ORNL/TM-6056

Actinide Partitioning and Transmutation Program Progress Report for Period April 1 to June 30, 1977

D. W. Tedder
J. O. Blomeke

OAK RIDGE NATIONAL LABORATORY
OPERATED BY UNION CARBIDE CORPORATION FOR THE ENERGY RESEARCH AND DEVELOPMENT ADMINISTRATION

DISCLAIMER

Printed in the United States of America. Available from
National Technical Information Service
U.S. Department of Commerce
5285 Port Royal Road, Springfield, Virginia 22161
Price: Printed Copy $9.25; Microfiche $3.00

ORNL/TM-6056

Contract No. W-7405-eng-26

CHEMICAL TECHNOLOGY DIVISION

ACTINIDE PARTITIONING AND TRANSMUTATION PROGRAM

PROGRESS REPORT FOR PERIOD APRIL 1 TO JUNE 30, 1977

Compiled by:

D. W. Tedder

J. O. Blomeke

Date Published: October 1977

OAK RIDGE NATIONAL LABORATORY
Oak Ridge, Tennessee 37830
operated by
UNION CARBIDE CORPORATION
for the
DEPARTMENT OF ENERGY

THIS PAGE

WAS INTENTIONALLY

LEFT BLANK

CONTENTS

FOREWORD

This is the second in a series of progress reports to be issued on the Actinide Partitioning and Transmutation Program, which is a multisite effort coordinated at the Oak Ridge National Laboratory. The first report was issued as ORNL/TM-5888. The overall program objective is to evaluate the feasibility and incentives for partitioning (separating) the long-lived biologically significant isotopes from fuel cycle wastes and transmuting (burning) them to shorter-lived or stable isotopes in power reactors.

During FY 1977 and 1978, the principal emphasis will be on the experimental evaluation of partitioning actinides, followed by their recovery in forms suitable for fabrication into transmutation targets. Detailed computer analyses will be undertaken to determine the effects on reactor and fuel cycle operations of recycling the partitioned actinides and to further verify the feasibility of transmutation itself. In FY 1979 the major effort will be directed toward a detailed assessment of the costs, risks, and benefits associated with this concept. The program is expected to produce: (1) realistic reprocessing and refabrication flowsheets which have been at least partly verified by experimental work, (2) several realistic transmutation schemes based on sophisticated reactor physics calculations, (3) an evaluation of partitioning and transmutation impacts on all phases of the nuclear fuel cycle, (4) a meaningful risk-cost-benefit analysis, and (5) a program plan for future development and demonstration requirements for eventual implementation in commercial operations. This analysis should constitute a reasonably firm technical basis for determining whether partitioning-transmutation represents a viable waste management alternative for managing long-lived waste nuclides that are generated by a nuclear power economy.

The program consists of 16 major tasks. This report summarizes the work done on each of these during the period April 1-June 30, 1977.

THIS PAGE

WAS INTENTIONALLY

LEFT BLANK

SUMMARY

Nonradioactive studies in PUREX PROCESS MODIFICATIONS on the extraction and stripping of uranium continue to demonstrate uranium losses of <0.01% in both continuous mixer-settler and batch countercurrent experiments. In anticipation of testing various flowsheet conditions in future hot-cell tests, investigations were made to establish the range of flow rates and impeller speeds which will ensure good operation of the mixer-settlers. Results showed that the two 16-stage mixer-settler units performed most satisfactorily at total flow rates up to 4.5 liters/hr and impeller speeds of 800 to 1100 rpm. Plutonium losses in batch countercurrent extraction tests (four extraction and four scrubbing stages) were found to be <0.01% using an extractant-to-aqueous volume ratio of 2. Stripping of plutonium was relatively poor when plutonium solubilized in 30% TBP was aged before stripping with 0.3 M HNO_3, but was relatively good for the unaged condition.

Efforts in ACTINIDE RECOVERY FROM SOLIDS during this report period were directed toward determining the dissolution parameters in various reagents for PuO_2, UO_2, U_3O_8, PuO_2-UO_2 solid solutions, and AmO_2-PuO_2 mixed solids. Several reagents were examined, including various concentrations of HNO_3, HNO_3-HF, HNO_3-H_2SO_4, HNO_3-$(NH_4)_2Ce(NO_3)_6$, and HNO_3-HF-H_2SO_4. Both Na_2CO_3 and Na_2CO_3-KNO_3 were investigated as possible salt fusion agents using simulated PuO_2-contaminated HEPA filter media. The weight percent actinide dissolved was measured for each of the mixtures, and plutonium adsorption isotherms were developed to determine whether any of the dissolved plutonium was being adsorbed by the filter medium. The HNO_3-$(NH_4)_2Ce(NO_3)_6$ mixture appears to give acceptable decontamination factors for refractory plutonium using a series of crosscurrent decontamination stages. The salt mixtures do not appear to be acceptable as fusion agents; in addition, severe corrosion problems are associated with this approach. Conceptual flowsheets are presented based on the most promising systems examined thus far.

Work relative to AMERICIUM-CURIUM RECOVERY WITH OPIX, TALSPEAK, AND CEC during this period consisted of: (1) settling rate measurements of rare-earth oxalates under semicontinuous precipitation conditions, (2) an

evaluation of the OPIX potential for removing residual traces of neptunium and plutonium from the HLLW, (3) Talspeak mixer-settler runs on the first cycle, (4) Talspeak distribution coefficient measurements, (5) studies of methods for removing monoethylhexylphosphoric acid from the Talspeak extractant, and (6) an examination of the effects of zirconium on the behavior of Talspeak. It was found that the volume of oxalate precipitate after complete settling was about 1% of the total solution volume. Batch precipitation tests indicate that about 99.5% of the plutonium can be removed when the plutonium is trivalent. Encouraging results were obtained for the first cycle of the Talspeak flowsheet as performed in the mixer-settler run; however, the distribution coefficient studies indicate that flowsheet modifications will be required. In addition, significant amounts of interfacial solids are formed in the Talspeak extraction when zirconium is present in the first-cycle feed in concentrations greater than 10^{-4} M. Also, the ethylene glycol scrub systems would have to be operated at nearly 1:1 volume ratios with the organic extractant. Consequently the ethylene glycol will have to be purified, possibly by ion exchange.

This quarter the studies in AMERICIUM-CURIUM RECOVERY USING BIDENTATE EXTRACTANTS involved measuring extraction, scrub, and strip distribution coefficients for actinides and other key elements between synthetic LWR waste solution, made 0.1 M in nitrite, and 30% dihexyl-N,N-diethylcarbamylmethylene phosphonate (DHDECMP) in diisopropylbenzene (DIPB).

Work concerning AMERICIUM-CURIUM RECOVERY USING INORGANIC ION EXCHANGE MEDIA focused on the effect of pH on the affinity of titanate, niobate, and zirconate ion exchange materials for rare-earth ions. Results obtained during the previous report period implied that these affinities would display a strong pH dependence.

Flowsheets were developed in the area of RECOVERY ALTERNATIVES APPLICABLE TO WASTE STREAMS for the extraction of Np, Pu, Am, Cm, Tc, and Pd from high-level liquid waste. The process involves three basic parts: first, the extraction of U, Np, Pu, Am, and Cm together with fission product Zr, Nb, Mo, Y, and rare earths using 0.5 M dihexoxyethylphosphoric acid (HDHoEP) in diethylbenzene (DEB) followed by stripping of Np, Pu, Zr, Nb, and Mo with oxalate and stripping of Am, Cm, and rare earths with 8 M HNO_3; second, the purification of Np and Pu from the Zr, Nb, Mo, and oxalate using 0.25 M

tricaprylmethylammonium nitrate ($TCMA \cdot NO_3$) in DEB; and third, the extraction of Tc and Pd from the raffinate of the first part using 0.1 M $TCMA \cdot NO_3$ in DEB. The process has been studied using synthetic liquid waste. Distribution ratios for selected actinides and fission products using HDHoEP and $TCMA \cdot NO_3$ are presented.

In the study of ACTINIDE RECOVERY FROM COMBUSTIBLE WASTE, the evaluation of leaching, acid digestion, and fusion methods for actinide recovery from incinerator ash was continued. High-fired plutonium oxide (with ^{241}Am present in tracer amounts) was used in each case. Solubilization and recovery of the actinides served as the measure of method efficiency. Fusion with 90 wt % Na_2CO_3--10 wt % $NaNO_3$ gave the best actinide recovery ($\geq$97%).

Emphasis in ACTINIDE RECOVERY AND RECYCLE PREPARATION FOR WASTE STREAMS was centered on the assessment of methods and recycle preparation for salt waste and waste-water streams. Further progress was made in a feasibility study for removing actinides from the salt wastes with a bidentate organophosphorous extraction process and a combined bidentate--tributyl phosphate extraction process. An evaluation of adsorbents for removing detergents from waste-water streams was initiated.

Work relating to RADIATION EFFECTS focused on completing the analysis for ion exchange materials. An interim report is expected to be in final form during the next period. This report will provide a compilation of the available information which has been converted to a consistent set of units. Additional rules of thumb, as well as sample calculations demonstrating the table usage, will also be included.

The FUEL AND TARGET FABRICATION STUDIES during this period were concerned with preliminary evaluations of alternative transmutation target forms. These considerations include the analysis of alternative diluents and the use of annular target rods.

LMFBR TRANSMUTATION STUDIES focused on the selection of a model LMFBR and its refuel material. Reference values for burnup, power density, k_{eff}, and breeding ratio were computed. The calculations were performed using 2-D, multigroup diffusion theory.

THERMAL REACTOR TRANSMUTATION STUDIES are described for three configurations of target material: (1) actinides uniformly dispersed in LWR fuel rods; (2) actinides concentrated in separate elements in an LWR fuel

assembly; and (3) actinide-containing rods comprising separate assemblies, surrounded by uranium-containing LWR fuel assemblies. In case 1, about 15% of the waste actinide inventory is fissioned and about 50% is converted to plutonium isotopes for fissioning later (after 20 years of recycling operations). In case 2, about 50% of the waste actinide inventory is fissioned after 20 years of operations. Case 3 is least attractive of the three because the flux in the separate target assemblies is four to ten times lower than in regular fuel assemblies. However, we anticipate that this situation can be largely alleviated by salting the waste actinide elements with fissile material.

The task areas FUEL CYCLE IMPACT STUDIES, RISK/BENEFIT ANALYSIS, and the DETAILED ECONOMIC ANALYSIS were inactive during this period.

Under ANALYSIS, COORDINATION, AND EVALUATION, alternative incineration flowsheets were drawn up. The incineration combination consisting of conventional air incineration and molten-salt fusion of the ashes for actinide recovery does not appear to result in significant reductions in salt waste volumes as compared with fluidized-bed incineration with sodium carbonate. The tandem system, however, would probably decrease the chances of significant actinide losses. Work during this period also included a continued review of the various ongoing programs with redirection as necessary. Editing continues on the forthcoming preliminary assessment of the concept, to be published as ORNL/TM-5808.

1. PUREX PROCESS MODIFICATIONS

W. D. Bond, F. A. Kappelmann, S. Katz, and F. M. Scheitlin
(Oak Ridge National Laboratory)

This task focuses on modifications to the Purex process which should result in higher recoveries of uranium, neptunium, and plutonium. Modifications to the process operations are considered, as well as alternatives in cleanup systems which result in smaller waste volumes and actinide losses.

1.1 Introduction

The Purex process employs tributyl phosphate (TBP), usually at a concentration of 30 vol %, in a hydrocarbon diluent (n-dodecane) to extract uranium and plutonium from fuel dissolver solutions. The theoretical degree of recovery is dictated both by the extent of extractability of these actinides from an aqueous solution salted by nitric acid and by the effectiveness of stripping the actinides from the extractant. Nominally, each of the extractable actinides undergoes at least two cycles (extraction and stripping) of solvent extraction to achieve the necessary decontamination from fission products and separation from each other. Any actinides not extracted from the solution of dissolved fuel remain with the high-level aqueous waste, whereas any actinides not stripped from the organic phase report to the wastes resulting from the regeneration and recycle of the extractant. In existing Purex plants, the extractant is purified for recycle by scrubbing it with an aqueous sodium carbonate solution which removes most of the principal solvent degradation products as well as the actinides and fission products. Thus, the sodium carbonate solution may become a transuranic waste stream and require further treatment in salt waste management. The actinide values remaining in nitric acid streams from the second and third Purex cycles (purification cycles) appear to be amenable to recycle if appropriate oxidation and reduction methods are used to separate the actinides from each other.

Experiments are being carried out on the Purex process relative to the countercurrent extraction and stripping of actinides using both continuous mixer-settlers and batch equipment. The purpose of these

experiments is to determine the effects on actinide losses by either including additional stages of extraction and stripping or using an additional Purex cycle to remove actinides from the high-level waste stream. The effects of the increased extraction of the zirconium and ruthenium fission products are also being evaluated. It is not known whether the increased radiation damage caused by the additional extraction stages (or cycles) will result in additional interfacial precipitates and cruds. Zirconium compounds formed with degradation products are reported to be of limited solubility both in the organic and aqueous phases and have been observed to impair operability when high-burnup fuels are processed.

All laboratory work to date has been carried out using simulated, nonradioactive fuel dissolver and high-level waste solutions as feeds. Plutonium work is carried out at the tracer level.

1.2 Studies Using Mixer-Settlers

Thirteen experimental runs were made using continuous, countercurrent mixer-settler equipment. Runs R-3 and R-4 examined the extraction of uranium followed by a subsequent strip with 0.3 M HNO_3 (Fig. 1.1). Eleven runs (S series) were made using 0.1 M HNO_3 for stripping uranium (Fig. 1.2). The concentrations and volumes of the effluents shown in Figs. 1.1 and 1.2 were estimated using the SEPHIS computer code.[1] In addition to providing data on uranium recovery, the S series of experiments also evaluated the hydraulic performance of the mixer-settler units and the range of operating conditions that should be used in future hot-cell tests. The use of stirrer speeds and flow rates that gave good hydraulic performance resulted in uranium losses that were less than 0.01%.

1.2.1 R series experiments

Conditions for the R series experiments are shown in Table 1.1. In the first two runs (R-1 and R-2), which were reported last quarter, it was necessary to use divided flow of the aqueous stream to the stripping bank (0.5 liter/hr to stage 1 and 3.0 liters/hr to stage 5). The need to divide the flow was eliminated when the split stirrer paddles in the stripping bank were replaced with solid stirrer paddles (Fig. 1.3) to improve mixing characteristics. Some further improvement in operation was also obtained

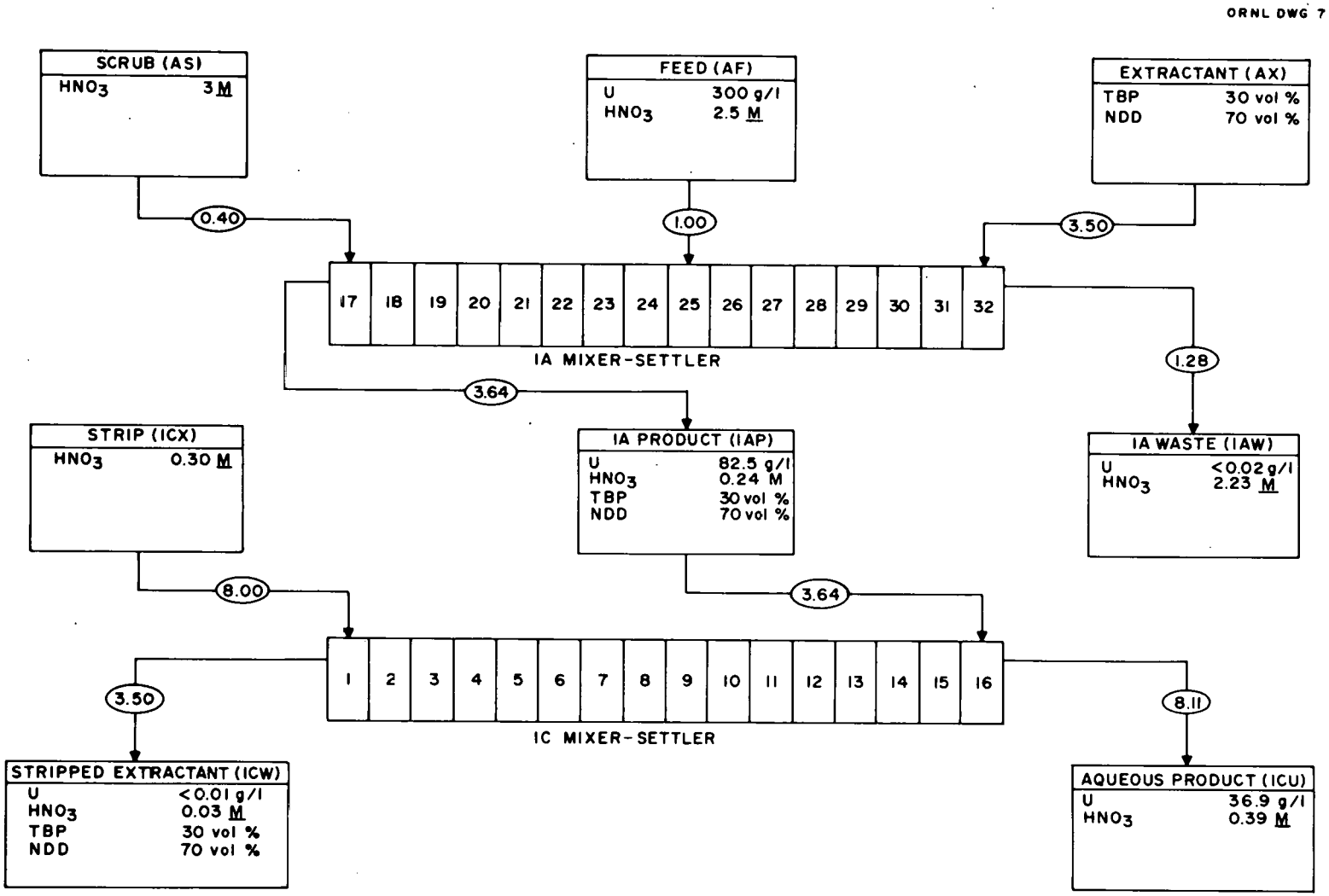

Fig. 1.1. Purex flowsheet using 0.3 M HNO_3 in stripping (R series).

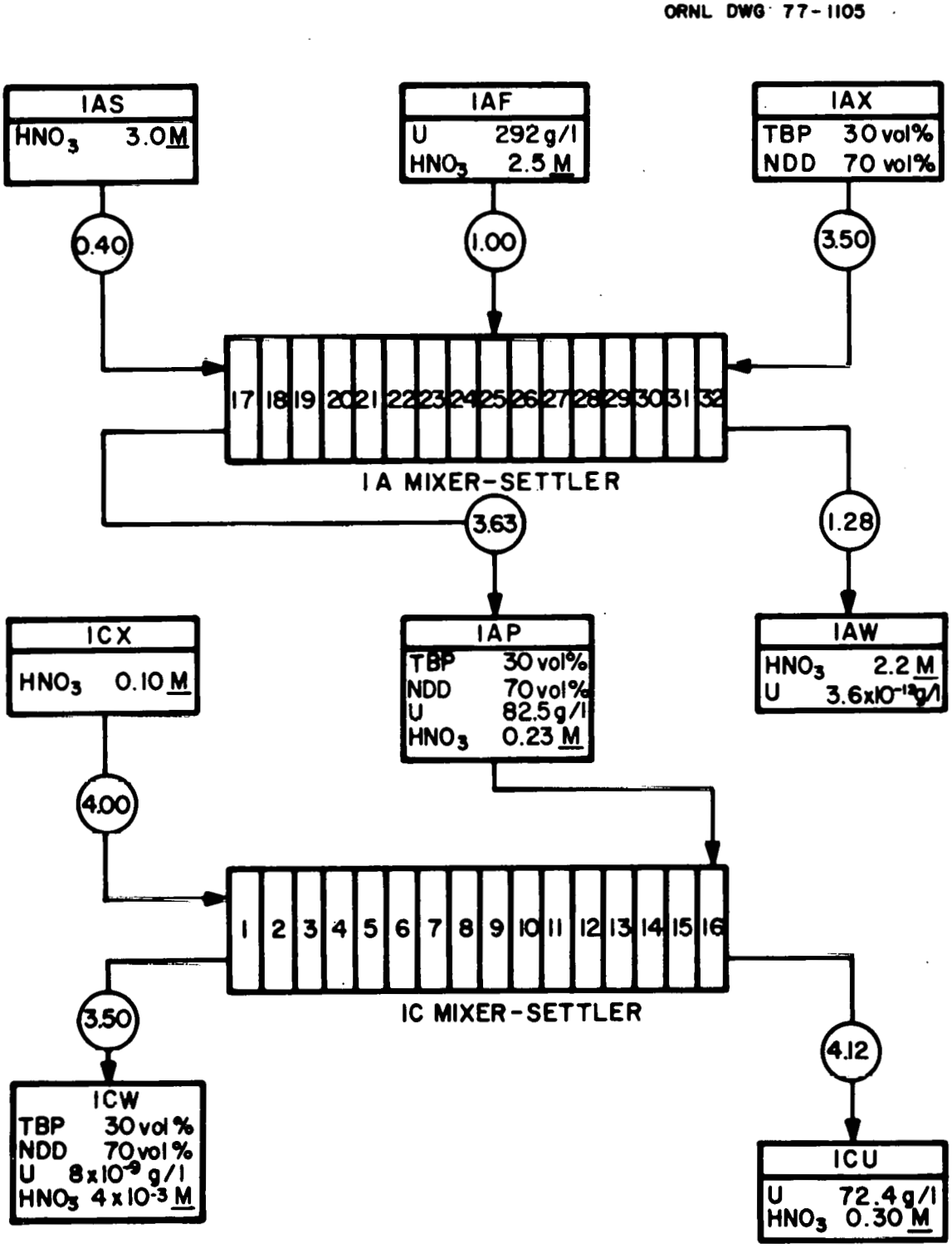

Fig. 1.2. Purex flowsheet using 0.1 M HNO_3 in stripping (S series).

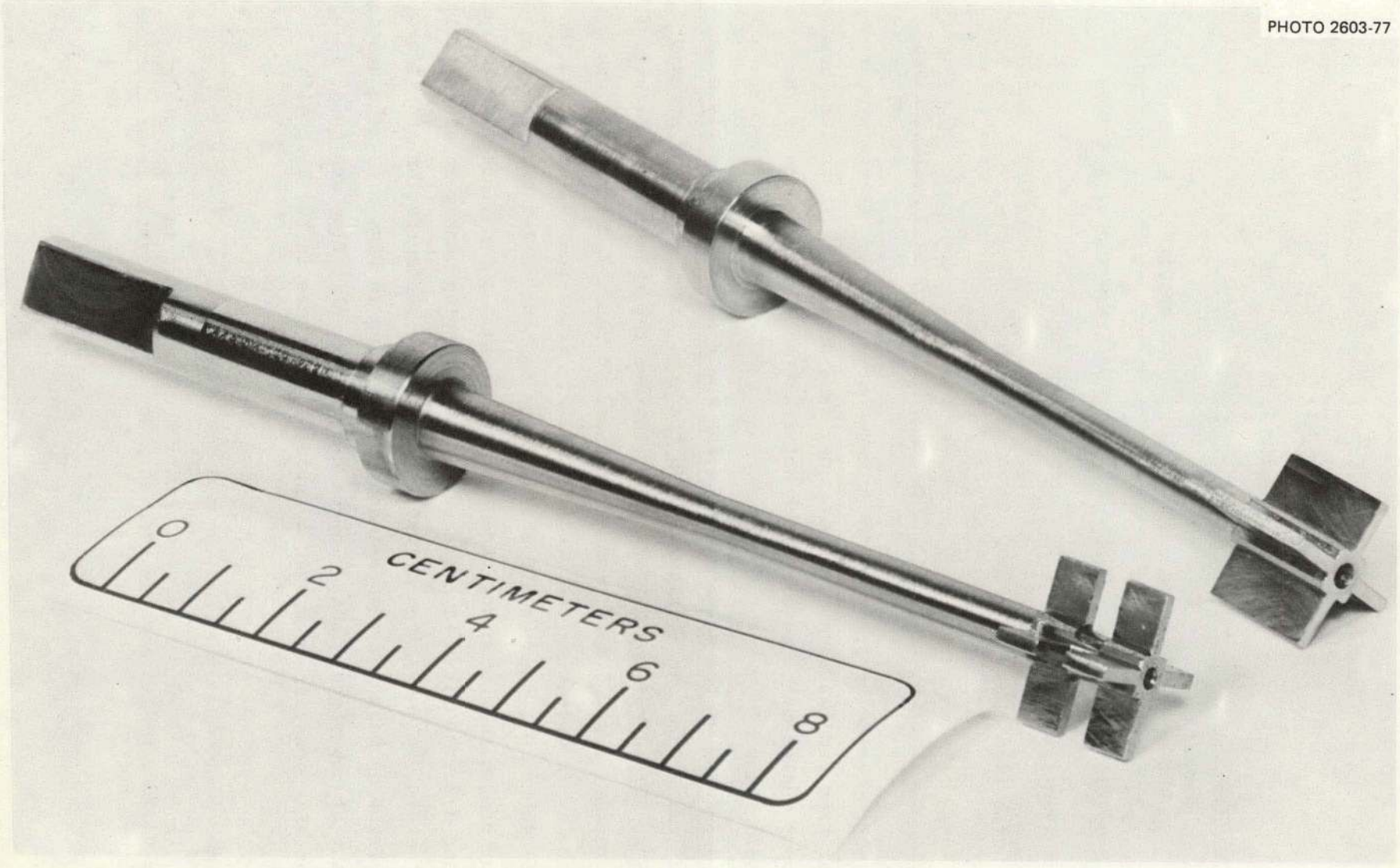

Fig. 1.3. Types of agitators used in mixer-settlers: (a) split blades, and (b) solid blades.

Table 1.1. Flowsheet conditions for R series experiments

Temperature = 43°C

Stirrer speed: 1100 rpm

Process stream	Flow rate (liters/hr)	Composition
Feed (1AF)	0.50	∿300 g U/liters and ∿2.5 M HNO_3
Solvent (1AX)	1.75	30% TBP-NDD
Scrub (1AS)	0.20	3.0 M HNO_3
Strip (1CX)	4.00	0.3 M HNO_3

by a more precise leveling of the mixer-settler units. At the same time the stirrer paddles were replaced, new feed pumps were installed; however, the pump replacement had either or no effect on the operation of the stripping bank.

A summary of the uranium losses for the R series runs is given in Table 1.2. Losses were calculated on the analysis of effluent streams taken at the end of the run and were greatest for the stripped organic (CW). The greatest loss, 0.032%, was experienced in run R-2 where there was difficulty in operating the stripping bank. Stage-to-stage distribution coefficients, D_A^o,* measured for the stripping bank of R-2 were about a factor of 2 higher than for the other runs. With the divided flow in runs R-1 and R-2, the first five stages of the stripping bank were essentially ineffective. A comparison of the organic-phase concentration profiles of the stripping bank for runs R-1 and R-4 is shown in Fig. 1.4. The uranium content of the organic phase in run R-1, where split flow was used, is essentially constant in stages 1 through 5, whereas in run R-4, with

*D_A^o is defined as the concentration of a species in the organic phase divided by its aqueous concentration when the system is at chemical equilibrium.

Table 1.2. Uranium recovery in R series runs

Run number	Run time (hr)	Additives to feed	Product conc. (g U/liter)		% U loss[a]		% U recovery[b]
			1AP	1CU	1AW	1CW	
R-1	12	None	82.9	41.5	2×10^{-4}	4×10^{-3}	99.996
R-2	11	Cold FP's[c]	92.5	36.1	2×10^{-4}	3×10^{-2}	99.970
R-3	10	None	96.1	37.1	9×10^{-4}	4×10^{-3}	99.995
R-4	10	Zr (1.3 g/liter)	76.3	28.8	8×10^{-4}	1×10^{-3}	99.998

[a]Based on effluent stream analysis at steady state.

[b]Calculated from losses.

[c]FP's = fission products.

ORNL DWG 77-1104

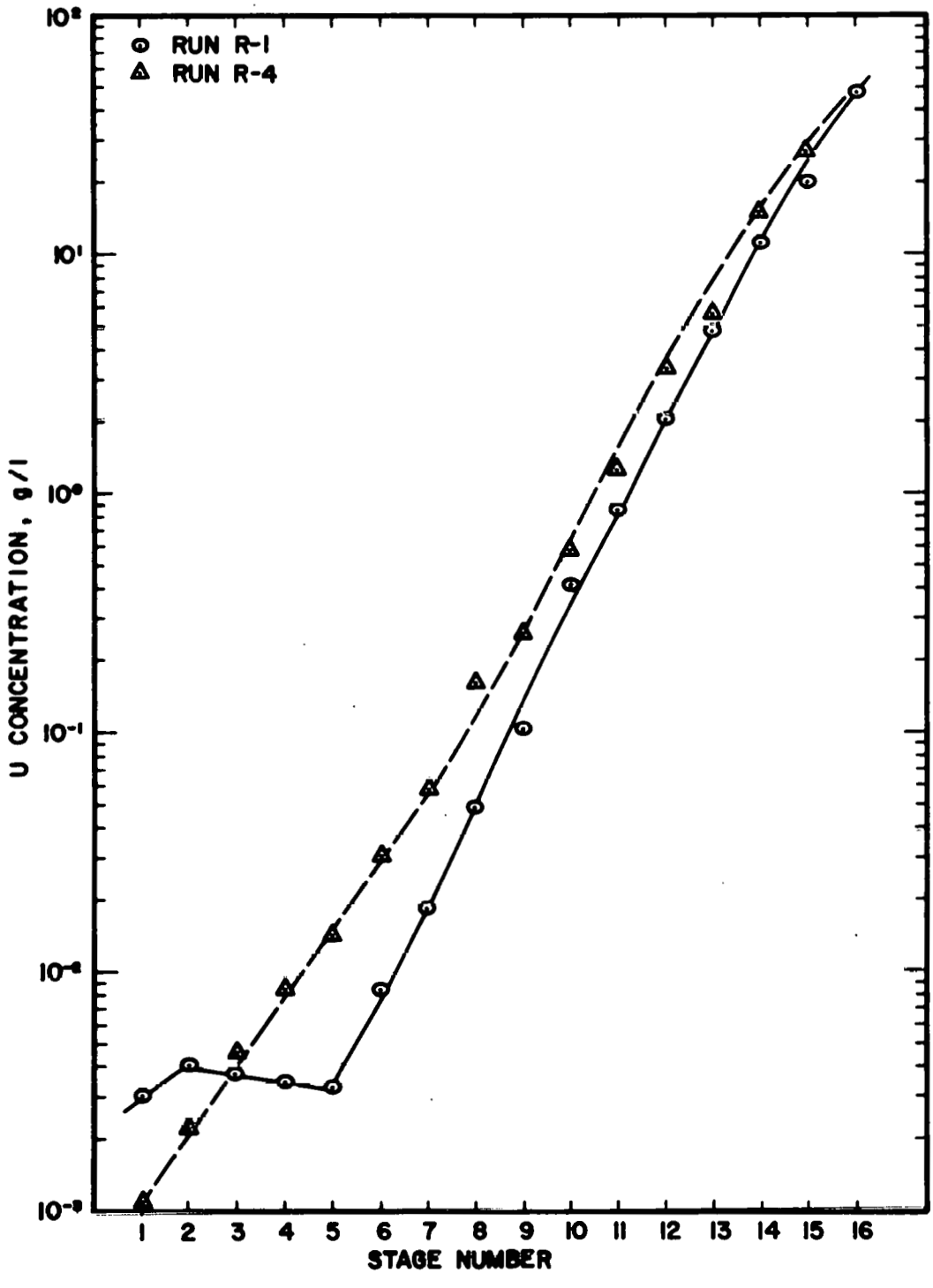

Fig. 1.4. Concentration profile of the organic phase in the stripping bank.

single flow, the uranium continues to strip out. The concentration profiles for the organic and aqueous phases in the extraction bank of run R-4 (see Fig. 1.5) are typical of all the runs.

Steady-state operation was apparently achieved in about 4 hr (Figs. 1.6 and 1.7), although considerable scatter was observed in the analysis. In runs R-3 and R-4, the equipment was shut down overnight after 6 hr of operation, leaving the inventory in the system, and then run an additional 4 hr on the following day (Fig. 1.8). The uranium concentrations of the products reached about the same value the second day; however, the losses to the raffinates appeared to increase, even though they were still low values. This suggests that shutdown operations would not necessarily increase uranium losses to unacceptable levels.

Measurement of stage-to-stage distribution coefficients for uranium, $D_A^o(U)$, gave reasonable agreement in runs R-3 and R-4 for both the extraction and stripping banks (Tables 1.3 and 1.4). The uranium concentrations in the phases were quite different in some stages, although the runs were essentially identical. In the R series runs, samples of each were taken via means of band-operated pipets. Some intermixing of liquids from different stages could have occurred, and this may partly explain the observed differences in runs R-3 and R-4. Also, attempts to measure the distribution coefficients of zirconium in run R-4, and zirconium and ruthenium in run R-2, were unsuccessful in that the chemical analytical methods used proved to be unreliable both at low levels and when these elements were present along with appreciable amounts of uranium.

1.2.2 S series experiments*

The objectives of these experiments were: (1) to establish the ranges of total flow rates and impeller speeds which would give stable operation, and (2) to determine the product losses and stage efficiencies attained under stable operating conditions. In addition, these runs were made to

---

*Work carried out in collaboration with H. C. Savage and V. C. A. Vaughen. Data obtained are of mutual interest to LWR program (ERDA Activity No. KX-0201-04-0).

ORNL DWG 77-1103

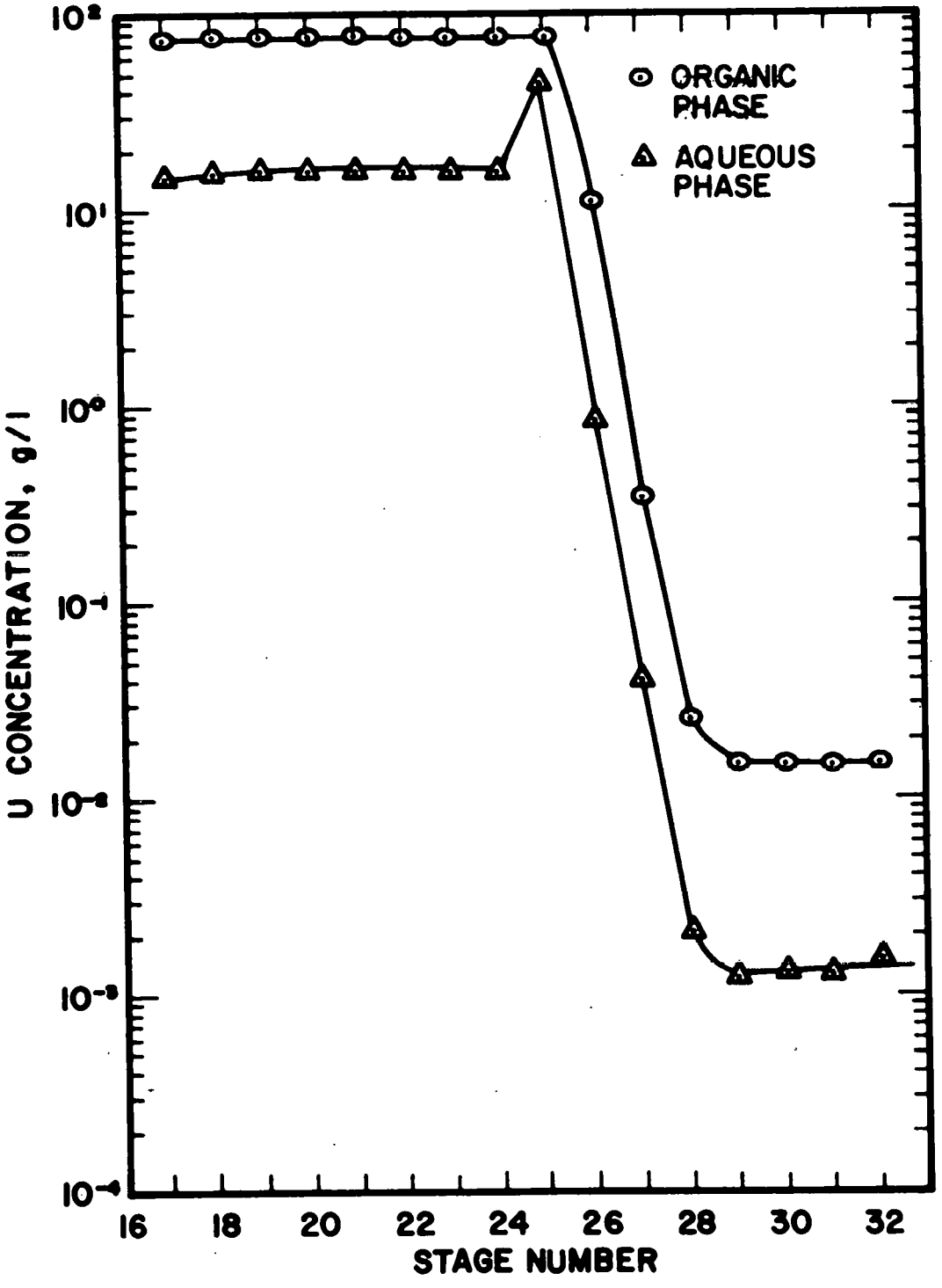

Fig. 1.5. Concentration profile of uranium in the extraction bank (run R-4).

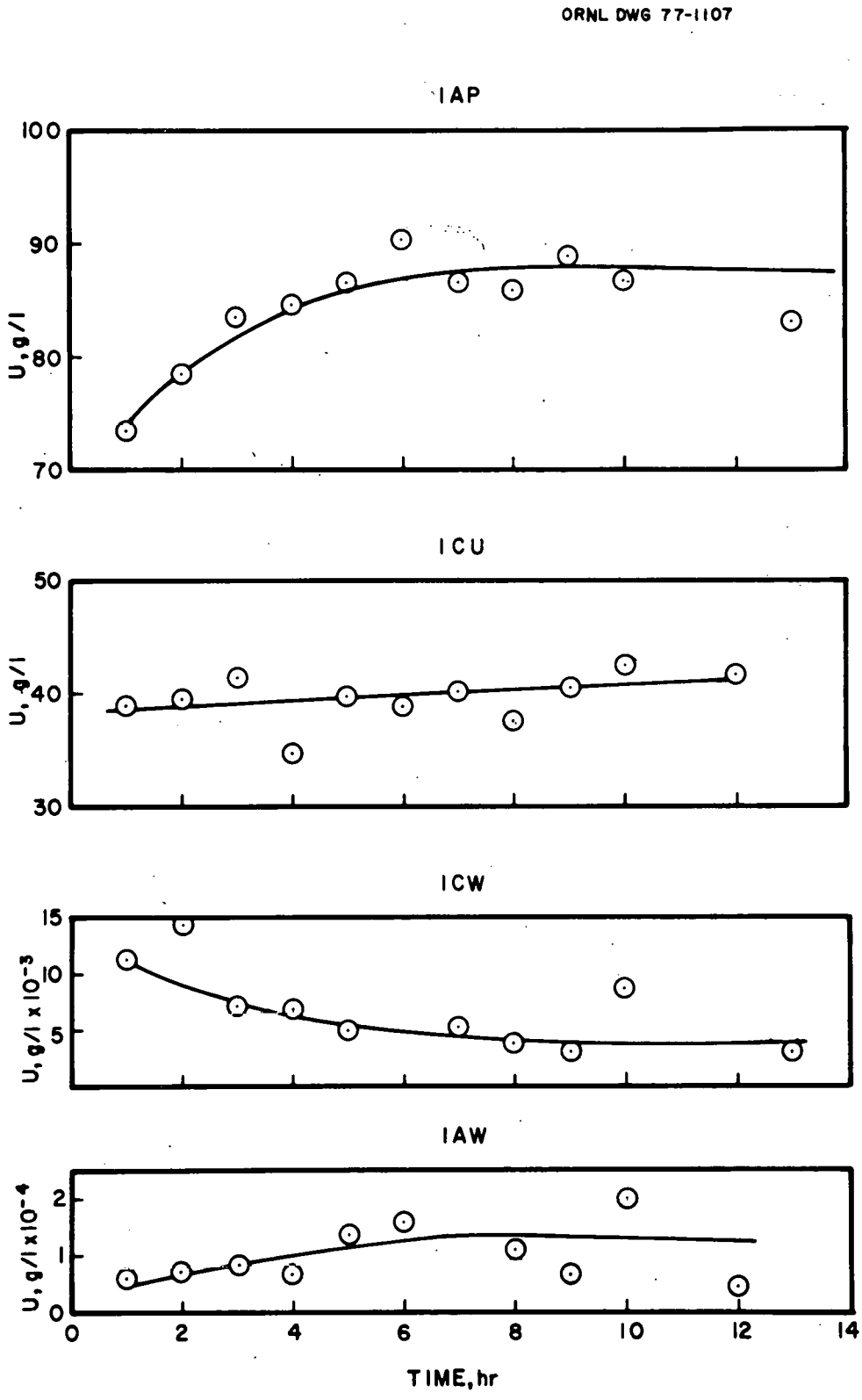

Fig. 1.6. Uranium concentration of end streams as a function of time (run R-1).

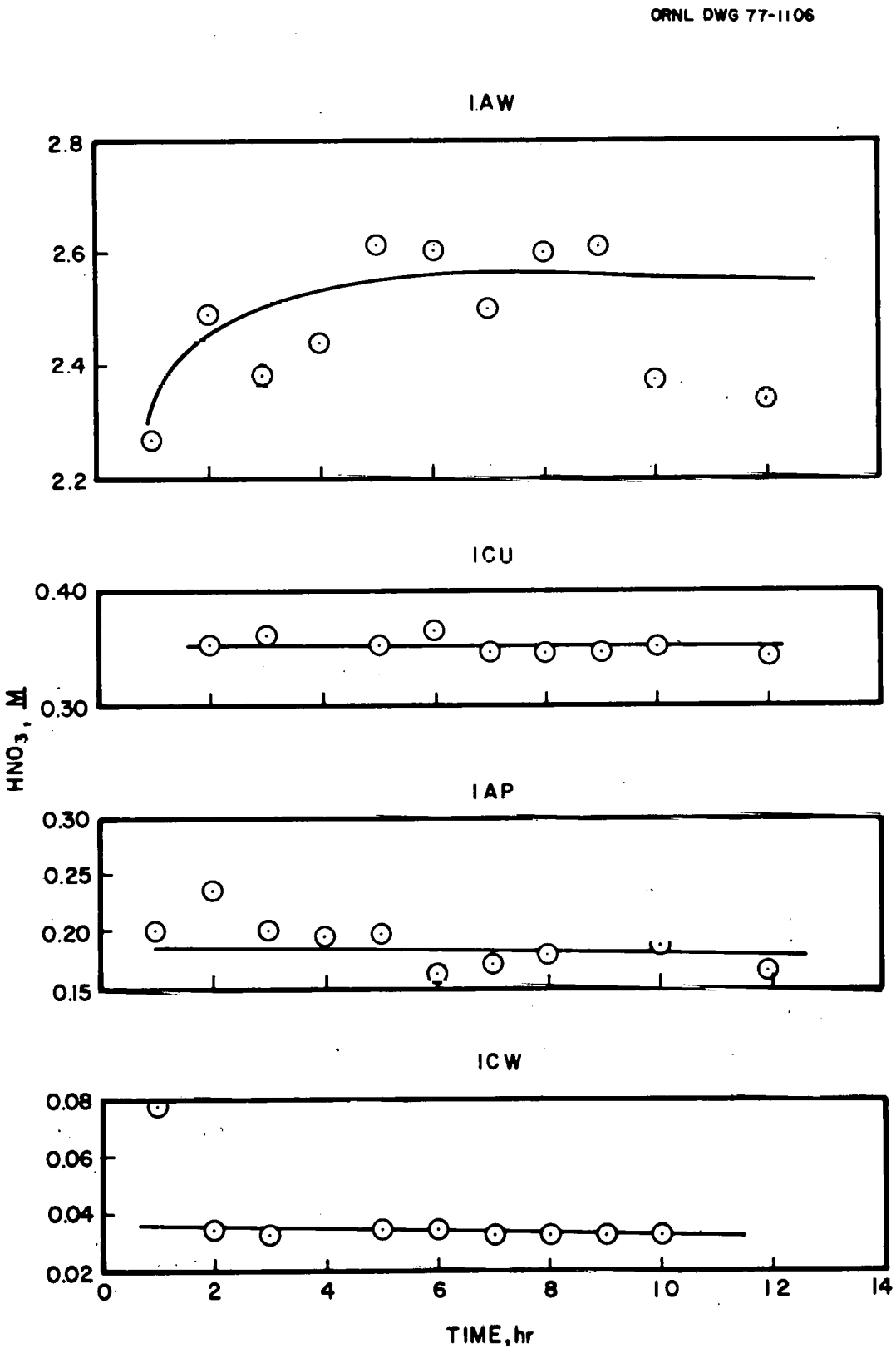

Fig. 1.7. Nitric acid concentration of end streams as a function of time (run R-1).

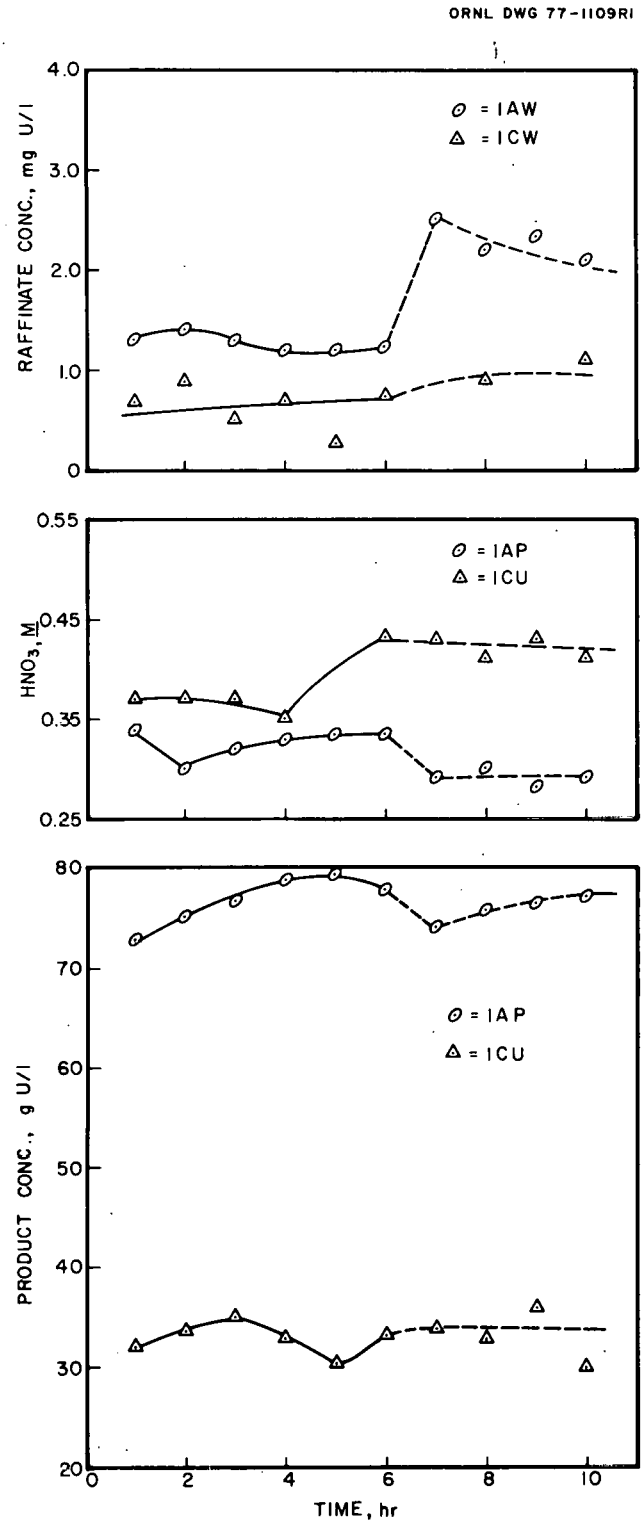

Fig. 1.8. Uranium and nitric acid concentrations of end streams of run R-4 as a function of time. The dashed-line portion of each curve denotes resumption of the run after shutdown overnight.

Table 1.3. Operating uranium concentrations and distribution coefficients in the extraction bank

Stage number	R-3		R-4	
	Aqueous U concentration (g/liter)	$D_A^o(U)$	Aqueous U concentration (g/liter)	$D_A^o(U)$
17	17.8		13.0	5.86
18			14.2	5.56
19	17.2		14.0	5.78
20			13.8	5.88
21	17.7		13.6	5.57
22			13.4	5.93
23	16.6	5.28	13.2	6.15
24	16.4	5.29	13.4	6.06
25	52.3	1.66	44.0	1.99
26	0.98	14.9	0.31	35.2
27	2.7×10^{-2}	14.2	1.0×10^{-2}	31.0
28			1.4×10^{-3}	50.0
29			1.1×10^{-3}	14.7
30	1×10^{-3}	21	1.1×10^{-3}	13.6
31			1.2×10^{-3}	11.7
32	2×10^{-3}	9.0	1.7×10^{-3}	8.8

Table 1.4. Operating uranium concentrations and distribution coefficients, $D_A^o(U)$, in the stripping bank

Stage number	R-3		R-4	
	Aqueous U concentration (g/liter)	$D_A^o(U)$	Aqueous U concentration (g/liter)	$D_A^o(U)$
1	0.003	1.1	0.0008	1.3
2			0.002	1.1
3			0.004	1.0
4	0.017	1.6	0.009	0.92
5			0.016	0.85
6			0.030	0.96
7			0.060	0.97
8			0.110	1.5
9	0.725	1.1	0.250	1.0
10	1.53	0.90	0.530	1.1
11	3.14	0.73	1.11	1.1
12	4.89	1.2	2.73	1.2
13	10.1	1.2	5.43	1.0
14	17.4	1.5	10.4	1.4
15	25.9	1.4	20.8	1.3
16	37.1	1.6	28.8	1.6

provide reasonable operating conditions for future hot-cell experiments. A mixer-settler is operable over a fairly wide range of impeller speeds and liquid throughputs, as shown in Fig. 1.9.[2]

Experimental. Eleven experimental runs were made in the S series. These runs differed from those in the R series with regard to the acid concentration and the volume used in the stripping bank (Figs. 1.1 and 1.2). The compositions of the process streams and their flow ratios (relative to the feed stream) are given in Fig. 1.2. Both the 1A and 1C units were operated at 43°C, which permits excellent phase separation.

The operating conditions for the S series experiments are shown in Table 1.5. Impeller speeds of 800, 1100, and 1700 rpm were employed. Total flow rates of the reference value (R), 0.5R, and 1.5R were used (Table 1.5) while maintaining flow ratios fixed at the values shown in Fig. 1.1. The time used for each run was that observed to reach at least 99% of steady state in both mixer-settler banks. In two runs, 1A and 2A, the mixer-settlers used for the A and C units were switched. The purpose of switching these mixer-settlers was to determine the effect, if any, of the stirrer configuration (each mixer-settler utilized stirrers with different blade configurations) on the performance characteristics in extraction and stripping. For runs 1 through 9, the back stirrer in the 1C unit had four blades (1.27 cm long × 0.56 cm wide × 0.16 cm thick). The stirrers in the A bank had eight blades and were similar to the stirrers in the C bank except for the 0.32-cm slot separating the blades (0.48 cm long × 0.56 cm wide × 0.16 cm thick) along the stirrer shaft (Fig. 1.3). In the following discussions, the four-bladed stirrers are referred to as solid-blade stirrers and the eight-bladed stirrers are called split-blade stirrers. An originally scheduled run (run 6) using a flow rate of 1.5R and an impeller speed of 800 rpm was not made because the results obtained in runs 4 and 5 indicated that the higher flow rates would not provide satisfactory operation.

The mixer-settler contained both organic and aqueous phases at the beginning of each run. Every run, except run 1, was started with an initial inventory of uranium in the mixer-settler. In each succeeding run, the initial inventory included the uranium that was distributed throughout the

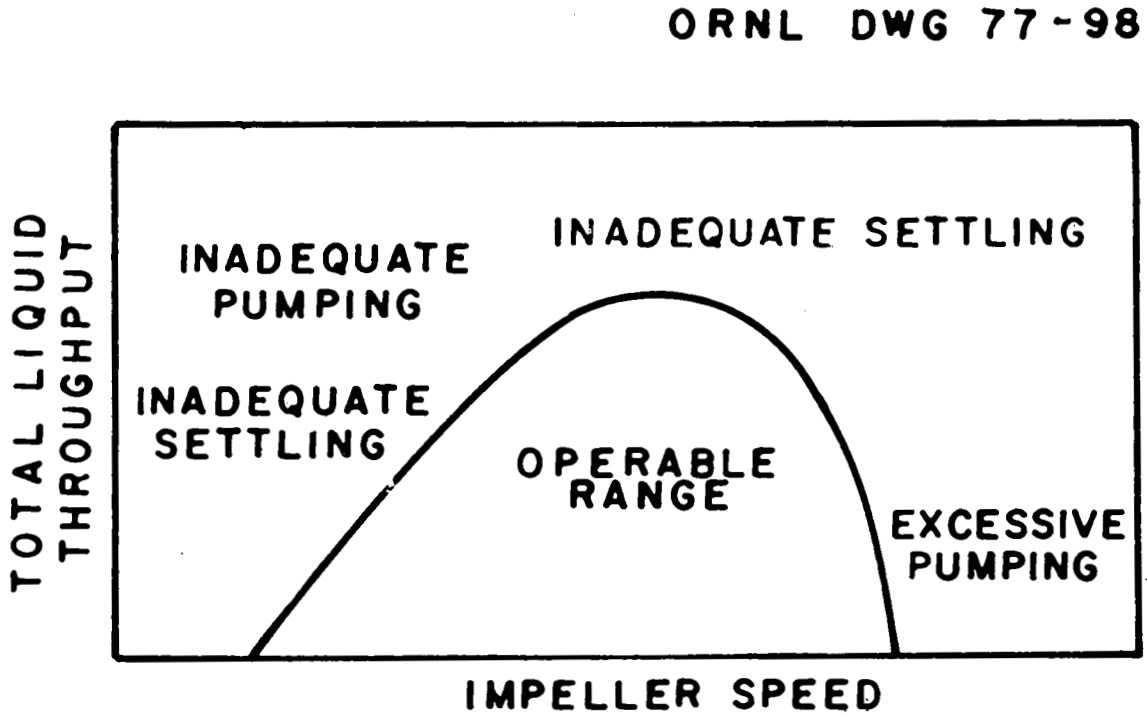

Fig. 1.9. Diagrammatic representation of operating regions for mixer-settlers.

Table 1.5. Operating parameters for Purex experimental runs in 16-stage mixer-settlers

Run number	Run time (hr)	Flow rate[a] (liters/hr)	Agitator speed (rpm)
1	4	Reference	1100
2	4	Reference	1700
3	4	Reference	800
1R[b]	4	Reference	1100
4	4	1.5 × reference	1100
5	4	1.5 × reference	1700 extraction bank; 1300 strip bank
7	6.25	0.5 × reference	1100
8	5	0.5 × reference	1700
9	7	0.5 × reference	800
1A[c]	4.5	Reference	1100
2A[c]	5	Reference	800

[a]Reference flow rate: Feed (AF) = 0.50 liter/hr
Solvent (AX) = 1.75 liters/hr
Scrub (AS) = 0.20 liter/hr
Strip (CX) = 2.00 liters/hr

[b]Repeat of run 1.

[c]A and C banks reversed to test effect of solid and split agitator blades.

stages from the previous run. The runs were performed in the order listed in Table 1.5. The initial inventory of solvent and aqueous phases at the start of run 1 was accumulated by feeding the banks with nitric acid solutions and 30% TBP (preequilibrated with 0.01 M HNO_3). Prior to run 1, the A bank inventory was accumulated by substituting 2.5 M HNO_3 for the uranium feed solutions, using the same flow rate as in run 1. All other input streams and flow rates to the A bank were the same as those shown in Fig. 1.2. The initial C bank inventory was obtained by feeding the organic phase exiting from the A bank to the C bank under the conditions shown in Fig. 1.2.

During each run, samples of the product and waste streams were withdrawn on an hourly basis until the last hour of operation; at that time samples were taken every 15 min (Fig. 1.10). Flow rates were monitored every 30 min and adjusted when necessary. Temperatures were checked periodically by inserting a thermometer into the solutions in the mixer-settlers. Agitator speeds, which were maintained within ±50 rpm, were monitored continuously by the speed-control panel meter and occasionally by means of a Strobatic.

At the end of the run, samples of both the organic and aqueous phases from each of the 32 settling chambers of the A and C banks were taken via a multiple sampler device (Fig. 1.11), which permits rapid removal of 2.5-ml volumes of each phase. These samples were analyzed for their uranium and nitric acid concentrations. Equilibrium distribution coefficients of four preselected stages were determined by removing aqueous and organic samples from these stages, performing batch equilibrium shakeouts, and analyzing the phases for uranium content. Samples of the composite AW and CW streams were also taken and analyzed for uranium.

Results. Each experimental run was evaluated by several methods, including: (1) determination of uranium concentrations in the product and waste streams, (2) calculation of uranium material balance, (3) estimation of overall stage efficiencies from McCabe-Thiele diagrams, and (4) visual observation of the settling chambers during operation (to detect any flooding, emulsion at the aqueous-organic interface, etc.). These methods were insufficient to quantitatively specify the optimum operating conditions;

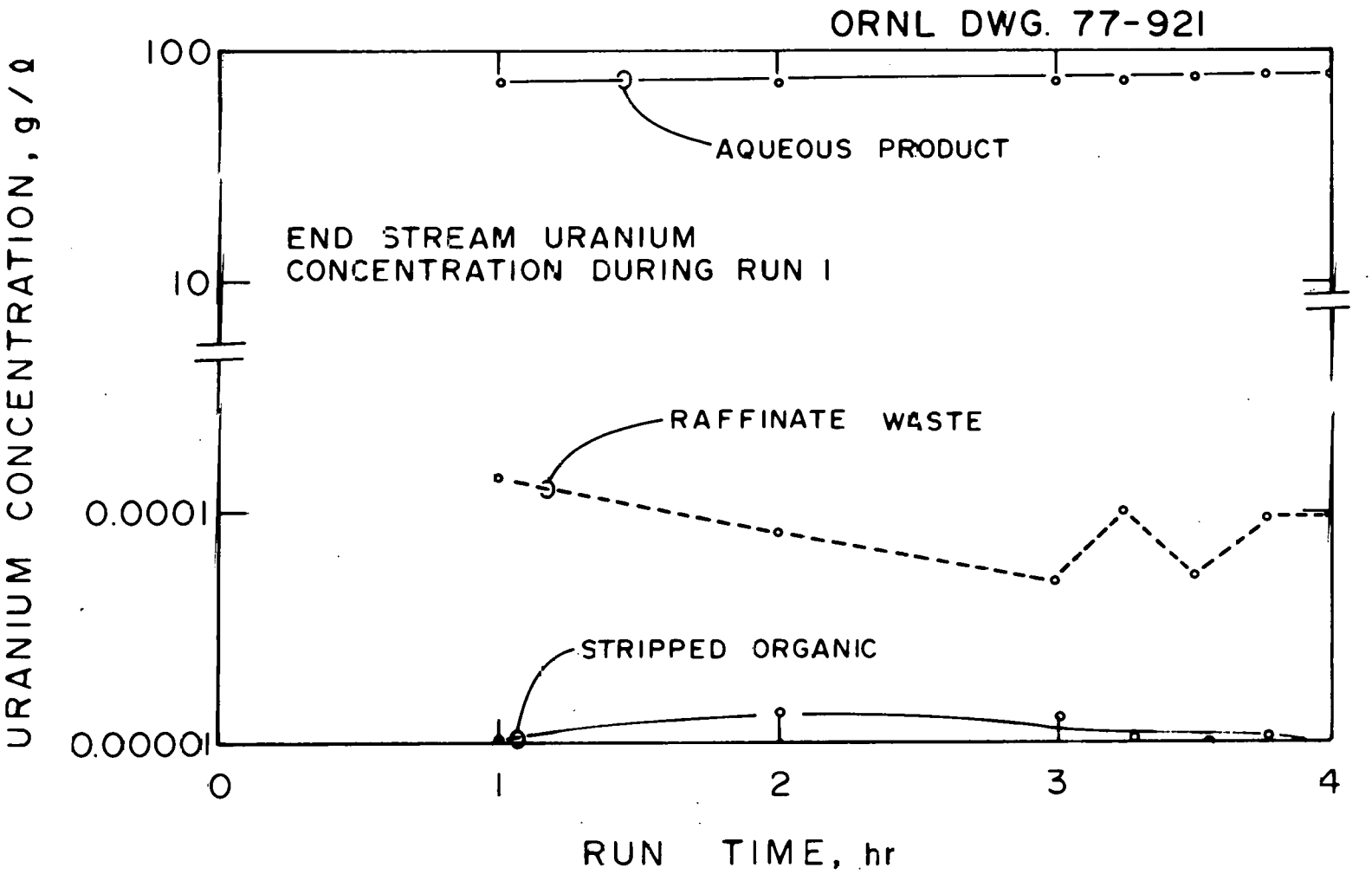

Fig. 1.10. End stream concentration vs operating time during run 1.

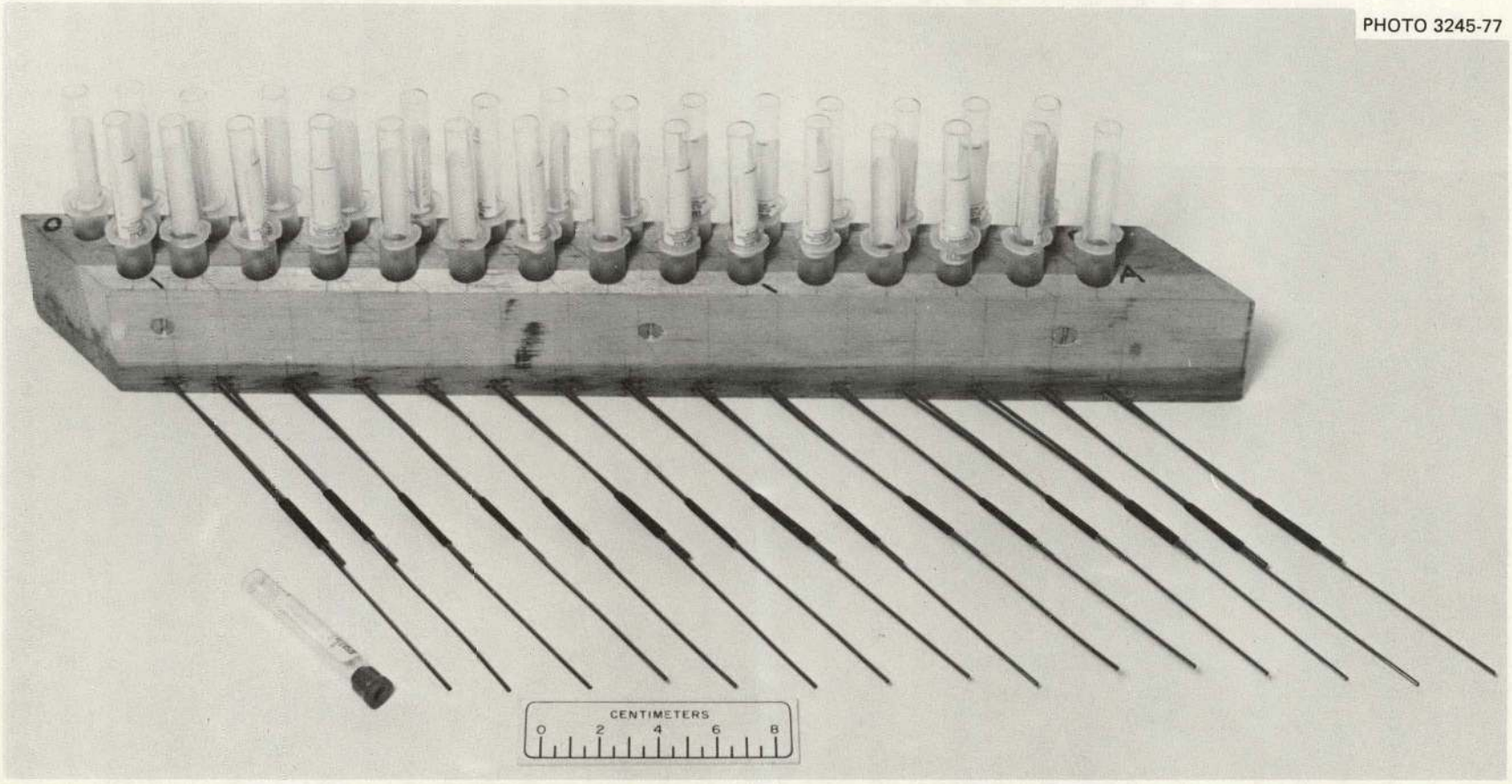

Fig. 1.11. Multiple sampler device for mixer-settlers.

however, the summation of all results and observations gave a good qualitative indication of the system performance at each of the run conditions. The relative value and limitations of each evaluation method are discussed in the following paragraphs.

The final uranium concentration in the aqueous raffinate (1AW) from the extraction bank varied from 2.6×10^{-5} to 3.4×10^{-3} g/liter, while that in the organic waste (1CW) from the strip bank varied from 1×10^{-5} to 11.2 g/liter (Table 1.6). The analytical limit for uranium is about 2×10^{-5} g/liter, and significant errors can be expected below about 1×10^{-4} g/liter. Therefore, no significance was attached to variations in the uranium concentration in the aqueous raffinate or organic waste unless the value exceeded about 1×10^{-4} g/liter. (For reference purposes, SEPHIS calculations predict uranium concentrations of about 3×10^{-12} and about 8×10^{-8} g/liter in the aqueous raffinate and organic waste, respectively, which are values far below our analytical capability.) Uranium concentrations in the organic and aqueous product streams from the extraction and stripping banks ranged from about 68 to 99 g/liter.

Material balances for uranium in the extraction and stripping banks, as well as an overall balance for both banks, were made. The apparent overall material balance for uranium ranged from 97 to 110%, with the exception of run 5 (133%) in which flooding was observed in the stripping bank (Table 1.7). Since the material balance depends directly on uranium analyses and flow rate, the values of both these parameters must be accurately known. The extraction bank product stream (1AP) is the input stream to the stripping bank, and the material balances for each bank depend on the analysis of this stream. The uranium concentrations in end streams are based on multiple samples taken during the run and should be considered a good estimate. Thus, the overall uranium material balance for both banks is also dependent on the accuracy of the flow rate measurements (+5%).

Overall efficiencies of the extraction and stripping banks were estimated from the McCabe-Thiele diagrams in which the number of actual stages required to produce given aqueous raffinate and organic waste uranium concentrations are compared with the number of theoretical stages to produce the same concentrations based on SEPHIS calculations (Table 1.7).

Table 1.6. Operating conditions and uranium analyses of product and waste streams for Purex experimental runs in 16-stage mixer-settlers

Run number	Run time (hr)	Flow rates[a]	Agitator speed (rpm)	Uranium concentration[b] (g/liter)				Uranium loss (%)[c]	
				AW	AP	CW	CU	AW	CW
1	4	Reference	1100	9.4×10^{-5}	91.4	1.0×10^{-5}	81.3	4.5×10^{-5}	1.2×10^{-5}
2	4	Reference	1700	2.6×10^{-5}	87.1	1.3×10^{-3}	80.1	1.2×10^{-5}	1.6×10^{-3}
3	4	Reference	800	4.0×10^{-5}	92.2	7.0×10^{-5}	80.0	1.9×10^{-5}	8.4×10^{-5}
1R	4	Reference	1100	4.1×10^{-5}	84.9	3.3×10^{-5}	73.7	2.0×10^{-5}	4.0×10^{-5}
4	4	1.5 × reference	1100	2.6×10^{-5}	80.9	1.0×10^{-2}	77.8	1.2×10^{-5}	1.2×10^{-5}
5	4	1.5 × reference	1700 ext.; 1300 strip	1.6×10^{-4}	99.2	11.2	89.6	7.7×10^{-5}	13.4
7	6.3	0.5 × reference	1100	3.4×10^{-3}	83.7	4.3×10^{-4}	74.5	1.6×10^{-3}	5.2×10^{-4}
8	5	0.5 × reference	1700	7.6×10^{-4}	81.7	6.3×10^{-2}	67.9	3.6×10^{-4}	7.6×10^{-2}
9	7	0.5 × reference	800	1.1×10^{-4}	79.3	7.1×10^{-5}	72.7	5.3×10^{-5}	8.5×10^{-5}
1A[d]	4.5	Reference	1100	2.8×10^{-4}	85.0	1.4×10^{-4}	73.6	1.3×10^{-4}	1.7×10^{-4}
2A[d]	5	Reference	800	2.2×10^{-4}	85.7	8.4×10^{-4}	73.7	1.1×10^{-5}	1.0×10^{-3}
Uranium concentrations predicted by SEPHIS				3.6×10^{-12}	82.5	8.1×10^{-8}	73.7		

[a]Reference flow: AF = 0.50 liter/hr; AX = 1.75 liters/hr; AS = 0.20 liter/hr; CX = 2.00 liters/hr.
[b]Feed (AF) = 292 g U/liter
[c]Loss calculated from uranium analyses at the end of run.
[d]Split-blade agitators in strip bank; solid-blade agitators in extraction bank.

Table 1.7. Uranium material balance and estimated overall stage efficiencies for Purex experimental runs in 16-stage mixer-settlers

Run number	Uranium material balance: output/input			Estimated[a] overall stage efficiency (%)		Observations
	Extraction (%)	Strip (%)	Extraction + strip (%)	Ext.	Strip	
1	100	105	106	65	85	Extraction bank organic continuous. Strip bank organic continuous except stages 1 and 3.
2	94	105	99	55	d	Foaming on surface of organic phase - all stages.
3	101	105	106	80	d	All stages organic continuous. Stable operation.
1R[b]	119	87	104	75	d	Same as Run 1.
4	93	106	99	55	<<75	Extraction bank same as 1. Strip bank organic continuous except stages 1, 10, 11.
5	111	120	133	55	d	Strip bank flooding.
7	104	105	109	55	<75	All stages organic continuous. Stable operation.
8	101	96	97	55	-	Foaming on surface of organic phase - all stages. Stripping poor. Uranium visible at stage 3.
9	98	112	110	55	75	Extraction bank organic continuous. Strip bank organic continuous except stages 1, 3, 9, 11, 12.
1A[c]	105	99	104	~100	75	Emulsion in strip bank.
2A[c]	113	92	103	80	75	Extraction bank stable. Emulsion in stage 16 with organic loss to product (CU).

[a]Estimated from McCabe-Thiele diagrams.
[b]Uncertainty in organic (AX) feed rate.
[c]Split-blade agitator in strip bank; solid-blade agitator in extraction bank.
[d]Not determined.

As noted previously, analyses could not reliably determine uranium concentrations below about 1×10^{-4} g/liter. For this reason, the number of ideal stages in each bank was compared with the number of actual stages required to reach about 1×10^{-4} g/liter. Based on SEPHIS calculations, the number of ideal stages is about 3.5 for the extraction bank and about 12 for the stripping bank. Estimated overall efficiencies for the extraction and stripping banks for those runs for which sufficient data were obtained are shown in Table 1.7. Samples taken from preselected stages for equilibrium shakeouts had uranium concentrations that were too low for accurate analyses and hence could not be used to determine stage efficiencies.

A quartz window allows observation of all 32 settling chambers in the mixer-settlers. Thus, abnormal or unsatisfactory operation (i.e., flooding, emulsion at the aqueous-organic interface, etc.) during a run could easily be determined visually. Pertient observations for each run, along with analytical results, are recorded in Table 1.7.

Discussion and Conclusions. As discussed in the previous section, the various methods used to determine optimum operating conditions for the 16-stage mixer-settlers are only qualitative; however, summation of all results and observations provide a reasonably good indication of system performance at each of the run conditions. In particular, very poor or very good operation was easily determined. Based on the results summarized Tables 1.3 and 1.4, the mixer-settler system was operable at the reference flow rate and at one-half the reference flow rate using agitator speeds of 800 and 1100 rpm. System performance was unsatisfactory at agitator speeds of 1700 rpm at all of the flow rates tested. System performance was poor at a flow rate of one and one-half times the reference flow rate and an agitator speed of 1100 rpm. The run at an agitator speed of 800 rpm and a flow rate of one and one-half times the reference flow rate was not made due to time limitations; however, it is believed that system performance would have been less satisfactory than at the lower flow rates. The results are shown diagrammatically in Fig. 1.12.

The performance of the two types of stirrers was evaluated by comparing runs 1 and 2 (solid blades in the stripping bank, split blades in the extraction-scrub bank) with runs 1A and 2A (split blades in the stripping

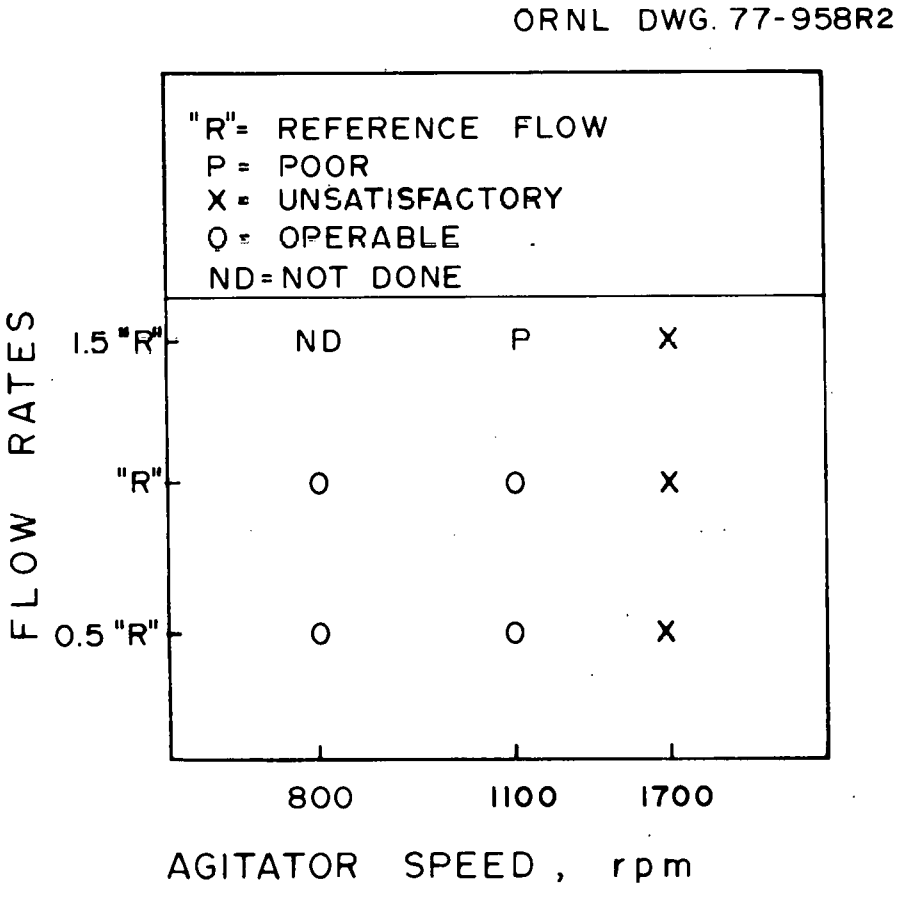

Fig. 1.12. Conclusions on the effects of operating parameters of mixer-settler performance in series S runs.

bank, solid blades in the extraction-scrub bank). Some emulsion was observed at the aqueous-organic interface in the stripping bank in run 1A, while some organic loss to the product stream (CU) was observed in run 2A. Also, uranium stripping was poorer in run 1A than in run 1 (Fig. 1.13). Thus it is concluded that the solid-blade agitators performed more effectively in the stripping bank. The data indicate improvement in the efficiency of the extraction-scrub bank with the split-blade agitators as compared with the solid-blade agitators (80 to 100% vs 75 to 80%). However, since these efficiencies are somewhat qualitative and based on only two runs, a preference for either type of stirrer blades in the extraction-scrub unit cannot be made at this time.

Uranium losses were quite low under the conditions that were determined to be operable, apparently ranging from about 2×10^{-5} to 5×10^{-4} %. The losses in the S series runs are lower than those in the R series runs primarily because of the lower nitric acid concentrations used in stripping.

1.3 Batch Countercurrent Extraction Tests

Extraction and stripping experiments are being carried out to generate distribution coefficient data for the extraction of uranium, plutonium, and key fission products into TBP and to evaluate the feasibility of significantly reducing the amounts of uranium and plutonium in high-level wastes. Distribution coefficient data are necessary to predict the number of stages required for a given recovery value.

1.3.1 Experimental

Batch countercurrent extraction tests employ four extraction stages and four scrubbing stages (Fig. 1.14). The feed stage (No. 4) is considered to be both an extraction stage and a scrubbing stage. We carry out the operations diagrammed in Fig. 1.14 until 16 cycles are completed, which ensures that >99.9% of steady state is attained. On completion of the 16 cycles, stage compositions are equal to those determined for continuous operations. In all extraction tests, the feed solution enters at stage 4, the scrub solution at stage 1, and the extractant at stage 7. The aqueous raffinate exits from stage 7, while the organic extract exits from stage 1. Stripping tests are carried out in a manner similar to that used in the

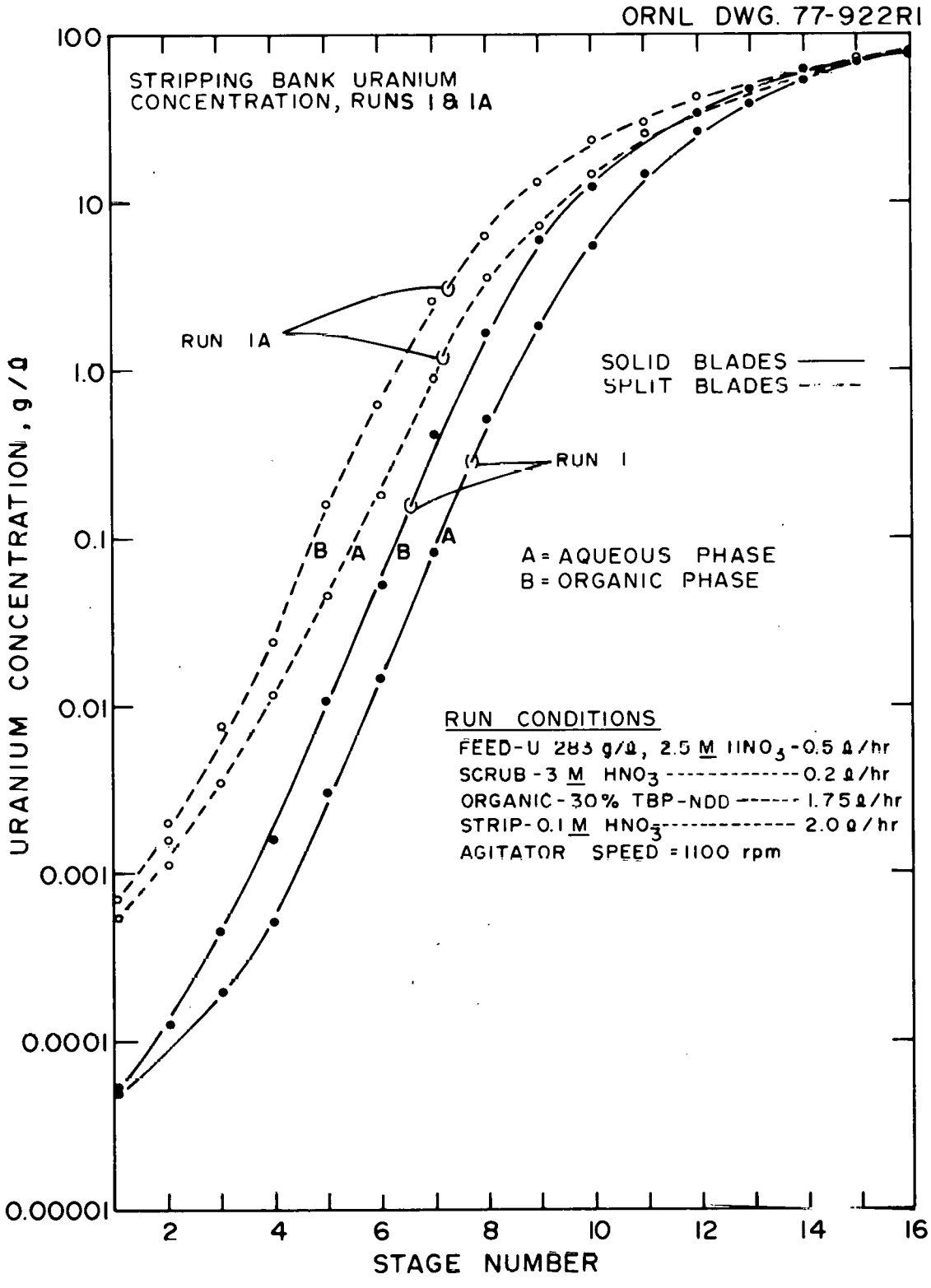

Fig. 1.13. Comparison of uranium concentration profiles in the stripping bank using solid- and split-blade stirrers.

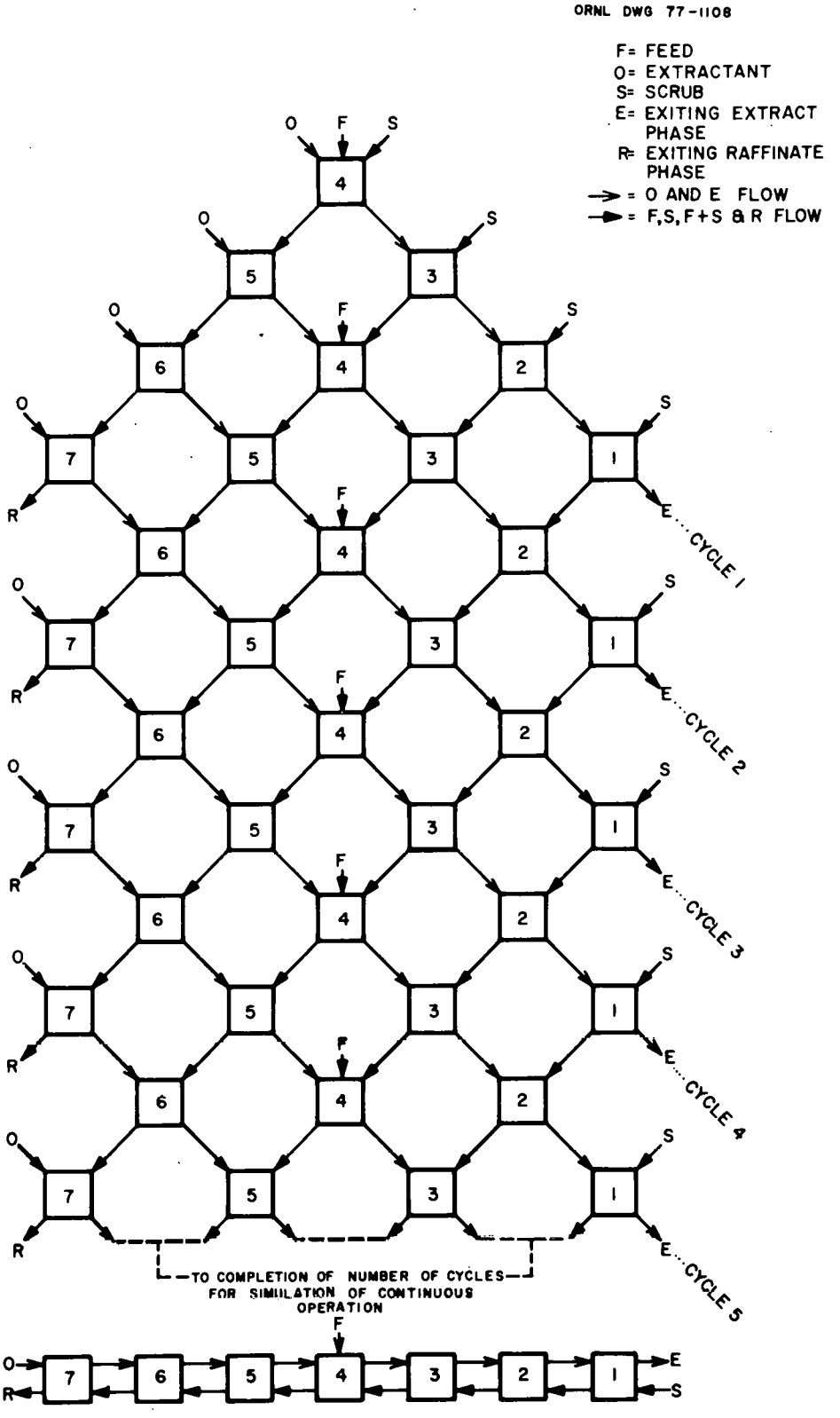

Fig. 1.14. Diagram of operational procedure used in batch countercurrent extraction tests.

extraction-scrub tests. In a few cases, however, less than seven stages were employed. In all our tests, the organic phase entered at the highest-numbered stage and the stripping solution entered at stage 1. This numbering system was used because it is compatible with the computer program for SEPHIS calculations.

The apparatus used in the batch countercurrent tests (see Fig. 1.15) consists of seven 125-ml separatory funnels which are water-jacketed for temperature control. The water jackets are connected in series and require only a single flow intake of heating or cooling water. Two such sets of separatory funnels are utilized. One is located in a laboratory hood for cold work, while the other is located in an alpha glove box for studies involving plutonium extractions.

1.3.2 Uranium

Tests continued to show that four extraction stages and four scrub stages are sufficient to reduce the uranium losses to 0.01%. Seven stages of stripping with 0.3 M HNO_3 using A/O* ratios of 1.7 to 2.2 were insufficient for removing >99.99% of the uranium. Distribution coefficients, $D_A^o(U)$, in the range of 1.5 to 2.0 were obtained by using organic feeds which had uranium concentrations in the range of 15 to 85 g/liter and were 0.2 to 0.4 M in HNO_3. The measured values of $D_A^o(U)$ suggest that 99.99% of the uranium would be stripped using 12 to 16 stages and an A/O ratio of 2. Data obtained with mixer-settler runs (see Sect. 3.3.1) confirm that 16 stages are sufficient.

Previously reported problems related to HNO_3 concentration measurements in the presence of uranium were resolved; however, our accuracy of measuring HNO_3 at concentrations of 0.1 M and below in the organic phase is of the order of ±50%. Samples of stock solutions were submitted weekly over a period of 6 weeks to determine reproducibility of measurements. Table 1.8 gives the average values ($\bar{X}$) and the corresponding standard deviations (σ) for the six samples of each stock solution.

Equilibrium distribution data obtained for the extraction of uranium and HNO_3 in six runs are given in Tables 1.9 and 1.10. Concentrations in the feed ranged from 72 to 316 g of uranium per liter and 1.9 to 2.5 M HNO_3.

---

*A/O designates the aqueous-to-organic volumetric flow ratio.

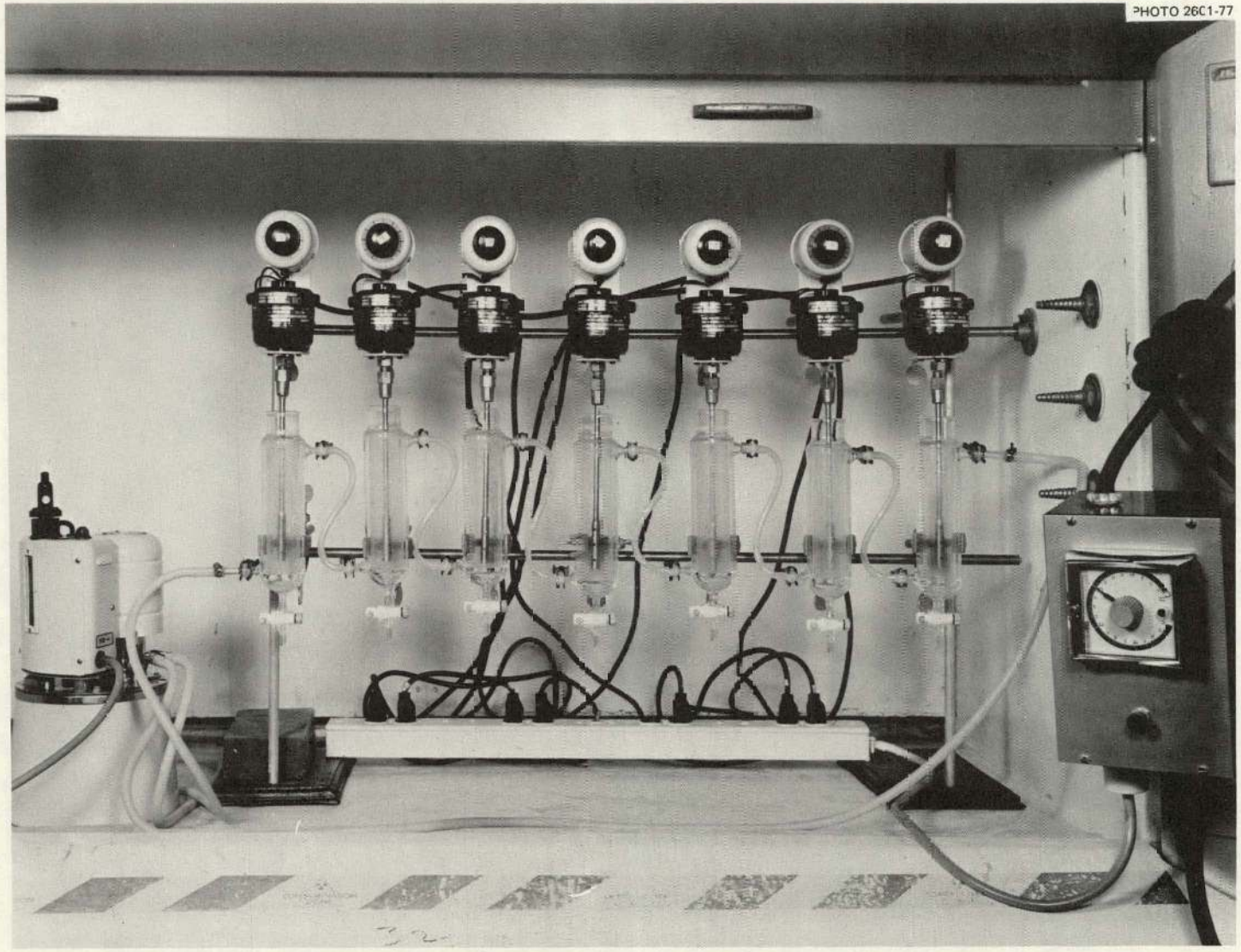

Fig. 1.15. Equipment used for batch countercurrent extraction tests.

Table 1.8. Average values and standard deviations of uranium and nitric acid analyses

	Uranium			HNO_3		
	$\bar{X}$ (g/liter)	σ(U)	%	$\bar{X}$ (M)	$\sigma(HNO_3)$	%
			Aqueous phase			
Stock 1	313.7	0.67	0.2	2.06	0.13	6.3
2	156.6	0.50	0.3	1.04	0.05	4.6
3	95.52	0.65	0.7	2.01	0.03	1.4
4	47.88	0.34	0.7	2.10	0.01	0.6
5	1.56	0.02	1.4	1.98	0.07	3.5
			Organic phase[a]			
Stock 1	108.8	0.64	0.6	0.12	0.04	33
2	54.0	0.39	0.7	0.06	0.02	33
3	0.53	0.006	1.1	0.04	0.023	60

[a] 30% TBP-NDD.

Table 1.9. Batch countercurrent extraction of uranium with 30% TBP

Temp. = 43°C; volume ratio of extractant/feed/scrub = 50/15/10

	Run					
	Q	R	IA	T	AD	AF
Feed composition						
U, g/liter	313	315	316	309	303	72.2
HNO_3, M	2.01	2.20	2.53	2.00	2.04	1.89
Scrub solution						
HNO_3, M	2.70	2.94	3.03	3.10	3.06	2.19
Equilibrium organic, g U/liter						
Stage 1	95.4	96.3	81.4	93.3	87.8	24.8
2	102	99.8	87.2	97.2	89.8	22.0
3	102	105	86.4	94.5	92.5	20.9
4	102	108	85.6	97.2	94.3	21.0
5	28.2	38.9	37.3	10.4	12.8	0.80
6	1.06	1.26	0.20	0.20	0.36	0.004
7	0.051	0.081	0.005	0.021	0.003	0.001
Equilibrium aqueous, g U/liter						
Stage 1	33.3	37.9	22.3	19.0	16.4	2.58
2	46.4	46.5	26.2	25.0	20.2	2.51
3	53.1	54.1	23.4	20.3	22.3	2.19
4	57.0	--	31.7	25.0	22.7	2.64
5	2.55	4.11	6.37	1.14	0.76	0.16
6	0.068	0.097	0.013	0.023	0.014	0.031
7	0.0016	0.021	5×10^{-4}	0.007	<0.001	0.006
D_A^O(U)						
Stage 1	2.86	2.54	3.65	4.92	5.35	9.62
2	2.17	2.15	3.33	3.89	4.44	8.77
3	1.92	1.94	3.69	4.65	4.16	9.53
4	1.78	1.28	2.70	3.90	4.16	7.94
5	11.1	9.46	5.86	9.14	16.9	5.02
6	15.7	13.0	14.8	8.52	25.4	--
7	31.9	3.86	9.8	3.0	>3.4	--
Material balance, %	102	102	86	101	97	114
% loss	9×10^{-4}	1.1×10^{-2}	3×10^{-4}	3.8×10^{-3}	$<6 \times 10^{-4}$	1.4×10^{-2}

Table 1.10. Equilibrium distribution of nitric acid in batch countercurrent extraction tests

	Run[a]					
	Q	R	IA	T	AD	AF
Organic HNO_3, M						
Stage 1	0.19	0.24	0.21	0.28	0.24	0.49
2	0.18	0.24	0.20	0.24	0.23	0.47
3	0.20	0.22	0.22	0.32	0.24	0.43
4	0.21	0.21	0.24	0.28	0.28	0.42
5	0.57	0.54	0.67	0.67	0.60	0.42
6	0.64	0.64	0.58	0.65	0.61	0.35
7	0.45	0.51	0.34	0.50	0.46	0.22
Aqueous HNO_3, M						
Stage 1	2.74	2.89	3.26	3.09	3.02	2.42
2	2.80	2.89	3.41	2.90	2.99	2.24
3	2.52	2.94	3.67	3.15	3.07	2.15
4	3.23	3.14	4.01	3.43	3.32	2.05
5	3.39	3.38	3.69	3.42	3.27	1.74
6	2.96	3.04	2.94	3.15	2.89	1.52
7	2.06	2.20	1.71	2.25	2.01	1.05
$D_A^o(HNO_3) \times 10^{-2}$						
Stage 1	6.9[b]	8.3	6.5	9.1	7.9	20
2	6.4	8.3	5.9	8.3	7.7	21
3	7.9	7.5	6.1	10	7.8	20
4	6.5	6.7	5.9	8.0	8.4	20
5	17	16	18	20	18	24
6	22	21	20	21	21	23
7	21	23	20	22	23	21

[a]See Table 1.9 for run conditions.

[b]Read as 6.9×10^{-2}.

The nitric acid concentration in the scrubbing solution varied from 2.2 to 3.0 M. Uranium losses to the aqueous raffinate varied from about 0.001 to 0.01%. Material balances ranged from 86 to 114% for the five runs. Runs T and AD were nearly identical with regard to conditions, and the variance in $D_A^o(U)$ reflects the precision of the experiments. The $D_A^o(U)$ values determined in stages where the uranium concentration was less than 0.1 g/liter were not reproducible. The $D_A^o(U)$ values for all runs except AF would be expected to be almost identical for stages 5, 6, and 7 because here the HNO_3 concentrations in the organic and aqueous phases are almost identical. Also, the total uranium concentration is low so that the effect of uranium complexing on the free TBP concentration is nearly immeasurable. Further study is required to determine whether the analytical procedure, interstage entrainment, or contamination of samples is involved. Nitric acid concentrations in the organic are nearly constant throughout the scrubbing sections (stages 1 through 4). The $D_A^o(HNO_3)$ values are also nearly constant in both the extraction and scrubbing stages, although they are different in the two sections.

Tests of the stripping of uranium from 30% TBP with 0.2 to 0.4 M HNO_3 using A/O phase ratios of approximately 1.7 to 2.2 showed distribution values in the range of about 1.0 to 2.5 (Table 1.11). The percent of uranium remaining unstripped is determined primarily by the HNO_3 concentration of the strip solution. The HNO_3 concentration of the original 30% TBP feed had little or no effect on HNO_3 concentrations in stages 1 through 4 of the seven-stage stripping tests for initial concentrations of 0.2 to 0.4 M HNO_3. Under the conditions used to obtain the data presented in Table 1.12, about 12 to 16 stages would be required to strip 99.99% of the uranium. Mixer-settler tests (see Sect. 1.2) confirmed that 16 stages are sufficient.

1.3.3 Plutonium

Plutonium losses to the aqueous raffinate were less than 0.01% in extraction tests. Anomalous results were obtained in the reductive stripping of plutonium with 0.3 M HNO_3. Poor stripping apparently resulted from aging phenomena related to the time span between extraction and stripping

Table 1.11. Batch countercurrent stripping of uranium from 30% TBP

	Run				
	K(A)	K	AE	AG	Z
Temperature, °C	25	25	25	43	25
Aqueous/organic ratio	2.20	2.20	1.67	1.67	1.67
Feed concentrations[a]					
U, g/liter	84.3	73.0	64.4	18.6	13.7
Pu, g/liter	*	*	*	*	0.324
HNO_3, M	0.20	0.17	0.29	0.41	0.32
Strip solution acidity					
HNO_3, M	0.30	0.33	0.31	0.30	0.37
Equilibrium organic, g U/liter					
Stage 1	5.45	5.31	4.68	0.118	3.44
2	11.5	10.9	9.58	0.334	5.91
3	21.1	14.3	16.41	0.880	8.19
4	33.1	19.5	23.0	1.890	10.3
5	53.7	23.5	31.3	4.29	12.4
6	b	36.7	42.2	9.09	14.4
7	b	44.4	59.0	17.20	15.9
Equilibrium aqueous, g U/liter					
Stage 1	3.29	1.69	2.50	0.154	1.45
2	7.16	4.39	5.07	0.358	2.67
3	13.5	6.14	9.04	0.850	3.79
4	20.9	13.5	12.5	1.93	4.97
5	36.6	14.0	17.6	4.15	6.07
6	b	21.6	24.8	7.81	6.84
7	b	29.4	30.9	8.50	6.00
D_A^o(U)					
Stage 1	1.66	3.14	1.87	0.77	2.37
2	1.61	2.48	1.89	0.93	2.21
3	1.56	2.33	1.82	1.04	2.16
4	1.58	1.44	1.83	0.98	2.08
5	1.47	1.68	1.78	1.03	2.05
6	b	1.70	1.70	1.16	2.10
7	b	1.51	1.91	2.02	2.65
U material balance, %	102	96	87	77	98
Unstripped U, %	6.5	7.3	7.3	0.6	25

[a]Asterisk denotes where that element is absent.

[b]Five-stage stripping run.

Table 1.12. Equilibrium distribution of nitric acid in batch countercurrent stripping tests

	Run				
	K(A)	K	AE	AG	Z
Organic HNO_3, M					
Stage 1	0.033	0.039	0.06	0.06	0.08
2	0.033	0.034	0.08	0.10	0.07
3	0.030	0.026	0.08	0.08	0.06
4	0.026	0.025	0.08	0.06	0.06
5	0.023	0.028	0.09	0.08	0.07
6	a	0.013	0.10	0.09	0.06
7	a	0.002	0.12	0.12	0.09
Aqueous HNO_3, M					
Stage 1	0.30	0.28	0.33	0.33	0.32
2	0.30	0.27	0.34	0.31	0.38
3	0.31	0.27	0.35	0.31	0.38
4	0.33	0.28	0.36	0.31	0.38
5	0.39	0.28	0.37	0.39	0.38
6	a	0.30	0.38	0.36	0.40
7	a	0.29	0.38	0.58	0.53
$D_A^o(HNO_3) \times 10^{-2}$					
Stage 1	11[b]	14	18	18	21
2	11	13	23	32	18
3	10	10	23	26	16
4	8	9	22	19	16
5	6	10	24	21	18
6	a	4	26	25	15
7	a	0.6	31	20	17

[a] Five-stage stripping run.

[b] Read as 0.11.

experiments. Crosscurrent stripping tests showed that the plutonium stripped normally when there was no appreciable time delay (<2 days) between extraction and stripping.

Results of batch countercurrent extraction tests are shown in Table 1.13. Losses of plutonium to the aqueous raffinate under the conditions used were less than 0.01%. This degree of extraction could be accomplished either in the presence or in the absence of nonradioactive (cold) fission product elements and with uranium saturations of the organic phase as great as 20%. The distribution coefficients decrease in stages 6 and 7 because of the lower HNO_3 concentrations of the aqueous phases of those stages. The HNO_3 extraction by the incoming fresh organic is the greatest in these stages (since organic-phase loading is low) and thus produces lower concentrations of HNO_3 in the corresponding aqueous phases. The concentration profile for plutonium throughout the extraction and scrubbing stages for run X (Fig. 1.16) is representative of the other runs given in Table 1.13.

Plutonium was stripped normally from a 30% TBP phase when the time delay between extractions and stripping was less than about 2 days. The results are summarized in Table 1.14. As shown, the D_A^o(Pu) values increase with increasing aging time of the organic feed solutions in the tests with 0.3 M HNO_3 (runs AC, Y, and AH). Similar behavior is noted in the 0.4 M HNO_3 tests (runs AB and Z). The stripping behavior was essentially normal for feed aged up to 2 days. This was confirmed by carrying out a seven-stage crosscurrent stripping test of a freshly prepared solution of plutonium in 30% TBP (0.437 g of plutonium per liter). Spectrophotometric investigations with the aid of M. H. Lloyd of ORNL are under way to determine whether accelerated hydrolysis of TBP is responsible for the process stripping in aged feed solution.

The sources of the organic feeds were composite, extract phases generated from our extraction runs (see Fig. 1.13, Sect. 3.3.1). These composites were used as feeds for stripping tests in order to save time since the work with plutonium is carried out in a glove box. Extrapolations of literature data to the acidity of our feed solutions indicated that room-temperature hydrolysis of TBP would be too slow to produce significant amounts of

Table 1.13. Batch countercurrent extraction of plutonium with 30% TBP

Volume ratio of extractant/feed/scrub = 50/15/10
Four extraction and four scrubbing stages

	Run			
	S(A)	W	X	AA
Temperature, °C	43	25	43	43
Feed solution[a]				
Pu, g/liter	2.26	2.48	1.49	1.56
U, g/liter	*	*	66	*
Cold FP elements, M	*	*	0.05[c]	0.05[c]
HNO_3, M	2.5	2.5	2.1	2.4
Scrub solution				
HNO_3, M	2.0	2.1	2.2	2.2
Equilibrium organic, g/liter				
Stage 1	0.708	0.758	0.441	0.435
2	0.714	0.781	0.446	0.457
3	0.736	0.803	0.453	0.457
4	0.723	0.778	0.445	0.452
5	3.3×10^{-2}	6.5×10^{-2}	2.3×10^{-2}	0.025
6	2.4×10^{-3}	6×10^{-3}	1.2×10^{-3}	1.0×10^{-3}
7	1.8×10^{-4}	6×10^{-4}	8.4×10^{-5}	1.1×10^{-4}
D_A^o(Pu)				
Stage 1	11.7	7.8	10.0	13.0
2	10.5	7.5	8.6	12.4
3	8.80	6.6	10.1	13.0
4	7.4	7.5	5.1	7.5
5	ND[b]	4.7	10.4	10.5
6	ND	3.0	9.2	7.9
7	ND	ND	6.1	4.4
Pu material balance, %	140	102	101	108
Pu loss, %	0.003	<0.01	0.001	0.003

[a] Asterisk denotes where that element is absent.

[b] Not determined. Alpha pulse analyses on aqueous phases were not sensitive enough to differentiate plutonium from americium and hence determind D_A^o (Pu) with any accuracy. In runs X and AA, extraction with thenoyltrifluoroacetone (TTA) were utilized to separate and to measure the plutonium.

[c] Corresponds to 33,000 MWd/tonne of burnup of LWR fuel.

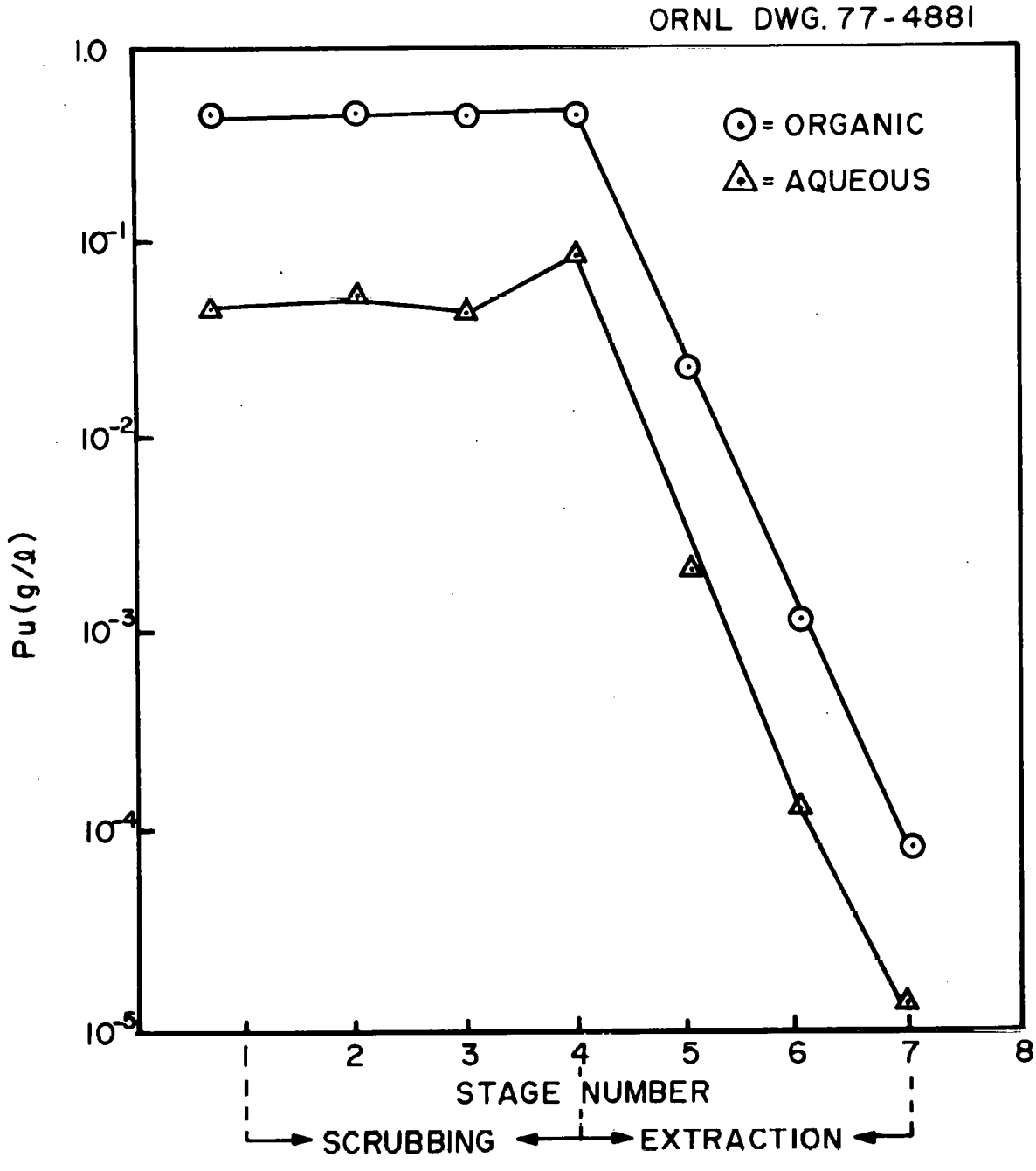

Fig. 1.16. Concentration profile of plutonium in batch countercurrent extraction (run X).

Table 1.14. Batch countercurrent stripping of plutonium from aged 30% TBP extracts

Organic feed enters stage 7

	Run				
	AC	AB	Y	Z	AH
Aqueous/organic ratio	1.67	1.67	2.00	1.67	2.00
Temperature, °C	25	25	25	25	43
Feed solution[a]					
Pu, g/liter	1.64	0.448	0.409	0.324	0.725
U, g/liter	*	*	19.0	13.7	*
HNO_3, M	0.08	0.53	0.43	0.32	0.22
Aging time, days	2	5	6	26	35
Strip solution					
HNO_3, M	0.29	0.44	0.28	0.37	0.29
D^{o}_{A}(Pu)					
Stage 1	3.6	5.4	15.2	21.4	20.5
2	2.4	4.2	5.7	9.4	17.1
3	2.3	3.0	3.4	5.7	11.9
4	1.5	2.0	1.7	3.9	6.0
5	0.84	1.6	4.4	3.1	4.4
6	0.61	1.5	0.6	2.3	1.9
7	0.56	0.1	0.1	2.6	1.1
Pu material balance, %	87	83	78	102	113
Pu unstripped, %	0.4	12	4	38	31

[a]Asterisk denotes where that element is absent.

dibutyl phosphoric acid. The results of our studies, when completed, may have implications with regard to minimum holdup times in stripping operations, particularly in the plutonium purification cycles.

1.3.4 Comparison of experimental distributions of uranium, plutonium, and nitric acid with values calculated by the SEPHIS code

SEPHIS calculations of the distributions of uranium, plutonium, and HNO_3 in several of our batch countercurrent extraction and stripping runs (Tables 1.15-1.17) were performed by R. H. Rainey of ORNL. Experimental results for uranium distributions agreed reasonably well with the calculated values with respect to trends in the data and to the magnitude of concentrations. Although not shown for the uranium runs, the calculated values of HNO_3 distribution in the extraction and stripping agreed reasonably well with experimental values, except for the organic-phase concentrations in the stripping runs. In the stripping runs, the HNO_3 concentrations in the organic phase are below 0.1 M, where experimental errors are most significant (see Tables 1.8 and 1.12).

Calculations of plutonium distributions also agreed reasonably well with observed values, particularly in stages 4 through 7 (Table 1.17). The distribution coefficient for plutonium, $D_A^{\circ}(Pu)$, decreased substantially from stage 4 to stage 7, primarily because of the lower concentration of HNO_3 in these stages. The extractant (30% TBP preequilibrated with 0.01 M HNO_3) enters at stage 7, where HNO_3 extraction is greatest; extraction of HNO_3 gradually decreases down to the feed stage (stage 4).

It is perhaps fortuitous that SEPHIS calculations predicted the concentrations of uranium and plutonium reasonably well in the last extraction or stripping stage. An accurate prediction for product losses should be possible for a given number of stages if the SEPHIS calculations are applicable over a wide range of concentrations and combinations of uranium, plutonium, and HNO_3. Further comparisons of SEPHIS calculations with data from experimental runs on the coextraction and costripping of uranium and plutonium are planned.

Table 1.15. Comparison of experimental distribution of uranium (g/liter) in extraction runs with values calculated by the SEPHIS code

	Stage number						
	1	2	3	4	5	6	7
Run AF							
Aqueous phase							
Exptl.	2.58	2.51	2.19	2.64	0.16	0.031	0.006
SEPHIS	2.05	2.13	2.16	2.19	0.090	4.4×10^{-3}	3.4×10^{-4}
Organic phase							
Exptl.	24.8	22.0	20.9	21.0	0.80	4.0×10^{-3}	1.0×10^{-3}
SEPHIS	21.2	21.6	21.6	21.6	1.06	4.3×10^{-2}	2.0×10^{-3}
Run AD							
Aqueous phase							
Exptl.	16.4	20.2	22.3	22.7	0.76	0.014	$<1.0 \times 10^{-3}$
SEPHIS	20.1	25.0	26.0	25.3	0.40	5.8×10^{-3}	1.3×10^{-4}
Organic phase							
Exptl.	87.8	89.8	92.5	94.3	12.8	0.36	3.4×10^{-3}
SEPHIS	87.3	91.1	92.0	92.2	12.1	0.19	2.7×10^{-3}

Table 1.16. Comparison of experimental distribution of uranium (g/liter) in stripping runs with values calculated by the SEPHIS code

	Stage number						
	1	2	3	4	5	6	7
Run AE							
Aqueous phase							
Exptl.	2.50	5.07	9.04	12.5	17.6	24.9	30.9
SEPHIS	3.66	7.84	12.5	17.6	23.6	30.9	35.2
Organic phase							
Exptl.	4.68	9.58	16.4	23.0	31.3	42.2	59.0
SEPHIS	4.99	11.3	18.4	26.3	35.0	45.2	57.6
Run AG							
Aqueous phase							
Exptl.	0.15	0.36	0.85	1.93	4.15	7.81	8.50
SEPHIS	0.20	0.64	1.55	3.34	6.43	10.0	10.9
Organic phase							
Exptl.	0.12	0.33	0.88	1.89	4.29	9.09	17.2
SEPHIS	0.15	0.49	1.24	2.80	5.84	11.08	18.2

Table 1.17. Comparison of experimental distribution of plutonium and nitric acid in extraction run AA with values calculated by the SEPHIS code

	Stage number						
	1	2	3	4	5	6	7
Plutonium, g/liter							
Organic phase							
Exptl.	0.435	0.457	0.457	0.452	0.025	1.0×10^{-3}	1.1×10^{-4}
SEPHIS	0.459	0.469	0.469	0.469	0.026	1.6×10^{-3}	1.0×10^{-4}
Aqueous phase							
Exptl.	0.0334	0.0368	0.0351	0.0601	0.0024	1.3×10^{-4}	2.5×10^{-5}
SEPHIS	0.0538	0.0544	0.0537	0.0531	0.0032	2.4×10^{-4}	2.9×10^{-5}
Nitric acid, M							
Organic phase							
Exptl.	0.61	0.58	0.59	0.57	0.54	0.44	0.30
SEPHIS	0.50	0.50	0.51	0.51	0.48	0.42	0.28
Aqueous phase							
Exptl.	2.36	2.34	2.38	2.32	2.14	1.90	1.34
SEPHIS	2.22	2.24	2.25	2.26	2.14	1.88	1.32
D_A^O(Pu)							
Exptl.	13	12.4	13.0	7.5	10.5	7.9	4.4
SEPHIS	8.5	8.7	8.7	8.9	8.2	6.5	3.6

1.4 References for Section 1

1. S. B. Watson and R. H. Rainey, Modifications of the SEPHIS Code for Calculating the Purex Solvent Extraction System, ORNL/TM-5123 (December 1975).

2. J. T. Long, Engineering for Nuclear Fuel Reprocessing, p. 393, Gordon and Breach Science Publishers, Inc., New York, 1967.

2. ACTINIDE RECOVERY FROM SOLIDS

E. L. Lewis and D. F. Luthy (Mound Laboratory)

The objective of this task is to measure the ability to decontaminate solids using reagents which are compatible with the reprocessing and refabrication flowsheets. The initial studies focus on the ability to decontaminate HEPA filters.

2.1 Experimental Work

2.1.1 Adsorption studies

The decontamination of HEPA filters is a complex process involving several phenomena. Actinides may be dissolved by a leaching reagent, but then adsorbed by a solid matrix in the mixture. If the latter effect occurs, it could limit the overall decontamination factor (DF) and should be considered in the conceptual design.

Initially, two types of plutonium dissolution tests were conducted with 8 M HNO_3 to determine if adsorption effects by the filter material could be observed. In one, PuO_2* was placed in the acid at boiling temperature. In the other, contaminated filter medium was added to the boiling acid. In both tests, samples were taken and filtered through a 4-μ Pyrex filter. The resulting percentage of plutonium in the aqueous phase (a sparkling clear solution) was measured as a function of time by the alpha activity in the acid.

The results of these initial scouting tests are shown in Fig. 2.1. The small number of observations and the large scatter make it difficult to determine if any difference in the dissolutioning rates (i.e., the slopes of the lines) resulted from the addition of the filter material; however, a slight shift downward in the percentage of plutonium in the aqueous phase after extended heating appears to have occurred. These tests suggested, therefore, that some of the plutonium was adsorbing on the filter material.

---

*The PuO_2 was a mixture of 80 wt % ^{238}Pu, 16 wt % ^{239}Pu, 2.5 wt % ^{240}Pu, 0.2 wt % ^{242}Pu, and small amounts of other actinides calcined at 750°C. The average particle size was about 20 μ.

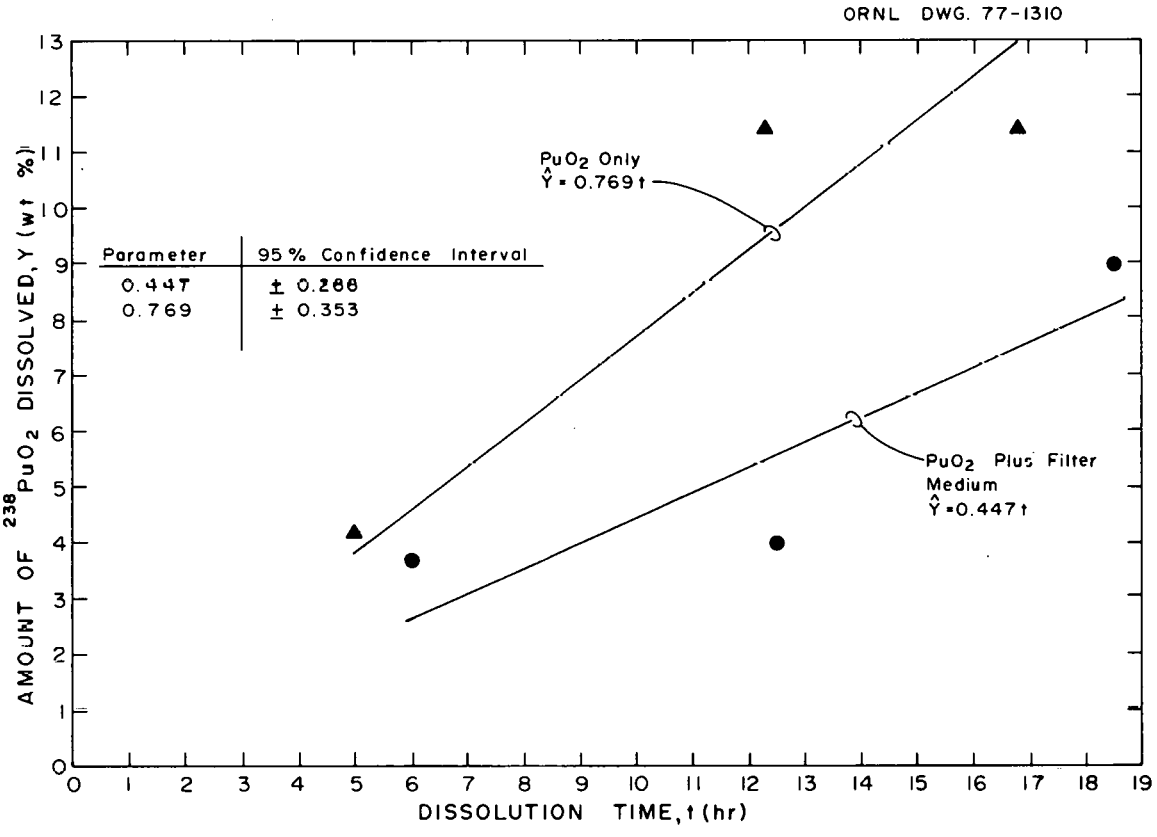

Fig. 2.1. Effect of presence of filter material on the dissolutioning of PuO_2 in 8 M HNO_3.

Consequently, plutonium adsorption isotherms were developed to determine the magnitude of this effect more accurately and assess its possible significance in limiting the ultimate DF which could be achieved.

Adsorption isotherms were determined for Pu-HNO_3 and Pu-HNO_3-HF systems. A stock plutonium solution was prepared by filtering an aqueous plutonium solution produced by refluxing the plutonium in 8 M HNO_3. Aliquots were subsequently withdrawn from the stock solution to make up standard plutonium solutions using conventional volumetric flasks and the desired acid strength. Filter material was shredded and ball-milled to less than 40 mesh. An adsorption test was performed by mixing 1 g of the uncontaminated, shredded filter material with 100 ml of a standard plutonium solution, stirring the mixture magnetically for several hours, and allowing the system to equilibrate overnight. A blank sample was run without filter material to correct for adsorption on the test beakers. All tests were performed at ambient temperature (∿20°C).

After equilibration had been achieved in each test, the aqueous-phase volume was measured; then the solution was filtered and the plutonium concentration in the filtrate measured by alpha counting. The variable X (milligrams of ^{238}Pu adsorbed) was obtained by differencing the apparent change in plutonium concentration in the aqueous phase and correcting for any volume changes.

In many adsorption studies, the solid phase is chemically inert and does not react appreciably with the fluid phase. In these systems, however, some of the filter material is dissolved by the acids; thus this effect should be considered. For example, after extended periods of mixing, ∿30 wt % of the filter material dissolves in 8 M HNO_3 and ∿50 wt % dissolves in 8 M HNO_3-0.1 M HF.

Consequently, the solid mass is reduced during an adsorption test until the acid is depleted and chemical equilibrium is attained. This effect is taken into account simply by measuring the final solid weight at the end of the experiment. Thus, the resulting solid mass was filtered, washed, and dried. Since firing at 1000°C had only a small effect on the final weight compared with the drying step, the weight of the dried solids was used for

the variable m (final milligrams of HEPA material after correcting for the analytical filter ash).

Figure 2.2 shows a comparison of the adsorption of plutonium by the HEPA filter medium in 8 M HNO_3 vs 8 M HNO_3-0.1 M HF. The ordinate is X/m as calculated from the variables defined above. The abscissa, C, is the final ^{238}Pu concentration expressed as milligrams per milliliter of solution. The Freundlich equation[1] relates X/m and C as follows:

$$X/m = kC^{1/n} , \tag{2.1}$$

or

$$\log(X/m) = \log (k) + (1/n)\log (C) . \tag{2.2}$$

The plot of log(X/m) vs log(C) should, therefore, be linear with a slope of 1/n and an intercept of log(k). This relationship appears to be valid for the 8 M HNO_3 system over the small concentration range that has been examined. The addition of HF apparently reduces the adsorption over this same concentration range. Experimental results indicate, however, that even for the HNO_3 system this adsorption effect is relatively small compared with the large effects of leachant compositions on the resulting percentage of plutonium dissolved (see Sect. 2.1.2). One additional point has been evaluated for the HNO_3-$(NH_4)_2Ce(NO_3)_6$ system; it lies between the HNO_3 and HNO_3-HF plots.

2.1.2 Effects of aqueous reagent composition on dissolution of PuO_2 from synthetic wastes

Contaminated HEPA filter material was prepared by mixing PuO_2 powder with shredded filter material. The ^{238}Pu concentration in the mixture was 11 mg per cubic centimeter of prepared medium. Small samples of this prepared mixture (~3 g) were added to glass beakers containing 250 ml of the leaching solution. All tests were performed at boiling temperature. Samples were withdrawn periodically and the ^{238}Pu concentration of the solution determined after filtration of the aliquot. The contents of the beakers were stirred every 2 hr. The volume and the concentration of the solution were kept constant by adding acid of proper concentration in order to replace that lost by evaporation.

ORNL DWG. 77-1331

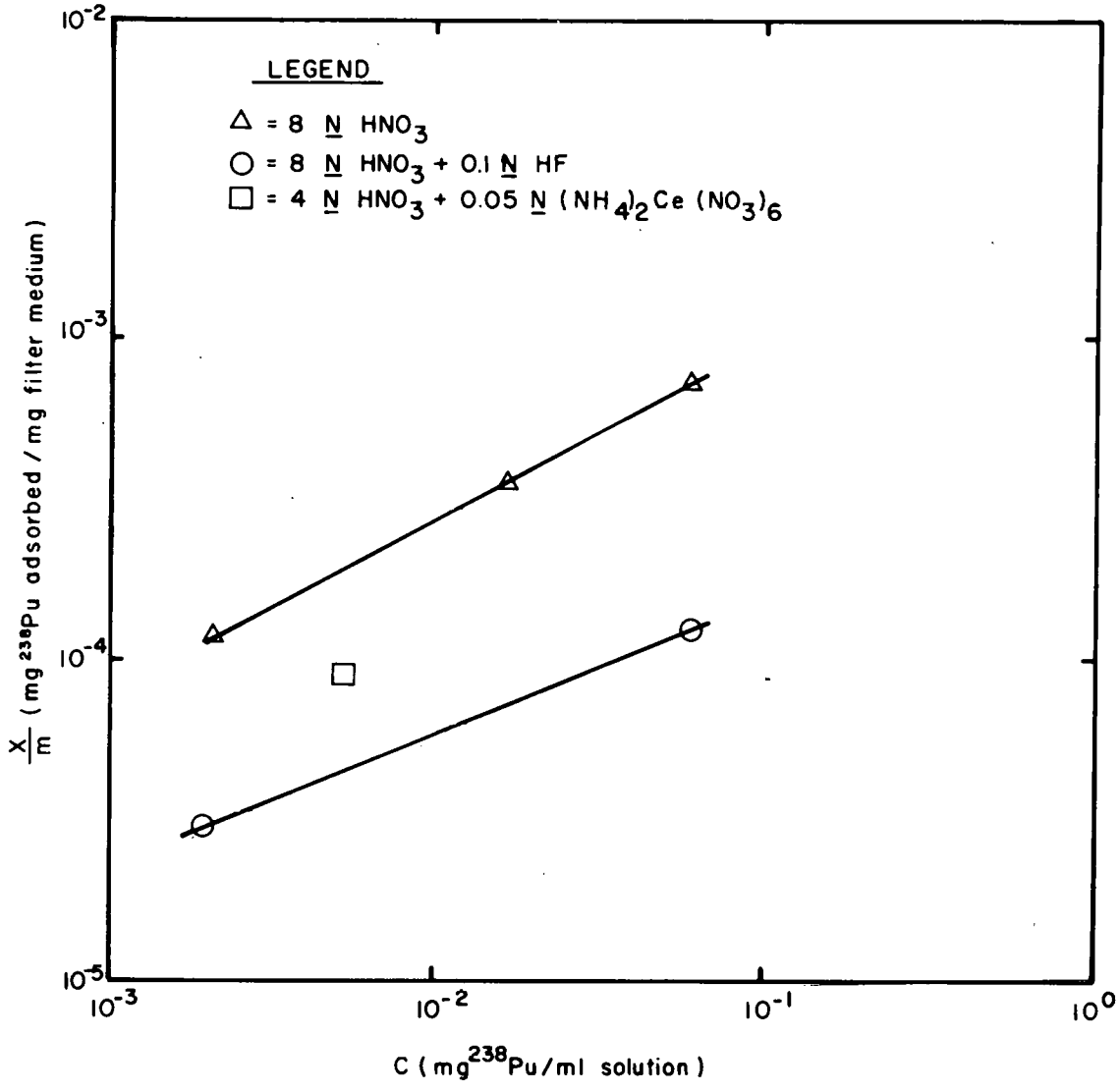

Fig. 2.2. Adsorption of plutonium by filter medium in HNO_3, HNO_3-HF, and HNO_3-Ce(IV).

Table 2.1 lists the results from these tests as observed for various reagent mixtures. The results for the acid mixtures are plotted in Fig. 2.3; the data shown in Fig. 2.1 are also plotted in Fig. 2.3. In analyzing the data shown in Fig. 2.1, a time trend was assumed to occur. In Fig. 2.3, the same data were analyzed using the assumption that the system was at chemical equilibrium throughout the sampling period. Comparison of these two figures indicates that the adsorption effect described above is relatively small compared with the effect of reagent composition on the percentage of plutonium dissolved.

Under the chemical equilibrium hypothesis, the data are analyzed simply by calculating the means and standard deviations for the samples. Although some time dependence of the percentage dissolved exists initially, this dependence does not appear to be statistically significant during the sampling period; hence it has been neglected in favor of the equilibrium hypothesis. In addition, the data for different reagent mixtures were pooled when a statistical difference between the two sample means did not appear to exist, based on a simple t-test. Consequently, in Fig. 2.3, the dissolutioning data for all runs containing either 0.1 or 0.05 N HF have been pooled. Also, since no significant effect for adding 0.1 N vs 0.5 N H_2SO_4 appears to exist, these data were pooled.

Comparison of the sample means shown in Fig. 2.3 indicates that the presence of fluoride ion has the largest effect. Sulfuric acid appears to enhance the dissolutioning of refractory plutonium, compared with nitric acid alone, but this effect is also limited.

A similar analysis was performed for the dissolutioning data obtained by adding varying amounts of ceric ammonium nitrate. These results (see Fig. 2.4) clearly show that the cerium enhancement effect is about the same order of magnitude as that observed for HF.

The dissolutioning reaction mechanism for dissolving refractory plutonium oxide in HNO_3-Ce^{4+} solutions is probably as shown in Eqs. (2.3) and (2.4):

$$2Ce^{4+} + 2e^- \rightleftarrows 2Ce^{3+} \qquad (2.3)$$

$$Pu^{4+} \rightleftarrows Pu^{6+} + 2e^- \qquad (2.4)$$

Table 2.1. Dissolution of PuO_2 with various reagents in aqueous systems

Acid test number	Reagent composition	Time heated (hr)	PuO_2[a] dissolved (wt %)
19-1	4 N HNO_3-0.05 M CAN[b]	5.75	42.9
19-2	4 N HNO_3-0.05 M CAN	12.25	41.4
19-3	4 N HNO_3-0.05 M CAN	18.75	38.5
20-1	8 N HNO_3-0.1 N H_2SO_4	5.75	14.4
20-2	8 N HNO_3-0.1 N H_2SO_4	12	12.7
20-3	8 N HNO_3-0.1 N H_2SO_4	18	15.9
21-1	12 N HNO_3-0.1 N HF-0.1 N H_2SO_4	4.75	115.2
21-2	12 N HNO_3-0.1 N HF-0.1 N H_2SO_4	10.50	107.1
22-1	12 N HNO_3-0.1 N HF	1.75	87.0
22-2	12 N HNO_3-0.1 N HF	6.75	94.1
22-3	12 N HNO_3-0.1 N HF	11.50	107.9
25-1	4 N HNO_3-0.005 M CAN	2.25	11.1
25-2	4 N HNO_3-0.005 M CAN	7.75	13.4
25-3	4 N HNO_3-0.005 M CAN	13.25	11.9
25-A-1	4 N HNO_3-0.005 M CAN-$KMnO_4$	3	13.4
25-A-2	4 N HNO_3-0.005 M CAN-$KMnO_4$	8.50	18.9
25-A-3	4 N HNO_3-0.005 M CAN-$KMnO_4$	14.75	26.3
26-1	12 N HNO_3-0.01 N HF	1.75	31.6
26-2	12 N HNO_3-0.01 N HF	7.25	41.0
26-3	12 N HNO_3-0.01 N HF	12.75	40.9
27-1	12 N HNO_3-0.1 N H_2SO_4-0.01 N HF	1.25	30.1
27-2	12 N HNO_3-0.1 N H_2SO_4-0.01 N HF	6.75	33.1
27-3	12 N HNO_3-0.1 N H_2SO_4-0.01 N HF	12.25	36.3
28-1	12 N HNO_3-0.01 N H_2SO_4-0.1 N HF	1	96.3
28-2	12 N HNO_3-0.01 N H_2SO_4-0.1 N HF	6.50	100.9
28-3	12 N HNO_3-0.01 N H_2SO_4-0.1 N HF	12	101.8
29-1	8 N HNO_3-0.5 N H_2SO_4	5.50	15.8
29-2	8 N HNO_3-0.5 N H_2SO_4	10.75	17.4
29-3	8 N HNO_3-0.5 N H_2SO_4	15.25	17.4
30-1	12 N HNO_3-0.05 N HF-0.01 N H_2SO_4	3	95.9
30-2	12 N HNO_3-0.05 N HF-0.01 N H_2SO_4	8.25	88.0
30-3	12 N HNO_3-0.05 N HF-0.01 N H_2SO_4	14.50	97.7
31-1	4 N HNO_3-0.1 M CAN	3	87.7
31-2	4 N HNO_3-0.1 M CAN	8.25	88.0
31-3	4 N HNO_3-0.1 M CAN	14.25	80.6
32-1	8 N HNO_3-$K_2S_2O_8$	3	0.86
32-2	8 N HNO_3-$K_2S_2O_8$	7.50	0.82
32-3	8 N HNO_3-$K_2S_2O_8$	13.50	1.89
33-1	4 N HNO_3+0.15 M CAN	5.25	98.1
33-2	4 N HNO_3+0.15 M CAN	11.25	99.1
33-3	4 N HNO_3+0.15 M CAN	17.5	93.5

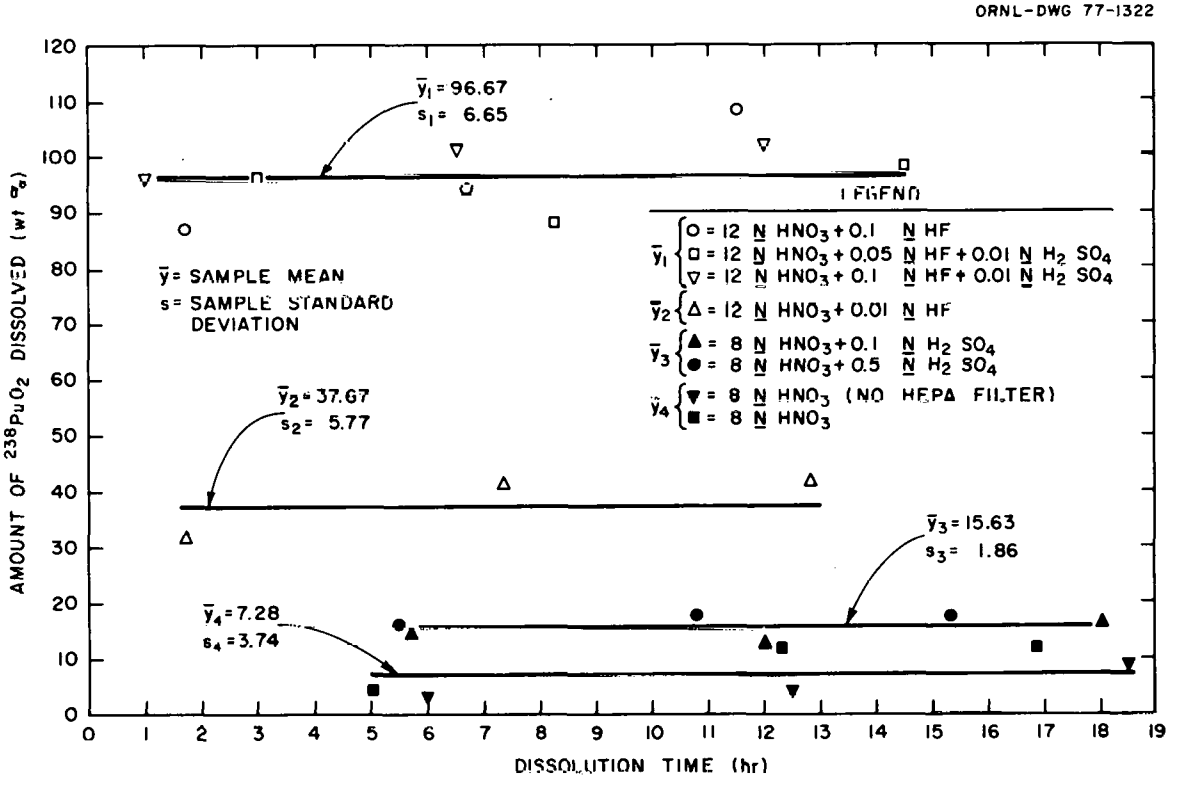

Fig. 2.3. Effect of various acid mixtures on wt % PuO_2 dissolved in the presence of shredded HEPA filters.

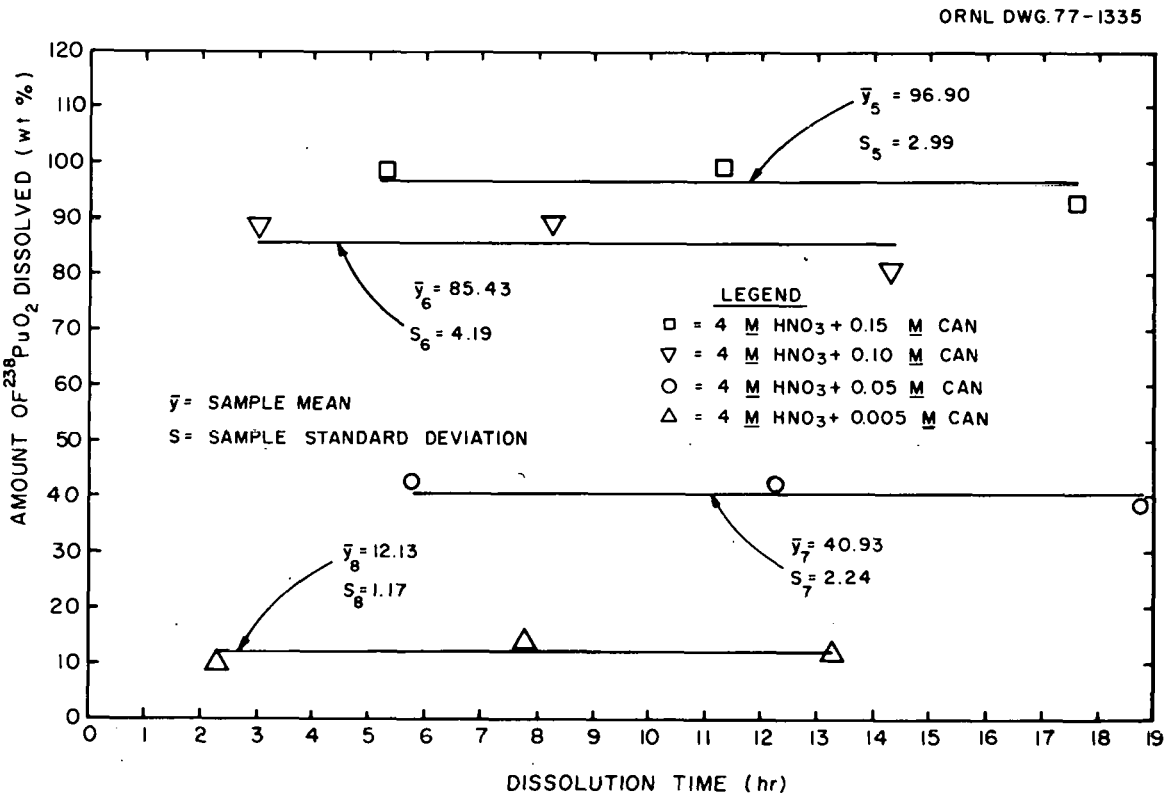

Fig. 2.4. Effect of the initial ceric ion concentration on the percent of PuO_2 dissolved in the presence of shredded HEPA filters.

Because stoichiometric quantities of Ce^{4+} are required for complete dissolution of the PuO_2, large amounts of Ce^{4+} are required to dissolve large quantities of PuO_2. Therefore, it would seem advantageous to use small amounts of Ce^{4+} and then add oxidizing compounds to reoxidize the Ce^{3+} to Ce^{4+}. An example of this would be the addition of $KMnO_4$ to the depleted solution. In the resulting reaction, the permanganate would be reduced and the depleted cerium would be reoxidized; that is,

$$3Ce^{3+} \rightleftarrows 3Ce^{4+} + 3e^{-} \quad , \tag{2.5}$$

$$Mn'^{+} + 3e^{-} \rightleftarrows Mn^{4+} \quad , \tag{2.6}$$

where 1 mole of manganese oxidizes 3 moles of cerium. This approach was used in acid tests 25 and 25A (see Table 2.1). Approximately 1 g of $KMnO_4$ was added to a depleted 4 N HNO_3-0.005 M $(NH_4)_2Ce(NO_3)_6$ solution and the solution heated an additional 15 hr. During this period of time, the amount of dissolved PuO_2 increased significantly from 12 wt % in the depleted solution to 26 wt % in the regenerated solution. This method does, however, add manganese and potassium to the dissolved salts of the waste stream.

2.1.3 Plutonium dissolution from actual HEPA glove-box filter material using aqueous reagents

Small test samples of ∿3 g each were removed from an actual glove-box filter contaminated with PuO_2*. Each sample contained ∿55 mg of ^{238}Pu. The samples were placed in a glass beaker containing 100 ml of the leaching reagent — either 4 N HNO_3-0.1 M $(NH_4)_2Ce(NO_3)_6$ or 12 N HNO_3-0.05 N HF-0.01 N H_2SO_4. The tests were performed at boiling temperature. The contents of the beakers were stirred every hour, and samples were withdrawn periodically for filtration and plutonium analysis. The volume and the acid concentration of the solution were kept constant by adding acid of proper concentration in order to replace that lost by evaporation. The results obtained in these experiments are summarized in Table 2.2. The amount of

---

*The same type of oxide as described in Sect. 2.1.1.

Table 2.2. Dissolution of small samples of actual HEPA filters

Acid test number	Reagent composition	Time heated (hr)	PuO_2 dissolved (wt %)	Liters of acid per gram ^{238}Pu
3265-3A	4 N HNO_3-0.1 M CAN[a]	3.5	103.2	1.84
3265-3B	4 N HNO_3-0.1 M CAN	5	103.3	1.84
3265-3C	4 N HNO_3-0.1 M CAN	11.75	81.9	1.84
3265-3D	4 N HNO_3-0.1 M CAN	14.75	81.5	1.84
3265-4A	12 N HNO_3-0.05 N HF-0.01 N H_2SO_4	3.5	96.9	1.83
3265-4B	12 N HNO_3-0.05 N HF-0.01 N H_2SO_4	5	89.1	1.83
3265-4C	12 N HNO_3-0.05 N HF-0.01 N H_2SO_4	12.5	93.9	1.83

[a]Abbreviation for ceric ammonium nitrate.

PuO_2 dissolved averaged 92.5 wt % using 4 N HNO_3-0.1 M $(NH_4)_2Ce(NO_3)_6$ and 93.3 wt % using 12 N HNO_3-0.05 N HF-0.01 N H_2SO_4. These percentages compare well with those found for the dissolution of simulated filter samples (85.4 and 93.9 wt % respectively).

Larger samples (40 g) of an actual HEPA filter were treated with 12 N HNO_3-0.05 N HF-0.01 N H_2SO_4. These experiments were conducted similarly to those previously described (using 3-g samples) except that different ratios of acid volume (liters) to ^{238}Pu weight (grams) were used. Also, the filter medium was processed through several successive, identical stages in an attempt to obtain the greatest overall DF (see Table 2.3). An acid volume/PuO_2 weight ratio of 0.67 yields a 99.35% dissolution in five stages. On the other hand, a volume/weight ratio of 2.35 produces a 99.53% dissolution in three stages. Thus we have a DF of 154 for the smaller volume/weight ratio and 213 for the higher ratio. These final dissolution percentages and DFs were determined by calorimetry and gamma counting* of the final filter media residues. All other dissolution percentages and DFs were determined by alpha counting of solution samples.

A possible explanation for the fact that a larger acid volume to PuO_2 weight ratio increases the extent of dissolution is thought to be as follows: The HF in the leaching solution is reacting with both PuO_2 particles and glass present in the filter material. When a small amount of leachant is added to a relatively large amount of contaminated fiberglass filter, the F^- concentration of the solution is quickly depleted as SiF_4 gas is produced. The remaining HF is not sufficient to dissolve 90% of the PuO_2 present, as desired. Conversely, if a large amount of leachant is added to the same amount of contaminated filter, sufficient HF is present to react with the glass and dissolve 90% (or greater) of the PuO_2. What is needed, therefore, is a larger amount of HF in the first stage of the process. This could be accomplished by using a larger volume of 12 N HNO_3-0.05 N HF-0.01 N H_2SO_4 or a higher concentration of HF in the acid mixture. For the subsequent

---

*After being water washed and dried, the filter residues were assayed for plutonium content using an alpha decay colorimeter and gamma counting.

Table 2.3. Multistage dissolution of large samples of actual HEPA filters

Acid test number	Reagent composition	Stage	Cumulative wt % PuO_2 dissolved	Liters of acid per gram ^{238}Pu	Time heated (hr)
3265-7-1	12 N HNO_3-0.05 N HF-0.01 N H_2SO_4	1	84.9	0.67	3.5
3265-7-2	12 N HNO_3-0.05 N HF-0.01 N H_2SO_4	2	88.9	0.67	5.25
3265-7-3	12 N HNO_3-0.05 N HF-0.01 N H_2SO_4	3	93.3	0.67	5.75
3265-7-4	12 N HNO_3-0.05 N HF-0.01 N H_2SO_4	4	95.8	0.67	7.25
3265-7-5	12 N HNO_3-0.05 N HF-0.01 N H_2SO_4	5	99.35	0.67	6.5
3265-9-1	12 N HNO_3-0.05 N HF-0.01 N H_2SO_4	1	94.2	2.35	10.5
3265-9-2	12 N HNO_3-0.05 N HF-0.01 N H_2SO_4	2	97.6	2.35	10.75
3265-9-3	12 N HNO_3-0.05 N HF-0.01 N H_2SO_4	3	99.53	2.35	7

stages, a HF concentration of 0.05 N should be sufficient since most of the glass has reacted.

2.1.4 Plutonium recovery by salt fusion

Sodium carbonate and Na_2CO_3-KNO_3 fusions were completed using PuO_2*-contaminated filters. Small samples were prepared by thoroughly mixing 0.1 g of PuO_2 and 1.5 g of filter material. Approximately 13 g of salt (Na_2CO_3 or Na_2CO_3-KNO_3) and 1.5 g of contaminated filter were placed in a platinum crucible, mixed thoroughly, and heated slowly to 950°C. The crucible and its contents were maintained at 950°C for 1 hr before being allowed to cool slowly to ambient temperature. The cooled melt was then removed from the crucible and dissolved in 4 M HNO_3. The acid was maintained at boiling temperature for at least 1 hr and subsequently sampled for ^{238}Pu concentration.

Table 2.4 tabulates the results achieved in these fusion experiments. As can be seen, the maximum dissolution obtained was 71% using a salt mixture of Na_2CO_3-30 wt % KNO_3. When the percent PuO_2 dissolved is plotted as a function of KNO_3 concentration, the solubility dependence appears to be linear between 0 and 16% KNO_3 and then levels off at higher KNO_3 concentrations. The acid concentration was increased to 8 N and the heating time increased to 7 hr with little increase (2%) in the amount of PuO_2 dissolved. Such results confirm what we had suspected, that is, that the PuO_2 had not been converted to a compound which was readily soluble in nitric acid. Also, because of time limitations, only three Na_2CO_3-KNO_3 fusions were performed and the maximum weight percent KNO_3 used was 30%. If time permits, more fusions will be completed next quarter using higher concentrations of KNO_3. It should be noted that the greater the weight percent of KNO_3 in the fusion matrix, the more vigorous the reaction.

The 71% recovery obtained using Na_2CO_3-30% KNO_3 is considered unsatisfactory for our purposes. The extent of dissolution must be greater than 90% in order to achieve large DFs, and this goal might be achieved by using KNO_3 concentrations greater than 30%.

---

*The same type of oxide as described in Sect. 2.1.1.

Table 2.4. Na_2CO_3-KNO_3 fusion of PuO_2

Fusion test number	Salt composition (wt %)	Time heated (hr)	Operating temperature (°C)	PuO_2 solubilized (wt %)
Pu-38	100% Na_2CO_3	1	950	8.83
Pu-39	Na_2CO_3-8% KNO_3	1	950	27.8
Pu-40	Na_2CO_3-16% KNO_3	1	950	48.7
Pu-41	Na_2CO_3-30% KNO_3	1	950	71.0

2.1.5 PuO_2-75 wt % UO_2 solid solution studies

The solid solution used in these studies was composed of plutonium and ^{238}U oxides which had been fired at 1600°C in a reducing atmosphere. A total of six dissolution tests were performed; the results are summarized in Table 2.5. The powdered PuO_2-UO_2 solid solution was mixed thoroughly with shredded filter material using a ratio of 1 g of solid solution to 12 g of filter. A small sample of the mixture (~3 g) was added to a glass beaker containing 250 ml of leaching solution. Samples were withdrawn periodically, filtered, and the percentage solid solution dissolved was determined. The volume and the concentration of the solution were kept constant by adding acid of proper concentration in order to replace that lost by evaporation.

As can be seen in Table 2.5, four reagents were successful in dissolving greater than 93% of the PuO_2-UO_2 in 2 hr. These were 12 N HNO_3-0.1 N HF, 12 N HNO_3-0.05 N HF-0.01 N H_2SO_4, 4 N HNO_3-0.1 M $(NH_4)_2Ce(NO_3)_6$, and 8 N HNO_3. Both the 4 N HNO_3 and the 4 N HNO_3-0.1 N H_2SO_4 were unsuccessful in providing a 90% dissolution even when leaching times of 7 hr were used. Therefore, it can be concluded that 8 N HNO_3, 12 N HNO_3-0.1 N HF, 12 N HNO_3-0.05 N HF-0.01 N H_2SO_4, and 4 N HNO_3-0.1 M $(NH_4)_2Ce(NO_3)_6$ would be acceptable leachants for PuO_2-UO_2 solid solution, while 4 N HNO_3 and 4 N HNO_3-0.1 N H_2SO_4 are unacceptable.

2.1.6 UO_2 and U_3O_8 dissolution studies

Contaminated filter samples were prepared by mixing 0.2 g of either UO_2 or U_3O_8* with 2.8 g of shredded filter material. These samples were combined in a glass round-bottom flask containing 250 ml of the desired leaching reagent. The flasks were then attached to reflux condensers, and the contents were heated and refluxed at boiling temperature. Samples were withdrawn periodically, filtered, and the uranium concentration of the solution determined.

---

*Depleted ^{238}U oxide.

Table 2.5. PuO_2-UO_2 solid solution dissolution

Acid test number	Reagent composition	Time heated (hr)	PuO_2-UO_2 dissolved (wt %)
Pu-U-1	12 N HNO_3-0.1 N HF	2	100.0
Pu-U-2	12 N HNO_3-0.05 N HF-0.01 N H_2SO_4	2	97.6
Pu-U-3	4 N HNO_3-0.1 M CAN[a]	2	94.8
Pu-U-4A	8 N HNO_3	1	71.8
Pu-U-4B	8 N HNO_3	2	93.2
Pu-U-5A	4 N HNO_3	2.5	49.6
Pu-U-5B	4 N HNO_3	4.5	54.2
Pu-U-5C	4 N HNO_3	7	60.0
Pu-U-6	4 N HNO_3-0.1 N H_2SO_4	3.75	80.2

[a]CAN is abbreviation for ceric ammonium nitrate.

Table 2.6 lists the results of the dissolution tests with various acid mixtures. As can be seen, the uranium oxides dissolved rapidly and the extent of dissolution was greater than 90% in every test. Eight normal HNO_3 performed as well as any of the acid mixtures, dissolving essentially 100% of the UO_2 or U_3O_8 after 6 hr of heating. As a comparison, the amount of PuO_2 dissolved after 6 hr was only ∿7% (see Fig. 2.3).

2.1.7 Americium-plutonium dissolution studies

Leaching studies were performed using a procedure identical to that employed in the PuO_2-UO_2 solid solution experiments. Contaminated filter material was prepared by mixing AmO_2-PuO_2 powder with shredded filter. Small samples of this mixture were then treated with various leaching reagents, including 4 N HNO_3-0.1 M $(NH_4)_2Ce(NO_3)_6$, 12 N HNO_3-0.05 N HF-0.01 N H_2SO_4, 12 N HNO_3-0.1 N HF-0.1 N H_2SO_4, and 8 N HNO_3. These experiments have not yet been completed; therefore, the results will be summarized and discussed in the next quarterly report.

2.2 Conceptual Flowsheets

Based on the studies performed thus far, it appears that multiple-stage decontamination will be required to achieve high actinide removals, expecially for refractory plutonium. Figure 2.5 represents a four-stage decontamination process and assumes a 90% actinide removal in each stage. The dissolution agent used is 12 N HNO_3-0.05 N HF-0.01 N H_2SO_4, which proved effective on refractory plutonium oxide.

Figure 2.6 represents an alternative decontamination flowsheet using $(NH_4)_2Ce(NO_3)_6$ in varying concentrations with 4 N HNO_3. The concentrations of $(NH_4)_2Ce(NO_3)_6$ shown are also based on calculations using experimental data. These calculations indicate that 0.01 mole of Ce^{4+} is required for each curie of actinides in order to achieve a dissolutioning of 90% or greater. Therefore, this process, even under unfavorable circumstances, should provide an overall DF of 10,000 for the four stages. One disadvantage of this process, however, is the large amount of the expensive

Table 2.6. UO_2 and U_3O_8 dissolution studies

Acid test number	Reagent composition	Time heated (hr)	UO_2 or U_3O_8 dissolved[a] (wt %)
UO_2-1-1	12 N HNO_3-0.01 N HF-0.1 N H_2SO_4	0.5	92.8
UO_2-1-2	12 N HNO_3-0.01 N HF-0.1 N H_2SO_4	6.5	94.1
UO_2-2-1	12 N HNO_3-0.1 N HF-0.01 N H_2SO_4	1	91.0
UO_2-2-2	12 N HNO_3-0.1 N HF-0.01 N H_2SO_4	7	99.6
UO_2-3-1	12 N HNO_3-0.1 N H_2SO_4	4.75	99.3
UO_2-4-1	8 N HNO_3	5.75	102.8
U_3O_8-5-1	8 N HNO_3	1	107.0
U_3O_8-6-1	12 N HNO_3-0.1 N H_2SO_4	1	103.0

[a]Expressed as weight percent uranium metal.

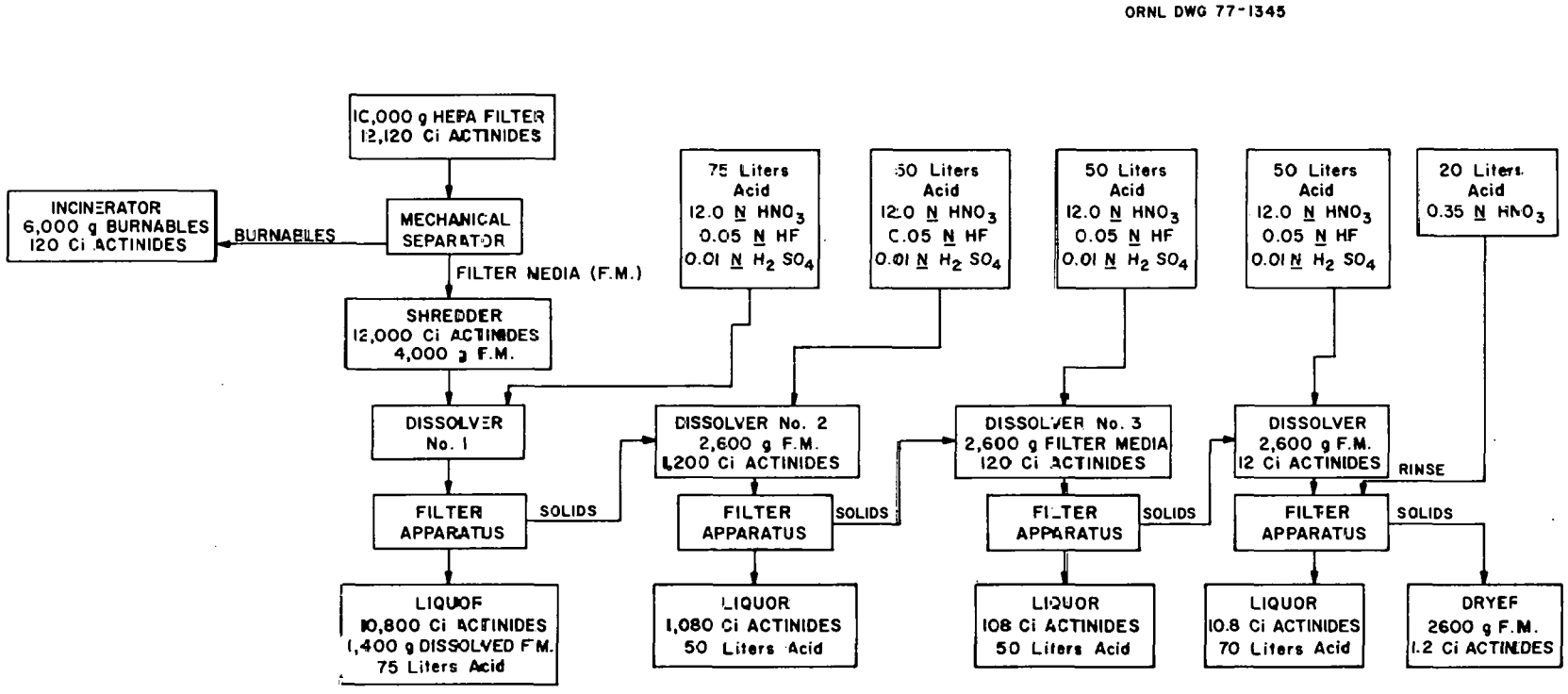

Fig. 2.5. Flowsheet for HEPA filter process. Basis: one 10,000-g HEPA filter.

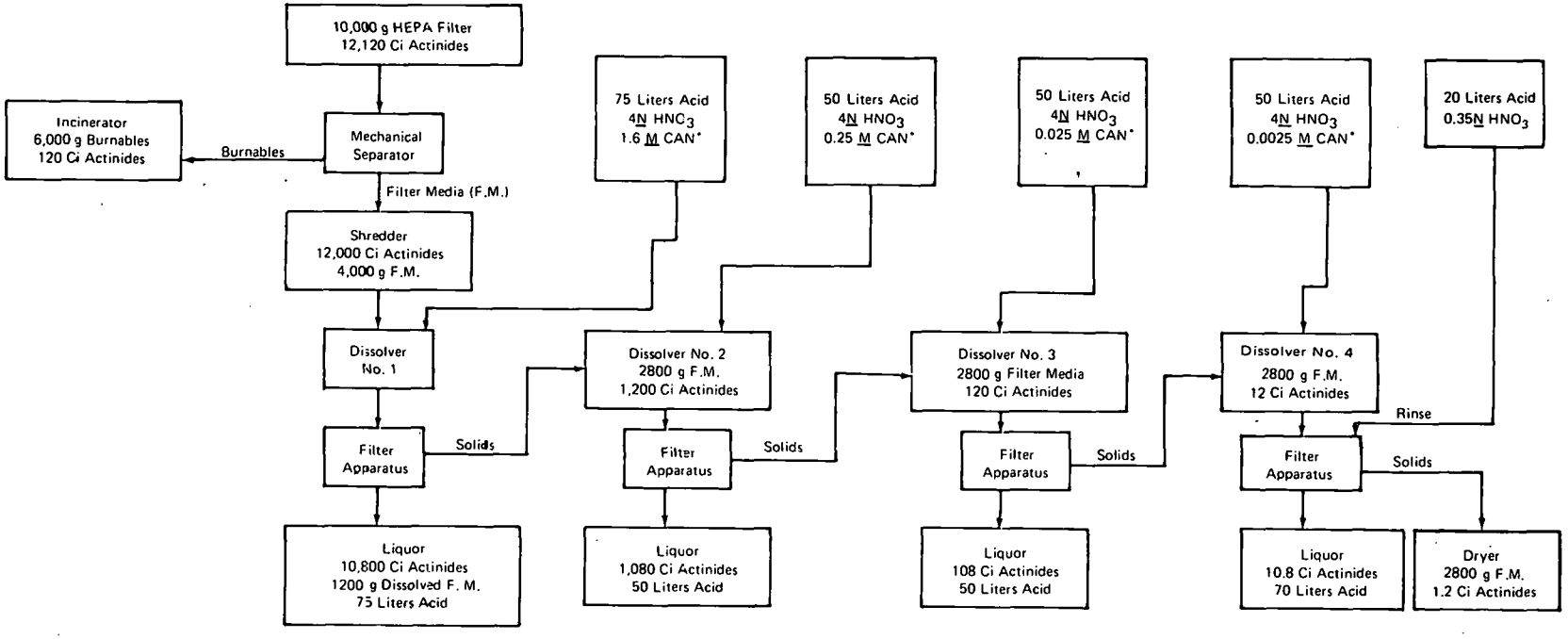

*CAN is abbreviation for Ceric Ammonium Nitrate

June 22, 1977

Fig. 2.6. Conceptual flowsheet for HEPA filter process. Basis: one 10,000-g HEPA filter.

$(NH_4)_2Ce(NO_3)_6$ reagent that is required (∿20 times the stoichiometric amount). In addition, a subsequent separation of the cerium and trivalent actinides would also be required, and this difficult separation would further increase the processing costs.

2.3 Summary and Conclusions

Earlier studies reported last quarter, in which the temperature of the HNO_3 solution was varied, showed a slight increase in the dissolutioning rate of refractory PuO_2 with temperature. A subsequent Arrhenius plot indicated that the apparent activation energy for plutonium dissolution by HNO_3 alone was about 4.8 kcal/g-mole (±9.45 kcal/g-mole)*. This relatively low activation energy suggests that the rate-controlling step is some type of physical process (e.g., film or pore diffusion, or physical adsorption or desorption) rather than a chemical process.

Plutonium adsorption isotherms were developed for the Pu-HNO_3 and Pu-HNO_3-HF systems which proved that the filter medium did adsorb plutonium. The $\frac{X}{m}$ ratio for the Pu-HNO_3-HF system was less than that for the Pu-HNO_3 system for all concentrations measured. The significance of this result is that higher DFs can probably be obtained with HNO_3-HF (assuming that each leaching reagent is equally effective for dissolving PuO_2).

Dissolution tests with HNO_3-H_2SO_4 acid mixtures were conducted on filter medium contaminated with PuO_2. Results showed that these mixtures were relatively ineffective as leaching reagents. The best leachants were found to be mixtures of HNO_3-HF and HNO_3-HF-H_2SO_4, in which the HF concentration was 0.05 N or greater. These solutions dissolved greater than 90% of the plutonium in 15 hr. It was also found that 4 N HNO_3-0.15 M $(NH_4)_2Ce(NO_3)_6$ dissolved 93% of the plutonium in approximately 5 hr. Addition of $KMnO_4$ to HNO_3 and $(NH_4)_2Ce(NO_3)_6$ solutions appears to reoxidize the cerium and thus allows more of the plutonium to dissolve with slightly reduced concentrations of ceric ion. However, the reagent containing 0.15 M ceric ion but no permanganate is a recommended leachant at this time.

---

*Approximate 95% confidence interval.

Both small and large samples of actual HEPA glove-box filters (contaminated with PuO_2) were treated with various leaching solutions. The reagent 12 N HNO_3-0.05 N HF-0.01 N H_2SO_4 proved superior to 4 N HNO_3-0.1 M $(NH_4)_2Ce(NO_3)_6$ for small samples, with greater than 89% of the PuO_2 being dissolved. For larger samples, an increase in the ratio of acid volume to PuO_2 weight was found to increase the dissolution percentage significantly.

Neither Na_2CO_3 nor Na_2CO_3-KNO_3 was satisfactory as a fusion agent for PuO_2. The highest PuO_2 recovery, 71%, was achieved using a Na_2CO_3-30 wt % KNO_3 salt mixture. Also, serious corrosion problems are associated with this process. For example, the platinum crucibles and the furnace used in these experiments were severely attacked by the resultant vapors. Additional fusion tests using higher KNO_3 percentages are planned for next quarter.

The PuO_2-75% UO_2 solid solution dissolved readily in 8 N HNO_3, 12 N HNO_3-0.1 N HF, 12 N HNO_3-0.05 N HF-0.01 N H_2SO_4, and 4 N HNO_3-0.1 M $(NH_4)_2Ce(NO_3)_6$. All of these would be acceptable leaching reagents since each dissolved greater than 93% of the PuO_2 in 2 hr at boiling temperature. Hueda[2] has reported that PuO_2-UO_2 can be dissolved in HNO_3 alone (up to 35% PuO_2). Baehr and Dippel[3] report that UO_2-15% PuO_2 fired at 1600°C will dissolve easily in 14 M HNO_3. These sources substantiate recent findings at Mound Laboratory.

Several dissolution tests were completed with UO_2- and U_3O_8-contaminated filters. Each of the leaching reagents used in the tests dissolved the uranium oxide rapidly. Eight normal HNO_3 performed as well as any of these reagents, dissolving ~100% of the UO_2 or U_3O_8 in 6 hr.

2.4 References for Section 2

1. J. A. Ayres, Decontamination of Nuclear Reactors and Equipment, Pacific Northwest Laboratory Battelle Memorial Institute, Ronald Press, New York, 1970.
2. A. Uriarte Hueda, Dissolution of Nuclear Fuels, Junta de Energia Nuclear, JEN-201-DMa/I-22 (1968).
3. W. Baehr and T. Dippel, The Dissolution of PuO_2-Containing Breeder Fuels in HNO_3 for Aqueous Reprocessing by Purex Method, Institute for Heisse Chemie, EUR-3704 (July 1967).

3. AMERICIUM-CURIUM RECOVERY WITH OPIX, TALSPEAK, AND CEC

W. D. Bond, C. W. Forsberg, F. A. Kappelmann, S. Katz, and F. M. Scheitlin
(Oak Ridge National Laboratory)

This work examines the use of oxalate precipitation and cation exchange (OPIX process) to remove the lanthanides and transplutonium actinides from the high-level liquid waste produced by the Purex solvent extraction process. Talspeak solvent extraction and cation exchange chromatography (CEC) are studied as methods of separating the lanthanides and trivalent actinides.

The conceptual flowsheets described by Tedder[1] are used as a guide in experimental studies. A number of steps in these tentative flowsheets require experimental verification and additional data so that a greater degree of confidence can be provided.

Work during this report period has centered on certain areas of the OPIX and Talspeak flowsheets (Figs. 3.1-3.3). The objective of the work is to obtain sufficient data for evaluation of the technical feasibility of these processes and their potential for scale-up.

3.1 OPIX Process

Semicontinuous precipitation of rare-earth oxalates was carried out to determine the settling characteristics and nature of the precipitates, and the assembly of equipment for continuous precipitation studies was completed. A few laboratory scouting tests were conducted on the removal of Np(IV) and Pu(III) using OPIX.

3.1.1 Semicontinuous precipitation of rare-earth oxalates

While the continuous precipitation equipment was undergoing installation, a short series of semicontinuous precipitation experiments was carried out. The purpose of these experiments was to duplicate a continuous process with a batch technique. A 150-ml solution prepared by mixing a synthetic waste solution and oxalic acid in a flask with a magnetic stirrer was used in most of the experiments. A 15-ml sample was withdrawn from the flask every 10 min. After each sampling, the

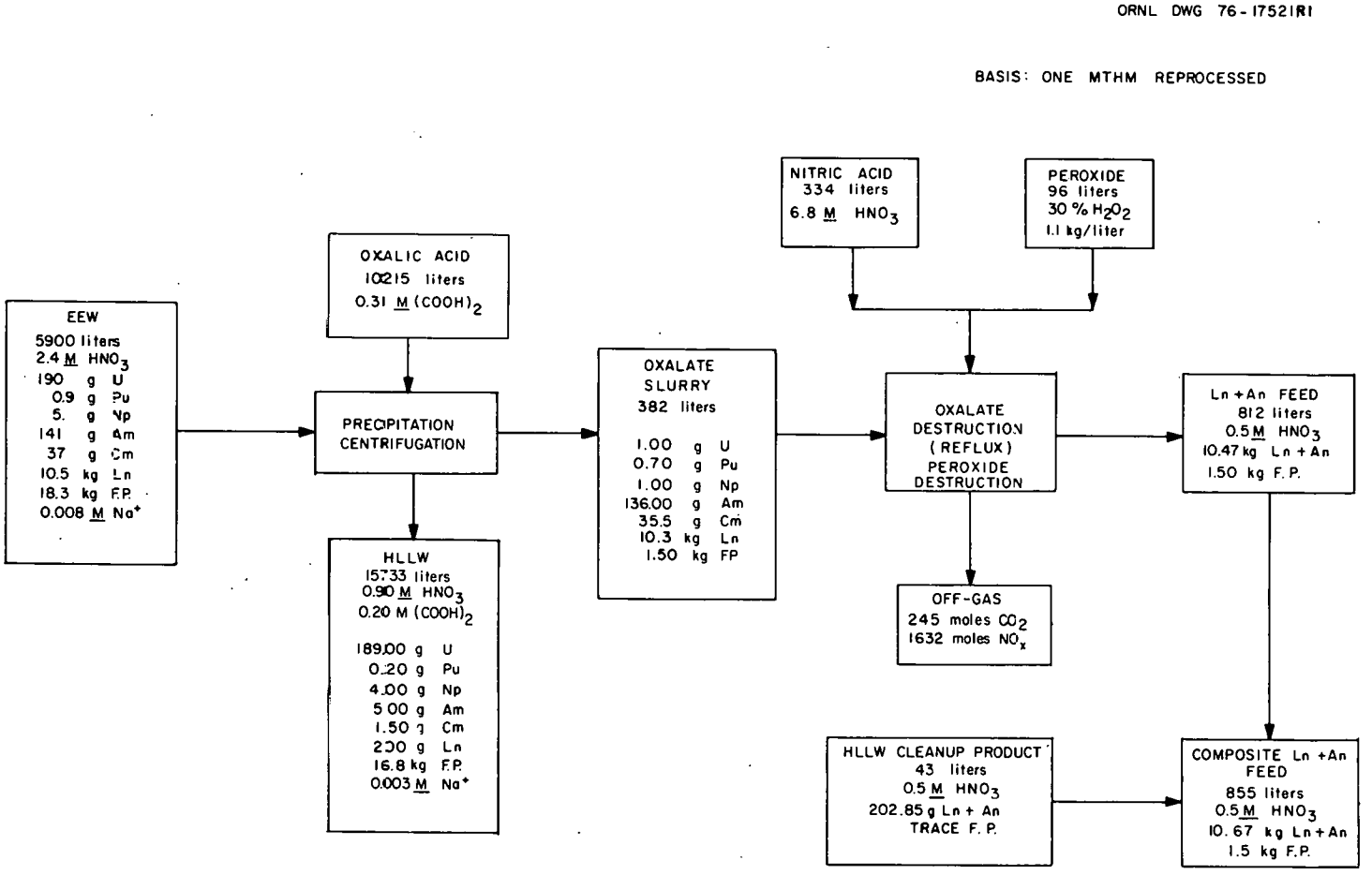

Fig. 3.1. Conceptual flowsheet for oxalate precipitation.

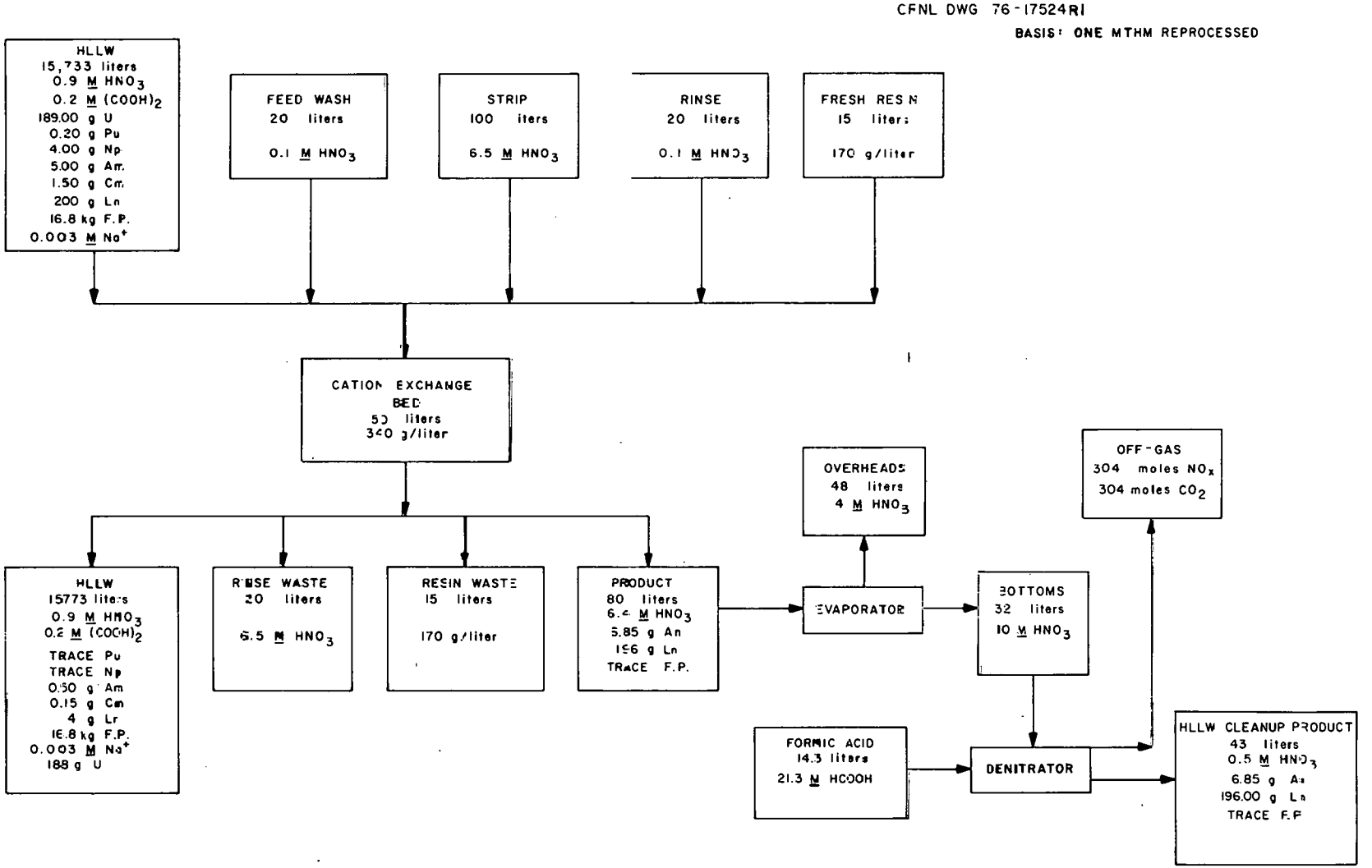

Fig. 3.2. Conceptual flowsheet for HLLW cation exchange cleanup.

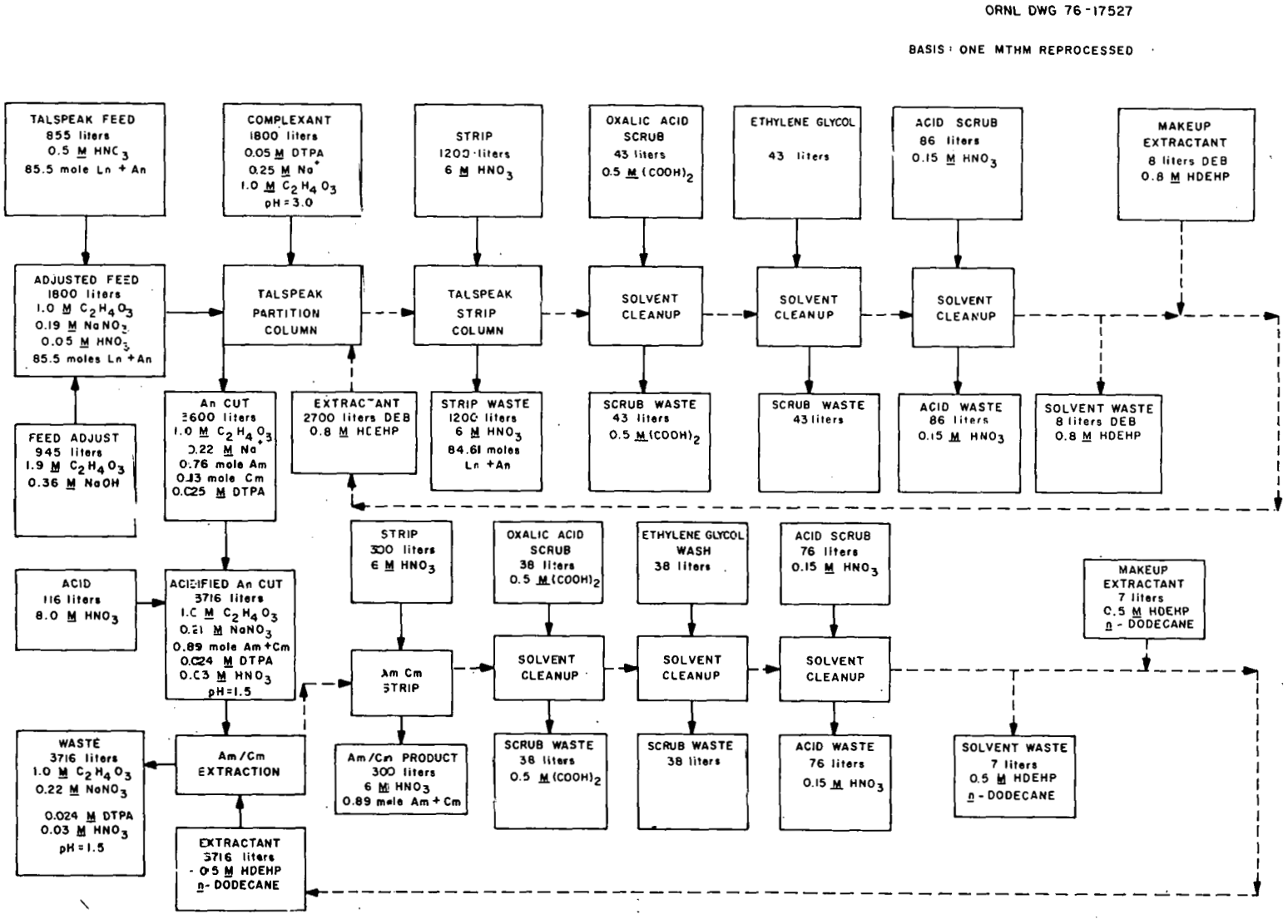

Fig. 3.3. Conceptual flowsheet for Talspeak.

following solutions were added to the flask: (1) 10 ml of a 0.3 M $(COOH)_2$-0.15 M HNO_3 solution; and (2) 5 ml of a synthetic waste solution which contained rare earths, at a concentration of 1.8 g/liter, and other fission products, and was 2.4 M in HNO_3. After six or seven samplings, the slurry in the flask began to approach equilibrium.

A pipettor, which is a constant-volume sampling device capable of taking fairly representative samples, was used to withdraw the samples. These samples, which consisted of slurries of crystals and solution, were then poured into 25-ml graduated cylinders, and the settling rate of the solids was measured as a function of time. Photographs of the precipitate were taken in each case.

Table 3.1 summarizes the results of these experiments. The following conclusions can be drawn from the results:

1. Strontium and barium interfere with rare-earth precipitation, as shown by the series of identical runs made using different types of synthetic waste solutions (Table 3.1). Wastes made of pure neodymium precipitated rapidly compared with completely synthetic waste solutions. Additional experiments, in which ruthenium, zirconium, barium, and strontium were successively added, showed that the barium and strontium caused the slower precipitation. Pure barium and strontium do not precipitate in oxalic acid under the present experimental conditions. About 15 min was required for approximately 99% settling of synthetic waste solutions containing barium and strontium. Thus, it is believed that some barium and strontium are coprecipitated with the rare earths and that this interferes with rapid crystal growth.
2. Microscopic examination of the precipitate indicated that crystals, not agglomerates of crystals, were formed. The pure crystals are rods with a length-to-diameter ratio of 5 (Fig. 3.4). Rod length is about 0.001 in. (2.5×10^{-3} cm). Many crystals are formed imperfectly with faulted crystal growth. In such cases, the crystal may appear spherical but, upon close examination, is found to consist of a number of rodlike crystal projections which have grown from a central point.

Table 3.1. Semicontinuous precipitation of rare-earth oxalates

Run number	Feed composition	Settling velocity (cm/min)		
		A[a]	B[a]	C[a]
1	Complete synthetic waste	0.733	0.808	0.685
2	Neodymium only, equivalent concentration	2.07	1.68	1.62
3	Zirconium only	No precipitate	No precipitate	No precipitate
4	Rare earths + Ru	1.05	1.85	1.36
5	Rare earths + Ru + Zr	1.59	1.91	1.72
6	Rare earths + Ru + Zr + Ba	0.378	0.310	0.264
7	Rare earths + Ru + Zr + Sr	0.294	0.264	0.353
8	Ba + Sr only	No precipitate	No precipitate	No precipitate

[a]Settling velocities were measured by following the clear-particulate interface as the particles settled in a graduated cylinder. A is the settling rate from the 15-cm^3 mark to the 13-cm^3 mark, B from 13 to 11, and C from 11 to 9.

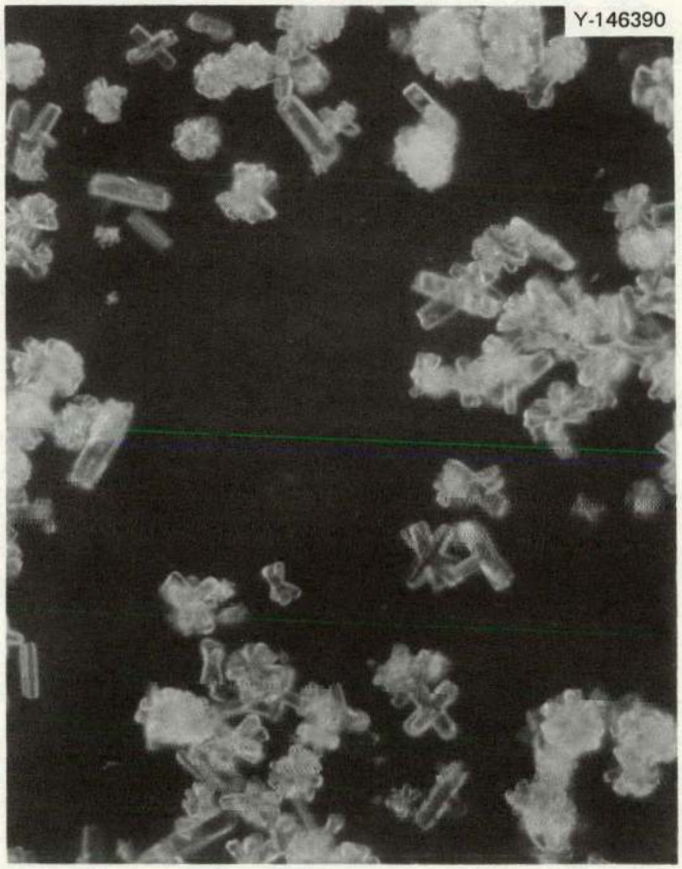

Fig. 3.4. Photomicrograph of rare-earth oxalate precipitate.

3. The volume of the settled precipitate cake was less than 1% of the volume of the mother liquor.
4. The size of the precipitate indicated that settling plus decantation may not be a workable method for achieving liquid-solid separation. Several experiments were attempted at 40°C. The laboratory equipment was not insulated, and thermal convection caused by cooling of graduated cylinder walls was sufficient to prevent settling of the precipitate. The higher levels of heating generated by radioactive decay in the precipitate may cause sufficient thermal convection to prevent separation, and either centrifugation or filtration will likely be required for the liquid-solid separation.
5. The density of the precipitate is about 2.0 g/cm^3. This is calculated from Stokes law by assuming a settling velocity of 0.75 cm/min, room-temperature operation, spherical crystals with a diameter of 6.0×10^{-4} in. (1.5×10^{-3} cm), and a viscosity equal to that of water. There is a great deal of uncertainty in this calculation, and future experiments will serve to quantify the results more accurately.

3.1.2 Studies on removal of Np(IV) and Pu(III)

Batch precipitation tests showed that the OPIX process was effective in removing about 99.5% of the plutonium from synthetic waste solution when the plutonium was trivalent. With an initial plutonium concentration of 0.2 mg/liter, ~3% of the plutonium remained in the supernate after precipitation and ~0.5% remained after passage through an ion exchange column (Table 3.2). A negligible amount of tetravalent neptunium appeared to be carried by the rare-earth oxalate precipitate; the concentration of neptunium remaining in the supernate gave values comparable to published data for the solubility of Np(IV) oxalate in 1 M HNO_3 and 0.2 M oxalic acid.[2] We used ^{237}Np in these experiments (specific activity, 8.01×10^5 counts min^{-1} mg^{-1}), and feed concentrations required to give good counting rates were on the order of 1 mg/ml. The experiments, therefore, could not detect any affinity of the rare-earth oxalates for Np(IV). Next quarter, the experiments will be repeated using feed concentrations that are lower by factors of 10 to 100. The neptunium in the supernate did not load on

Table 3.2. Precipitation of Np(IV) and Pu(III) oxalates along with rare-earth oxalates at 25°C

(Conditions: 0.2 M oxalic acid and 0.9 M HNO_3)

Element	Run	Aging time (hr)	Supernate		Ion exchange effluent		Net loss (%)
			Conc. (mg/liter)	% of total	Conc. (mg/liter)	% of total	
Np	1	2	20	5.7	20	a	5.7
	2	2	12	3.9	12	a	3.9
	3	18	31	8.8	31	a	8.8
	4	18	35	9.7	35	9.7	9.7
Pu	1	2	0.06	2.8	0.006	0.5	0.5

[a] Experiments not performed.

the ion exchange column, indicating that either the oxalate complexes are too strong or the neptunium was reoxidized to the pentavalent state. Further evidence of oxidation of Np(IV) to Np(V) was suggested by the observed increase of neptunium scavenging on aging the precipitates overnight in the mother liquor.

The plutonium that was loaded on the ion exchange resin eluted poorly. Only about 50% was recovered with 40 column volumes of 3 M HNO_3 (Table 3.3). These results may indicate that the principal species is Pu(IV) rather than Pu(III).

Table 3.3. Elution of plutonium from OPIX column with 3 M HNO_3[a]

(Conditions: Column volume consists of 200-400 mesh Dowex 50X8 resin)

Column volumes	Percent Pu eluted
18	7
23	10
29	35
34	42
40	52

[a]Cumulative values are used for column volumes and percent plutonium eluted.

For convenience, 0.01 M ferrous sulfamate was used in these tests to reduce the Np(V) and Pu(IV) in the stock solution to the tetravalent and trivalent species respectively. A reduction time of 1 hr was allowed. In upcoming tests, this procedure will be examined to determine whether the conditions allow complete reduction.

3.2 Talspeak Studies

3.2.1 Mixer-settler studies

One mixer-settler run was made on the first cycle of the Talspeak[3] reference flowsheet (Fig. 3.5). In this run, neodymium was used to represent the extraction and stripping behavior of rare earths and to evaluate the general performance of the mixer-settler units using the reference flowsheets. The conditions used in the run are given in Table 3.4. The operational and sampling procedures employed were the same as those used in the Purex runs (see Sect. 1.3.2). The total run time was 7.5 hr, with an initial 3.5-hr operation, an overnight shutdown, and 4 hr of operation the following day. The analyses for neodymium and the percent of neodymium in the exiting product and waste streams are listed in Table 3.5. The results show that ∿0.5% of the neodymium was present in the americium-curium product solution (1AP), while ∿0.15% was left in the stripped extractant (2AP). Samples were taken of the aqueous and organic phases of all 32 stages after 4 hr of operation on the second day, but the results of these analyses are not yet available. The neodymium losses to the 1AP and 2AP streams were greater than would be expected on the basis of previously reported data in the literature.[1,3]

3.2.2 Batch solvent extraction studies

Laboratory-scale batch extraction studies are being carried out to obtain values of the distribution coefficient (D_A^o) for selected rare earths and actinides. In future experiments, we plan to measure D_A^o's for other fission products which may be present as impurities in Talspeak feeds. These distribution coefficient data could lead to a revision of our reference, conceptual Talspeak flowsheet (see Fig. 3.2, Sect. 3.2).

Last quarter we measured D_A^o's for americium and plutonium between 1 M glycolic acid-0.025 M DTPA solutions and HDEHP using either DIPB or normal dodecane (NDD) as the diluent for the HDEHP. The method employed radiometric assay of plutonium and americium. The distributions of plutonium and americium in samples were determined by gross alpha determinations using alpha pulse-height analysis. Plutonium distribution

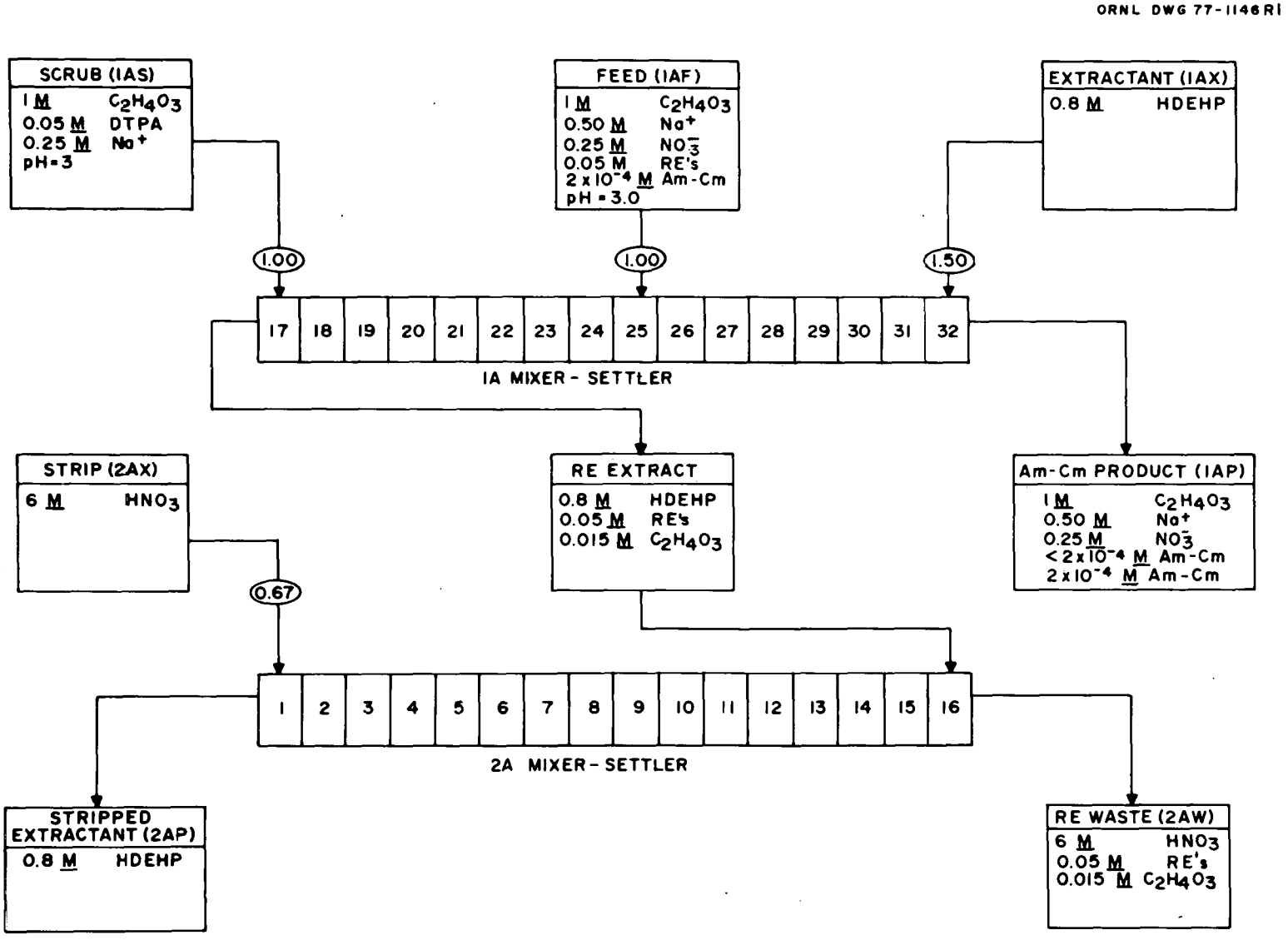

Fig. 3.5. Flowsheet for experimental run on first Talspeak cycle in 16-stage mixer-settlers.

Table 3.4. Run conditions for input streams in mixer-settler flowsheet test (run TAL 1)

(Temperature: 43°C; stirrer speeds: 1A, 800 rpm and 2A, 1100 rpm)

Feed stream	Composition	Flow rates (ml/hr)	
		Desired	Measured[a]
1 AF	4.84 g/liter Nd, 1.0 M $C_2H_4O_3$, 0.36 M Na, pH 2.87	500	494
1 AS	1.0 M $C_2H_4O_3$, 0.05 M DTPA, pH 3.00	500	467
1 AX	0.8 M HDEHP in DEB	750	800
2 AX	6 M HNO_3	375	440

[a]Measured by changes of volume of the feed tanks.

Table 3.5. Concentrations and percentages of neodymium in effluent streams

Time (hr)	Nd concentration (g/liter)			% of Nd feed		
	1 AP	2 AP	2 AW	1 AP	2 AP	2 AW
1	7.5×10^{-3}	3.5×10^{-3}	2.83	0.32	0.14	55
2	1.4×10^{-2}	6.5×10^{-3}	6.88	0.55	0.21	115
3	1.1×10^{-2}	5.4×10^{-3}	6.36	0.48	0.18	125
		Overnight shutdown				
1	1.5×10^{-2}	4.6×10^{-3}	a	0.53	0.13	a
2	1.7×10^{-2}	3.8×10^{-3}	a	0.72	0.12	a
3	1.2×10^{-2}	4.3×10^{-3}	a	0.47	0.14	a
4	1.0×10^{-2}	1.8×10^{-3}	5.85	0.43	0.06	93

[a]Analysis not made.

coefficients were always determined in the presence of americium, using the 5.15-MeV peak for plutonium and the 5.50-MeV peak for americium.

The D_A^o values for americium decreased by factors of 2 to 4 when the pH of the aqueous phase was increased from 2.4 to 3.0 (Table 3.6). Plutonium behavior was erratic, and the D_A^o values showed no particular trend with changing pH. The D_A^o values for Am are about a factor of 3.5 higher (4.86 vs 1.48) at pH 2.7 when NDD rather than DIPB is employed as the diluent (Table 3.7). The D_A^o values for americium pass through a maximum at about pH = 1 for the pH range 0.6 to 2.7. Plutonium coefficients appeared to decrease with increasing pH over the range of 0.6 to 2.7. A pH of about 1 would appear to be a more desirable value to use for reextraction of americium than the value of 1.5 used in our reference flowsheet. However, this observation requires verification at other concentrations of DTPA. An average concentration of 0.025 M DTPA as used in the reference flowsheet is too low to prevent losses of americium. Increasing the DTPA concentration in the reference flowsheets is more desirable than changing the flow ratios.

3.2.3 Recycle of Talspeak extractants

Practical methods are not available for the purification of HDEHP from degradation products expected to be generated by radiation and hydrolysis, and from highly extractable elements which are likely to be present as impurities in the aqueous feed to the Talspeak process. The principal degradation product expected from HDEHP is mono-2-ethylhexylphosphoric acid (H_2MEHP). Highly extractable, difficult-to-strip elements that are expected to be impurities in Talspeak feeds include zirconium, molybdenum, plutonium, neptunium, and possibly ruthenium. In addition, the solubility limits of these elements in the extractant and aqueous phases may lead to formation of precipitates or of a third organic phase. An aqueous oxalic acid solution has tentatively been selected in our reference flowsheet as the scrubbing reagent for the elements that are difficult to strip from HDEHP, and ethylene glycol has been selected for removal of H_2MEHP. An important criterion in the choice of scrubbing solutions is that the HDEHP solubility be low, so that excessive losses are avoided. Solubility data are needed, particularly with regard to ethylene glycol where losses are expected to be significant.

Table 3.6. Distribution coefficients of Am and Pu(IV) between 0.8 M HDEHP in DIBP and 1.0 M glycolic acid--0.025 M DTPA at 25°C

pH	D_A^o	
	Pu	Am
2.4	a	2.20
	a	2.30
	a	2.45
	a	2.74
	0.058	2.53
	0.047	1.77
	a	2.29
	0.76	2.74
2.56	0.24	1.44
2.74	0.70	1.48
2.78	0.022	1.43
3.01	0.020	0.99

[a]Element not present.

Table 3.7. Distribution coefficients of Am and Pu(IV) between 0.5 M HDEHP in NDD and 1.0 M glycolic acid--0.025 M DTPA at 25°C

pH	D_A^o	
	Pu	Am
0.64	0.64	2.43
1.12	0.037	20.8
1.22	0.030	13.4
2.71	0.018	4.86

During this quarter, we measured H_2MEHP and HDEHP distributions throughout the extraction and scrubbing operations depicted in the reference Talspeak flowsheet, and observed interfacial solid formations when zirconium was present in Talspeak feed solutions at concentrations of 10^{-4} M or greater.

3.2.4 Distributions of H_2MEHP and HDEHP

The distribution coefficients for H_2MEHP were determined by analyses of the aqueous phase only. Measured amounts of H_2MEHP were added to the 0.7 M HDEHP in diethylbenzene (DEB) or to the 0.5 M HDEHP in NDD. High-purity HDEHP was used to prepare the HDEHP and diluent solutions. The distribution coefficients were determined by making successive contacts (1:1 volume ratio) with fresh portions of the appropriate aqueous or ethylene glycol phase and subsequently analyzing that phase. The analysis consisted of converting the aqueous- or glycol-soluble organic phosphoric acids to PO_4^{3-} and determining the total phosphate. The aqueous solubility of H_2MEHP is considerably higher than that for HDEHP and could be determined by difference. The solubility of HDEHP in scrubbing liquids could be measured directly using the pure compound.

The distribution coefficients were determined from linear regression analyses of plots of the logarithms of the H_2MEHP concentrations in the scrubbing phase vs the number of contacts. The slope of the curve is $-\log (1 + D_o^S)$ for extractable species whose distribution coefficients are constant. The following equation* was derived for the scrubbing of H_2MEHP from HDEHP-diluent mixtures using equal-volume contacts:

$$\log C_s = -n[\log(1 + D_o^S)] + \log(I_o\ D_o^S), \qquad (3.1)$$

where

C_s = equilibrium concentration of H_2MEHP in scrubbing phase of contact n,

---

*With these assumptions: (1) phase equilibrium, (2) constant volumes, and (3) negligible changes in the distribution coefficients between scrubs.

n = number of phase contacts,

D_o^S = ratio of concentration of H_2MEHP in scrub to that in the HDEHP phase,

I_o = initial concentration of H_2MEHP in HDEHP phase before contact,

and σ defines a 95% confidence interval.

Equation (3.1) can be used for volume ratios other than unity by substituting the extraction factor, E_o^S, for D_o^S in the $\log(1 + D_o^S)$ term, giving the general case:

$$\log C_s = -n[\log(1 + E_o^S)] + \log(I_o D_o^S), \qquad (3.2)$$

where

$$E_o^S = D_o^S \frac{V_s}{V_o},$$

V_s = volume of scrub solution,

V_o = volume of HDEHP (or any phase containing the extractable species).

Equations (3.1) and (3.2) are particularly useful for the estimation of distribution coefficients when an analytical method is not readily available for the phase initially containing the impurity or extractable species. An equation similar to Eq. (3.2) can easily be derived for the change in concentrations of the phase initially containing the extractable species with repeated contacts, in the event that an analysis for the scrub or transfer phase is not readily available.

Tables 3.8 and 3.9 show the results of linear regressions using the experimental data obtained. In Eq. (3.1), the accuracy of the determination of distribution coefficients is reflected in the 95% confidence limits, $\sigma(95)$, of $\log(1 + D_o^S)$ and in the range of the D_S^o values calculated using these confidence limits. To ensure consistency with our other extraction studies, we have reported the coefficient D_S^o, which is the reciprocal of D_o^S. Also, difficulties encountered in the analytical procedure for total phosphate lead to uncertainty in the values of line slopes (Figs. 3.6 and 3.7). However, the overall results show the magnitude of the separations that can be expected. The following conclusions can be drawn from the D_S^o values that were determined:

Table 3.8. Scrubbing of H_2MEHP from 0.7 M HDEHP in DEB at 25°C

Scrubbing phase	Run number	Number of contacts	$\log(1 + D_O^S) \pm \sigma(95)$	D_S^o Mean	D_S^o High	D_S^o Low	HDEHP concentration in scrub liquid (M × 10^{-4})
pH 3.0, 0.05 M DTPA with 1 M glycolic acid	1	4	0.4624 ± 0.0815	0.53	0.71	0.40	3[a]
	2	5	0.4336 ± 0.0415	0.58	0.69	0.50	3
	3	6	0.3086 ± 0.0208	0.97	0.88	1.06	6
2 M glycolic acid	1[b]	6	0.2442 ± 0.1231	1.33	3.10	0.75	6
pH 1.5, 0.05 M DTPA with 1 M glycolic acid	2[b]	6	0.0805 ± 0.0272	4.91	7.65	3.55	2
		6	0.1002 ± 0.0326	3.85	5.93	2.80	3
Ethylene glycol	1	4	0.5671 ± 0.1510	0.37	0.62	0.24	42
10% oxalic acid	1	5	0.1427 ± 0.0283	2.57	3.32	2.07	7

[a] Read as 3×10^{-4}.

[b] Using Zr and Eu initial concentrations in the aqueous phase of 0.001 and 0.05 M, respectively.

Table 3.9. Scrubbing of H_2MEHP from 0.5 M HDEHP in NDD at 25°C

Scrubbing phase	Number of contacts	$\log(1 + D_o^S) \pm \sigma(95)$	D_S^o Mean	D_S^o High	D_S^o Low	HDEHP concentration in scrub liquid (M × 10^{-4})
pH 1.5, 0.05 M DTPA with						
1 M glycolic acid	6	0.1248 ± 0.0072	3.00	3.21	2.82	4
1 M glycolic acid	5	0.1621 ± 0.0573	2.21	3.66	1.52	5
2 M glycolic acid	6	0.1298 ± 0.0849	2.87	9.18	1.56	2
Ethylene glycol	5	0.3992 ± 0.1292	0.66	1.16	0.42	35

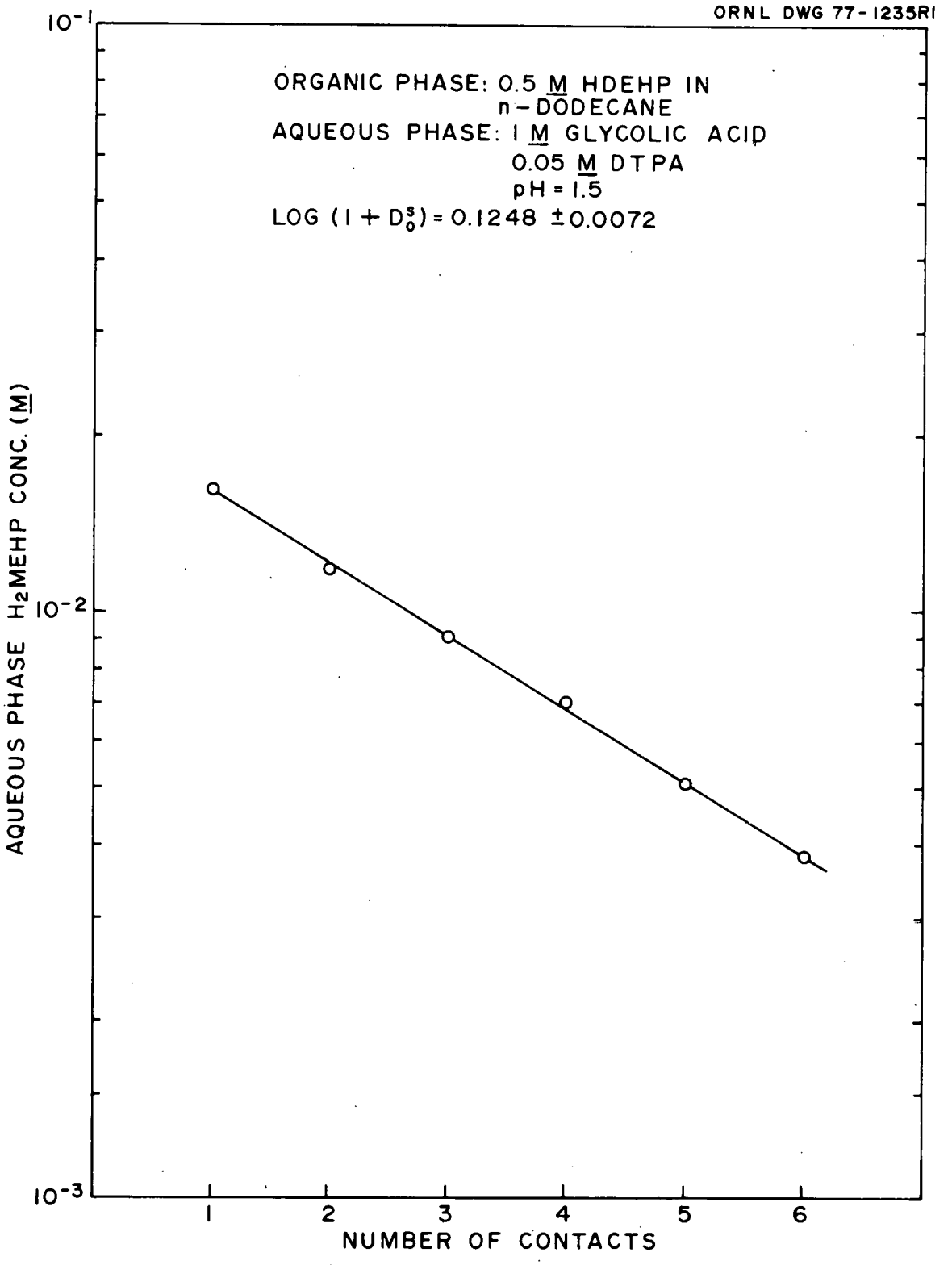

Fig. 3.6. Concentration of H_2MEHP in 1 M glycolic acid-0.05 M DTPA as a function of the number of contacts.

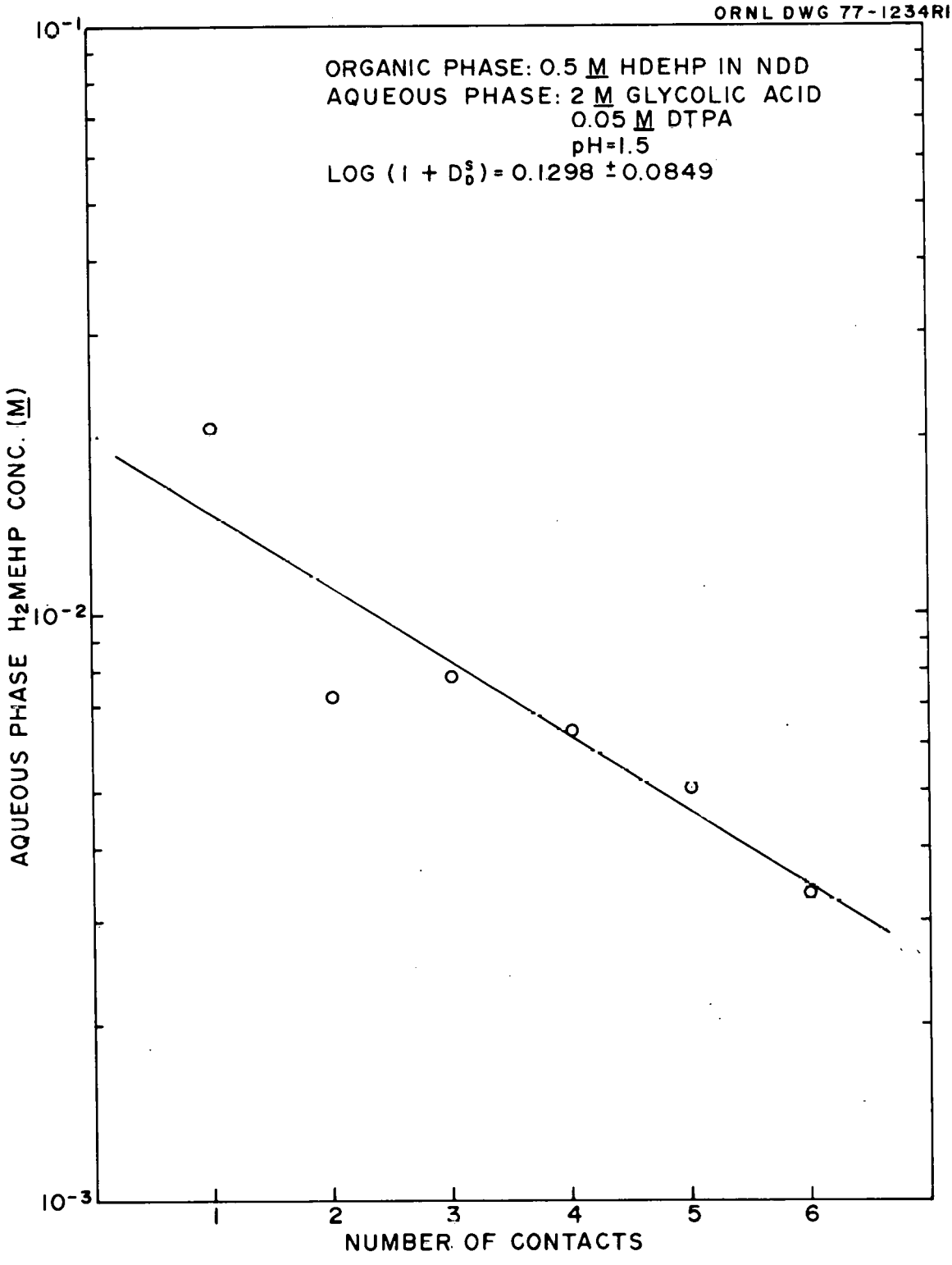

Fig. 3.7. Concentration of H_2MEHP in 2 M glycolic acid-0.05 M DTPA as a function of the number of contacts.

1. H_2MEHP is more soluble in the aqueous phase than in the organic phase with the pH 3.0, glycolic acid-DTPA solutions, using DEB as the diluent for HDEHP. With pH 1.5 solutions, however, it is more soluble in the organic phase using either DEB or NDD as the diluent. The distributions were unaffected by the presence of 10^{-3} M zirconium and 0.05 M europium, within the confidence limits of the experiments. The import of these results is that H_2MEHP will be scrubbed out (50 to 70% per cycle) in the aqueous actinide product in the rare-earth extraction step (pH 3) of Talspeak. In the actinide extraction step (pH 1.5 aqueous), the H_2MEHP will be reextracted to a high degree as evidenced by the D_S^o values for that step of $\sim$3.
2. Ethylene glycol is effective in scrubbing H_2MEHP from the HDEHP (D_S^o = 0.4 to 0.7); however, significant volumes of this liquid would be required, depending on the degree of removal sought and the volumes of HDEHP to be purified. For the same reasons, the solubility of HDEHP (4×10^{-3} M or 1.3 g/liter) in ethylene glycol may be excessive for its use as a scrubbing agent.

3.2.5 Interfacial, zirconium-bearing solids

A few tests were made to determine the effect of the presence of zirconium in aqueous Talspeak solutions. Although the tests consisted of simple physical observations, the results are worthy of reporting. High-purity HDEHP was used in these tests. When the feed contained zirconium at a concentration of 10^{-4} M, we observed only small amounts of an interfacial solid (or organic third phase) from rare-earth extractions, and interference with separation of the phases was minimal. When zirconium was present at a concentration of 10^{-3} M, however, the effect was marked, making separation by gravity-settling difficult. We plan to evaluate the operational behavior of our mixer-settler with zirconium concentrations of 10^{-3} to 10^{-4} M in the feed solutions.

3.3 References for Section 3

1. A. G. Croff, D. W. Tedder, J. P. Drago, J. O. Blomeke, and J. J. Perona, A Preliminary Assessment of Partitioning and Transmutation as a Radioactive Waste Management Concept, ORNL/TM-5808 (September 1977).

2. J. A. Porter, Ind. Eng. Chem., Process Design Dev. 3, 289 (1964).

3. B. Weaver and F. A. Kappelmann, Talspeak: A New Method of Separating Americium and Curium from Lanthanides by Extraction from an Aqueous Solution Aminopolyacetic Acid Complex with a Monoacidic Phosphate or Phosphonate, ORNL-3559 (August 1964).

4. AMERICIUM-CURIUM RECOVERY USING BIDENTATE EXTRACTANTS

L. D. McIsaac, J. D. Baker, R. E. LaPointe, and N. C. Schroeder
(Allied Chemical Corporation-Idaho Chemical Programs)

The objective of this task is to study the usefulness of neutral bidentate extractants in recovering the transplutonium actinides from the HLLW. One phase of this study involves the development of flowsheets which describe the extraction of the actinides and lanthanides, their decontamination from other fission products, the stripping of the extractant, and the cleanup of the used solvent for recycle.

4.1 Studies Using Synthetic LWR Waste

Additional distribution coefficients for actinides and other key elements between synthetic commercial LWR waste solution and 30% dihexyl-N,N-diethylcarbamylmethylenephosphonate (DHDECMP) in diisopropylbenzene (DIPB)* have been measured. Extraction, scrub, and strip data reported in Table 4.1 were obtained by using the same procedures described last quarter. Table 4.1 is a composite of newly obtained data and values reported in the previous report in this series.[1]

Under the conditions used for the extraction contact (0.1 M nitrite), favorable distribution coefficients were obtained for actinides and lanthanides. Of the nonactinide and lanthanide elements present in synthetic LWR solution, only zirconium, yttrium, technetium, palladium, niobium, molybdenum, and ruthenium are extracted to any large extent. Of these, zironium, niobium, and molybdenum are removed from the organic phase by contacting it with 3 M HNO_3-0.05 M $H_2C_2O_4$ scrub solution. Strip contacts with 0.05 M HNO_3-0.05 M $NH_2OH \cdot HNO_3$ show that only uranium, ruthenium, palladium, and technetium are not removed from the organic phase. Additional distribution data, using 0.05 M HNO_3-0.05 M $H_2C_2O_4$ and 0.5 M Na_2CO_3

---

*Technical grade DIPB: ~10% ortho, 50% meta, and 40% para isomers.

Table 4.1. DHDECMP extraction-scrub-strip studies with synthetic Purex first-cycle waste (HAW) solution made 0.1 M in nitrite

Feed component	Extraction contact	Distribution coefficients				
		Scrub contacts		Strip contacts		
		1	2	1	2	3
Cm(III)	3.0	2.9	3.7	0.50	0.11	0.10
Am(III)	4.3	4.1	5.7	0.70	0.13	0.18
Pu(IV)	304.	122.	25.	0.70	0.068	0.16
Np(V,VI)	2.2	2.0	3.6	0.060	0.84	
U(VI)	51.	62.	52.	13.9	2.74	2.40
Gd(III)	2.1	2.4	2.6	0.33	0.061	
Eu(III)	2.9	3.2	3.3	0.46	0.086	0.048
Sm(III)	3.4					
Pm(III)	4.2					
Nd(III)	4.3					
Pr(III)	5.3					
Ce(III)	5.8	5.2	7.1	1.02	0.18	<0.1
La(III)	6.5	6.1	7.8	1.01	0.16	0.085
Ba(II)	0.013	0.012				
Cs(I)	0.00050					
Te(IV)	0.020	0.0084				
Sb(V)	0.036					
Sn(IV)	0.002					
Cd(II)	0.0067					
Ag(I)	0.028	0.026				
Pd(II)	0.53	0.47	0.41	1.10	1.20	2.8
Rh(III)	0.018					
Ru(III,IV)	0.27	0.96		15.	15.	
Tc(VII)	2.3	1.40		8.3	5.1	
Mo(VI)	0.39	0.10	0.041			
Nb(V)	0.51	0.017	0.75			
Zr(IV)	1.8	0.022	0.0028			
Y(II)	0.60	0.66	0.70	0.076	<0.1	
Sr(II)	0.017	0.019				
Rb(I)	0.00064					
Fe(III)	0.0015					
Cr(III)	0.0033					
H^+	0.23					

solutions, are presented in Table 4.2. Uranium and ruthenium are efficiently stripped by carbonate; technetium is also stripped, but less efficiently.

Preliminary extraction distribution coefficients for various key elements from reduced synthetic LWR solution, 0.01 M $Fe(SO_3NH_2)_2$-0.02 M HSO_3NH_2, are shown in Table 4.3. For comparison, values obtained using 0.1 M $NaNO_2$ are listed in the far right-hand column. Ferrous sulfamate was prepared by dissolving stoichiometric quantities of ferrous ammonium sulfate and sulfamic acid in water. This solution was made SO_4^{2-}- and Cl^--free by passing it through a sulfamate anion exchange column. A new method of preparation[2] for a 1:2 molar ratio of $Fe(SO_3NH_2)_2$:HSO_3NH_2 involves the addition of iron filings to sulfamic acid at a mole ratio of 1:4. Care should be taken to protect this solution from oxygen, light, and heat. Experimental procedures for obtaining the data in Table 4.3 were the same as those used for obtaining the results shown in Table 4.1. As expected, neptunium shows a much higher distribution coefficient when reduced to the quadrivalent state. Niobium and ruthenium also extracted to a greater extent under these conditions. Other elements to be measured include plutonium, uranium, and rhodium.

Experiments were run to determine whether neptunium would maintain a high distribution coefficient for several scrub contacts after being extracted from reduced synthetic LWR waste solution. Normal scrubs, two 0.2-volume contacts with 3 M HNO_3-0.05 M $H_2C_2O_4$, failed to maintain a high distribution coefficient ($D < 5$). However, when the scrub was changed to 3 M HNO_3-0.05 M $H_2C_2O_4$-0.02 M HSO_3NH_2-0.007 M $Fe(SO_3NH_2)_2$, the distribution coefficients for the first and second scrubs were maintained at 70 and 22 respectively.

The capacity of DHDECMP to load with rare-earth elements was determined in an experiment in which varying concentrations of lanthanum were extracted from 3.0 M HNO_3 into 30% DHDECMP-DIPB. These results are given in Fig. 4.1, which is a plot of aqueous- vs organic-phase lanthanum concentrations at equilibrium. As expected, the D_{La}* is inversely proportional to

---

*In accordance with the ISEC-74, this notation will be used in all future reports. This notation replaces E_a^o.

Table 4.2. Oxalic acid and sodium carbonate strip data

Element	Distribution coefficients	
	0.05 M $H_2C_2O_4$-0.05 M HNO_3	0.5 M Na_2CO_3
Cm	0.20	
Am	0.12	
Pu	0.16	
Np	7.5	
U	0.095	0.006
Pd	0.8	
Ru	11.0	0.05
Tc		0.58

Table 4.3. Distribution coefficients for key elements from reduced synthetic LWR waste solution

Element	0.01 M $Fe(SO_3NH_2)_2$--0.02 M HSO_3NH_2	0.1 M $NaNO_2$
Mo	0.37	0.39
Nb	1.50	0.51
Tc	2.2	2.3
Zr	2.0	1.8
Pd	0.54	0.53
Ru	0.50	0.27
Ba	0.011	0.013
Cs	~0.0004	0.0005
Ce	5.8	5.8
Eu	2.9	2.9
Np	98	2.2

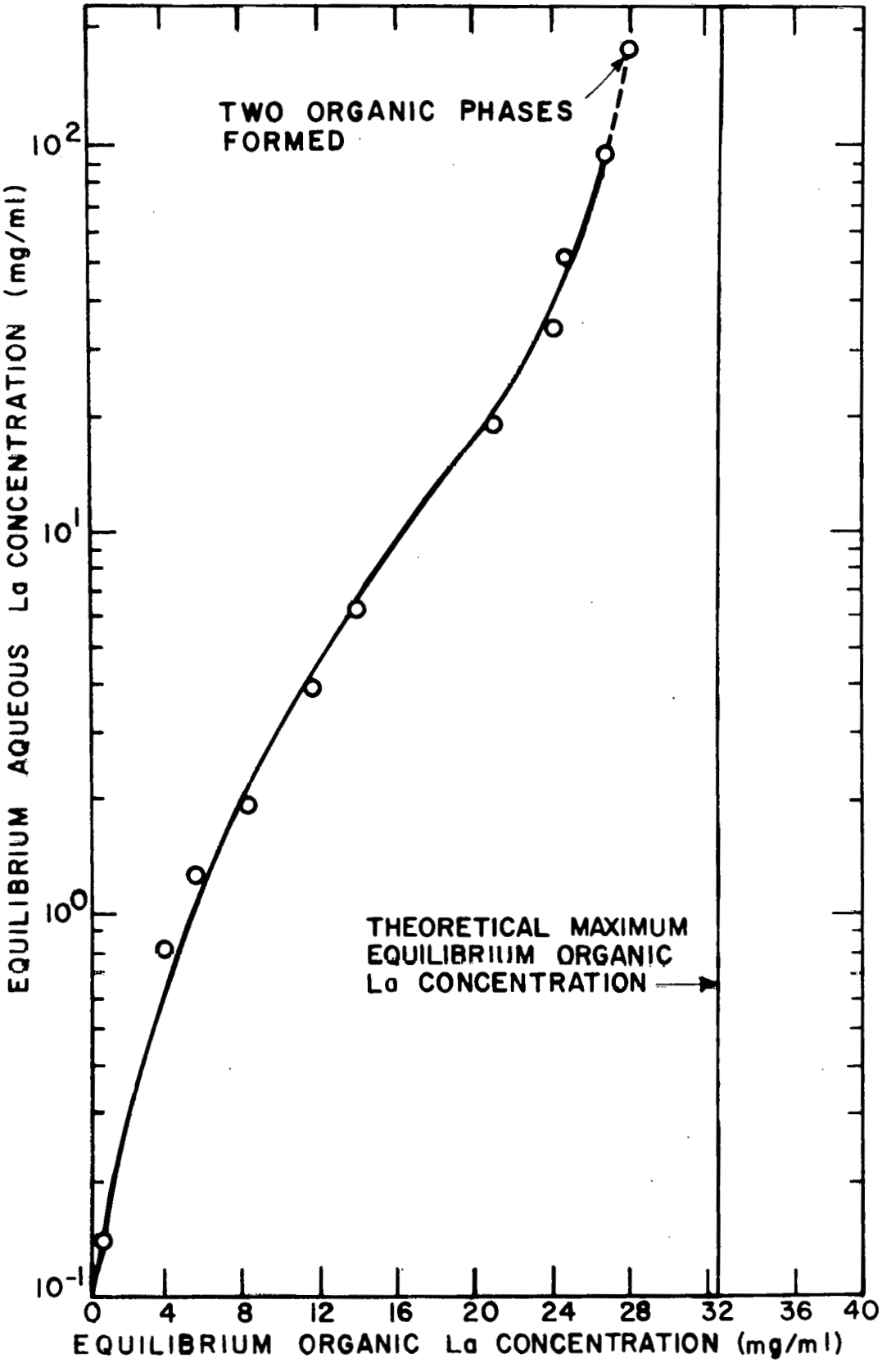

Fig. 4.1. Lanthanum loading of 30% DHDECMP-DIPB.

the concentration of lanthanum in the extractant. The value of D_{La} fell below 1 when the extractant was loaded to ∿70% of its theoretical capacity. It should also be noted that the organic separated into two phases when loaded to ∿86% of its capacity. In the actinide removal process envisioned for LWR waste, the extractant would be loaded to ∿5% of its capacity; hence there would be no loading problem due to rare-earth elements.

4.2 Extraction Mechanisms

Distribution coefficients for Pu(IV) between 30% DHDECMP in DIPB and various concentrations of HNO_3 were determined during this report period. The results are shown in Fig. 4.2, along with data obtained last quarter. Plutonium was set in the quadrivalent state by adding 1 drop of 30% H_2O_2 to the nitrate tracer and taking it to incipient dryness in concentrated HNO_3. The tracer was then taken up with the particular HNO_3 concentration being studied and made 0.025 M in nitrite. The sample was subsequently capped to prevent loss of NO_2 and allowed to stand for 1 hr. After this period, 1:1 extractions were performed in the manner described in previous reports.

Efforts to determine distribution coefficients for Pu(III) using 0.025 M $Fe(SO_3NH_2)_2$ or 0.25 M sodium formaldehyde sulfoxylate ($NaCH_2OSO_2$) were successful with HNO_3 concentrations up to 1 M. At higher concentrations, however, oxidation to Pu(IV) readily occurred.

Other areas of interest that are basic to understanding the extraction capabilities of DHDECMP are being pursued. Additional studies will be made to determine how the variance in nitrate and hydrogen ion concentrations independently affects americium distribution coefficients.

The nature of the extracted complex also presents an interesting problem. Evidence in the literature[3] indicates that one of the methylene protons in DHDECMP could be acidic. Considering the similarity in the structure of DHDECMP to acetylacetone about the methylene carbon, this is not too surprising. Acidic methylene hydrogens could have important roles in the ability of DHDECMP to form complexes. Loss of a methylene proton would allow neutral complexes of metals to be extracted into the organic

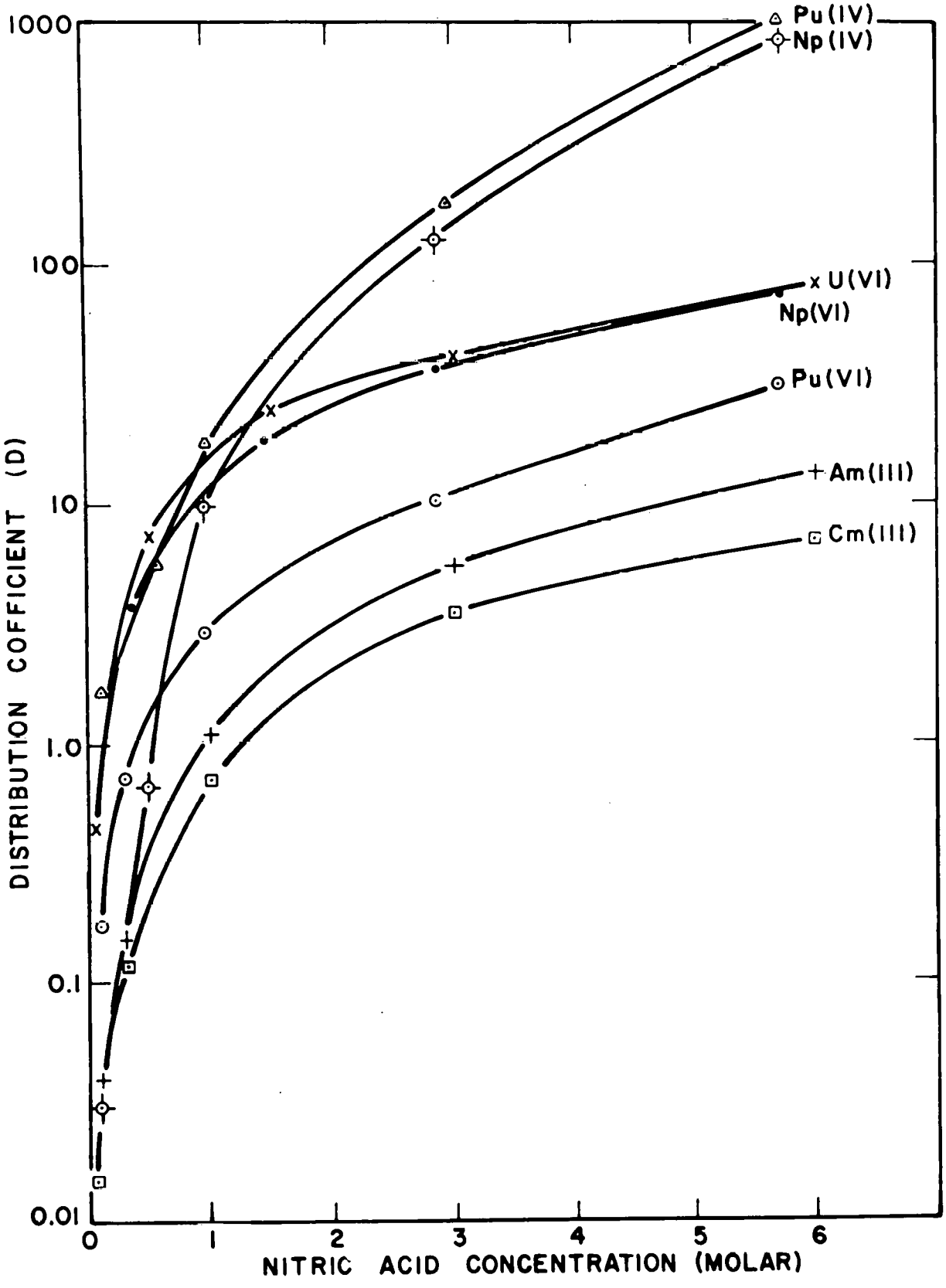

Fig. 4.2. Distribution coefficients for actinides between 30% DHDECMP-DIPB and HNO_3.

phase. In addition, aromaticity similar to metal complexes of acetylacetone might exist in these complexes:

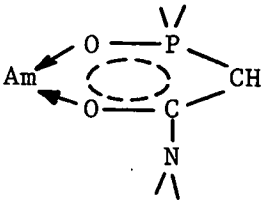

The correct number of π electrons (i.e., six) are available for this structure. Whether or not enough planarity exists for effective π orbital overlap is speculative. Efforts to obtain a metal complex of DHDECMP will be attempted. An NMR spectrum of this complex should show a large downfield shift if aromaticity does exist.

4.3 Conceptual Flowsheet

The batch equilibrium distribution coefficients presented in Table 4.1 were used to prepare a preliminary material balance flowsheet for actinide removal. The basis for this flowsheet (see Fig. 4.3) is 1 tonne of PWR-U fuel processed as described in the literature.[4] Decontamination factors (DFs) used in this flowsheet are based on operation at 23°C.* Therefore, the feed to the extraction contactor (HAW stream) would need to be cooled, clarified, and adjusted to an as yet undetermined concentration of HNO_2. The desired americium DF (ref. 5) of 1000 would be accomplished using five extraction stages. The necessary DFs for other actinides[5] would also be achieved by five extraction stages. The organic stream is scrubbed to remove the extracted zirconium. All of the lanthanides, americium, curium, and neptunium, as well as 99+% of the plutonium are removed in the first strip contactor. The second strip contactor removes any residual plutonium, along with ∿50% of the uranium. In the first solvent wash contactor, the remaining uranium and acidic degradation products are

*The americium distribution coefficient decreases in magnitude by approximately 5%/°C with increased temperature.

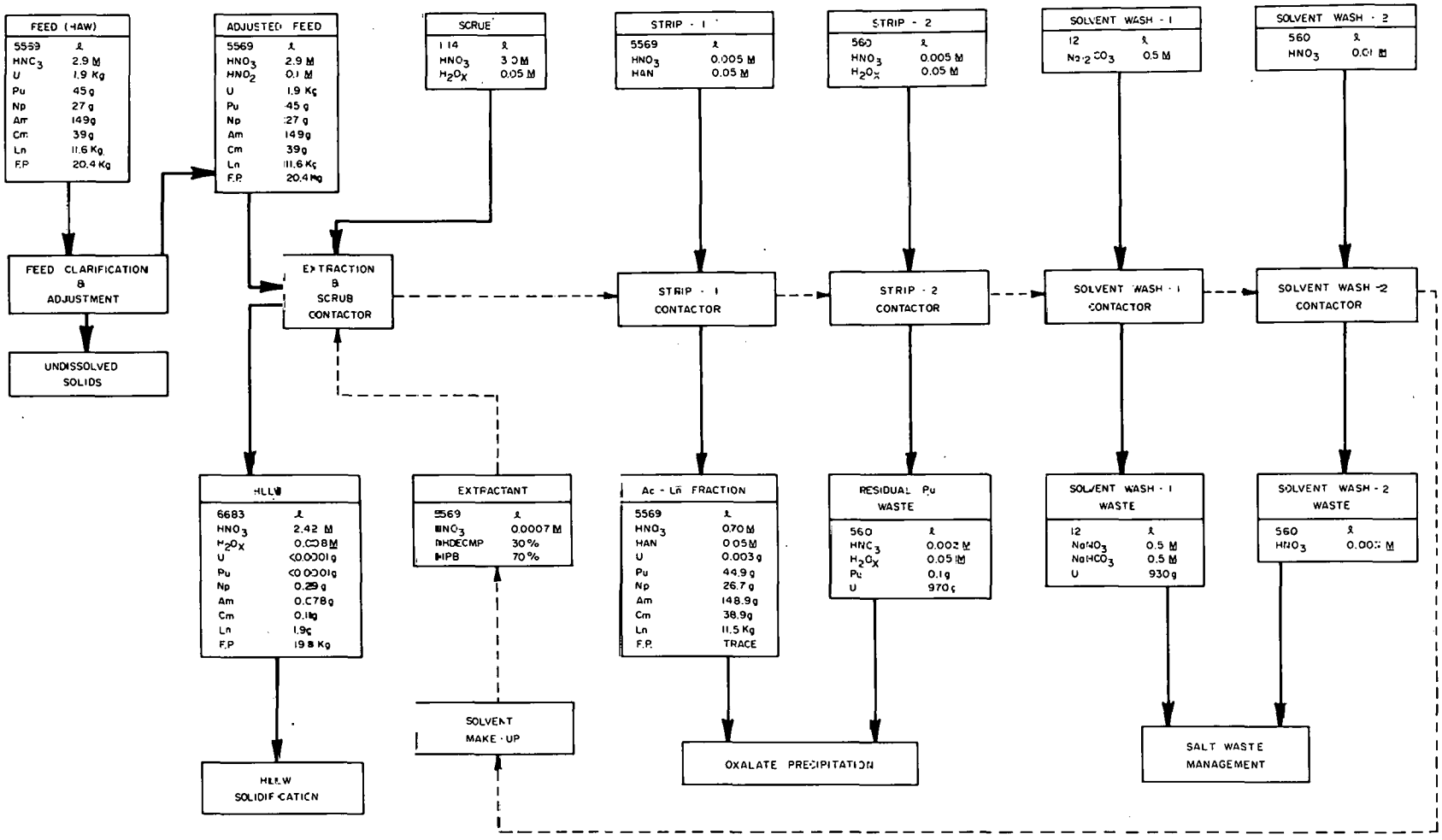

Fig. 4.3. Conceptual actinide partitioning flowsheet for HAW from reprocessing LWR fuel.

scrubbed from the extractant. Solvent purification is completed in the second solvent wash contactor. Before recycling, the organic would be routed to a solvent makeup tank for analysis and adjustment of DHDECMP and diluent concentrations.

Tentatively, the actinide-free HLLW would be solidified, the solvent washes would be sent to salt waste management, and the actinide streams would be subjected to an oxalate precipitation step preparatory to the Talspeak process. Several areas in this flowsheet need further investigation. For example, the optimal HNO_2 concentration in the feed is not known, and the D_{HNO_2} has not yet been determined. In addition, extractant recycle needs to be proved. The relative volumes of each stream also need to be determined. Investigation of a mixed diluent, decalin-DIPB, is under way. It is believed that the DHDECMP in this diluent gives a sufficiently high americium distribution coefficient to permit operation of the contactor at 45 to 50°C. This is the expected ambient temperature of the HAW feed solution.

4.4 References for Section 4

1. J. O. Blomeke and D. W. Tedder, Actinide Partitioning and Transmutation Program Progress Report for Period October 1, 1976 to March 31, 1977, ORNL/TM-5888 (June 1977).

2. M. C. Thompson, Savannah River Laboratory, Aiken, S.C., personal communication to L. D. McIsaac.

3. M. R. Yoninou et al., "Coordination of Organophosphorous Anions. 6'. Characterization of Nitrato Complexes of Cobalt(II), Nickel(II) and Zinc(II). Crystal and Molecular Structure of the Dimeric Nitrato (γ-piperidino β-ketophosphonate) Cobalt(II), " Inorg. Chem. 16(4), 872 (1977.

---

*The americium distribution coefficient decreases in magnitude by approximately 5%/°C with increased temperature.

4. W. D. Bond and R. E. Leuze, Feasibility Studies of the Partitioning of Commercial High-Level Wastes Generated in Spent Nuclear Fuel Reprocessing: Annual Progress Report for FY-1974, ORNL-5012 (January 1975).

5. H. C. Claiborne, Effect of Actinide Removal on the Long-Term Hazard of High-Level Waste, ORNL/TM-4724 (January 1975).

5. AMERICIUM-CURIUM RECOVERY USING INORGANIC ION EXCHANGE MEDIA

D. R. Tallant (Sandia Laboratories)

The objective of this study is to determine the usefulness of certain inorganic ion exchange media for separating the trivalent actinides and lanthanides. During the first year, feasibility will be determined. If successful, flowsheets will be developed during the second year.

During this quarter, work focused on determining the effect of pH on the affinities of titanate, niobate, and zirconate ion exchange materials for rare-earth ions. The results obtained during the last report period implied that these affinities would display a strong pH dependence.

The experiments were carried out by contacting a 5 ppm lanthanum solution with weighed amounts of the hydrogen forms of the various ion exchange materials. The pH of each solution was adjusted by adding dilute HNO_3 or ammonia and was monitored with a pH meter and glass electrode. After an equilibration period of >60 hr, the solution was analyzed for remaining lanthanum using inductively coupled plasma-optical emission spectroscopy. The results of these experiments are plotted in Fig. 5.1, which presents affinities in terms of distribution coefficients, K_d, where

$$K_d = \frac{(\text{fraction of } La^{3+} \text{ on ion exchanger})}{(\text{fraction of } La^{3+} \text{ in solution})} \cdot \frac{(\text{ml of solution})}{(\text{g of ion exchanger})} .$$

In the figure, upward- and downward-pointing arrows denote, respectively, points for which only lower and upper limits of the K_d's were determinable. K_d's for europium on the niobate material were also determined as a function of pH and were found to exhibit nearly the same pH dependence as the lanthanum K_d's.

As expected, the K_d's are strongly dependent on pH. Further, the positions on the pH axes of the K_d curves for the three ion exchange materials are in line with their acid strengths (niobate > titanate > zirconate), since it would be expected that a stronger acid would tend

ORNL DWG-77-6011

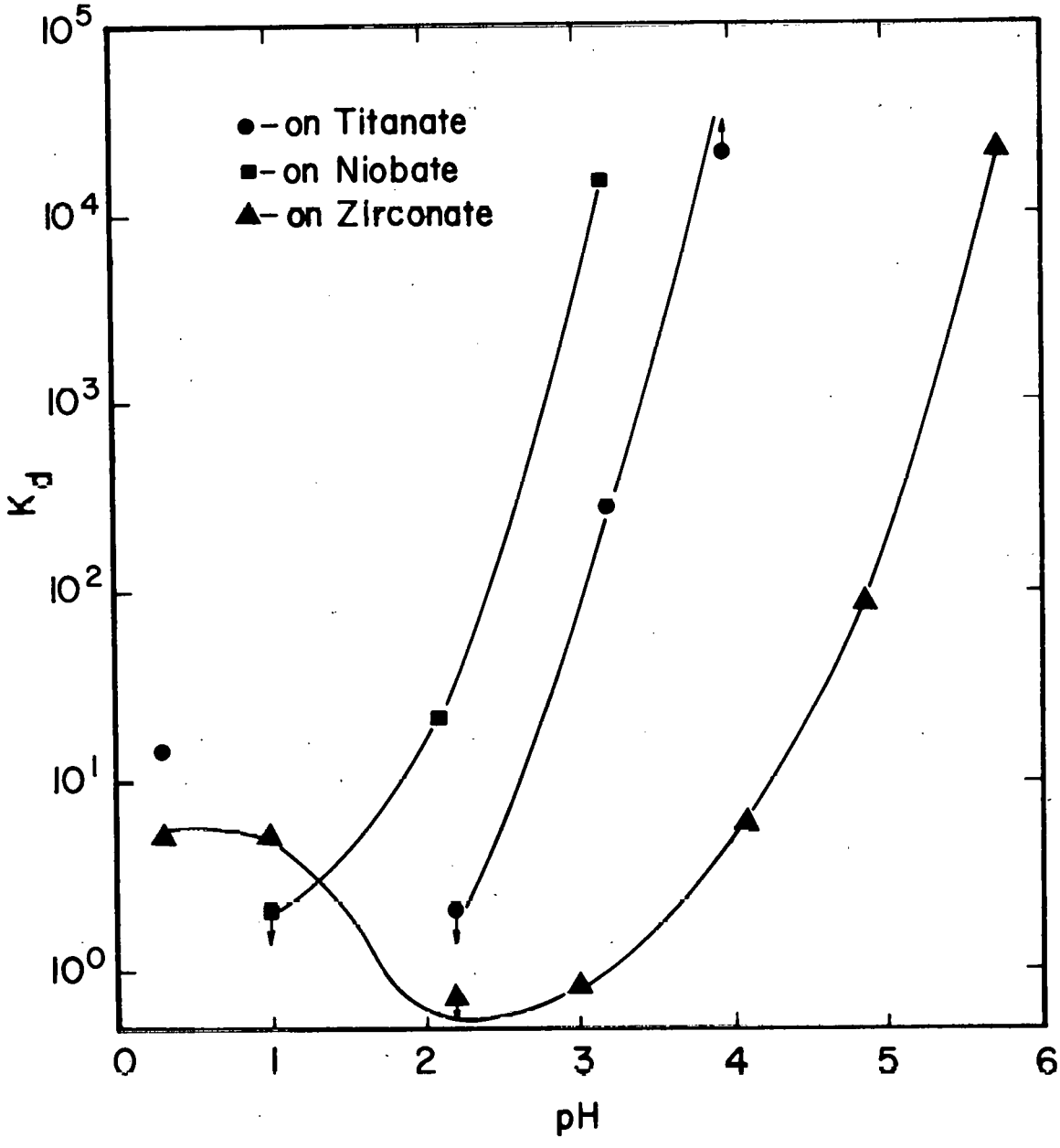

Fig. 5.1. Effect of pH on the affinity of lanthanum for various inorganic ion exchange materials.

to exchange H^+ for La^{3+} more easily (i.e., at a lower pH) than a weaker acid.

The strong dependence on pH of the K_d's is encouraging in that differences in K_d-vs-pH curves between lanthanides and actinides could be exploited as a basis for partitioning. Experiments are planned or in progress to establish K_d-vs-pH curves for europium, gadolinium, promethium, americium, and curium through the use of radiotracers.

6. RECOVERY ALTERNATIVES APPLICABLE TO WASTE STREAMS

E. P. Horwitz, W. H. Delphin, G. W. Mason, and M. Steindler
(Argonne National Laboratory)

This task focuses on processing alternatives for recovering actinides and technetium from high-level liquid waste. Additional work will examine alternatives for separating the lanthanides from the trivalent actinides and for recovering actinides from salt wastes.

6.1 Introduction

The present program is directed toward the examination of the feasibility of recovering macro amounts of long-lived actinides, neptunium, plutonium, americium, and curium, and fission product technetium and palladium from commercial high-level waste (HLLW), using dihexoxyethyl phosphoric acid (HDHoEP) and tricaprylmethyl ammonium nitrate (TCMA·NO_3). To date, the process is divided into three distinct parts. These parts have been developed in sufficient detail to permit flowsheet construction. An additional americium/curium-lanthanide separation step is being developed and will be incorporated into the flowsheet next quarter.

The first part of the process involves the extraction of uranium, neptunium, plutonium, americium, and curium from synthetic HLLW solution using HDHoEP in diethylbenzene (DEB). Zirconium, niobium, molybdenum, iron, yttrium, and the lanthanides are also extracted by the HDHoEP. An oxalate strip is used to back-extract the neptunium and plutonium, together with the zirconium, niobium, molybdenum, and iron. The americium, curium, yttrium, and lanthanides, which remain in the organic phase during the oxalate strip, are then back-extracted using 8 M HNO_3.

The second part of the process involves the purification of neptunium and plutonium from the zirconium, niobium, molybdenum, and iron and the oxalate strip solution using TCMA·NO_3 in DEB. Neptunium and plutonium are extracted into the organic phase and stripped with formic acid.

The third part of the process involves the extraction of technetium and palladium from the raffinate of the first part, using TCMA·NO_3 in DEB. Six molar nitric acid is used to back-extract the technetium and palladium.

Extensive extraction equilibria data have been obtained using HDHoEP and TCMA·NO_3. Preliminary conceptual flowsheets based on these data have been prepared and tested on synthetic HLLW. In constructing the flowsheet, emphasis was placed on achieving a high decontamination of actinides, technetium, and palladium from the HLLW.

The chemical information developed in the experimental program will be supplemented by several types of ongoing reviews aimed at evaluation of the feasibility of the above flowsheet. For example, the liquid-liquid extraction schemes will be tested in high-speed centrifugal contactors. Radiation stability and macro loading studies of HDHoEP and TCMA·NO_3 are already in progress. Some effort will also be directed at obtaining process-related information (e.g., corrosion of and compatibility with materials of construction, commercial availability of or estimated costs to produce reagents, safety-related properties, etc.).

A study of the feasibility of carrying out the third part of the separation scheme, as well as developing a flowsheet for salt-waste processing, using high-speed liquid-liquid chromatography (LLC) is under way. Early efforts have been directed at the evaluation of various inert supports for the stationary phases and at an assessment of column stability. The LLC studies will be described in the next quarterly report.

6.2 Experimental

6.2.1 Extractants

The quaternary amine employed in this study was TCMA·NO_3. A technical grade of this amine (called Aliquat-336 chloride*) was obtained from General Mills, Inc. This amine was either used as received for the flowsheet testing or was purified by liquid-liquid extraction using a cyclohexane-50:50 water:acetonitrile system for K_d measurements. The quaternary amine remains

---

*Trade name of General Mills, Inc., Kankakee, Ill.

in the acetonitrile phase, whereas the tertiary and lower amines concentrate in the cyclohexane phase. Two batch extractions (organic/aqueous ratio = 1) of the acetonitrile-water phase with cyclohexane are normally employed. Following the extraction, the acetonitrile-H_2O is removed from the quaternary amine by means of a commercial rotary evaporator. No detectable difference in the purified and technical-grade Aliquat-336 was observed. The HDHoEP was synthesized and purified following the procedure of Peppard, Mason, and Giffin.[1]

6.2.2 Measurements of K_d

Distribution ratio measurements were performed in the conventional manner using standard scintillation and gamma counting techniques. The K_d measurements* made at 50°C were carried out by placing 7-ml culture tubes containing the two phases in a constant-temperature water bath. After 5 min, the tubes were removed from the water bath and the phases were equilibrated for 15 sec by means of a vortex mixer. The culture tubes were then returned to the bath for 1- to 2-min intervals before being withdrawn and remixed for 15 sec. Four 15-sec equilibrations were used for K_d measurements at 50°C. However, one to two 15-sec equilibrations were used for flowsheet testing in order to simulate phase contact times in high-speed centrifugal contactors. Phases were never vortex-mixed longer than 15 sec before returning the tubes to the constant-temperature bath.

Hydroxylammonium nitrate (HAN), ferrous nitrate, and hydrazinium dinitrate were used as a reducing agent, a catalyst, and a nitrous acid scavenger respectively. The HAN was prepared from the hydrochloride salt by neutralizing the hydrochloride with Dowex 2-X8 on the hydroxyl cycle and the neutralizing the resultant hydroxyamine with HNO_3. The HAN was stored in 0.1 M HNO_3. Ferrous nitrate was prepared from ferric nitrate and HAN. A 0.17 M Fe(II)-0.50 M HAN stock solution was used in making the Np(IV) and Pu(III) K_d measurements. Hydrazinium dinitrate was also prepared from the

*The ratio of the organic to aqueous concentration at chemical equilibrium.

dihydrochloride salt by neutralizing the hydrochloride with Dowex 2-X8 on the hydroxyl cycle and then neutralizing the resultant hydrazine with HNO_3. The $N_2H_6(NO_3)_2$ was stored in 0.1 M HNO_3.

Tetramethylammonium hydrogen oxalate (TMA·HOx) was prepared by neutralizing standard 1 M oxalic acid solution with the stoichiometric quantity of standard tetramethylammonium hydroxide* solution.

6.2.3 Preparation of synthetic liquid waste

Synthetic waste solution was prepared by mixing HNO_3 solutions of salts of nonradioactive isotopes of fission products according to the procedure described by Bond and Leuze.[2] The quantities of fission product elements used corresponded to those calculated for a typical LWR fuel irradiated to a burnup of 33,000 MWd per tonne of heavy metal. The products from 1 tonne of this fuel were assumed to be present in either 5569 liters of 2.9 M HNO_3 (HAW waste stream) or 5900 liters of 2.4 M HNO_3 (EEW waste stream). (The EEW waste stream is formed from exhaustive TBP extraction of the HAW waste stream.) In addition to the fission products, 0.19 g of iron per liter (as ferric nitrate) was introduced into the synthetic waste (EEW waste stream) to simulate corrosion products. The presence of iron in the waste solution is particularly important in the proposed process because it is a catalyst for the reduction of Np(V) to Np(IV). Synthetic waste solution was filtered after preparation from stock solutions as described by Bond and Leuze.[2] Separate portions of the synthetic waste were spiked with $\sim 10^8$ dis/min of either ^{239}Np, ^{239}Pu, or ^{241}Am for flowsheet testing.

6.3 Results and Discussion

6.3.1 Extraction of Actinides using HDHoEP

The partitioning of the actinides from HLLW using the dialkylphosphoric acid, HDHoEP, is based on the high distribution ratios of tri-, tetra-, and hexavalent actinides from acidic solution. Figure 6.1 shows the K_d's of selected actinides as a function of HNO_3 concentration using 0.5 M HDHoEP

---

*Obtained from Eastman Organic Chemicals.

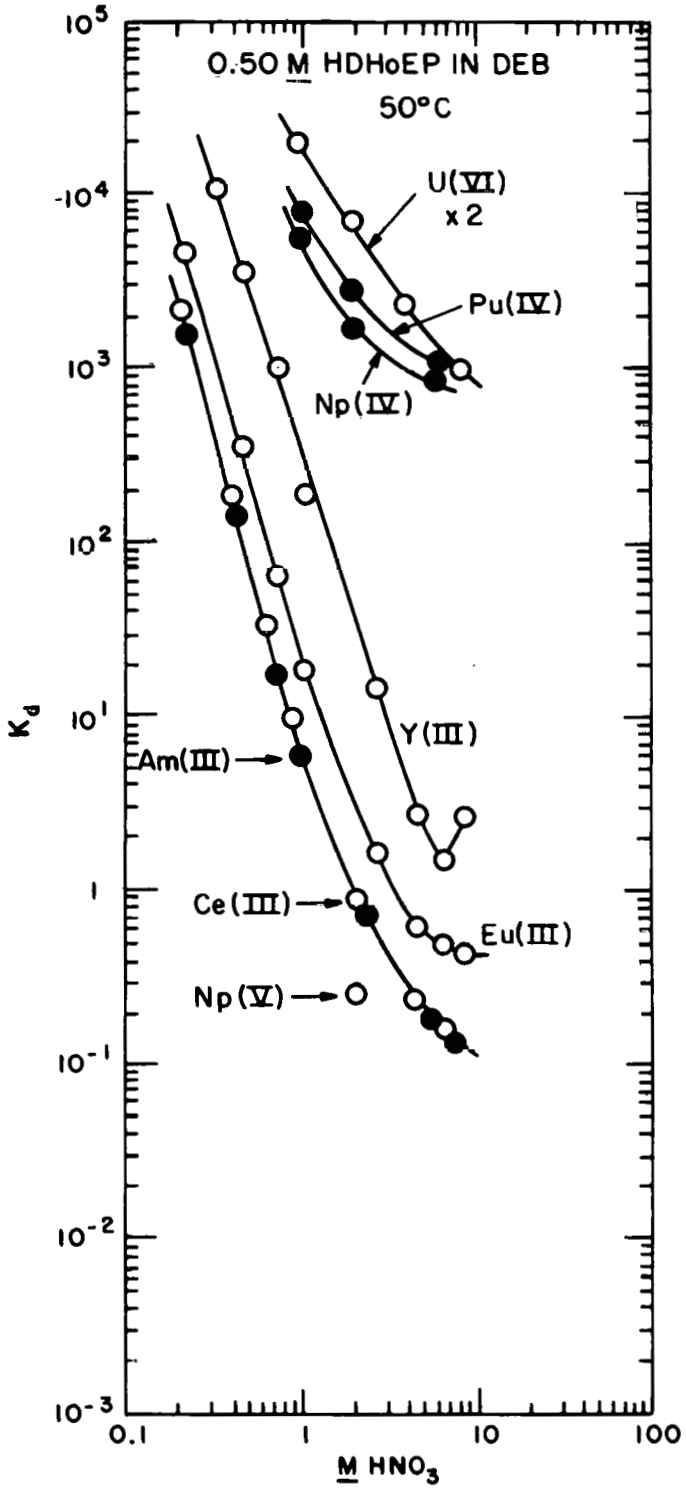

Fig. 6.1. Distribution ratios of selected actinides and of cerium, europium, and yttrium as a function of HNO_3 concentration. Organic phase - 0.05 M HDHoEP in DEB. U(VI) data - $K_d \times 2$; Pu(IV) - (0.05 M $NaNO_2$ + HNO_3); Np(IV) - (0.05 M HAN + 0.017 M Fe + 0.06 M N_2H_4 + HNO_3); Np(V) - (0.05 M HAN + HNO_3); Ce(III) - (0.05 M HAN + HNO_3). Pu(IV) and Np(IV) data were obtained by back-extraction.

in DEB at 50°C. The higher temperature was selected because of the self-heating effects which take place in HLLW. Distribution ratios for selected lanthanides were included for comparison. The K_d for Am(III) is slightly lower than that of Ce(III). Figure 6.2 shows the K_d of Am(III) in 1 M HNO_3 as a function of HDHoEP concentration in NDD and DEB. The lower K_d values for the aromatic diluent are expected because of the interaction of the benzene ring with the phosphate group. However, the difference in slopes and the change in curvature of the extractant dependency data are not easily explained. Peppard, Mason, and Giffin[1] found a significant difference between the aggregation of HDHoEP in an aromatic diluent and that in an aliphatic diluent. The average values of the molecular aggregation for a 0.1 M HDHoEP solution in benzene and cyclohexane are 2 and 3 respectively. These differences in aggregation cannot explain all the features of the extractant dependency curves. Vandegrift and Horwitz[3] have shown that, in the case of the extraction of Ca(II) by HDEHP, interfacial reactions enter into the equilibria and influence the reaction orders and thus the extractant dependencies.

The K_d data in Figs. 6.1 and 6.2 show high to moderate extractabilities of Am(III) from HNO_3 concentrations, even up to 1.5 M, using HDHoEP. The equilibria for the extraction of actinide(III) ions may be described by the following equations:

$$M^{3+} + n(HY)_m \rightleftarrows MH_{nm-3}Y_{nm} + 3H^+ \qquad (6.1)$$

$$Am^{3+} + 3/2(HDHoEP)_2 \rightleftarrows Am(DHoEP)_3 + 3H^+ \qquad (6.2)$$

at HNO_3 concentrations less than 1.5 M, and

$$MNO_3^{2+} + n(HY)_m \rightleftarrows M(NO_3)H_{nm-2}Y_{nm} + 2H^+ \qquad (6.3)$$

at HNO_3 concentrations above 1.5 M, where HY is the acid HDHoEP, Y is the anion $DHoEP^-$, and m is the degree of association of the extractant. The extraction of the nitrato complex at higher HNO_3 concentrations is indicated by the change in the acid dependency slope from -3.5 at low acidity to a slope of -2 at 4 M HNO_3. (A slope of -3.5 is expected for a tripositive ion

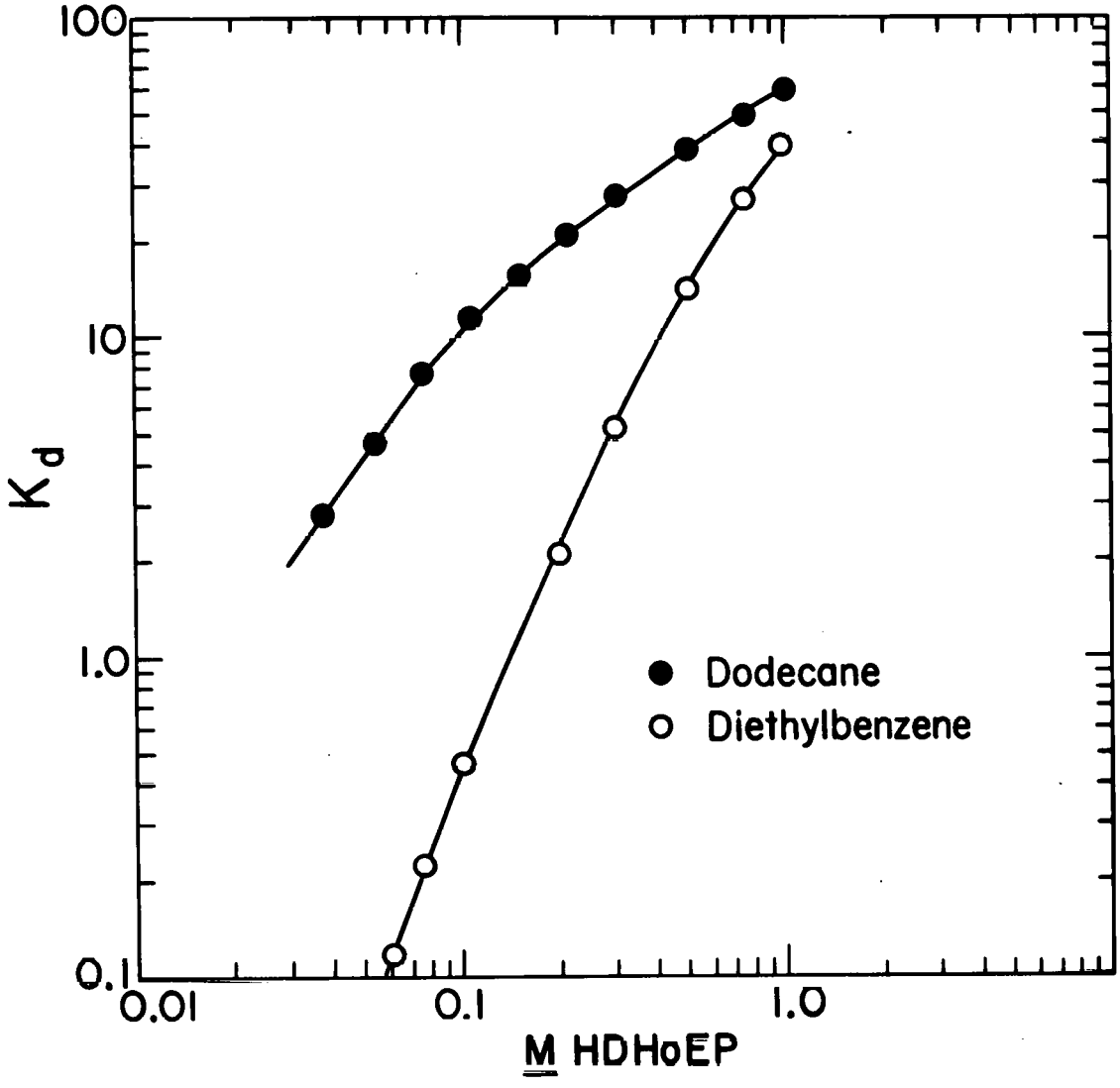

Fig. 6.2. Distribution ratio of Am(III) as a function of the molarity of HDHoEP in dodecane and in diethylbenzene. Aqueous phase - 1.0 M HNO_3; temperature = 25°C.

when the ionic strength is not held constant.) Lenz and Smutz[4] have shown that Nd(III) and Sm(III) also form nitrato complexes when extracted from high HNO_3 concentrations by HDEHP.

Extraction of macro concentrations of La(III), Nd(III), and Eu(III) from HNO_3 by 0.5 M HDHoEP in DEB has shown that saturation of the extractant occurs at a HDHoEP/M(III) ratio of 3.0 [note Eq. (6.2)]. No formation of precipitate took place on saturation, although the lanthanide-loaded organic phases did become rather viscous. An equilibrium curve for the extraction of macro concentrations of Eu(III) is shown in Fig. 6.3. The solubility of Ln(III)-HDHoEP complexes is strikingly different from the behavior of Ln(III) in HDEHP, which forms a precipitate when the Ln(III)/HDEHP ratio exceeds 1/6. It is possible that HDHoEP is acting as a tridentate ligand with the ether group, forming a seven-membered ring with the metal ion. Thus the M^{3+} ion would have a coordination number of nine, which in dilute solution is the case[5] for hydrated La^{3+} to Nd^{3+}.

The extraction of Am(III) was studied as a function of three independent variables, namely, acidity, extractant concentration, and temperature using a two-level, three-factorial experimental strategy. From these data a predictive model equation was derived expressing the log K_d as a function of acidity, extractant concentration, and temperature. The levels (ranges) of the three independent variables and the predictive modeling equations are shown in Table 6.1.

Separation factors* (α) at 50°C for selected trivalent metal ions relative to Am(III) at $\leq$2 M HNO_3 are as follows: Cm/Am = 1.1, Ce/Am = 1.2, Pm/Am = 1.9, Eu/Am = 3.0, and Y/Am = 33.0. These values agree fairly well with the data of Peppard, Mason, and Giffin[1] for HDHoEP in benzene vs $HClO_4$ at 25°C. The separation factors change somewhat at higher acidities. For example, the α for Y/Am decreases to 9.0 at 6 M HNO_3, which makes it possible to strip Y(III) along with Am(III) using 6 M HNO_3.

Figure 6.1 shows that the extraction of tetra- and hexavalent actinides is very high at all HNO_3 concentrations studied. This behavior is well

---

*Separation factor is defined as the ratio of distribution coefficients for two different extractable species at the same conditions.

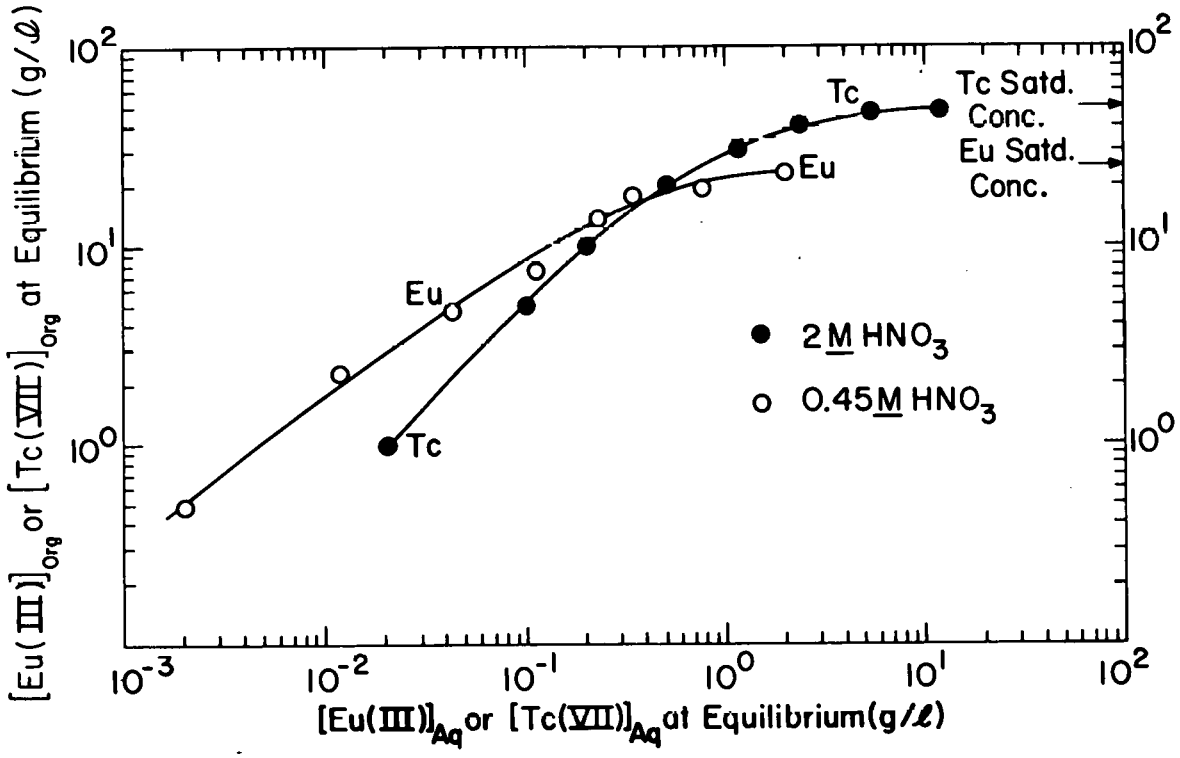

Fig. 6.3. Equilibrium curve for the extraction of Eu(III) from 0.45 M HNO_3 using 0.5 M HDHoEP in DEB and the extraction of Tc(VII) from 2 M HNO_3 using 0.50 M TCMA·NO_3 in DEB. Temperature = 50°C.

Table 6.1. Predictive model equations for the extraction of Am(III) by HDHoEP in DEB[a]

Equation number	High and low limits of independent variable		
	Acidity (M HNO_3)	Extractant concentration (M HDHoEP)	Temperature (°C)
1	0.413-2.0	0.05-0.1	50-25
2	0.413-2.0	0.10-0.5	50-25
3	0.413-2.0	0.50-1.0	50-25

Eq. (1)

$$\log K_d = -0.724 - 1.037X_1 + 0.393X_2 + 0.156X_3$$

$$X_1 = \frac{\log [HNO_3] + 0.0415}{0.343} \; ; \; X_2 = \frac{\log [HDHoEP] + 0.151}{1.151} \; ;$$

$$X_3 = \frac{(\frac{1}{t}°K) - 3.23 \times 10^{-3}}{1.3 \times 10^{-4}}$$

Eq. (2)

$$\log K_d = 0.422 - 1.110X_1 + 0.754X_2 + 0.130X_3$$

X_1 and X_2 same as in Eq. (1); $X_2 = \frac{\log [HDHoEP] + 0.651}{0.350}$

Eq. (3)

$$\log K_d = 1.369 - 0.499X_1 + 0.194X_2 + 0.097X_3$$

X_1 and X_2 same as in Eq. (1); $X_3 = \frac{\log [HDHoEP] + 0.151}{0.151}$

[a]These models will predict K_d to within $\pm$ 4% approximately 95% of the time for the defined ranges of the independent variables.

known for other dialkylphosphoric acid extractants (e.g., HDEHP). The difficulty in utilizing dialkylphosphoric acids as extractants for tetra- and hexavalent actinides lies in the problem of stripping these elements from the organic phase. This problem will be discussed below. The extraction of Np(IV) and Pu(IV) with HDHoEP, in all probability, involves the extraction of nitrato complexes, even from 1 M HNO_3. The slopes of acid dependency curves are less than 3, and the formation constants of actinide(IV)-nitrato complexes are higher than similar complexes for actinide(III) ions. Peppard, Mason, and McCarty[6] have conclusively shown that nitrate is transferred to the organic phase for the extraction of Th(IV) by HDEHP. The following equations describe some possible equilibria:

$$Pu(NO_3)_2^{2+} + (HDHoEP)_2 \rightleftarrows Pu(NO_3)_2(DHoEP)_2 + 2H^+, \quad (6.4)$$

$$Pu(NO_3)_3^{+} + (HDHoEP)_2 \rightleftarrows Pu(NO_3)_3(DHoEP)(HDHoEP) + H^+, \quad (6.5)$$

$$Pu(NO_3)_3^{+} + n(HY)_m \rightleftarrows Pu(NO_3)_3H_{nm-1}Y_{nm} + H^+, \quad (6.6)$$

where the abbreviations are defined as discussed previously. Similar equilibria may be written for the extraction of UO_2^{2+}:

$$UO_2^{2+} + 2(HDHoEP)_2 \rightleftarrows UO_2(DHoEP)_2 \cdot 2(HDHoEP) + 2H^+, \quad (6.7)$$

$$UO_2(NO_3)^{+} + n(HY)_m \rightleftarrows UO_2(NO_3)H_{nm-1}Y_{nm} + H^+ . \quad (6.8)$$

It is interesting to note that HDHoEP is acting as both an acidic and a neutral extractant in Eqs. (6.5) and (6.7), and possibly Eqs. (6.1), (6.3), (6.6), and (6.8). Similar behavior has been reported for the extraction of Nd(III) and Sm(III) by HDEHP.[4]

6.3.2 Extraction of selected fission and corrosion products using HDHoEP

Figure 6.4 shows the K_d's of selected fission products and corrosion products as a function of HNO_3 using 0.5 M HDHoEP in DEB at 50°C. As expected (based on previous experience with HDEHP), the K_d's for Fe(III),

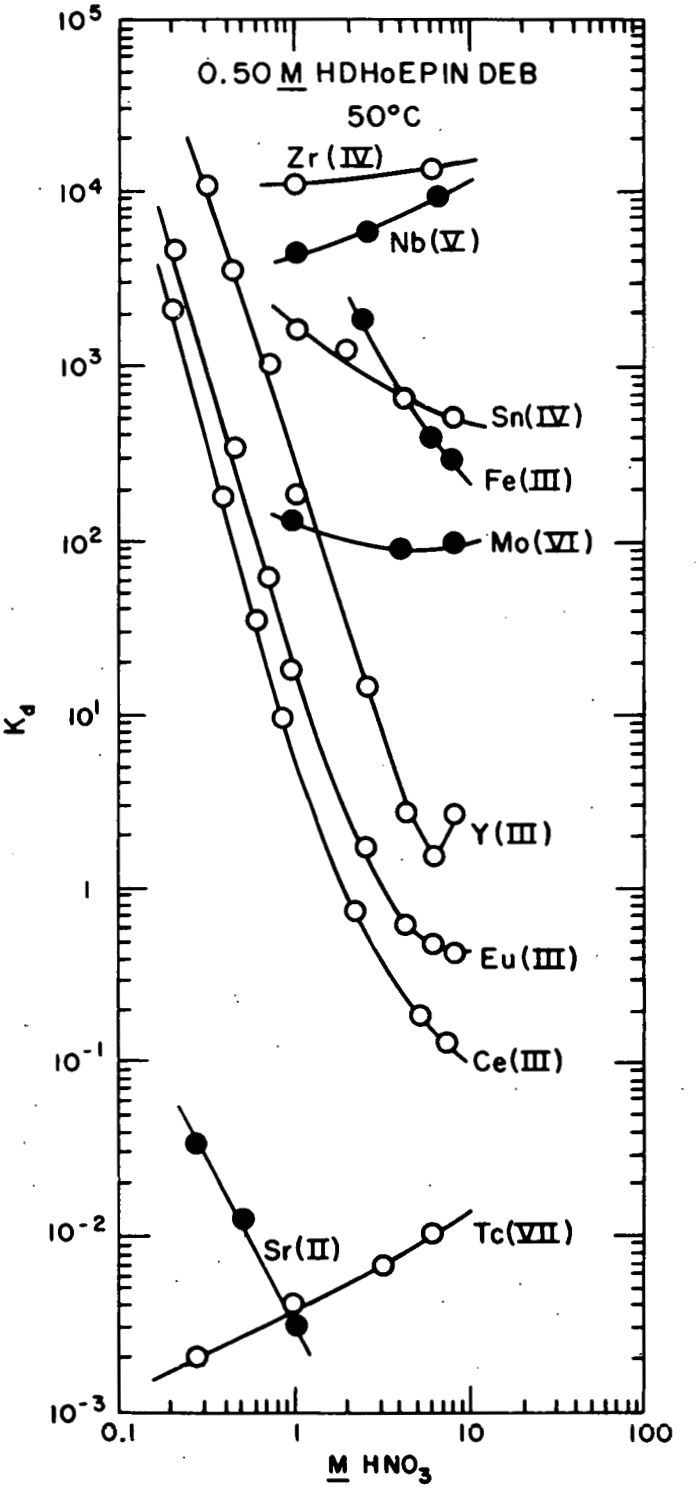

Fig. 6.4. Distribution ratios of selected fission products as a function of HNO_3 concentration. Organic phase - 0.05 M HDHoEP in DEB. Zr(IV), Nb(V), Mo(VI), and Fe(III) data were obtained by back-extraction.

Zr(IV), Nb(V), and Mo(VI) are high at all HNO_3 concentrations studied but have somewhat poor reproducibility because of variations in the species present in the aqueous phase (hydrolysis products with different extractabilities are apparently formed). Equations analogous to those used to describe the extraction of tetra- and hexavalent actinides may be written as follows:

$$ZrO^{2+} + 2(HDHoEP)_2 \rightleftarrows ZrO(DHoEP)_2 \cdot 2HDHoEP + 2H^+, \quad (6.9)$$

$$MoO_2^{2+} + 2(HDHoEP)_2 \rightleftarrows Mo(DHoEP)_2 \cdot 2HDHoEP + 2H^+. \quad (6.10)$$

The K_d's for Zr(IV) and Nb(V) were obtained by reverse extraction, that is, by equilibrating organic phase which contained the extracted nuclide with fresh aqueous phase. The reverse K_d's for Zr(IV) and Nb(V) are higher, by a factor of 1.5 and 20, respectively, than the forward K_d's.* The Fe(III) and Mo(VI) data were also obtained by reverse extraction. Nevertheless, Zr(IV), Nb(V), and Mo(VI) are all extracted to 98% or greater in 15-sec equilibrations. The extraction of Fe(III) by HDHoEP is somewhat slow, as is the case with HDEHP.

Figure 6.4 also shows the very poor extractibility of Sr(II) and Tc(VII). Although additional data on other fission products will be obtained in the near future, the following fission and corrosion products would be expected to be poorly extracted, based on experience with HDEHP:[7] rubidium, ruthenium, rhodium, palladium, silver, cadmium, tellurium, cesium, barium, nickel, and chromium. The extractibility of Sb(III) by HDHoEP, although uncertain, will probably be similar to that of some of the lanthanides. The K_d's of Sb(V) should be much less than those for the lanthanides.

6.3.3 Extraction of actinides from HLLW using HDHoEP

Figure 6.5 shows a conceptual flowsheet for the extraction of actinides from HLLW (EEW waste stream)[2] using 0.5 M HDHoEP in DEB. This flowsheet was

---

*Forward K_d's are probably lower because of hydrolysis products with different extractabilities, which are formed in the aqueous phase.

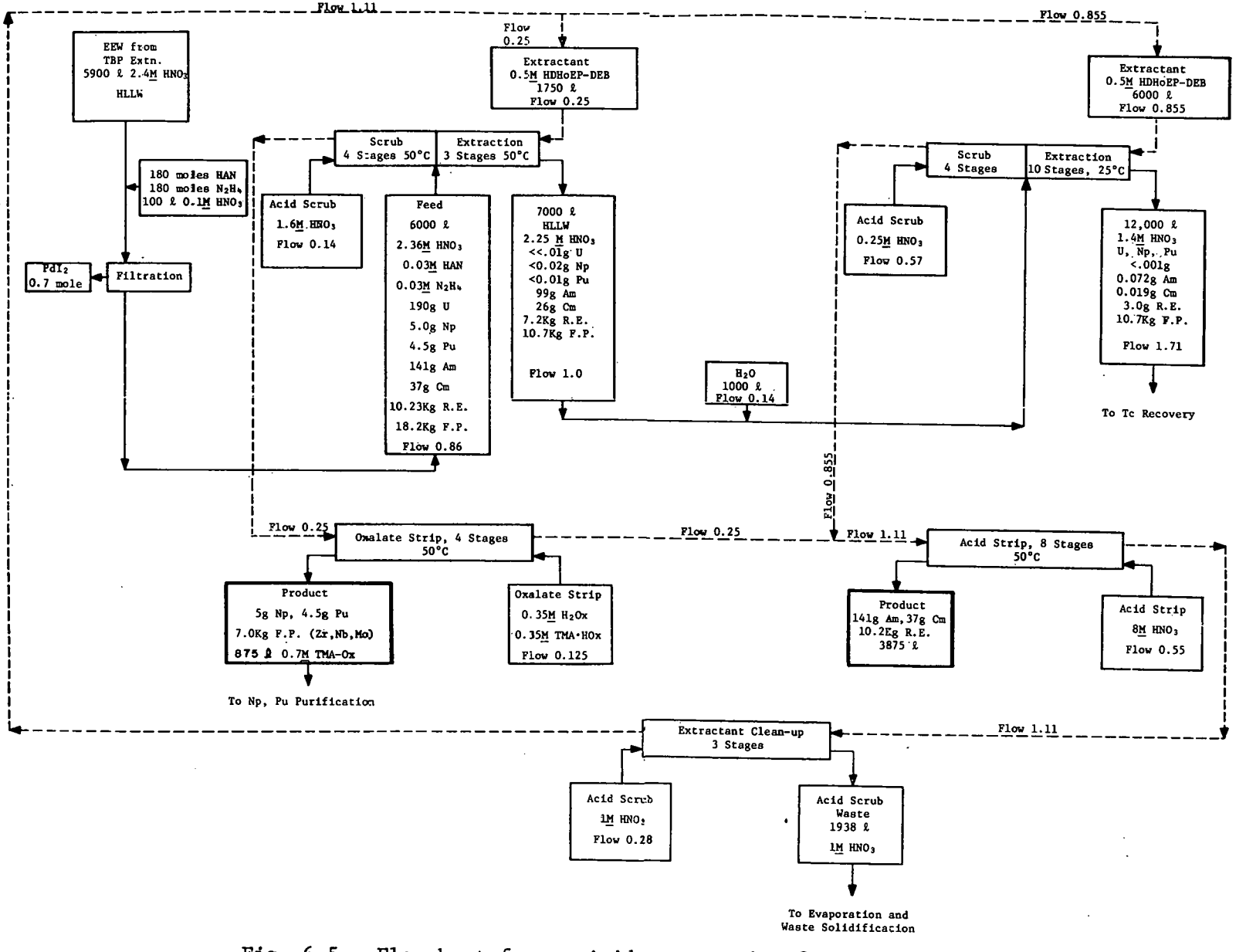

Fig. 6.5. Flowsheet for actinide extraction from HLLW using HDHoEP in DEB. Basis: 1 MTHM.

developed and is being tested using synthetic waste solution. The first step in the flowsheet involves the introduction of HAN and hydrazinium nitrate ($N_2H_4 \cdot 2HNO_3$) in order to adjust the oxidation states of neptunium and plutonium.[8,9] The HAN reduces Np(VI) to Np(V) and, in the presence of Fe(II), reduces Np(V) to Np(IV). Since iron is always present in the HLLW from corrosion of stainless steel, Fe(II) is produced from Fe(III) by reduction with the HAN. Hydrazinium nitrate is also introduced, along with the HAN, to remove excess HNO_3, which would destroy the HAN. These reducing agents would serve to reduce IO_3^- to I^-, which is subsequently precipitated by the excess Pd(II) present.

The PdI_2 could be removed by filtration or centrifugation before carrying out the subsequent liquid-liquid extraction (LLE), since the solid tends to concentrate at the organic-aqueous interface. A substantial portion (>90%) of the ^{129}I present in solution could probably be removed by this technique, although we have not investigated this process. It is expected, however, that in fuel reprocessing $\geq$99% of the iodine will report to the dissolver off-gas train. Any iodine remaining in the dissolver feed would be extracted by tri-n-butyl phosphate (TBP) during the exhaustive extraction and in the HA column. By introducing excess HI into the HLLW along with the HAN, one could probably remove the palladium and rhodium via precipitation of their iodides.

The HAN-Fe(II) mixture also reduces some Pu(IV) to Pu(III). However, it was found that Fe(II) was readily oxidized in 2 M HNO_3 by the acid. The destruction of the Fe(II) resulted in oxidation of Pu(III) to Pu(IV), but significantly, Np(IV) was not appreciably affected. A similar observation was made by Thompson, Burney, and Hyder[10] while studying the valence adjustment of neptunium and plutonium in enriched-uranium processing using ferrous sulfamate. The net effect of the HAN-N_2H_4 mixture is that neptunium and plutonium are adjusted to their tetravalent oxidation states.

Two separate streams of HDHoEP are used to extract the actinides from EEW waste. Calculations from the measured K_d values show that the first stream removes >99.5% of the uranium, neptunium, and plutonium and 30% of the americium, curium, and rare earths. Using an organic/aqueous phase ratio of 0.25 (that includes a scrub stream), about 34% of the capacity of

the HDHoEP would be consumed by the zirconium, molybdenum, yttrium, and iron which are extracted along with the actinides. However, both phases separate rapidly and cleanly. The extraction of americium and curium during the first stages is somewhat more complicated than the extraction of Np(IV) and Pu(IV) because of the influence of the macro amounts of zironium on the K_d's of the trivalent metal ions. The K_d of americium was found to be a factor of four times higher in the first stage (K_d = 2.4) than in the second and third stages (K_d = 0.6). This phenomenon may be explained by the interaction of macro quantities of zirconium with HDHoEP. Weaver[11] has shown that zirconium forms complexes with acidic phosphorus-based extractants, which are better extractants for metal ions than the original extractant. However, we believe that the effect of zironium is not large with HDHoEP, and once the bulk of this element is extracted (i.e., after the first stage), the K_d's of americium from the synthetic waste solution should be close to those measured using pure HNO_3.

The quantities of neptunium, plutonium, and americium extracted were calculated for an ideal, steady-state, countercurrent* LLE using the following equation:[12]

$$x_r = x_f \left[\frac{(RK) - 1}{(RK)^{n+1} - 1} \right] , \qquad (6.11)$$

where x_r and x_f are the concentrations of solute in the raffinate and the feed solution, respectively, R is the organic/aqueous phase ratio, K is the distribution ratio, and n is the number of stages (and hence RK is the usual extraction factor). In situations where the K_d was not constant for each stage, the following equation was substituted in the denominator of Eq. (6.11):

$$[1 + RK_1 + R^2K_1K_2 + R^3K_1K_2K_3], \qquad (6.12)$$

---

*The following assumptions also apply to Eq. (6.11): (1) constant K_d's, (2) constant organic/aqueous volume ratios, (3) phase equilibrium, (4) negligible backmixing, and (5) negligible interfacial effects for each stage.

where K_1, K_2, and K_3 are the distribution ratios in stages 1, 2, and 3, respectively. The squeous feed is introduced into stage 1. Equation (6.11) was also used in the following modified form to calculate the concentration of solute remaining in the aqueous phase after countercurrent stripping:

$$x_o = x_f \left[\frac{(R'K') - 1}{(R'K')^{n+1} - 1} \right] , \qquad (6.13)$$

where x_o and x_f are the concentrations of solute in the stripped organic and feed organic solutions, respectively, and R'K' (the conventional stripping factor) is the reciprocal of RK.

Table 6.2 gives the experimental RK values obtained for neptunium, plutonium, and americium using synthetic EEW. The low RK values for neptunium and plutonium in the second and third stages suggest the presence of primarily Np(V) and Pu(III), respectively. Essentially all of the Np(IV) and Pu(IV) are extracted in the first stage. Since curium has almost the same K_d as americium and the average K_d's for lanthanum-europium are also close to the K_d of americium, it was assumed that the fraction of curium and rare earths remaining in the raffinate would be the same as that of americium. On the other hand, more than 99.5% of the yttrium should be extracted by the HDHoEP.

Table 6.2. Experimental extraction factors for neptunium, plutonium, and americium from synthetic EEW

(Organic/aqueous ratio = 0.25; T = 50°C)

Element	Stage number		
	RK_1	RK_2	RK_3
Np	100	1	1
Pu	500	0.2	0.2
Am	0.58	0.14	0.14

The aqueous raffinate from the first HDHoEP extraction, which still contains 70% of the americium, curium, and lanthanides (lanthanum-europium), is diluted with H_2O and extracted again with 0.5 M HDHoEP in DEB. This treatment reduces the acidity to 1.4 M HNO_3, which increases the K_d for americium. In addition, the temperature is reduced to 25°C in order to further increase the K_d (see Table 6.1). Measured K_d's for americium using synthetic waste were in the range of 4 to 5. Assuming an RK of 2, a ten-stage, ideal, countercurrent LLE should give an overall americium-curium DF of $>10^3$.

The two loaded HDHoEP-DEB streams could be combined at this stage, passed through the americium, curium, and lanthanide stripping stages, and then routed to the plutonium, neptunium, zirconium, molybdenum, and iron stripping stages. However, it is more efficacious to keep the streams separated at this point because only the first HDHoEP-DEB stream contains any appreciable quantities of neptunium, plutonium, zirconium, molybdenum, and iron.

The neptunium and plutonium, together with the zirconium, niobium, molybdenum, and iron (but not uranium), are readily stripped from the loaded organic phase using a 0.35 M oxalic acid (H_2Ox)--0.35 M tetramethylammonium hydrogen oxalate (TMA·HOx) mixture. Under these conditions, most of the americium, curium, and rare earths would remain in the organic phase. The chemical basis for this step lies in the fact that the formation constants of the oxalato complexes for Np(IV), Pu(IV), Zr(IV), Nb(V), Mo(VI), and Fe(III) are many orders of magnitude larger than the formation constants of the oxalato complexes of Am(III), Cm(III), and rare earths(III). Table 6.3 contains a list of the formation constants (β_1 and β_2) of the oxalato complexes of U(VI), Am(III), and Zr(IV)[13] and of Np(IV) and Pu(IV).[14] The theoretical reduction in the K_d of Am(III) in the presence of oxalate ion can therefore be calculated using the following equation:

$$K_d = \frac{K_d^o}{1 + \beta_1[C_2O_4^{2-}] + \beta_2[C_2O_4^{2-}]^2}, \qquad (6.14)$$

Table 6.3. Formation constants of oxalato complexes obtained from the literature and calculated K_d reductions for certain actinides and zirconium at 0.083 M $[H^+]$

(T = 25°C, μ = 1.0, K_1 = 8.32×10^{-2}, and K_2 = 2.79×10^{-4} for oxalic acid)

	β_1[a]	β_2[b]	$1/1 + \beta_1[C_2O_4] + \beta_2[C_2O_4]^2$
U(VI)	5×10^{16}	10^{12}	7.3×10^{-7}
Np(IV)	1.7×10^{9}	4.2×10^{16}	1.7×10^{-11}
Pu(IV)	5.4×10^{9}	2.4×10^{17}	3.1×10^{-12}
Am(III)	4.3×10^{4}	2.2×10^{8}	2.9×10^{-3}
Zr(IV)	2×10^{10}	2×10^{20}	3.7×10^{-15}

[a] $\beta_1 = \dfrac{[M(C_2O_4)^{2+}]}{[M^{4+}][C_2O_4^{2-}]}$.

[b] $\beta_2 = \dfrac{[M(C_2O_4)_2]}{[M^{4+}][C_2O_4^{2-}]^2}$.

where K_d^o and K_d are the distribution ratios in the absence and presence of the oxalate ion, respectively, and β_1 and β_2 are the first formation constant and the product of the first and second formation constants, respectively. The concentration of $[C_2O_4^{2-}]$ is readily calculated as a function of $[H^+]$ by using the following equation:

$$\alpha = \frac{[C_2O_4^{2-}]}{C_T} = \frac{K_1K_2}{[H^+]^2 + K_1[H^+] + K_1 \cdot K_2}, \qquad (6.15)$$

where C_T is the total analytical concentration of oxalic acid plus oxalate, α is the fraction of C_T present as oxalate anion $[C_2O_4^{2-}]$ and K_1 and K_2 are the acid dissociation constants of oxalic acid. Values of $\alpha \cdot C_T$ can be substituted for $[C_2O_4^{2-}]$ in Eq. (6.14). By taking the $[H^+]$ of an equimolar mixture of $H_2C_2O_4$ and $TMA \cdot HC_2O_4$ as 0.083 M, and $C_T = 0.70$, a value of $\alpha \cdot C_T = 1.17 \times 10^{-3}$ is obtained. Substitution of this value in Eq. (6.14) allows the reductions in the K_d^o's for uranium, neptunium, plutonium, americium, and zirconium to be calculated (see Table 6.3).

Only in the case of Am(III) is it possible to estimate the K_d^o at 0.083 M $[H^+]$. If we ignore the effect of temperature on the $[H^+]$ and β values, the K_d for Am(III) in the presence of 0.35 M H_2Ox + 0.35 M $TMA \cdot H_2Ox$ is estimated to be ~70. This result is fairly close to the experimental value, which is ~52. Nevertheless, the reductions in K_d's for uranium, neptunium, plutonium, and zirconium in the presence of H_2Ox + $TMA \cdot HOx$ appear to be excessive. Table 6.4 shows some experimental K_d's for selected actinides and fission products in the presence of oxalic acid and $TMA \cdot HOx$. Table 6.5 shows the experimentally observed effect of increasing concentration of $TMA \cdot HOx$ on the K_d's of U(VI) and Pu(VI). The data in these tables agree semi-quantitatively with the calculated reductions in K_d in the presence of oxalate shown in Table 6.3. For example, the calculated reduction factors predict that Pu(IV) would be slightly more effectively stripped than Np(IV) but much more effectively stripped than U(IV). Both results are observed experimentally. In addition, the reduction factors predict that Zr(IV) would be easier to back-extract with oxalate than any of the actinides,

Table 6.4. Experimental back-extraction data for selected actinides and fission products[a] from 0.5 M HDHoEP in DEB using $H_2C_2O_4$ and $H_2C_2O_4$ + $TMA \cdot HC_2O_4$ at 50°C

	K_d		
	0.5 M $H_2C_2O_4$	0.25 M $H_2C_2O_4$ + 0.25 M $TMA \cdot HC_2O_4$	
		First contact	Second contact
Np(IV)		0.70	0.58
Pu(IV)	2.7	0.13	0.078
Am(III)		64	
Y(III)	254	250	
Zr(IV)	0.7	0.22	0.054
Nb(V)		0.010	0.0057
Mo(VI)	0.03	0.0057	0.0080
Fe(III)	0.44	0.089	0.0047
		0.35 M $H_2C_2O_4$ + 0.35 M $TMA \cdot HC_2O_4$	
		First contact	Second contact
Np(IV)		0.1[b]	
Pu(IV)		0.08[b]	
Am(III)		52[b]	

[a]Assumed valence state.

[b]Measured using loaded organic from synthetic waste solution.

Table 6.5. Experimental K_d's of U(VI) and Pu(IV) from 0.5 M HDHoEP in DEB using $H_2C_2O_4$ and $TMA \cdot HC_2O_4$ at 50°C

Medium	K_d	
	U(VI)	Pu(IV)
0.70 M H_2Ox	174	0.49
0.53 M H_2Ox + 0.17 M TMA·HOx	68.3	0.26
0.35 M H_2Ox + 0.35 M TMA·Hox	20.9	0.044
0.17 M H_2Ox + 0.53 M TMA·HOx	10.9	0.026
0.70 M TMA·HOx	5.39	0.019

which is also observed experimentally. The back-extraction of Pu(IV) may be expressed by the following equilibria:

$$Pu(NO_3)_2(HDoEP)_{2(org)} + 2H_2C_2O_{4(aq)} \rightleftarrows Pu(C_2O_4)_{2(aq)} + (HDHoEP)_{2(org)} + 2HNO_{3(aq)}, \quad (6.16)$$

$$Pu(C_2O_4)_2 + C_2O_4^{2-} \rightarrow Pu(C_2O_4)_3^{2-}, \quad (6.17)$$

where Eq. (6.17) represents the formation of higher, more-soluble oxalato complexes. No formation of precipitate has been observed during the oxalate stripping of loaded organic phase obtained from synthetic waste processing.

An R'K' value of 5.0 (RK = 0.2) was employed to calculate the fractions of neptunium and plutonium remaining in the organic phase, using Eq. (6.13). After four equilibrium stages, these fractions would theoretically be reduced by a factor of 770. Even less zirconium, niobium, molybdenum, and iron would remain in the organic phase; however, U(VI) and yttrium, together with americium, curium, and the lanthanides, would not be stripped. The resultant oxalate strip solution containing the neptunium and plutonium, along with zirconium, niobium, molybdenum, and iron, would then be transferred to the neptunium, plutonium purification cycle, which is discussed in Sect. 6.3.4.

After the oxalate strip, the first HDHoEP-DEB stream is combined with the second, and the resulting 7750 liters of 0.5 M HDHoEP in DEB is transferred to the 8 M HNO_3 stripping stage. An eight-stage countercurrent extraction, RK = 0.4, leaves only 0.04% of the americium and curium in the organic phase. The stripped HDHoEP-DEB stream, which still contains uranium and yttrium, is then transferred to the extractant cleanup.

Extraction cleanup, as shown in Fig. 6.5, involves only the use of a 1 M HNO_3 scrub. This scrub removes radiolytic decomposition products from the HDHoEP plus any excess HNO_3 extracted into the organic phase from the 8 M HNO_3 strip. Since yttrium and uranium have not been stripped from the extractant, they would be recycled. If one used the same HDHoEP-DEB stream for 20 processing cycles, approximately 10% of the extractant capacity would

be consumed by yttrium and uranium. However, if one applied the flowsheet in Fig. 6.5 to HAW waste, then yttrium and uranium would consume ∿20% of the extractant capacity after 20 cycles. However, the uranium concentration could be held down by continually withdrawing a few percent of the solvent volume for incineration and continuously replacing it with fresh solvent.

Investigations of the use of phosphoric acid for extractant cleanup are in progress. Approximately 8 M H_3PO_4 not only strips uranium (K_d = 0.27) and yttrium (K_d = 0.36) from 0.5 M HDHoEP in DEB but would also probably back-extract radiolytic and hydrolytic decomposition products readily. However, a method must be found for removing the yttrium and uranium from the scrub solution and recycling the phosphoric acid.

The physical properties of HDHoEP in DEB are quite favorable. A 0.5 M HDHoEP solution in DEB has a density of 0.879 g/ml. Phase disengagement throughout the various extraction, scrubbing, and stripping sections was excellent. In addition, no formation of emulsions or interfacial precipitates was observed. Preliminary tests on the radiation stability of 0.5 M HDHoEP solution in DEB have been carried out. No detectable change in either forward or reverse K_d's has been observed up to an absorbed dose of 20 Whr/liter. The extractant is also easily synthesized and purified, and should be comparable in cost to HDEHP.

6.3.4 Purification of neptunium and plutonium from oxalate strip using TCMA·NO_3

Figure 6.6 shows a flowsheet for the purification of neptunium and plutonium from the oxalate strip solution using 0.25 M TCMA·NO_3 in DEB. The process is based on the high extractabilities of Np(IV) and Pu(IV) from HNO_3 using TCMA·NO_3. Figure 6.7 shows the K_d's of selected actinides at 50°C using 0.50 M TCMA·NO_3 in DEB and selected fission products at 25°C using 0.50 M TCMA·NO_3 in Solvesso*. The fission product data were obtained from Koch.[15]

---

*Product of Exxon Chemical Co., Houston, Tex.

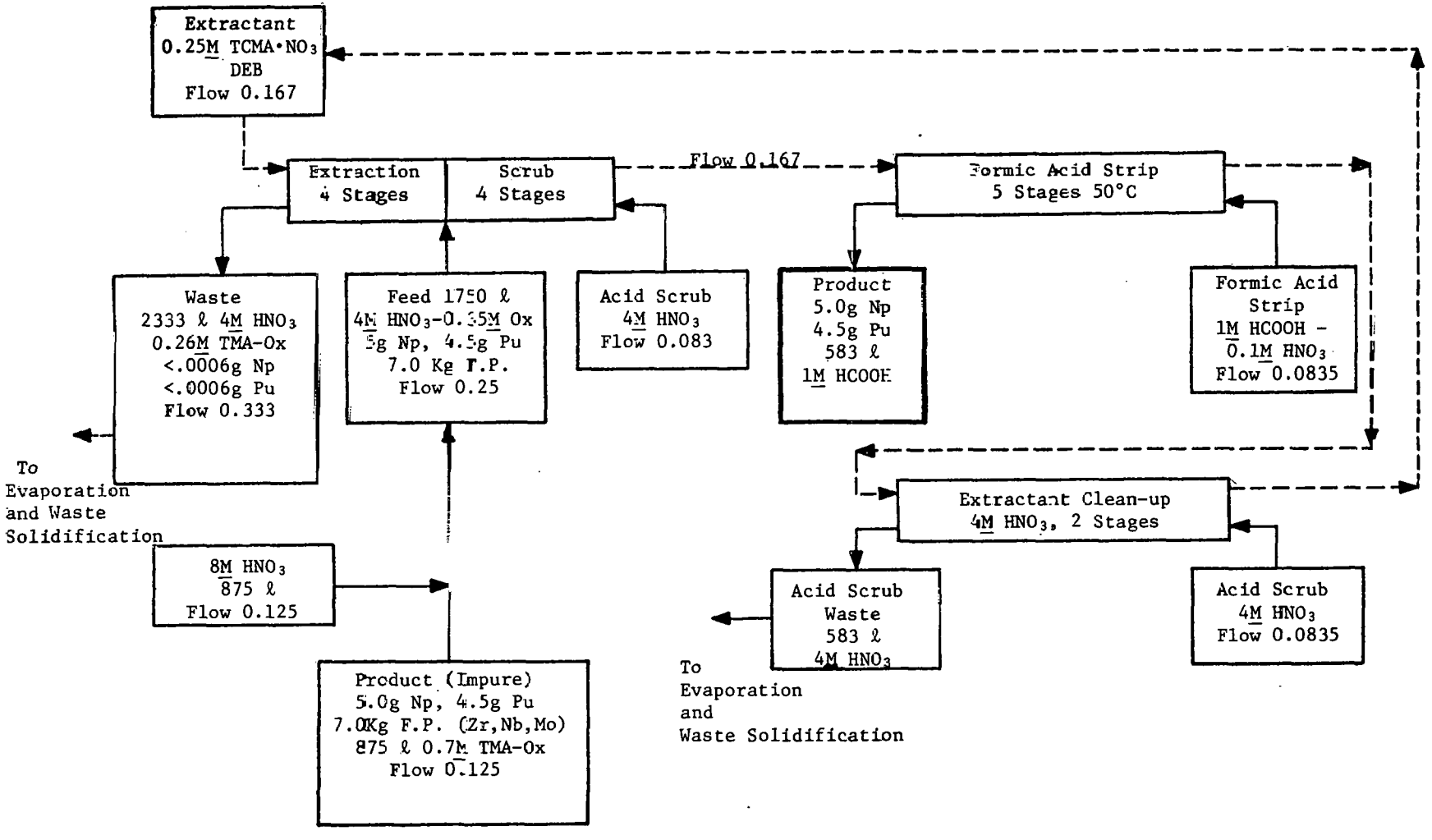

Fig. 6.6. Flowsheet for purification of neptunium and plutonium from oxalate strip. Basis: 1 MTHM.

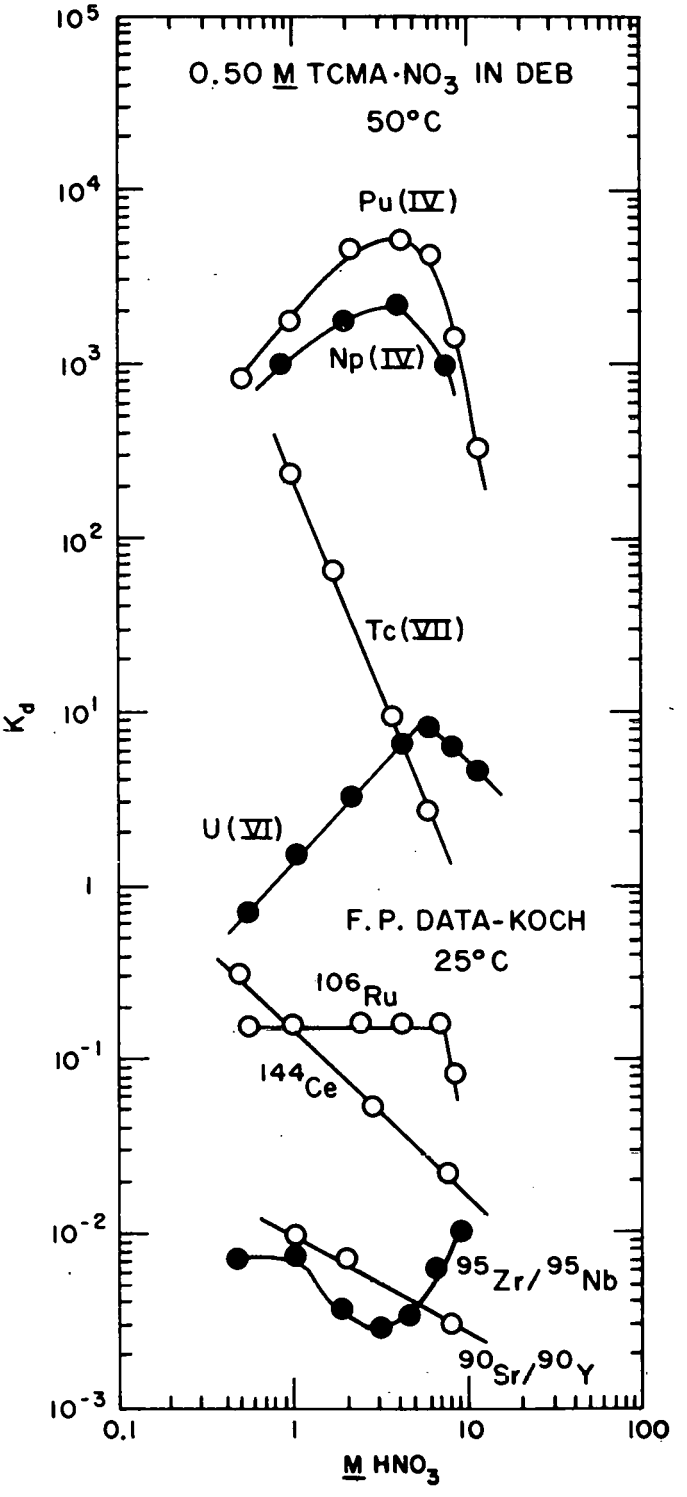

Fig. 6.7. Distribution ratios of selected actinides and fission products as a function of HNO_3 concentration. Organic phase - 0.50 M TCMA·NO_3 in DEB. Pu(IV) - (0.05 M $NaNO_2$ + HNO_3), Np(IV) - (0.05 M HAN + 0.017 M Fe + 0.06 M N_2H_4 + HNO_3). Pu(IV) and Np(IV) data were obtained by back-extraction.

The extraction of the tetranitrato complex of Pu(IV) by $TCMA \cdot NO_3$ is described by the following equilibrium:

$$Pu(NO_3)_{4(aq)} + 2R_3CH_3N^+NO_3^-{}_{(org)} \rightleftarrows (R_3CH_3N)_2Pu(NO_3)_{6(org)} , \qquad (6.18)$$

where R is a mixture of C_{10} and C_8 hydrocarbon chains. The stoichiometry of the extracted complex is supported by loading experiments and extractant dependency data.[15]

The first step in the process involves the addition of 8 M HNO_3 to the oxalate strip solution. The large increase in acidity effectively destroys the complexing ability of the oxalate ion. Since the H_2Ox-TMA·HOx back-extracts only tetravalent neptunium and plutonium and since $C_2O_4^{2-}$ stabilizes the tetravalent neptunium and plutonium, no valence adjustment step in the feed solution should be necessary. In order to ensure that the raffinate is decontaminated from neptunium and plutonium at least as well as the raffinate from the HDHoEP extraction, four ideal stages were used in the conceptual flowsheet, even though the RK was as high as 100 for plutonium and as low as 10^{-3} for zirconium.

The raffinate from the $TCMA \cdot NO_3$ extraction goes to an evaporation and waste solidification process. It is assumed at this stage that no difficulty will be encountered with the decomposition of $TMA \cdot HC_2O_4$. However, both this potential problem and the use of TMA·HOx as a possible substitute for $TMA \cdot HC_2O_4$ will be investigated.

The neptunium and plutonium are back-extracted from the organic phase using 1 M HCOOH-0.1 M HNO_3. (The presence of HNO_3 in the formic acid prevents formation of emulsions.) Table 6.6 shows the experimental K_d's for successive back-extractions of Np(IV) and Pu(IV) using 1 M HCOOH-0.1 M HNO_3. An RK value of 0.4 (R'K' = 2.5) was used to calculate the fractions of neptunium and plutonium remaining in the organic phase. After five equilibrium stages, these fractions would theoretically be reduced by a factor of 167.

The physical properties of $TCMA \cdot NO_3$ in DEB are also quite favorable. A 0.25 M $TCMA \cdot NO_3$ solution in DEB has a density of 0.87 g/ml. Phase disengagement was good, although somewhat slow during formic acid stripping. The radiation stability of $TCMA \cdot NO_3$ in xylene has recently been investigated by Contarini et al.[16] They found that absorbed doses in the range of

Table 6.6. Experimental K_d's of Np(IV)[a] and Pu(IV) from 0.25 M TCMA·NO_3 in DEB using 1 M HCOOH-0.1 M HNO_3 at 50°C

Contact	Np(IV)[a]	Pu(IV)
First	0.38	0.66
Second	0.24	0.25
Third	0.18	0.23

[a]Valence state is uncertain.

50 to 100 Whr/liter had relatively small negative effects on the extraction properties of Aliquat-336 nitrate in xylene. Thus, the extractant cleanup step using 4 M HNO_3 shown in Fig. 6.6 is little more than a preconditioning step to remove HCOOH.

6.3.5 Extraction of technetium and palladium from liquid waste using TCMA·NO_3 in DEB

Figure 6.8 shows a conceptual flowsheet for the extraction of technetium and palladium from the raffinate obtained from the HDHoEP extraction of americium and curium (see Fig. 6.5). The process is based on the high extractabilities of Tc(VII) and Pd(II) from $\leq$3 M HNO_3 using TCMA·NO_3. Figure 6.7 shows the K_d of Tc(VII) as a function of HNO_3 using 0.50 M TCMA·NO_3 in DEB at 50°C. Only preliminary K_d data on palladium extraction with TCMA·NO_3 are available at this time; however, these data indicate that Pd(II) has essentially the same or slightly lower K_d's than Tc(VII) from 1.5 and 6.0 M HNO_3 using 0.10 M TCMA·NO_3 in DEB. More complete distribution ratios for Pd(II) will be obtained during the next report period. Therefore, the results shown in Fig. 6.7 are tentative.

Figure 6.9 shows the extractant dependency of Tc(VII) on TCMA·NO_3 molarity in DEB from 1 M and 6 M HNO_3 and an extrapolated extractant dependency at 2 M HNO_3. The lines in Fig. 6.9 have slopes of 1.0, which indicates a simple 1:1 ratio of amine:pertectnetate:

$$TcO_4^- + R_3CH_3N^+NO_3^- \rightleftarrows R_3CH_3N^+TcO_4^- + NO_3^- \qquad (6.19)$$

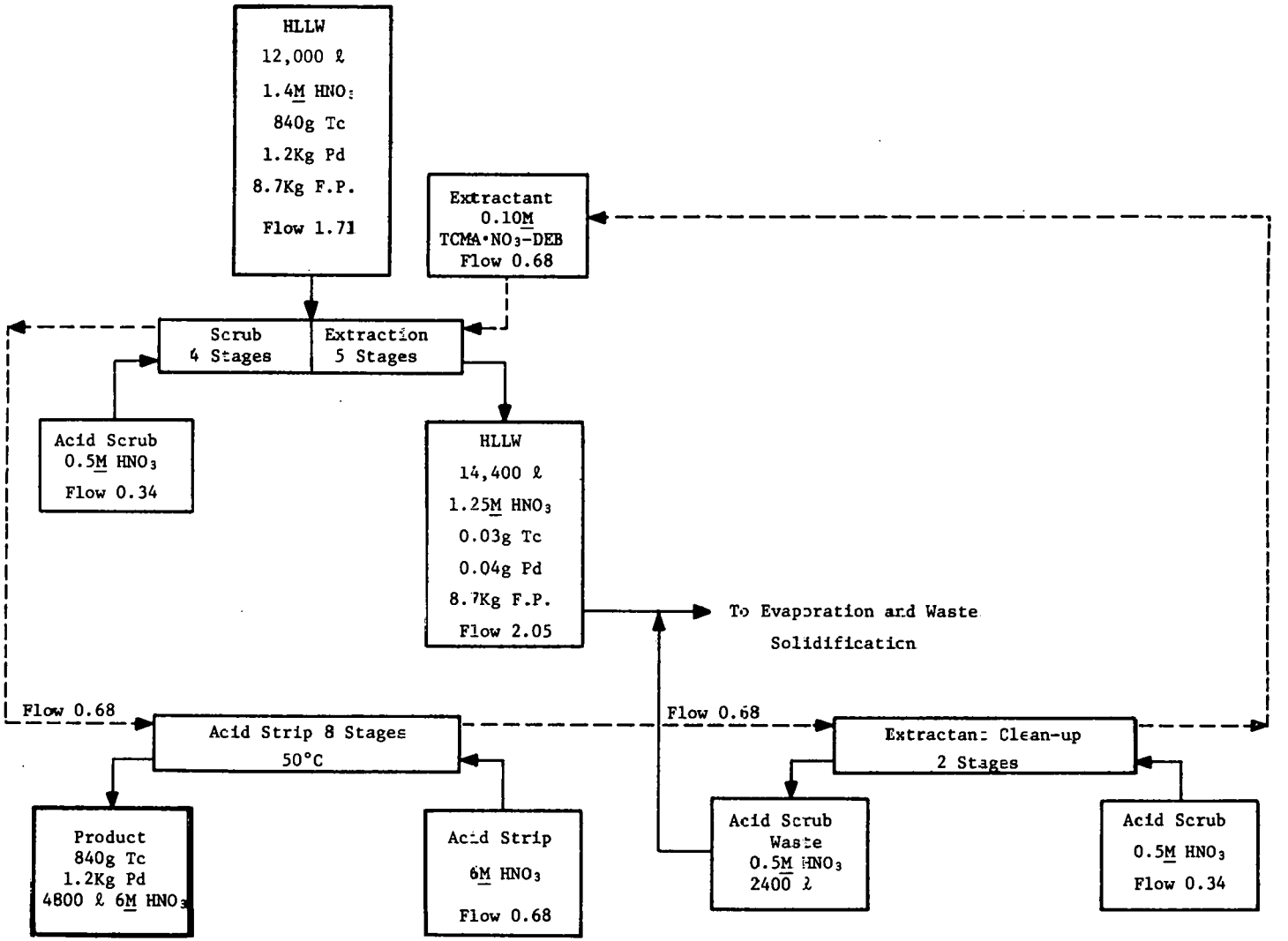

Fig. 6.8. Flowsheet for extraction of technetium and palladium from HLLW using $TCMA \cdot NO_3$ in DEB. Basis: 1 MTHM.

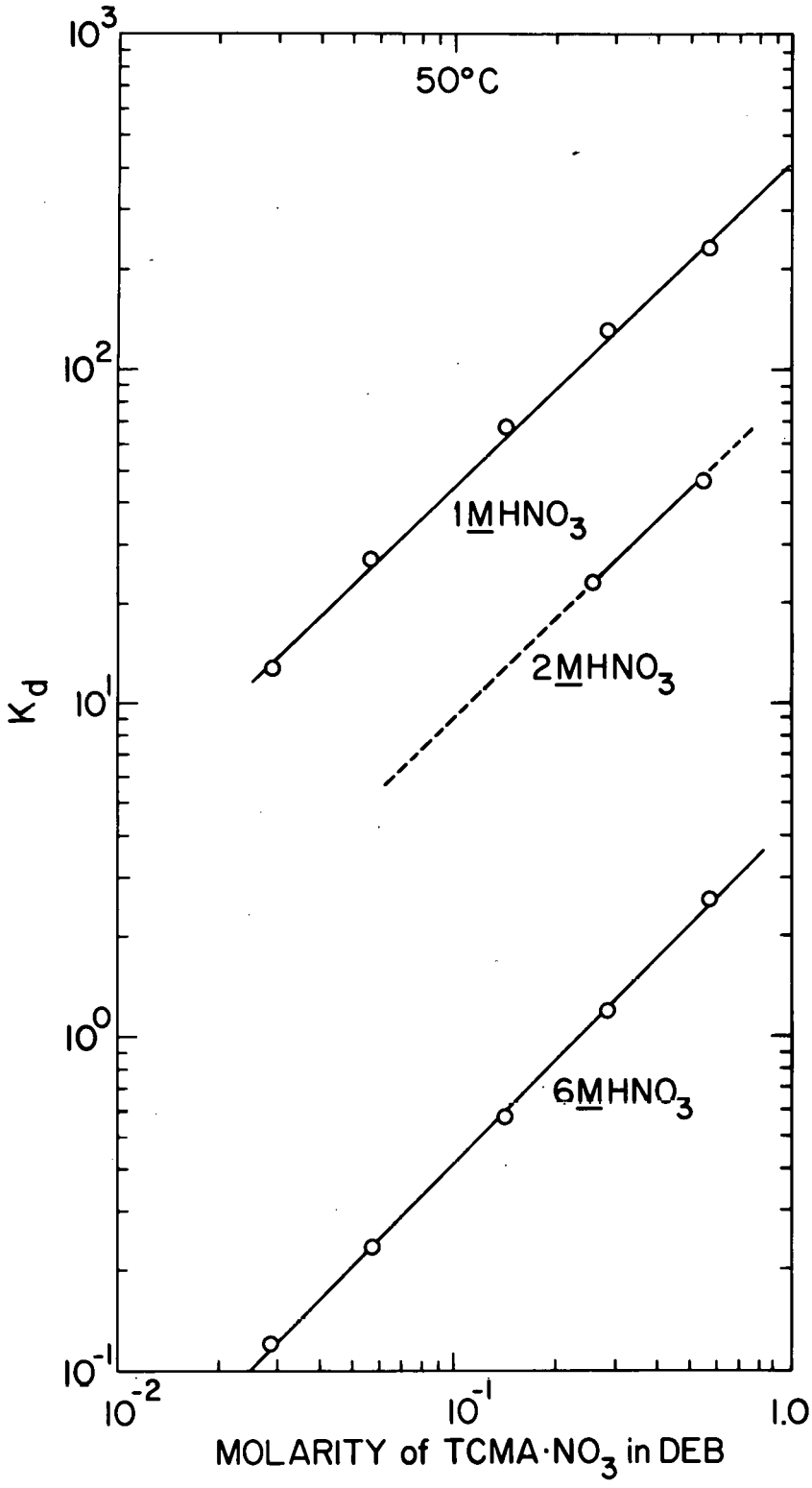

Fig. 6.9. Distribution ratio of Tc(VII) as a function of the concentration of $TCMA \cdot NO_3$ in DEB. Temperature = 50°C.

Extraction of macro concentrations of TcO_4^- from 2 M HNO_3 using 0.50 M TCMA·NO_3 in DEB have shown that saturation of the extractant occurs at a TCMA/TcO_4^- ratio of 1.0. No precipitate or third-phase formation took place on saturation. An equilibrium curve for the extraction of macro concentrations of TcO_4^- is shown in Fig. 6.3. Molecular weight data, on the other hand, show that the average aggregation number of high-purity trioctylmethylammonium nitrate (TOMAN) in xylene gradually increases from 1 in dilute solution ($\leq 10^{-2}$ M) to 8 in a 0.5 M solution.[17] This gradual change in aggregation number of the quaternary ammonium salt complicates the interpretation of the first-power extractant dependencies data. The explanation probably lies in the mechanism of the pertectnetate extraction, which is currently being investigated.[17]

The flowsheet described in Fig. 6.8 is based on the extraction of Tc(VII) and Pd(II) from 1.25 M HNO_3 using 0.10 M TCMA·NO_3 in DEB. The K_d and RK values for Tc(VII) from 1.25 M HNO_3 are ∿24 and ∿8, respectively, at 30°C. It was assumed that Pd(II) has a comparable K_d under these conditions. Approximately 6% of the extractant capacity would be consumed by the technetium and palladium, assuming that the TCMA/metal ratios are 1 for technetium and 2 for palladium. Using a low-molarity solution of TCMA·NO_3 makes it feasible to strip the technetium and palladium with nitric acid. The RK value is 0.42 for 6 M HNO_3 at 50°C.

As discussed in Sect. 6.3.4, the physical properties of the TCMA·NO_3 in DEB and its radiation stability appear to be very favorable. The extractant cleanup would probably be essentially a preconditioning step to remove excess HNO_3 from the organic phase.

6.4 Conclusions

A flowsheet for the extraction of neptunium, plutonium, americium, and curium, as well as fission product technetium and palladium, from HLLW has been developed based on laboratory batch extraction data obtained using synthetic waste. The process utilizes HDHoEP and TCMA·NO_3 as the extractants for the actinides and technetium, palladium, respectively. Either known or reasonably probable distribution coefficients were used in developing

the process and predicting the theoretical stages required for the desired separation factors. The flowsheets have been tested using synthetic liquid waste and appear to be functional. Physical properties and stability to radiation of the two extractants are very favorable; however, extractant cleanup is complicated by difficulties in stripping yttrium and uranium. Additional work on this problem and the separation of americium-curium from rare earths is in progress.

6.5 Acknowledgments

The authors wish to thank C. A. A. Bloomquist, H. Griffin, and S. Lewey for performing many of the K_d measurements. Appreciation is also expressed to W. B. Seefeldt and R. Leonard for helpful discussions in preparing the flowsheets.

6.6 References for Section 6

1. D. F. Peppard, G. W. Mason, and G. Giffin, "Extraction of Selected Trivalent Lanthanide and Actinide Cations by Bis(hexoxyethyl)Phosphoric Acid," J. Inorg. Nucl. Chem. 27, 1683 (1965).

2. W. D. Bond and R. E. Leuze, Feasibility Studies of the Partitioning of Commercial High Level Wastes Generated in Spent Nuclear Fuel Reprocessing: Annual Progress Report for FY-1974, ORNL-5012 (January 1975).

3. G. Vandegrift and E. P. Horwitz, "The Mechanism of Interfacial Mass Transfer of Calcium in the System: Di(2-ethylhexyl) Phosphoric Acid in Dodecane - Dilute Nitric Acid," J. Inorg. Nucl. Chem. (in press).

4. T. G. Lenz and M. Smutz, "The Extraction of Neodymium and Samarium by Di(2-ethylhexyl) Phosphoric Acid from Aqueous Chloride, Perchlorate, and Nitrate Systems," J. Inorg. Nucl. Chem. 30, 621 (1968).

5. F. H. Spedding, P. F. Cullen, and A. Habenschuss, "Apparent Molar Volumes of Some Dilute Aqueous Rare Earth Salt Solutions at 25°," J. Phys. Chem. 78, 1106 (1974).

6. D. F. Peppard, G. W. Mason, and S. McCarty,"Extraction of Thorium (IV) by Di Esters of Orthophosphoric Acid, $(GO)_2Po(OH)$," J. Inorg. Nucl. Chem. 13, 138 (1960).

7. G. Ghersini, in T. Braun and G. Ghersini (eds.), Extraction Chromatography, pp. 68-133, Elsevier, Amsterdam (1975).

8. J. M. McKibben and J. E. Bercaw, Hydroxylamine Nitrate as a Plutonium Reductant in the Purex Solvent Extraction Process, DP-1248 (January 1971).

9. G. S. Barney, "A Kinetic Study of the Reaction of Plutonium(IV) with Hydroxylamine," J. Inorg. Nucl. Chem. 38, 1677 (1976).

10. M. C. Thompson, G. A. Burney, and M. L. Hyder, Neptunium and Plutonium Valence Adjustment in Enriched Uranium Processing, DB-1396 (March 1976).

11. B. Weaver,"Enhancement by Zirconium of Extraction of Cations by Organophosphorus Acids, I. Monoacidic Phosphonates," J. Inorg. Nucl. Chem. 30, 2233 (1968).

12. L. Alders, Liquid-Liquid Extraction Theory and Laboratory Experiments, p. 95, Elsevier, 1955.

13. A. E. Martell, Stability Constants of Metal Ion Complexes, Supplement No. 1, Special Publication No. 25, The Chemical Society, Burlington House, London, 1971.

14. S. V. Bagawde, V. V. Ramakrishna, and S. K. Patil,"Oxalate Complexing of Tetravalent Actinides," J. Inorg. Nucl. Chem. 38, 1669 (1976).

15. G. Koch, in A. A. C. McKay, T. V. Healy, I. L. Jenkins, and A. Naylor (eds.), Solvent Extraction Chemistry of Metals, pp. 247-66, Chemical Rubber Co. Press, Cleveland, 1967.

16. M. Contarini, P. Pasquinelli, and L. Rigali,"The Effect of Gamma Irradiation on Extraction Properties of a Quaternary Ammonium Extractant," Radiochim. Acta 22, 88 (1975).

17. G. Dyrkacz, G. Vandegrift, M. Thomsen, and E. P. Horwitz,"The Kinetics of Pertectnetate Extraction by Quaternary Ammonium Salts," J. Inorg. Nucl. Chem. (to be published).

7. ACTINIDE RECOVERY FROM COMBUSTIBLE WASTE

G. H. Thompson, E. L. Childs, and D. L. Cash
(Rockwell International, Rocky Flats Plant)

The objective of this task is to determine the recoverability of actinides from incinerator ashes. During the second year, the distribution of actinides through the preferred recovery system will be measured.

7.1 Introduction

Combustible wastes produced during reactor fuel fabrication and reprocessing are comprised of paper, wood, plastics, rubber, cloth, spent solvent, activated carbon, and ion exchange resins. These wastes are incinerated or acid digested to reduce volume and organic content as well as to facilitate actinide recovery. The product is a residue containing actinides and fission products. The objective of this project is to evaluate methods for recovering actinides from these residues. ORNL has explicitly stated that only currently known recovery methods are to be evaluated. In order for a method to receive serious consideration, it must (1) provide efficient recovery of actinides from residues in a form suitable for recycle or transmutation, (2) result in little actinide entrainment in the process off-gas, (3) not materially increase final waste volumes, and (4) not deleteriously affect glass or concrete waste forms.

During the first report period, a preliminary literature survey was completed.[1] A preliminary evaluation of common leaching and fusion methods showed that fusion with commonly used reagents dissolves >60% of the ash from the fluidized-bed incinerator (FBI) process and leaching with concentrated HNO_3 dissolves 40 to 60% of the same ash. Preparation of plutonium-contaminated ash was initiated.

7.2 Experimental

7.2.1 Materials

An attempt was made to prepare contaminated ash by adding plutonium nitrate in 0.35 M HNO_3 to ash, drying the ash, and then fluidizing it in a

quartz reactor at 550°C. Although the amount of nitrate present was small, deflagration occurred at approximately 325°C. This was not unexpected since about 20% of FBI ash is carbon, but the outcome confirmed that a different approach will have to be used for preparing the ash.

Because the most difficult actinide to recover will be high-fired PuO_2 resulting from fuel fabrication operations, ORNL suggested that this material be used to evaluate the proposed recovery methods. Further, since trivalent actinides and lanthanides will be present during fuel fabrication, it was suggested that ^{241}Am tracer be included.

The PuO_2 used in the experiments was prepared as follows. Plutonium metal was dissolved in 12 M HCl with cooling. The solution was adjusted to 7 M NO_3^-, and the plutonium was sorbed on anion exchange resin. The column was then washed with five column volumes of 7 M HNO_3 and the plutonium eluted with 0.35 M HNO_3. The acidity was subsequently adjusted to 0.5 M by denitration with formic acid. Finally, a tracer amount of ^{241}Am was added and plutonium and americium were precipitated as the oxalates. After drying, the actinide oxalates were calcined at 925°C to constant weight. Analysis determined the americium concentration to be 2.27×10^{-4} g per gram of plutonium. All fusion and leaching agents used in these experiments were reagent-grade chemicals.

7.2.2 Procedure

An attempt was made to dissolve 0.1 g of the high-fired PuO_2 in 25 ml of concentrated HNO_3 (liquid:solid ratio of 250:1). The mixture was refluxed for 12 hr; a total reflux condenser was used to prevent liquid loss. After the mixture had been cooled sufficiently, it was filtered. The filtrate was subsequently diluted to a known volume and sampled. Undissolved PuO_2 was refluxed in a solution of 0.1 M F^- in 12 M HNO_3 for 2 hr. After the mixture had been cooled, it was filtered. The resulting filtrate was then diluted to a known volume and sampled.

Two tests were made of the acid digestion method developed by Lerch and Cooley.[2,3] Twenty milliliters of 95 vol % H_2SO_4 – 5 vol % HNO_3 was refluxed with 0.2 g of PuO_2 for 12 hr (test 1) and for 16 hr (test 2). Additional HNO_3 was added incrementally during this time (2 to 3 ml/hr).

After cooling, the acid was removed by filtration and the residue was washed with 4 M HNO_3 to solubilize plutonium and americium sulfates. The residue (undissolved oxide) was removed by filtration and then solubilized by refluxing in a solution of 0.1 M F^- in 12 M HNO_3, as described above.

For fusion experiments, 10 g of flux was mixed with 0.1 g of PuO_2 (flux:solid ratio of 10:1). NaOH fusions were done in both nickel and high-purity alumina crucibles. Other basic fluxes (Na_2CO_3, 90 wt % Na_2CO_3-10 wt % Na_2SO_4, 90 wt % Na_2CO_3-10 wt % $NaNO_3$, and 50 wt % Na_2CO_3-50 wt % $Na_2B_4O_7 \cdot 10\ H_2O$) were evaluated in the high-purity alumina crucibles. Acidic fusions (with $KHSO_4$ and $K_2S_2O_7$) were carried out in quartz crucibles. Samples were mixed and fused at the desired temperature for 2 hr. After cooling, the samples were solubilized in 4 M HNO_3 and filtered to remove any PuO_2 remaining; then the filtrate was diluted to a known volume and sampled. The residues were solubilized by refluxing in a solution of the composition 12 M HNO_3-0.1 M F^-. After cooling and filtration, these solutions were also diluted to a known volume and sampled.

The effect of time was evaluated via fusion tests of 8 hr duration. The actinide recovery methods were identical to those described above.

7.3 Results and Discussion

The results of the leaching and acid digestion experiments are summarized in Table 7.1. The results of the fusion experimenta are presented in Tables 7.1 and 7.2. Actinide recovery is expressed as the percent recovered of the original quantity.

Leaching with concentrated HNO_3 recovered only 0.09% and 3.5% of the plutonium and americium present, respectively. Such a low recovery is not surprising for PuO_2, and americium, which forms more soluble oxides, was apparently trapped within the plutonia matrix. This explanation is suggested by the similarity in the amount of plutonium and americium recovered, and a consistent trend was observed throughout for a given method.

The acid digestion process succeeds in solubilizing the high-fired oxides; however, it appears to be fairly slow and required frequent additions of HNO_3, with resultant evolution (at the $\sim$230°C reflux temperature) of NO_x. Additional study is needed for an adequate evaluation of this method.

The efficiency of NaOH fusion (Table 7.1) depended on the type of crucible used. For example, fusion in nickel crucibles gave much better

Table 7.1. Actinide recovery by leaching, digestion, and fusion

Leachant:solid ratio = 250:1
Digestant:solid ratio = 100:1
Flux:solid ratio = 100:1
Sample: Am-traced PuO_2 (2.27×10^{-4} g Am/g Pu) fired at 925°C to constant weight

Method	Temperature (°C)	Time (hr)	Actinide recovery (mean %, ± standard deviation) Pu	Am
15.7 M HNO_3 leach[a]	(Reflux)	12	0.09	3.5
H_2SO_4-HNO_3 digestion[a]	(Reflux)	12	94	88
H_2SO_4-HNO_3 digestion[a]	(Reflux)	16	97	96
NaOH fusion[b]	500	2	98 ± 0.97	96 ± 0.89
NaOH fusion[c]	500	2	34 ± 4.6	32 ± 4.0
Na_2CO_3 fusion	900	2	7.7 ± 2.5	6.9 ± 0.35
Na_2CO_3-Na_2SO_4 fusion	900	2	6.3 ± 3.9	6.7 ± 1.2
Na_2CO_3-$NaNO_3$ fusion	900	2	98 ± 2.3	98 ± 2.6
Na_2CO_3-$Na_2B_4O_7 \cdot 10\ H_2O$ fusion	900	2	96 ± 2.9	92 ± 0.62
$KHSO_4$ fusion	500	2	95 ± 2.8	94 ± 3.5
$K_2S_2O_7$ fusion	500	2	92 ± 5.3	89 ± 5.0

[a]Single determination.
[b]Nickel crucible.
[c]Alumina crucible.

Table 7.2. Actinide recovery by fusion

Flux: solid ratio of 100:1
Time: 8 hr
Sample: Am-traced PuO
(2.27×10^{-4} g Am/g Pu)
fired at 925°C to
constant weight

Flux	Temperature (°C)	Actinide recovery[a] (%)	
		Pu	Am
NaOH[b]	500	96	97
NaOH[c]	500	84	84
Na_2CO_3	900	29	27
90% Na_2CO_3--10% Na_2SO_4	900	23	13
90% Na_2CO_3--10% $NaNO_3$	900	99.8 ± 0.06	97.1 ± 1.2
$KHSO_4$	500	97	96
$K_2S_2O_7$	500	98	96

[a]Results of single determination, except for carbonate-nitrate (mean % ± standard deviation).

[b]Nickel crucible.

[c]Alumina crucible.

recoveries than fusion in alumina. Results were reproducible; if NaOH becomes a candidate for the recovery process, this phenomenon will be investigated further. Unfortunately, fusion with NaOH at temperatures greater than 500°C is difficult because the molten NaOH "crawls" out of the crucible, carrying material (e.g., ash or plutonia) with it. Fusion with Na_2CO_3 or 90 wt % Na_2CO_3-10 wt % Na_2SO_4 at 900°C is not an efficient way to recover the actinides. The most satisfactory flux tested in this study was a 90 wt % Na_2CO_3-10 wt % $NaNO_3$ mixture, which efficiently recovered plutonium and americium but did not attack the alumina crucible. The 50 wt % Na_2CO_3-50 wt % $Na_2B_4O_7 \cdot 10H_2O$, while efficiently recovering the actinides, also severely attacked the alumina crucible. The $KHSO_4$ and $K_2S_2O_7$ fusions gave high recoveries, but have the disadvantage of adding sulfate to the waste. Sulfate is deleterious to glass waste forms.

The effect of increasing the fusion time for the samples (i.e., to 8 hr) is shown in Table 7.2. Actinide recoveries were improved, especially for NaOH in alumina, Na_2CO_3, and 90 wt % Na_2CO_3-10 wt % Na_2SO_4. However, increasing the reaction time does not appear to be the most efficient way to increase recoveries. The fluxes that are effective in 2 hr are not improved to any great extent, while the ineffective fluxes, although significantly improved, still do not produce the desired results, Increasing the fusion temperatures will probably prove to be more advantageous.

7.4 Summary and Conclusions

The program to determine the feasibility of actinide recovery from combustible waste is continuing. During this quarter, an evaluation of leaching and solubilization methods using ^{241}Am-traced high-fired PuO_2 showed that:

1. Fusion with commonly used fluxes solubilizes $\geq$96% of high-fired plutonium-americium oxide.
2. Acid digestion with 95 vol % H_2SO_4-5 vol % HNO_3 (concentrated acids) will solubilize the high-fired oxide but requires lengthly refluxing.
3. Leaching with 12 M HNO_3 does not solubilize high-fired oxide.

Attempts to prepare simulated ash by fluidizing plutonium nitrate-traced ash in a quartz reactor failed because of ignition and rapid burning

of the high-carbon ash. A laboratory-scale FBI which will burn combustible waste is being built. Actinide recovery methods will be evaluated using the contaminated ash produced in this FBI system.

7.5 Future Work

Efforts involving the recovery of plutonium and americium from mixtures of ash and high-fired oxide are under way. Such mixtures simulate contaminated ash; actual contaminated ash will be prepared by adding plutonium to combustible waste and burning it in a laboratory-scale FBI system. This system, which is now in the final design stage, will be fabricated, installed, and checked out during the next few months. Combustible wastes to be burned in the FBI system will include general trash, ion exchange resins, and spent solvents.

The methods and techniques developed using cold ash and ash-oxide mixtures will be extended to actual contaminated ash. Promising primary and secondary recovery methods will be more extensively investigated until the end of FY 1977. At present, these methods comprise fusion techniques (for primary recovery) which do not introduce sulfate to the waste, and solubilization of the fused cake with dilute acid (secondary recovery). The candidate primary and secondary recovery methods will be selected by the end of FY 1977, and FY 1978 will be spent in investigating and documenting these methods. Determination of actinide and fission product losses to the off-gas system will be made concurrently with fusion experiments by means of a filter and scrubber system.

7.6 Acknowledgments

The authors gratefully acknowledge the assistance of D. L. Ziegler, L. J. Meile, and A. J. Johnson of the Pilot Plant Development Group of Chemistry Research and Development (CRD) and F. J. Miner of CRD, Rocky Flats Plant.

7.7 References for Section 7

1. J. O. Blomeke and D. W. Tedder, Actinide Partitioning and Transmutation Program Progress Report for Period October 1, 1976 to March 31, 1977, ORNL/TM-5888 (June 1977), p. 51.

2. R. E. Lerch and C. R. Cooley, Treatment of Low-Level Alpha Contaminated Solid Waste by Acid Digestion, HEDL-TME-73-22, Westinghouse Hanford Company, Hanford Engineering Development Laboratory, Richland, Washington (April 1973).

3. C. R. Cooley and R. E. Lerch, "The Acid Digestion Process for Treatment of Combustible Wastes," Proceedings of the Seminar on the Management of Plutonium-Contaminated Solid Wastes, Marcoule, France, October 14-16, 1974, CONF-741026, p. 172.

8. ACTINIDE RECOVERY AND RECYCLE PREPARATION FOR WASTE STREAMS

J. D. Navratil, L. L. Martella, and C. M. Smith
(Rockwell International, Rocky Flats Plant)

The objective of this task is to determine the feasibility of removing actinides from secondary aqueous waste streams likely to be produced during reactor fuel fabrication and reprocessing. The waste streams are part of two flowsheets entitled "Salt Water Management" and "Acid and Waste Water Management." Evaluation of methods for the salt waste and waste-water streams and recycle preparation problems will be the major emphasis of this task.

8.1 Introduction

Evaluation of methods on a laboratory scale for the salt waste and waste-water streams as well as recycle preparation problems will be the major emphasis of this task. Solvent extraction and ion exchange methods will be investigated to determine their utility in the processing of salt waste streams, and adsorption and membrane techniques will be examined for their application to treatment of waste-water streams. The best methods for both waste streams will be tested further to obtain process information for flowsheet analysis.

During the first report period, a program plan was written, a preliminary literature search was made, and waste streams were defined.[1] The testing of a bidentate organophosphorus extractant for removing actinides from salt waste streams was initiated. Extraction coefficients for uranium, plutonium, and americium were determined as a function of HNO_3 concentration. A program to determine the feasibility of using reverse osmosis (RO) for water purification was also initiated. Conceptual flowsheets were constructed for purifying waste water. The preliminary flowsheets were based on experience with RO at Rocky Flats.

8.2 Experimental

8.2.1 Salt waste processing

The testing of impure DHDECMP (dihexyl-N,N-diethylcarbamylmethylene phosphonate) for removing actinides from salt waste streams was continued.

Prior work showed high uranium extraction coefficients at low acidity, indicating that uranium stripping reagents other than water or dilute HNO_3 would be needed.[1] However, uranium extraction coefficients in dilute HNO_3 may be higher with DHDECMP subjected to Amberlyst A-26* resin treatment alone[1] than with DHDECMP purified via additional steps.

Various stripping agents, which were selected because of their compatibility with subsequent processing steps, were tested for removing uranium from 30 vol % DHDECMP-CCl_4. The extractant, containing 41 g of uranium per liter, was contacted with the stripping agents four times using an aqueous/organic ratio of 1. The accumulated percent of uranium stripped after each contact is plotted in Fig. 8.1. The results show that citric acid was the most effective stripping agent tested; however, it was not much better than four water contacts.

A synthetic salt waste solution was prepared and processed by both the DHDECMP and the TBP solvent extraction schemes. Prior to processing, two basic salt wastes [synthetic incinerator liquor (22 ml) and analytical waste (1.9 ml)] were combined and then acidified with 7 M HNO_3 (75 ml). The acidification process required care because considerable foam and heat were produced. Filtration after acidification indicated that no solids were present in the waste. The compositions of the two basic solutions prior to acidification are shown in Table 8.1.

The problem of actinide removal, especially plutonium, was evaluated using both extraction schemes. Figure 8.2 presents the plutonium and americium analyses of the acidified salt waste after consecutive contacts with 30 vol % TBP-dodecane and 30 vol % DHDECMP-CCl_4. An aqueous/organic ratio of 5 was used. The results show that the DHDECMP was more effective in removing actinides than TBP; however, the rate of plutonium extraction decreased, indicating the presence of a nonextractable species.

8.2.2 Waste-water processing

An evaluation of various adsorption materials for potential use in removing detergents and anions from waste water has begun. The initial

---

*Product of the Rohm and Haas Co., Philadelphia, Pa.

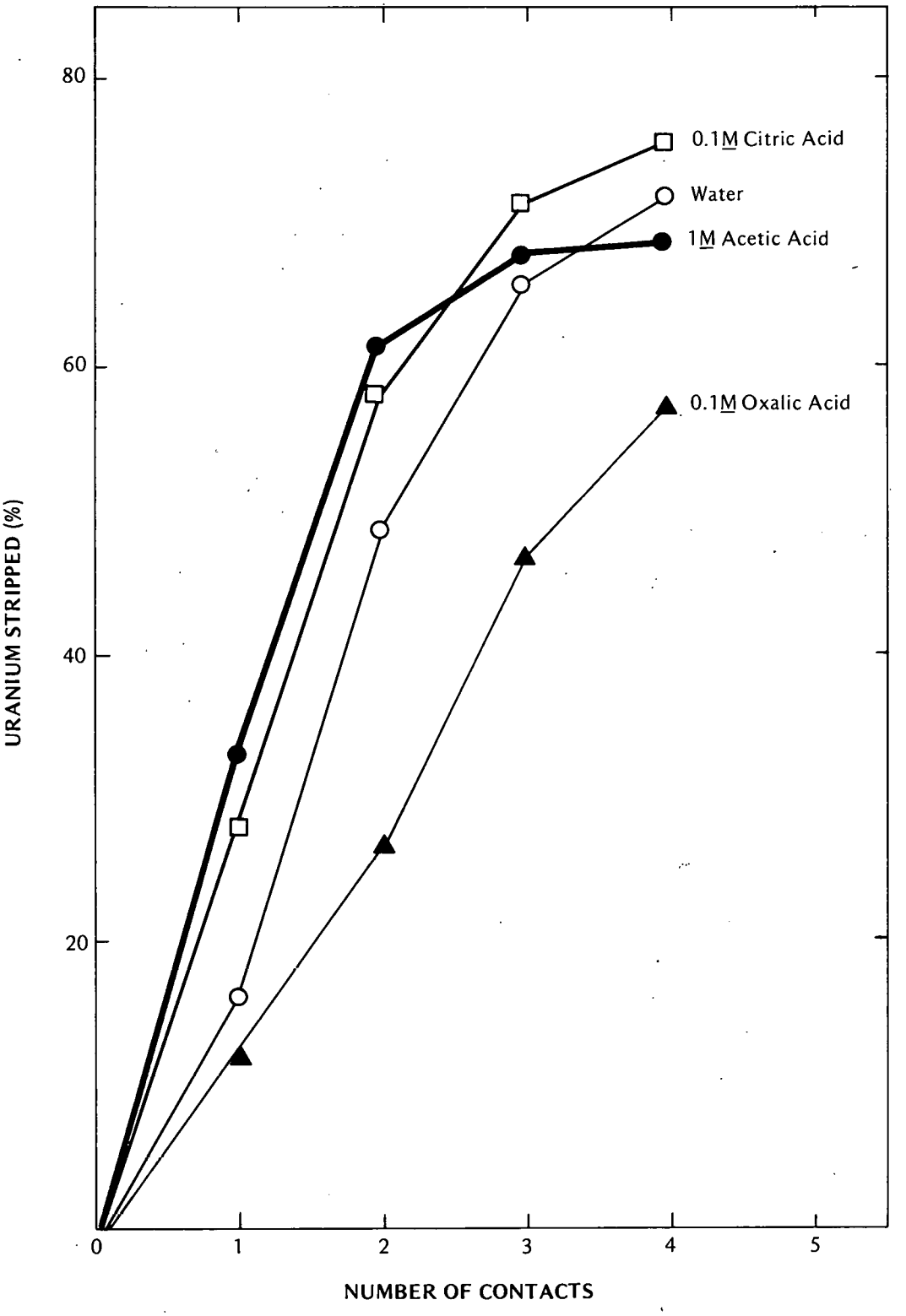

Fig. 8.1. Evaluation of uranium stripping with 30% DHDECMP-CCl_4. Aqueous/organic ratio = 1.

Table 8.1. Composition of synthetic basic wastes prior to acidification

Component	Concentration
Incinerator Liquor	
Na_2CO_3	1.36 M
Na_3PO_4	0.46 M
NaCl	0.52 M
Na_2SO_4	0.37 M
$NaNO_3$	0.07 M
Pu	0.0002 M
Am	0.00002 M
U	0.02 M
Fission products	0.14 g/liter
Analytical Waste	
HNO_3	1.5 M
HCl	0.1 M
$NaNO_3$	0.005 M
$K_2Cr_2O_7$	0.005 M

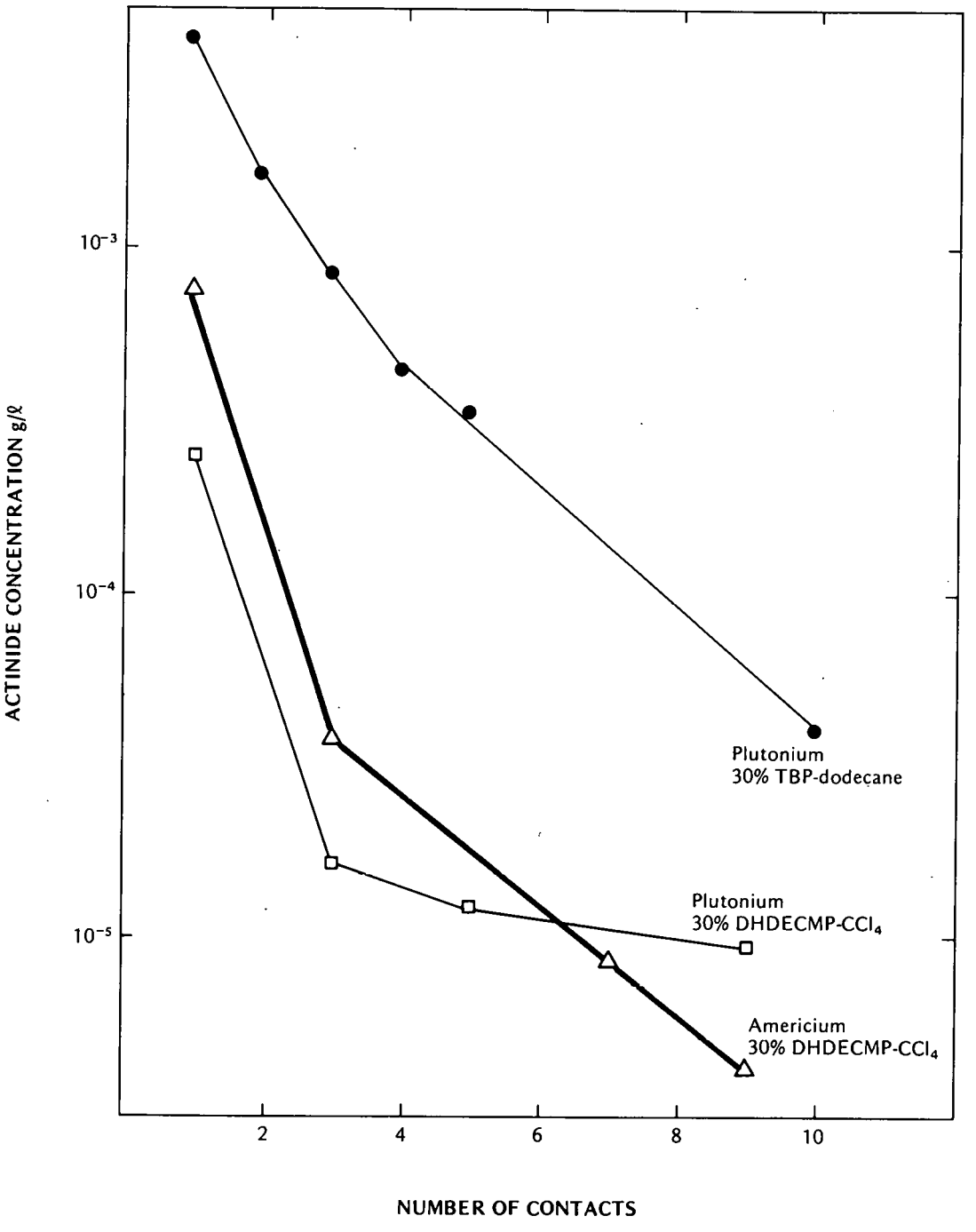

Fig. 8.2. Results of actinide removal with TBP and DHDECMP. Aqueous/organic ratio = 5; feed: 0.01 g of plutonium and 0.001 g of americium per liter.

effort will consist of comparing the breakthrough capacities of activated carbons, macroreticular resins, and polyurethanes.

Preliminary breakthrough curves were determined by passing a detergent solution (Proctor & Gamble Pierce Commercial Laundry Detergent dissolved in deionized water at a concentration of 2.6 g/liter) through a column containing about 1 g of adsorbent. Fractions (100 ml) were collected and analyzed for linear alkylate sulfonates (LAS).

The results of runs using Analab activated coconut carbon (40 to 50 mesh), Amberlite* XAD-4 macroreticular sorbent (20 to 50 mesh beads), and Analab polyurethane foam are shown in Fig. 8.3. The foam was substituted for the rigid open-pore polyurethane (OPP) because the high pH ($\sim$11) of the detergent solution resulted in breakage of the OPP-column bond. The carbon and resin appeared to have similar capacities, with the carbon having a slight advantage. Discrimination between the two would depend on changing the flow rate and/or the column design. The foam proved to be very inefficient, probably due to the lack of adsorption sites.

Since solutions of high pH are incompatible with OPP, a detergent solution having a pH of 3.5 was prepared to determine the breakthrough curve of OPP. Runs were also made with XAD-4 resin and two activated carbons to investigate the effect of pH on the adsorption of LAS. The results, presented in Fig. 8.4, show that the OPP and XAD-4 have the best adsorption capabilities. The decrease in pH enhances adsorption on the XAD-4, while the Analab carbon appears to experience a decrease in adsorption. The low adsorption on the Witco 517 could be due to large particle size (20 to 60 mesh).

The adsorbents were also tested to determine their chloride removal capability. All of the materials except the coconut charcoal achieved 100% chloride breakthrough with the first fraction. The coconut charcoal gave 100% breakthrough with the second fraction.

---

*Product of the Rohm and Haas Co., Philadelphia, Pa.

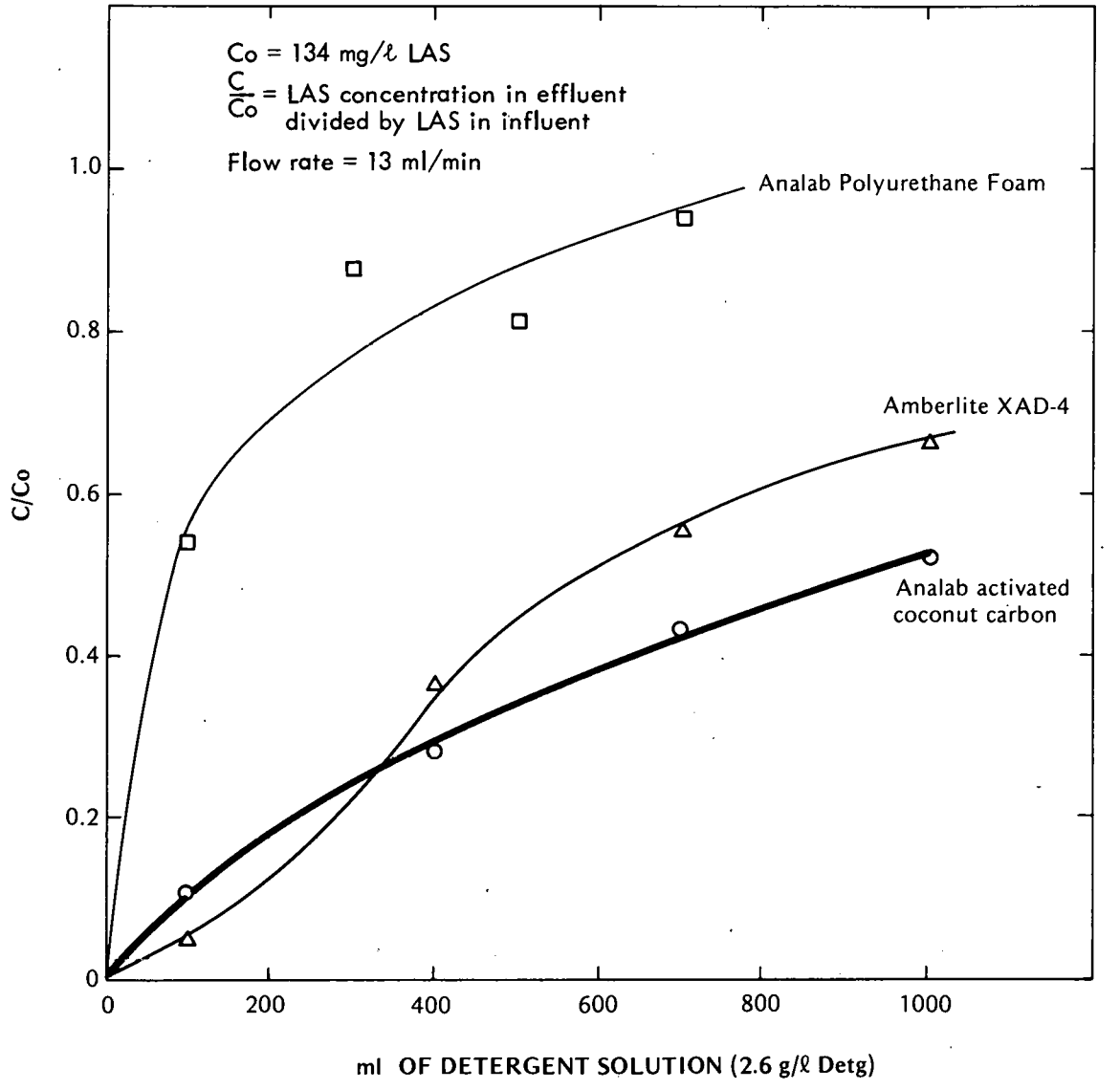

Fig. 8.3. Breakthrough curves for adsorbents, with alkaline detergent (pH 12).

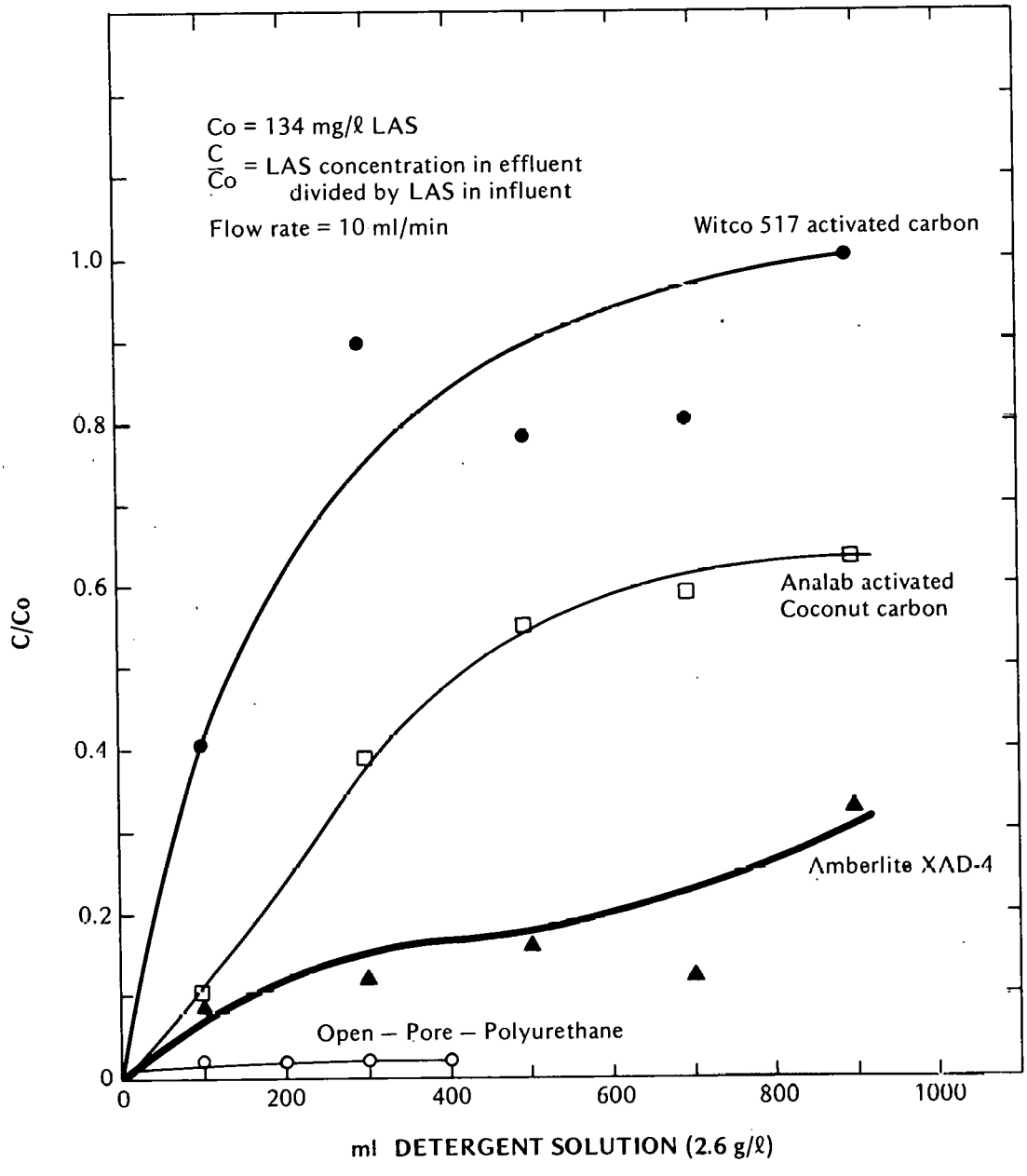

Fig. 8.4. Breakthrough curves for adsorbents, with acidified detergent (pH 3.5).

8.3 Summary and Conclusions

The evaluation of methods for the salt waste and waste-water streams and recycle preparation problems was continued. Preliminary runs were made with both a bidentate organophosphorus process and a combined bidentate-TBP extraction process to remove actinides from salt waste. The first process effectively removed actinides but prevented efficient stripping of uranium. More efficient uranium stripping agents than water were not found. The combined process appears to be more advantageous for removing actinides from salt waste. The TBP removes most of the uranium and plutonium, while the bidentate extractant removes most of the remaining actinides.

Tests were run with activated carbon, macroreticular resins, and polyurethanes to determine their relative capabilities for removing detergents and corrosive anions from waste water. The preliminary results show that an OPP resin has the highest capacity for detergent but a low capacity for anions.

8.4 Future Work

The bidentate extraction process will be evaluated further to determine whether it has utility for processing salt wastes. New and recycled extractants will be tested with synthetic waste to determine actinide DFs. The behavior of impurity ions in the process will also be studied.

The investigation of adsorption materials for removing detergents and corrosive anions from waste-water streams will be completed. Conceptual flowsheets for purifying waste water using membrane techniques will be evaluated.

8.5 Reference for Section 8

1. J. O. Blomeke and D. W. Tedder, Actinide Partitioning and Transmutation Program Progress Report for Period October 1, 1976 to March 31, 1977, ORNL/TM-5888 (June 1977), p. 58.

9. RADIATION EFFECTS

T. E. Gangwer, M. Goldstein, and K. K. S. Pillay
(Brookhaven National Laboratory)

This task examines the formation of radiation products in waste streams encountered in fuel reprocessing and refabrication plants which operate with a high degree of stream recycle. Analysis will provide methods of predicting the formation of chemical species which interfere with process operations or result in operating hazards.

9.1 Radiation Effects in Ion Exchange Materials

An intensive literature search was initiated to examine the present knowledge on the radiation effects of process chemicals. During this report period, our primary effort has been concentrated on reviewing available materials on the effect of ionizing radiation on ion exchange materials used in, as well as those with potential for possible use in, nuclear fuel and waste processing areas. A 1965 Russian publication[1] was identified as a useful starting point. While this book contains an extensive survey of Russian and East European publications up to 1964, it has not included several publications in the English language. Another significant publication[2] includes a comprehensive compilation of ion exchange materials, although it has not devoted any space for radiation effects.

Our efforts at assembling materials of relevance[3-49] has centered around pre-1964 papers not included in ref. 1 and reports and publications since 1964. It is generally felt that published works from Russia, Hungary, and Poland still dominate, while there are fewer publications from the United States, Britain, Germany, and Japan. Most of the material published in the open literature in the English language has been collected, and other sources are being researched. A few of the important foreign papers, identified as valuable from their abstracts, have been translated. We are planning to prepare a list of references from foreign sources, identified as valuable, but not translated. The process of compiling these materials into a convenient format is now in progress. The format used in the tabulation of experimental data from various research reports consists of the following:

1. Trade name(s) of the synthetic and natural ion exchangers--both organic and inorganic types.
2. The ionic forms used in the experiment.
3. Total exchange capacities expressed as milliequivalents per gram of the dry form of the ion exchanger.
4. Radiation sources used in experiments and their dose rates (in rads/hr).
5. Irradiation conditions used in experimental studies as well as process-related measurements.
6. Integral dose received by the ion exchange material (in rads).
7. Loss of exchange capacity as percent of initial exchange capacity.
8. G-values expressed as groups per 100 eV.
9. A listing of various other parameters studied during the investigation.
10. Reference numbers and relevant additional notations.

Very few experimental studies in the material reviewed thus far have provided all the above information. Also, the data presented show significant differences due to differences in the objectives of the original work as well as in the facilities and experimental conditions. For example, G-values have been reported by several investigators in a variety of ways such as the following:

1. The number of functional groups which have lost ion exchange capacity per 100 eV of absorbed radiation energy.
2. G-values for radiation decomposition products such as ammonia, primary amines, secondary amines, and tertiary amines.
3. Radiation yield calculated for gas yield (mostly for hydrogen) per 100 eV of absorbed radiation.
4. G-values for SO_4^{2-} ion formation from sulfonated resins.
5. G-values expressed in terms of other gaseous products of radiation decomposition, etc.

In compiling these experimental data, an attempt is being made to express all the data in some uniform units of measurement and to point out the differences in manner of presentation by some of the authors. Where possible, some of the data have been used to recalculate radiation doses and G-values for uniformity of presentation.

Most of the reports on radiation effects on ion exchange material deal with the phenomenonal aspects. Very few have attempted to study or explain the mechanisms.

The tabulation of experimental data has combined the data reported in ref. 1 with those from other collected papers. It is felt that, as part of this compilation, it would be desirable to include two additional tables -- one from ref. 1 and the other from ref. 2. Together, these two tables contain information which can be used as a ready reference to complement the tabulation described earlier. Additional information on new ion exchange materials, not included in the original tabulations, will be added where possible. One of these tabulations gives the structural formulas, active ion exchange group(s), and a description of the base materials used in the preparation of the exchangers. The other contains a listing of physical characteristics, operational controls, and descriptive information, including the manufacturers of the ion exchange materials.

The compilation of experimental data on the radiation effects on ion exchange resins will therefore include: (1) a chemically descriptive table, (2) a listing of general physical characteristics, and (3) a detailed tabulation of the experimental data on the effects of ionizing radiation on ion exchange resins, with an attempt to include as many of the ten parameters described above as possible.

A representative example of such a listing is shown in Table 9.1. This table contains several parameters that can be readily understood to make educated predictions on process-related problems when a particular exchanger is used. It also contains a detailed listing of the various parameters studied and references to the original work. Comments on the contents and format of this table are solicited with a view toward optimization of the utility of such a compilation before the final tabulation is made.

We have identified (not yet fully digested) over a hundred publications that <u>are not included</u> in ref. 1. Since a significant number of publications are still in Russian, Polish, Czech, and Rumanian, it has only been possible to compile and document materials available in English within the time period available.

Table 9.1. Effect of ionizing radiation on ion exchange materials

Resin	Ionic form	Exchange capacity (meq/g)	Source (rads/hr)	Radiation conditions	Internal dose (rads)	Exchange loss (%)	G[a]	Other parameters[b]	Ref.
Dowex 50X12	H^+, Na^+	4.40	x-ray ($\sim 10^6$)	Air dry	$\sim 10^9$	22.6	--	*a,b,c,d,e*	[37]
Dowex 50X12	H^+	5.17	γ-ray (?)	Water	8×10^7	--	1.4	*d,e*	[1]
Ku-2X8	H^+	4.9	e-accelerator (5.8×10^8)	Aq. acid	2.3×10^9	--	2.0	*e,f*	[1]
Amberlite IRA-400	OH^-	3.3	F.P. β, γ-rays (1.4×10^7)	Moist	Max: 2×10^8	5-25	--	*e,g*	[13,15]
Imac S5-40	OH^-	3.62	^{60}Co γ-ray (10^6)	Water	10^7	9.9	35	*e,f,g,h*	[20]
Imac S5-40	OH^-	3.62	10^6	Water	10^8	17.1	7	*e,f,g,h*	[20]
Av-17	PO_4^{3-}	3.45	e-accelerator (4.9×10^8)	Water	2.9×10^8	--	2.6	*e*	[1]
Av-17	OH^-	3.6	Reactor (1.1×10^7)	Water	2.5×10^8	--	32	*e*	[1]

[a] G-value expressed as groups/100 eV of absorbed radiation.

[b] Parameters are defined as follows:
a. weight change;
b. solubility;
c. thermal stability;
d. formation of SO_4^{2-}, H^+, Cl^-, etc.;
e. exchange capacity measurements;
f. products of decomposition;
g. water-soluble products;
h. mechanism proposed.

The report of this literature search will include:

1. A detailed write-up describing the terms and parameters employed and emplaining the use and cross-usage of the various tables.
2. A separate section presenting generalized information pertinent to the evaluation of radiation effects on ion exchange resins. This section will also point out contradictions in some of the reported results, where such data are reported.
3. An objective evaluation of the present knowledge, including both the virtues and limitations.
4. Graphic illustrations of some of the characteristics of ion exchange resins and the changes that occur as a result of radiation effects. The parameters being considered include radiation sources of differing LET values, variation in G-values with exposure time, influence of cross-linkage, moisture content, and ionic form of the resin.

It has become evident that information concerning the radiation effects on inorganic ion exchangers is limited. Therefore, instead of the tabulation-type presentation, a written version of the available information will be provided with the reference.

One important aspect of this literature survey will be the identification of both the strengths and the weaknesses of the available information. This will be provided in an objective manner with a view toward facilitating the evaluation of process-related phenomena.

When plausible, general rule-of-thumb statements will be cited. Some examples are:

1. Attrition of ion exchangers exposed to irradiation is much more extensive if the irradiation is carried out in water or aqueous solution than if conducted in air.
2. The irradiation of monofunctional sulfonated (cation) exchangers in air and in vacuo is usually accompanied by cross-linking. If these ion exchangers undergo radiolysis when swollen (due to contact with water or aqueous electrolytes), degradation is the predominant process.

3. In the course of radiolysis of (cation) exchangers, the exchange capacity of the sulfone group decreases. If these materials are irradiated in air or in water, new phenolic and carboxylic groups are formed.
4. In general, salt forms of (cation) exchangers are more stable than the H^+ form to radiation in air or in vacuo. Cation exchangers swollen in water or in aqueous electrolytes can be stabilized only by a few kinds of ions.
5. As a rule, the radiation resistance of ion exchangers increases with increase in the degree of cross-linkage.

9.2 References for Section 9

1. E. V. Egorov and P. D. Novikov, "Action of Ionizing Radiation on Ion-exchange Materials," Atomizdat, Moscow (1965); Israel Program for Scientific Translations, Jerusalem (1967).
2. I.A.E.A. Technical Report Series No. 78, Operation and Control of Ion-exchange Processes for Treatment of Radioactive Wastes, International Atomic Energy Agency, Vienna (1967).
3. P. G. Clay, G. R. Hall, M. K. Rahman, and M. Rashid, "The γ-Radiolysis of Zeocarb-225 Cation-exchange Resins," J. Appl. Polym. Sci. 14, 2167-70 (1970).
4. W. C. Yee and W. Davis, Jr., "Effects of Gamma Radiation on Cation-exchange Resin in a Flowing-water System," Nucl. Sci. Eng. 24, 1-5 (1966).
5. W. C. Yee and W. Davis, Jr., Effects of Gamma Radiation on Cation-exchange Resin in a Flowing-water System, ORNL-P-661 (1964).*
6. M. A. Kskarov, A. T. Dzhalilov, R. A. Nazinova, and G. S. Tsveshko, "Radiation Stability of Polycondensation Ion-exchange Resins Based on Furfural," translation from Zh. Prikl. Khim. 46(9), 2115-17 (1973).
7. E. A. Chuveleva, P. P. Nazarov, and K. V. Chmutov, "The Use of Radiation-resistant Resins for Separating Radioactive Elements by Means of Displacement Chromatography-I," translation (BNL-TR-646) from Zh. Fiz. Khim. 50(5), 1316-18 (1976).

*Available from National Technical Information Service, U.S. Dept. of Commerce, 5285 Port Royal Road, Springfield, Va.

8. E. A. Chuveleva, P. P. Nazarov, and K. V. Chumutov, "The Use of Radiation-resistant Resins for Separating Radioactive Elements by Means of Displacement Chromatography-II," translation (BNL-TR-647), Zh. Fiz. Khim. 50(5), 1318-21 (1976).

9. K. M. Semushin, I. P. Galitskaya, and I. A. Kuzin, "Radiation and Chemical Stability of Methacrylic Acid-Divinyl Benzene Copolymers," translation from Zh. Prik. Khim. 44(9), 2035-39 (1971).

10. T. Ichikawa and Z. Hagiwara, "Effect of Gamma Radiation on Cation Exchange Resin," J. Nucl. Sci. Technol. 10, 746-52 (1973).

11. V. Dannow, S. Specht, W. Weinlander, and H. J. Born, "Modification of the Efficiency of Chromatographic Systems During the Transition to Higher Activities--I. Comparison of α- and γ-Radiolysis of a Cation Exchanger with Respect to Modifications in Its Weights, Its Salt-splitting Capacity, Its Residual Capacity and Its Expansion Capacity," J. Radioanal. Chem. 24, 393-409 (1975).

12. T. Shigematsu and T. O'Shio, "Effect of ^{60}Co Gamma Radiation on Ion Exchange Resin," Bull. Inst. Chem. Res., Kyoto Univ. 37, 349-52 (1959).

13. E. W. Baumann, Radiolysis of Ion Exchange Resins Used in the Purification Systems of Savannah River Reactors, USAEC Report DP-977, Savannah River Laboratory, Aiken, S.C. (July 1965).

14. E. W. Baumann, "Gamma Irradiation of Individual and Mixed Ion-Exchange Resins," J. Chem. Eng. Data 11, 256-60 (1966).

15. E. W. Baumann, Depletion of Deionizer Resin in an SRP Reactor System, USAEC Report DP-973, Savannah River Laboratory, Aiken, S.C. (1965).

16. A. Basinski, A. Narebska, and M. Tempczyk, "Effect of Gamma Radiation on Ion Exchange Resins. I--Radiation Damage of Functional Groups in the Strongly Basic Anion-Exchange Resin Zerolit FF-IP," Nukleonika (English Translation) 14(5), 77-88 (1969).

17. A. Narebska, A. Basinski, and H. Litowska, "Effect of Gamma Radiation on Ion Exchange Resins. II--Investigation of the Effect of Gamma Radiation on Zerolit FF-IP by the IR-Method," Nukleonika (English Translation) 15(2), 30-39 (1970).

18. A. Narebska and B. Mazurkiewicz, "Effect of Gamma Radiation on Ion Exchange Resins. IV--Degradation and Cross-linking of Polystyrene Sulfonic Cation Exchange Resin, Zerolit-225 of Different DVB Contents," Nukleonika (in Polish) 27(3-4), 169-79 (1972).

19. M. Litowska and A. Basinski, "Effects of Gamma Radiation on Ion Exchange Resins. V--Kinetics of Radiation Damage of Strongly Alkaline Functional Groups in Anion Exchange Resin Zerolit FF-IP," Nukleonika (English Translation) 18(5), 1-6 (1973).

20. M. Litowska, A. Narebska, and J. Ostrowska, "Effects of Gamma Radiation on Ion Exchange Resins. VI--The Kinetics and Mechanism of Radiation-induced Decomposition of Functional Groups in an IMAC S5-40 Anion Exchange Resin," Nukleonika (English Translation) 19(1), 19-29 (1974).

21. M. Litowska and J. Ostrowska, "The Effects of Radiation on Ion Exchangers. VII--The Kinetics of Variation in Sulfonic Groups of the Cation Exchanger IMAC-C12," Nukleonika (in Polish) 19(4), 284-90 (1974).

22. L. L. Smith and H. J. Groh, The Effect of Gamma Radiation on Ion Exchange Resins, USAEC Report DP-549, Savannah River Laboratory, Aiken, S.C. (1961).

23. A. R. Kazanjian and D. R. Horrell, Radiation Effects on Ion-Exchange Resins. I--Gamma Irradiation of Dowex 50W, USAEC Report RFP-2140, Rocky Flats Division, Golden, Colo. (1974).

24. A. R. Kazanjian and D. R. Horrell, Radiation Effects on Ion-Exchange Resins. II--Gamma Irradiation of Dowex 1, USAEC Report RFP-2354, Rocky Flats Division, Golden, Colo. (1975).

25. A. R. Kazanjian and D. R. Horrell, Radiation Effects on Ion-Exchange Resins. III--Alpha Irradiation of Dowex 50W, USAEC Report RFP-2298, Rocky Flats Division, Golden, Colo. (1975).

26. A. R. Kazanjian, Radiation Effects on Dowex 11 Ion Exchange Resin, Internal Report No. CRDL-940250-101, Rockwell International, Rocky Flats Division, Golden, Colo. (February 1977).

27. A. R. Kazanjian, Effects of Radiation and Acids on the Thermal Stability of Ion Exchange Resins, Internal Report No. CRDL-940250-103, Rockwell International, Rocky Flats Division, Golden, Colo. (March 1977).

28. G. R. Hall and M. Streat, "Radiation Induced Decomposition of Ion-exchange Resins. Part I. Anion-exchange Resins," J. Chem. Soc. B, 5205-11 (1963).

29. M. T. Ahmed, P. G. Clay, and G. R. Hall, "Radiation-induced Decomposition of Ion-exchange Resins. Part II. The Mechanism of the Deamination of Anion-exchange Resins," J. Chem. Soc. B, 1155-57 (1966).

30. E. D. Kiseleva, K. V. Chmutov, V. M. Khasanova, and Z. A. Markova, "Radiation Stability of AN-25 and AN-25A Anion-exchange Resins," Russ. J. Phys. Chem. (English translation) 45(4), 499-502 (1971).

31. E. D. Kiseleva, V. M. Khasanova, and K. V. Chmutov, "The Radiation Stability of AVKh-8P and AVI-8P Quinoline and Isoquinoline Anion-exchange Resins," Russ. J. Phys. Chem. (English translation) 45(5), 667-69 (1971).

32. V. M. Khasanova, E. D. Kiseleva, and K. V. Chmutov, "An Infrared Spectroscopic Study of the Change in the Structure of AVKh-8P and AVI-8P Anion-exchange Resins under the Influence of Ionizing Radiation," Russ. J. Phys. Chem. (English translation) 45(5), 725-26 (1971).

33. G. Mohorcic, V. Kramer, and M. Pregelj, "Interaction of a Sulfonic Acid Ion Exchange Resin with Tritiated Water on γ-Irradiation," Int. J. Appl. Radiat. Isot. 25, 177-82 (1974).

34. S. A. Fisher, Effect of Gamma Radiation on Ion Exchange Resins, USAEC Report RMO-2528 (1954).

35. G. J. Moody and J. D. R. Thomas, "The Stability of Ion Exchange Resins; Part II--Radiation Stability," Lab. Pract. 21(10), 717-22 (1972).

36. J. A. Marinsky and A. J. Giuffrida, The Radiation Stability of Ion-exchange Materials, USAEC Report ORNL-1978, Oak Ridge National Laboratory (1957).

37. R. E. Wedemeyer, "The Stability of Ion Exchange Resins to X-rays," Ph.D. thesis submitted to Faculty of Graduate School of Vanderbilt University, Nashville, Tenn. (September 1953).

38. E. D. Kiseleva, K. V. Chmutov, and N. V. Kuligina, "The Mechanism of the Effect of Radiation on KU-2 Cation-exchange Resin," Russ. J. Phys. Chem. (English translation) 44(2), 264-67 (1970).

39. E. D. Kiseleva, K. V. Chmutov, and M. M. Klientovskaya, "Action of Ionizing Emissions from a Stream of Accelerated Elections on Polycondensation Cation-exchange Resins," Russ. J. Phys. Chem. (English translation) 42(11), 1518-20 (1968).

40. P. E. Tulupov and A. I. Kasperovich, "Effect of the Structure of Macromolecules of Sulfonic Acid Cation-exchange Resins in Their Stability to Radiation," Russ. J. Phys. Chem. (English translation) 42(8), 1040-43 (1968).

41. E. D. Kiseleva, K. V. Chmutov, M. M. Klientovskaya, and V. P. Li, Radiation Stability of KU-4 Cation-exchange Resin," Russ. J. Phys. Chem. (English translation) 41(7), 850-53 (1967).

42. O. R. Skorokhod and I. B. Stankevich, "Radiation Stability of the Sulfonated Cation-exchange Resin KU-2 in the Lithium, Sodium and Potassium Forms," Russ. J. Phys. Chem. (English translation) 42(2), 271-73 (1968).

43. P. E. Tulupov, A. M. Butaev, V. P. Greben, and A. I. Kasprovich, "Effect of Contents of Divinylbenzene in KU-2 Cation-exchange Resin on Its Resistance to Irradiation in Water," Russ. J. Phys. Chem. (English translation) 47(4), 551-53 (1973).

44. A. V. Nikolaev, I. N. Gribanova, N. I. Yakovleva, and I. D. Khol'kina, "Radiation Stability of Complex Forming Organophosphorus Resins," Russ. J. Phys. Chem. (English translation) 40(4), 456-57 (1966).

45. I. N. Gribanova, I. D. Khol'kina, Yu.N. Polovinkin, and A. V. Nikolaev, "Radiation, Chemical and Mechanical Stability of Porous Organophosphorus Cation Exchangers," Russ. J. Phys. Chem. 44(7), 983-85 (1970).

46. R. H. Wiley and G. Devenuto, "Irradiation Stability of Sulfonated Styrene Resins Crosslinked with Various Divinylbenzene Isomers and Mixtures Thereof," J. Appl. Polym. Sci. 9, 2001-7 (1965).

47. G. Mohrcic and V. Kramer, "Gases Evolved by ^{60}Co Radiation Degradation of Strongly Acidic Ion Exchange Resins," J. Polym. Sci., Part C 16, 4185-95 (1968).

48. J. Payne, "Investigation of the Mechanism of the X-ray Degradation of Dowex-50 Ion-exchange Resin," M. A. thesis submitted to the Faculty of the Graduate School of Vanderbilt University, Nashville, Tenn. (March 1956).

49. J. W. Utley, "The Chemical Effects of Low Energy X-Radiation on Ion-exchange Resins," Part I of Ph.D. thesis submitted to the Faculty of the Graduate School of Vanderbilt University, Nashville, Tenn. (June 1959).

10. FUEL AND TARGET FABRICATION STUDIES

A. G. Croff (Oak Ridge National Laboratory)

This task identifies primary and secondary transuranic waste streams and evaluates waste treatment processing options for fabrication plants that are operated under the actinide partitioning concept. Chemical and equipment flowsheets will be prepared for use in a detailed cost estimate of these plants. The effects of alternate fuel forms are also examined.

10.1 Introduction

The partitioning-transmutation (P-T) program is concerned with determining the feasibility and desirability of recovering and fissioning the noneconomic actinide values from primary and secondary transuranic waste streams. To ensure that this determination is defensible, it is important that the fuel cycle strategies selected for final analysis represent the best methods for implementing P-T. If this precaution is not taken, any negative conclusions of the program will continue to be questioned since a better strategy might change these conclusions, thus affecting the feasibility or desirability of P-T.

One aspect of P-T that appears to be particularly sensitive in this respect concerns the form of the waste actinides in the transmutation reactor. As a result of an information void concerning the fabricability and irradiation behavior of many potential fuel materials, we have thus far restricted our consideration to two cases: (1) homogeneous actinide recycle, and (2) recycle in target elements or assemblies with a UO_2 diluent. The diluent is required to reduce the power produced in a target element to levels comparable with those in normal fuel elements.

By definition, the homogeneous case is restricted to diluting the waste actinides with normal reactor fuel. Thus, there is no freedom to improve this system except by changing the type of reactor or fuel cycle (e.g., ^{235}U-enriched PWR vs plutonium-enriched PWR).

On the other hand, the target case might be improved by varying the chemical and physical forms of the waste actinides. The principal reasons

that UO_2 has been assumed to be the diluent thus far are: (1) it is probably compatible with the other actinide oxides, (2) it performs in a known and acceptable manner during irradiation, (3) it can be dissolved in HNO_3 alone during reprocessing, and (4) it breeds plutonium to aid in fueling the reactor.

The fourth advantage cited above must also be recognized as a disadvantage. If the plutonium bred in the target is recycled back to the target, the specific power of the target will be greater than in the case where it is not recycled. This will require the addition of more diluent which, in turn, will increase the volume of the waste-actinide-containing fuel. In a uranium-enriched PWR the target volume will increase by about a factor of 5, from 2% of the core to 10% of the core, as compared with the volume required with no uranium diluent. In an LMFBR, the volume will increase by roughly a factor of 2, to about 3% of the core. The alternative is to remove the plutonium from the targets and combine it with the normal plutonium produced in the reactor. This procedure would increase the ^{238}Pu content of the plutonium from about 1.7% to about 5% in the PWR, and from about 1% to 1.5% in an LMFBR. The increased heavy-metal content of the targets would also increase the volumes of the process streams generated at the target reprocessing plant.

Based on this analysis, the target recycle strategy can apparently be simplified and/or made more effective either by using an "inert" diluent or by eliminating the diluent altogether. In the subsections below, two different diluent concepts are presented and discussed.

10.2 Inert Diluents

The concept of an inert (i.e., no actinide production) oxide diluent is not new since it was one of the first ideas proposed after UO_2. The inert diluent must have the following properties:

1. chemical and physical stability up to about the maximum expected temperatures,
2. acceptable irradiation behavior,
3. small neutron absorption cross section,
4. solubility in aqueous HNO_3 and chemical dissimilarity from the actinides to aid in partitioning, and
5. chemical compatibility with the waste actinides and cladding.

Criterion 1 alone eliminates most chemical compounds because of melting or decomposition at unacceptably low temperatures. If it is assumed that waste actinide oxides will be used, criteria 1 and 5 will probably restrict the choice of compounds to metal oxides or a few metals. Criterion 4 eliminates virtually all metals and many oxides, which do not dissolve in HNO_3 because of their refractory nature, as well as most of the lanthanides, which are chemically similar to the actinides. The ultimate result is that only two oxides, MgO (magnesia) and CaO (lime), appear to have the requisite qualities. Some of the pertinent physical, chemical, and nuclear properties of these two oxides and of UO_2 are summarized in Table 10.1.

Based on the data given in Table 10.1, MgO appears to be superior to CaO because of its lower cross section and lower solubility in water. Even though the maximum useful temperature (1927°C) of MgO is much lower than that of UO_2 (2500°C), it is still acceptable as a diluent because its high thermal conductivity results in a MgO element centerline temperature of 1100°C when a UO_2 element with equivalent diameter and linear power would be beginning to melt.

Reagent-grade MgO is readily soluble in 8 M HNO_3 at room temperature. Magnesium oxide prepared by burning magnesium metal (ca. 2400°C), although somewhat less soluble in 8 M HNO_3 than the reagent-grade MgO, is still readily soluble. Fused MgO (temperature >2800°C), may not be readily soluble, but this condition is not expected to occur in commercial nuclear reactors. Mixtures of 2.71 wt % PuO_2 in MgO and 12.95 wt % PuO_2 in MgO have been irradiated to the equivalent of 4000 MWd/MTHM without problems[1] at a specific power equivalent to 107 MW/MTHM and at centerline temperatures ranging up to 2450°C. These irradiations were conducted in zirconium capsules with no apparent compatibility problems. Finally, the chemical dissimilarity of Mg^{2+} and the actinides should facilitate the reprocessing of the targets.

Based on specific power considerations alone, a MgO--waste actinide element in a uranium-enriched PWR would contain about 23 wt % (10 vol %) waste actinides. The waste actinide mixture would consist of ∿50% plutonium, 23% neptunium, and 23% americium-curium. This composition may require that additional UO_2 be added to form a solid solution with PuO_2, thus aiding

Table 10.1. Characteristics of MgO and CaO as compared with UO_2

Property	MgO	CaO	UO_2
Melting point, °C	2800	2570	2500
Max. useful temp., °C	1927	2315	2500
Boiling point, °C	3600	2850	?
Approximate centerline temperature of diluent corresponding to the melting point of the centerline of a UO_2 element, °C	1100[a]	800[a]	--
Specific gravity, g/cm^3	3.65	3.32	10.96
Thermal conductivity, cal/sec-cm-°C	0.076	0.17	0.022
Reaction with H_2O	Forms $Mg(OH)_2$	Forms $Ca(OH)_2$	None
Solubility, g/100 g H_2O	0.0009	0.165	Insoluble
Thermal expansion, 10^{-6} in./in.-°F	10	13	5
Effective thermal cross section, barns	0.05	0.35	10
Dissolves in nitric acid	Yes (unless fused?)	Yes	Yes
Irradiation experience	Very limited[b]	None	Extensive; good behavior
Chemical compatibility with cladding	OK	OK	OK

[a]Assumes that surface of element is at 500°F and that elements have the same diameter.

[b]See ref. 1.

subsequent target dissolution. This type of fuel element would comprise about 2% of the fuel rods in a PWR after five recycles.

A possible variant on this scheme would be to disperse actinide metal particles in the MgO matrix, thereby eliminating potential PuO_2 dissolution problems.

10.3 Annular Fuel Rods

A second method for reducing the linear power of a fuel rod containing waste actinides without adding UO_2 diluent is to make an annular fuel pellet, thus reducing the actinide mass per unit fuel rod length. After five recycles, the waste actinides in the fuel pellet should comprise about 10 vol % of a standard PWR fuel rod in order to obtain the correct linear power. If the outside diameter of the rod is 0.3225 in. and the density of heavy metal as oxide is 9.18 g/cm^3 (equivalent to 95% of the theoretical density of UO_2), the annulus would have a wall thickness of 0.0083 in. This thickness is far too small to support the pellet itself plus the pellets on top of it and still achieve reasonable burnups. Therefore, a waste actinide oxide annular fuel pellet does not appear feasible. There is, however, a method available for strengthening the annulus which could potentially be accomplished in either an oxide or a metallic system. This would involve using a slug of inert material as a substrate for a surface layer of actinides that would result in the correct power rating.

With an oxide substrate, a solid right cylinder of, for example, Al_2O_3 (alumina) would be formed. The alumina cylinder would then be surrounded with actinide oxide powder and hot pressed to give the desired actinide oxide surface layer. The resulting pellet would subsequently be ground, sintered, and so forth. After irradiation, the actinide oxides could hopefully be dissolved, leaving the unreactive alumina as a residue.

The advantage of this concept is that the volume of actinides that must be reprocessed is reduced by a factor of 10 to 20 if no UO_2 is added to promote PuO_2 dissolution.

The disadvantages of this concept are complexity and problems related to potential dissolution. The hot pressing, sintering, and grinding of an 8-mil oxide surface layer, assuming that this layer must remain intact during irradiation, promises to be extremely difficult. The difficulty encountered

when attempting to dissolve PuO_2 which is not in solid solution may require that UO_2 be added to aid in solubilizing such plutonium. This procedure would reduce the previously mentioned actinide volume reduction factor of 10 to 20 by about one-half (i.e., to 5 to 10); that is, it would double the waste actinide mass requiring dissolution and reprocessing.

The metallic substrate concept would involve fabricating a right cylinder of an inert metal (e.g., zirconium in LWRs and stainless steel in FBRs) and coating it with metallic waste actinides using an as yet undefined process. Because of the higher density of the actinide metals as compared with that of the oxides discussed above, the thickness of the surface layer would be reduced to about 0.005 in.

This concept would offer two distinct advantages. First, the volume of material that would be dissolved would be reduced by a factor of 10 to 20, thereby allowing a commensurate reduction in the scale of the target reprocessing plant. The second advantage is that the metallic actinides, plutonium in particular, will be much more amenable to dissolution than the oxides, which should serve to minimize insoluble residues in the dissolver. This also means that UO_2 diluent would not be required to bring the PuO_2 into solid solution as it might be if actinide oxides are used.

This process also has two disadvantages: (1) the actinides used for coating the substrate must be reduced to the metallic state, and (2) actinide metals tend to exhibit poor irradiation behavior. The first disadvantage does not appear to be serious since the number of subsequent fabrication operations should be reduced and since uranium and plutonium metals are routinely produced for weapons fabrication. It is hoped that the second disadvantage will not be realized since the actinide layer is very thin and receives its structural strength from the well-behaved substrate material.

10.4 Reference for Section 10

1. M. D. Freshley and D. F. Carroll, The Irradiation Performance of $MgO-PuO_2$ Nuclear Fuel, HW-SA-3127, General Electric Hanford Atomic Products Operation, Richland, Wash. (1963).

11. LMFBR TRANSMUTATION STUDIES

M. L. Williams and J. W. McAdoo (Oak Ridge National Laboratory)

The objective of this task is to examine the in-reactor aspects of long-lived nuclide transmutation in projected commercial LMFBRs. During FY 1977, this subtask will be concerned with scoping studies leading to the determination of one or two preferred transmutation modes which will be examined in detail in FY 1978.

During this quarter, the nuclide compositions of a model LMFBR and its refuel material were selected. Reference values for burnup, power density, k_{eff}, and breeding ratio were computed, based on the equilibrium configuration of the model. The calculations were performed using 2-D, multigroup diffusion theory.

The processing of "preliminary-preliminary" ENDF-V actinide cross sections has been completed, and the following libraries have been generated: 171 fine-group library, 51 intermediate-group library, 5 broad-group library, and ORIGEN library. In comparing these newer cross sections with Benjamin's data,[1] the general trend appears to be an increase in capture values and a decrease in fission values in the newer data.

Zero-dimensional ORIGEN calculations were used to determine actinide production by the model LMFBR. It was found that approximately 32 kg of neptunium, americium, and curium were produced every 337.5 days (270 full-power days, at 80% capacity factor). This material, along with 21 kg of actinides from a LWR, was recycled in the LMFBR until an equilibrium condition was achieved. The actinide inventory at equilibrium consisted of 486 kg of actinides in the reactor plus 127 kg of actinides at the reprocessing plant.

A study of the heterogeneous effects of lumping actinides in special target assemblies was completed. It was found that spatial self-shielding was small in the actinide assembly; thus homogeneous calculations are applicable to the heterogeneous case. Power peaking in the actinide assemblies was observed, and a parametric study was carried out to determine the effect of varying the concentration of ^{238}U diluent in the assembly.

Results showed that a substantial amount of diluent is required to reduce the power output of an actinide assembly to the same level as that of a fuel assembly. The required ^{238}U concentration may be as much as 70 to 80% of the heavy metal in the target assembly.

Spectral effects of lumping were also examined. It was found that an actinide assembly has a somewhat harder spectrum than a fuel assembly (44% $\emptyset$ > 2 keV, compared with 35% for a fuel assembly). The addition of ^{238}U diluent tends to soften the spectrum in the target assembly; and at 75% diluent concentration, the spectrum in the actinide assembly is fairly close to that in a fuel assembly.

11.1 Reference for Section 11

1. R. W. Benjamin, F. J. McCrossen, T. C. Gorrell, and V. D. Vandervelde, A Consistent Set of Heavy Actinide Multigroup Cross Sections, DP-1394 E. I. du Pont de Nemours and Co., Savannah River Laboratory (1975).

12. THERMAL REACTOR TRANSMUTATION STUDIES

T. C. Gorrell (Savannah River Laboratory)

The objective of this subtask is to study the in-reactor aspects of long-lived nuclide transmutation in thermal reactors. Uranium- and plutonium-enriched LWRs will be the principal reactor types examined, although "CANDU" and high-power-density (SRL production type) thermal reactors will also be considered. During FY 1977, this subtask will be concerned with scoping studies leading to the determination of one or two preferred thermal reactor transmutation modes which will be examined in detail in FY 1978.

Benchmark calculations of plutonium production in LWR fuel cells were completed. Measured values of the actinide content of H. B. Robinson fuel were compared with calculated results obtained from the GLASS code.[1] Normalization between calculations and measurements was achieved by a small reduction in the neutron width and capture width of the 6.7-eV resonance of ^{238}U. Results are given in Table 12.1 for three sets of parameters at two fuel exposures.

The ^{235}U remaining as calculated by GLASS* is a few percent less than measured. The calculated $^{239}Pu/^{238}U$ ratio is 2% higher than measured. Good agreement was also achieved in the plutonium isotopic ratios at the two exposures. The calculated ^{240}Pu contents are slightly higher, while the ^{241}Pu contents are lower, than measured.

The host lattice for the actinide transmutation calculations is described in ref. 2. The fuel elements, which are arranged in a 17 × 17 array, have an initial ^{235}U enrichment of 3.2 wt %. The total burnup achieved is 33,000 MWd/MTHM. Calculated actinide contents of the fuel at discharge are given in Table 12.2.

---

*Cross sections used were those in the standard SRL 84-group library, specified as STD.NUCPARAM.STANDARD and STD.MULTIGRP.STANDARD, as of March 1977.

Table 12.1. Comparison of measured and calculated contents of H. B. Robinson fuel

Ratio of ^{235}U/total U

Exposure, MWd/MTHM	Wt % ^{235}U	
	Measured	Calculated
0	2.56	-
24,570	0.81	0.80
30,920	0.60	0.55

Ratio of $^{239}Pu/^{238}U$

Exposure, MWd/MTHM	$^{239}Pu/^{238}U$ (%)	
	Measured	Calculated
24,570	0.496	0.508
30,920	0.520	0.531

Isotopic composition of Pu

Pu isotope	Wt % Pu			
	24,570 MWd/MTHM		30,920 MWd/MTHM	
	Measured	Calculated	Measured	Calculated
238	1.1	1.0	1.7	1.5
239	58.9	58.8	53.6	53.5
240	23.2	23.9	24.9	25.5
241	12.6	11.9	13.8	13.0
242	4.2	4.4	6.0	6.5

Table 12.2. Actinide content of irradiated PWR fuel[a]

Actinide	Charged (g/MTHM)	Discharged	
		g/MTHM	Wt %
Uranium			
U-234	288	152	
U-235	32,000	8,133	
U-236	0	4,009	
U-238	967,712	942,802	
Total	1,000,000	955,096	
Plutonium			
Pu-238		160	1.6
Pu-239		5,744	56.5
Pu-240		2,362	23.3
Pu-241		1,339	13.2
Pu-242		551	5.4
Total		10,156	100.0
Other actinides			
Np-237		512	
Am-241		48	
Am-243		109	
Cm-242		16	
Cm-244		34	

[a]Fuel is irradiated to 33,000 MWd/MTHM at an average specific power of 37.5 MW/MT.

Transmutation studies were made for three configurations of target material:

1. uniform dispersal of actinides in LWR fuel elements,
2. actinides concentrated in separate elements in a PWR fuel assembly, and
3. actinide-containing elements comprising separate assemblies, surrounded by uranium-enriched PWR fuel assemblies.

A summary of results for each case follows. Calculations were made using the SRL GLASS code, which computes multigroup neutron spectra and reaction rates for specified configurations of fuel and target assemblies.

Two methods were employed in assessing the effectiveness with which the waste actinides were fissioned in a given irradiation scheme. The first was simply to compare the number of grams of waste actinides that would remain after transmutation to that which would accumulate if there were no irradiation. In the second method, each actinide was weighted by half-life on a log scale of 0 to 1.0, with the 1.0 value set at 10^5 years (four times the half-life of ^{239}Pu). Actinides with half-lives less than or greater than 10^5 have weighting factors less than 1.0. Results obtained in this manner are designated "relative importance."

12.1 Uniform Dispersal in LWR Fuel

In this mode of recycle, actinides other than uranium and plutonium (i.e., the "waste actinides") were mixed uniformly with regular LWR uranium fuel, at an initial enrichment of 3.2 wt % ^{235}U. Loadings were in a 1:1 ratio; that is, waste actinides from one discharged fuel element were charged to one new element. Irradiation times were 3 years at an 80% capacity factor (33,000 MWd/MT), with 1 year of processing time; the uranium and plutonium were not recycled. After five recycle operations (total time, 20 years), the neptunium and americium contents had ceased to change with exposure; however, the contents of the higher actinides, especially ^{252}Cf, were still increasing.

In this case, the waste actinides were removed from the inventory in two ways: by fission, and by conversion of the ^{237}Np to plutonium, which was partitioned from the waste actinides and would be fissioned later when used as a fuel. After five recycles, only 15% of the waste actinides

had been fissioned. Figure 12.1 compares the relative waste actinide inventory (excluding uranium and plutonium) with the waste actinide accumulation in the no-recycle case. The conversion of ^{237}Np to plutonium accounts for most of the inventory reduction. The assay of plutonium obtained from a recycle 5 fuel element is compared with a no-recycle element below:

Pu isotope	Pu assay (%)	
	Recycle 5	No recycle
238	5.0	1.7
239	55.3	56.9
240	22.4	23.4
241	12.1	12.6
242	5.2	5.4

Figure 12.1 also shows that there is little difference between the two methods (i.e., mass vs relative importance) of accounting for the remaining actinides.

12.2 Actinides Concentrated in Separate Elements

Actinides other than uranium and plutonium from 100 elements were placed in a single element, with zirconium being used as a diluent to occupy the remaining volume. The waste actinides from 100 regular fuel elements were added to the inventory at the start of each 3-year irradiation period. Adjacent elements contained the standard uranium-enriched PWR loading of 3.2 wt % ^{235}U.

After five recycle operations, the specific power of the target element exceeded that of the uranium-enriched elements by 50% and was increasing with exposure. The recycle mode was repeated, with the concentration factor reduced to 50:1. The specific power of the target elements was acceptable for this case. Figure 12.2 shows the relative inventory for this case, including all actinides from uranium to californium. After five recycles, the gram inventory is 54% of that which would be experienced in the absence of irradiation. Using the relative importance index, the inventory is 64% of the no-recycle case.

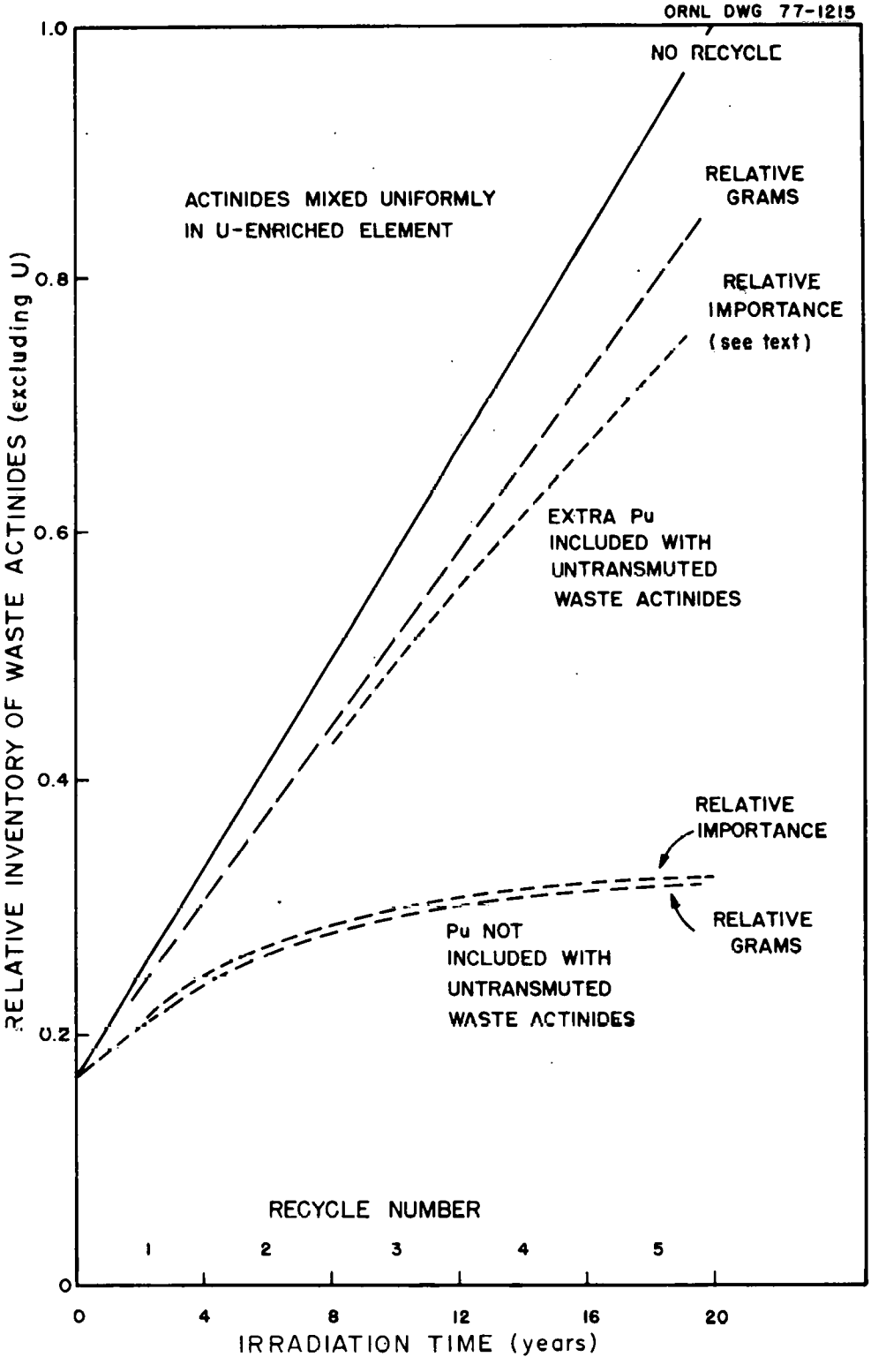

Fig. 12.1. Waste actinide inventories vs irradiation time when the actinides are uniformly dispersed within the fuel.

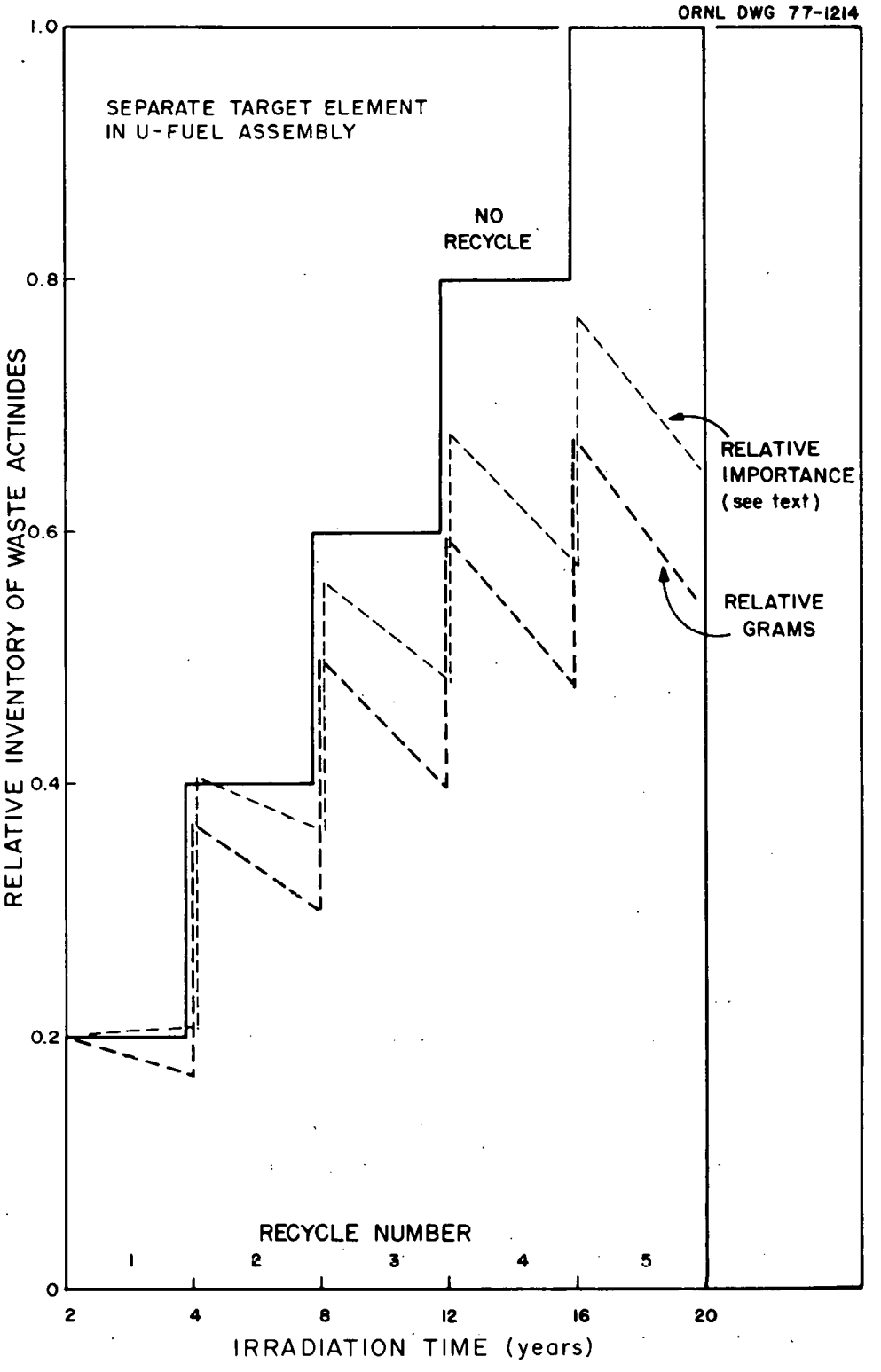

Fig. 12.2. Waste actinide inventories vs irradiation time when the actinides are concentrated in separate fuel elements.

Depleted uranium (0.2 wt % ^{235}U), rather than zirconium, was used as the actinide diluent in one set of calculations to simplify target dissolution. The power generated from ^{239}Pu produced by the ^{238}U in the diluent made it necessary to reduce the actinide concentration factor to 20:1. After three recycle operations (12 years), the total waste actinide inventory was equal to that for no recycle because the plutonium produced from the ^{238}U diluent in the target element was considered to be a waste actinide and recycled back to the target element. This case is not directly comparable to the homogeneous recycle case described in Sect. 12.1 and will be pursued further at a later date.

12.3 Actinide-Containing Assemblies

Two loading configurations for separate target assemblies were investigated using neutron flux spectrum calculations. In the first, all element locations in the square assembly (264) contained waste actinides with zirconium diluent. The thermal flux in the central elements was heavily depressed, to a value about one-tenth that of the adjacent uranium-enriched assemblies. The thermal flux in the outer actinide elements was four times that of the inner elements.

In the second configuration, waste actinides were charged only to the elements near the outside of the target assembly, with H_2O occupying inner positions. Approximately 36% of the element locations contained waste actinides. The thermal flux in the actinide elements was about one-half that of the uranium-enriched assemblies. These results indicate that there is little incentive to employ a standard, fully loaded LWR assembly for actinide depletion under these conditions. Alternate possibilities include: (1) salting the elements with highly enriched uranium or plutonium, (2) a new configuration with a higher H_2O/uranium ratio, or (3) a partially loaded assembly.

No depletion calculations have been made for the separate assembly case. GLASS calculations require about four times as much computer time as the other, simpler configurations. The GOSPEL code, which computes actinide transmutation for a fixed flux spectrum, is being modified to accommodate the PWR conditions.

12.4 Program for Next Quarter

During the next quarter, four additional cases will be studied with the GLASS code:

1. all actinides recycled except uranium, mixed with natural uranium in the concentration needed for reactivity,
2. all actinides recycled, with ^{235}U added as needed for reactivity,
3. waste actinide elements in the lattice comprised of mixed plutonium-uranium fuel, and
4. separate assemblies of waste actinides in a D_2O reactor system.

In addition, the irradiation period of some of the cases will be extended using the GOSPEL code, with neutron spectra obtained from GLASS.

12.5 References for Section 12

1. H. C. Honeck, JOSHUA System, DP-1380, E. I. du Pont de Nemours and Co., Savannah River Laboratory (1975).
2. Reference Safety Analysis Report, Vol. II, Westinghouse Nuclear Energy Systems, DOCKET-RESARA-23 (November 1973).

13. FUEL CYCLE IMPACT STUDIES

A. G. Croff (Oak Ridge National Laboratory)

The objective of this task is to analyze the impacts of partitioning-transmutation that are not being considered by other subtasks. Examples of such impacts are the effects of the recycled actinide neutron activity on nuclear fuel cycle operations and determination of the recycled actinide inventories in the fuel cycle.

This task was not active during the April-June report period.

14. RISK/BENEFIT ANALYSIS OF CONCEPT

(Oak Ridge National Laboratory and Battelle Northwest)

The objective of this task is to estimate the additional risks that are incurred as a result of increased handling of the long-lived nuclides, and the long-term benefits that would accrue as a result of the biologically significant, long-lived nuclide content of radioactive wastes being significantly reduced.

This task is inactive during FY 1977.

15. DETAILED ECONOMIC ANALYSIS OF FABRICATION AND REPROCESSING PLANTS IN A PARTITIONING-TRANSMUTATION FUEL CYCLE

(Oak Ridge National Laboratory)

This task will provide detailed cost estimates of fuel reprocessing and refabrication plants operating with and without partitioning and transmutation. The analysis will show the economic impacts of this option on the fuel cycle.

This task is inactive during FY 1977.

16. PARTITIONING-TRANSMUTATION ANALYSIS, COORDINATION, AND EVALUATION

D. W. Tedder, A. G. Croff, and J. O. Blomeke
(Oak Ridge National Laboratory)

This task coordinates all other efforts related to the program. Integrated flowsheets are developed from the experimental evaluation of subsystems within the fuel and target reprocessing and refabrication plants. Alternative flowsheets are evaluated; options are chosen for detailed analysis. Constraints are defined which facilitate the integration of the concept to all aspects of the fuel cycle.

16.1 Incineration Analysis

Additional analysis was conducted during this quarter to examine incineration alternatives in greater detail. This unit operation interacts with many other waste management steps in fuel reprocessing and refabrication, including the acid and water recycle systems, salt waste management, off-gas treatment, and the low- and intermediate-level waste immobilization systems.

Although small amounts of combustibles may be tolerated in a federal waste repository, requirements will likely dictate that all radwastes be chemically and radiologically stable. In addition, as much as 25% of the total actinide losses may be to combustible wastes. Although the toxicity indexes of these wastes are generally several orders of magnitude lower* than the index of the high-level waste, they are still important with respect to minimizing the total actinide losses and should not be ignored. Consequently, the integrated partitioning flowsheets include radwaste incineration and subsequent treatment, although the most attractive system has not yet been conclusively identified.

The assumed combustible wastes, which are summarized in Tables 16.1 and 16.2, include a variety of materials with different levels of contamination.

---

*Because the radioactivity is more dilute.

Table 16.1. Composition of combustible trash

Component	wt %
Cellulose	88
Latex	1
Neoprene	2
Hypalar	?
Polyvinyl chloride	4
Polyethylene	3

Table 16.2. Composition of combustible waste

Component	wt %
Trash	41
Activated carbon	27
Waste TBP solvent	25
Cation exchange resins	5
Kerosene	1
Mixed ion exchange resins	1
Anion exchange resins	1

Extensive pretreatment of these wastes would be required, regardless of the type of incineration used. Moreover, the required sorting, shredding, and tramp-metal removal operations are largely unavoidable and not subject to conceptual optimization. On the other hand, the incineration method is subject to optimization and several considerations appear important. These include: (1) actinide recoverabilities from the incinerator effluents, (2) resulting effluent compositions and volumes, (3) system safety and operability, and (4) long-term maintenance requirements and system availability. The relative costs are also important, but are not a dominant consideration in the context of actinide partitioning. Because of the many common constraints (e.g., remote operation, off-gas neutralization, etc.), radwaste incineration will probably be unavoidably expensive.

The current generation of reference flowsheets assumes that the radwaste will be incinerated in a fluidized bed of sodium carbonate[1] operated at about 500°C, as shown in Fig. 16.1. This system has several advantages, including in situ neutralization of acidic off-gases and low-temperature operation. It also has disadvantages, including (1) relatively high volumetric off-gas rates, (2) incomplete combustion of solid wastes, and (3) inability to solubilize refractory plutonium. In addition, it generates substantial quantities of salt wastes which must be managed.

In the reference flowsheets, the solid effluents from the fluidized-bed incinerator (FBI) are combined and treated for actinide recovery. This treatment involves four steps: (1) water wash of the combined solid effluents, (2) separation of the insoluble wastes (ashes) from the salt liquor, (3) HNO_3 leaching to recover actinides from the ashes, and (4) cation exchange to recover actinides from the salt liquor. The first step consists primarily of separating the undesirable phosphate, sulfate, and chloride anions from the insoluble ash residue. Since some actinides form water-soluble carbonates, the partitioning facility must be capable of recovering them, possibly as suggested in step 4.

Most of the actinides, however, are expected to remain with the water-insoluble ash, and step 3 would be complicated by two effects: (1) the possible organic contamination of the ash from incomplete combustion, and (2) the insolubility of refractory plutonium in HNO_3 alone. The first

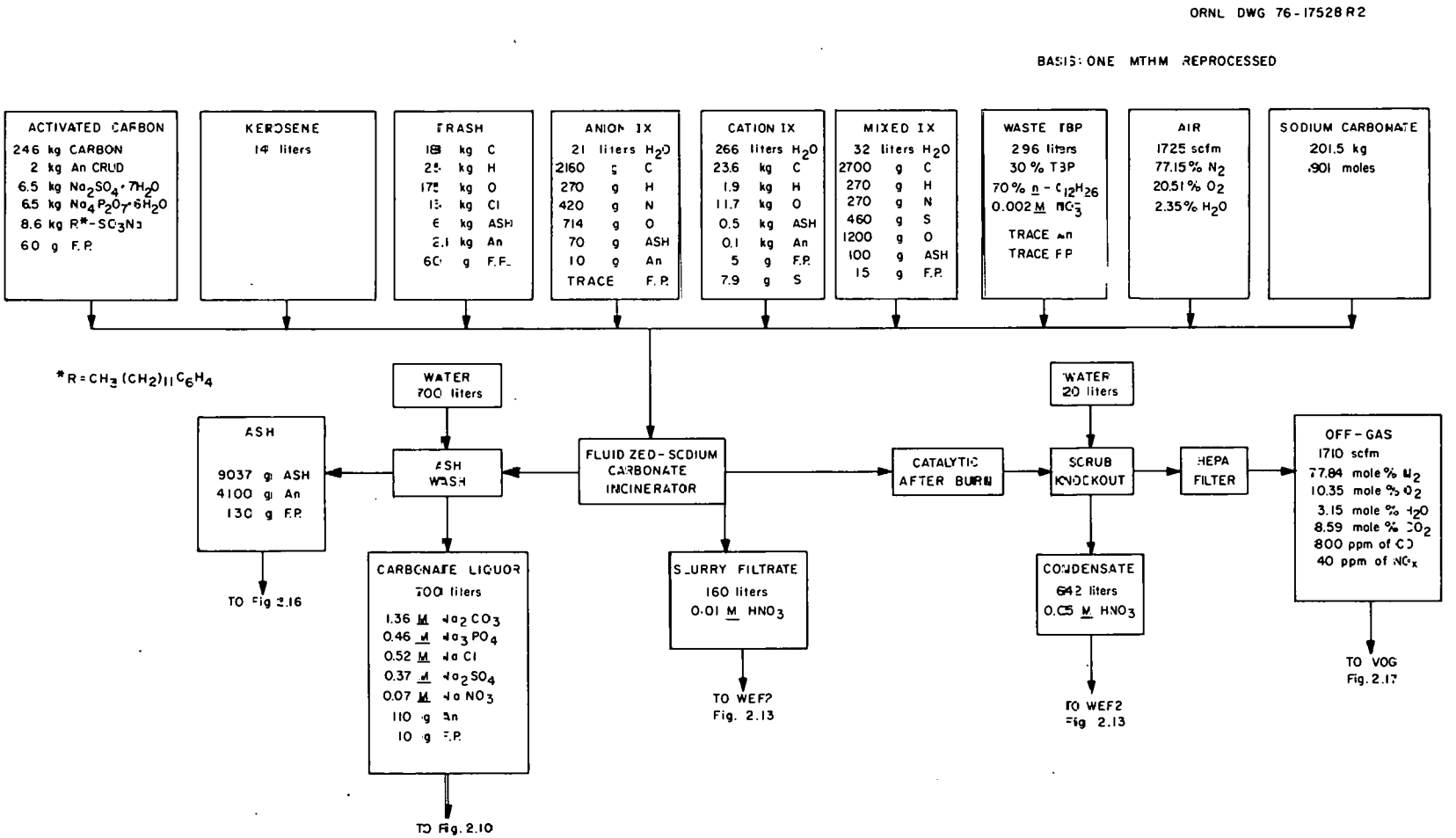

Fig. 16.1. Fluidized-bed incineration.

consideration may result in hazardous operating conditions due to the potential formation and accumulation of nitrated organic explosives. The second consideration indicates that significant plutonium losses would probably occur if refractory plutonium is eventually introduced into the incinerator in large amounts. These losses could be kept low, of course, if only uranium-enriched fuels are processed; however, they may become unacceptably high during the processing of fast reactor fuels or transmutation targets.

Figures 16.2 and 16.3 outline one possible alternative incineration system, which burns the same wastes as the FBI in Fig. 16.1 but utilizes a combination of conventional, controlled-air incineration[2] and molten-salt fusion.[3] The controlled-air incinerator burns the ion exchange resins, waste kerosene, and general trash. A caustic scrub neutralizes the corrosive off-gases. In Fig. 16.3, a molten-salt bed achieves a more complete combustion of carbon in the controlled-air incinerator ashes and also burns the phosphate-bearing wastes, which otherwise tend to form a dense, black smoke. The salt effluent should have only a very low content of unoxidized carbon and potentially will contain only ionic plutonium, which will readily dissolve in HNO_3.

Since the salt fusion system also dissolves the silicates, it then becomes necessary to perform a gelatin strike[4] subsequent to nitration of the salt cake. Otherwise, polysilicates would form a nonfilterable gel in the acid solution. The resulting gelatin-silicate precipitate can be easily filtered, however, and past experience[4] suggests that significant actinide losses to the precipitate can be avoided by simple washes with 0.1 M HNO_3. Unfortunately, zirconium tends to remain with the precipitate; thus it would probably be necessary to incorporate this precipitate into the high-level glass. Although the presence of gelatin could cause safety problems in the solidification operation, the excess gelatin in the resulting supernate is not expected to interfere adversely with any subsequent actinide recovery operations or salt waste immobilization in concrete.

In comparing the effluents from these two incinerators, differences exist with respect to both effluent compositions and volumes. The controlled air incinerator, for example, would facilitate a separation of the actinides

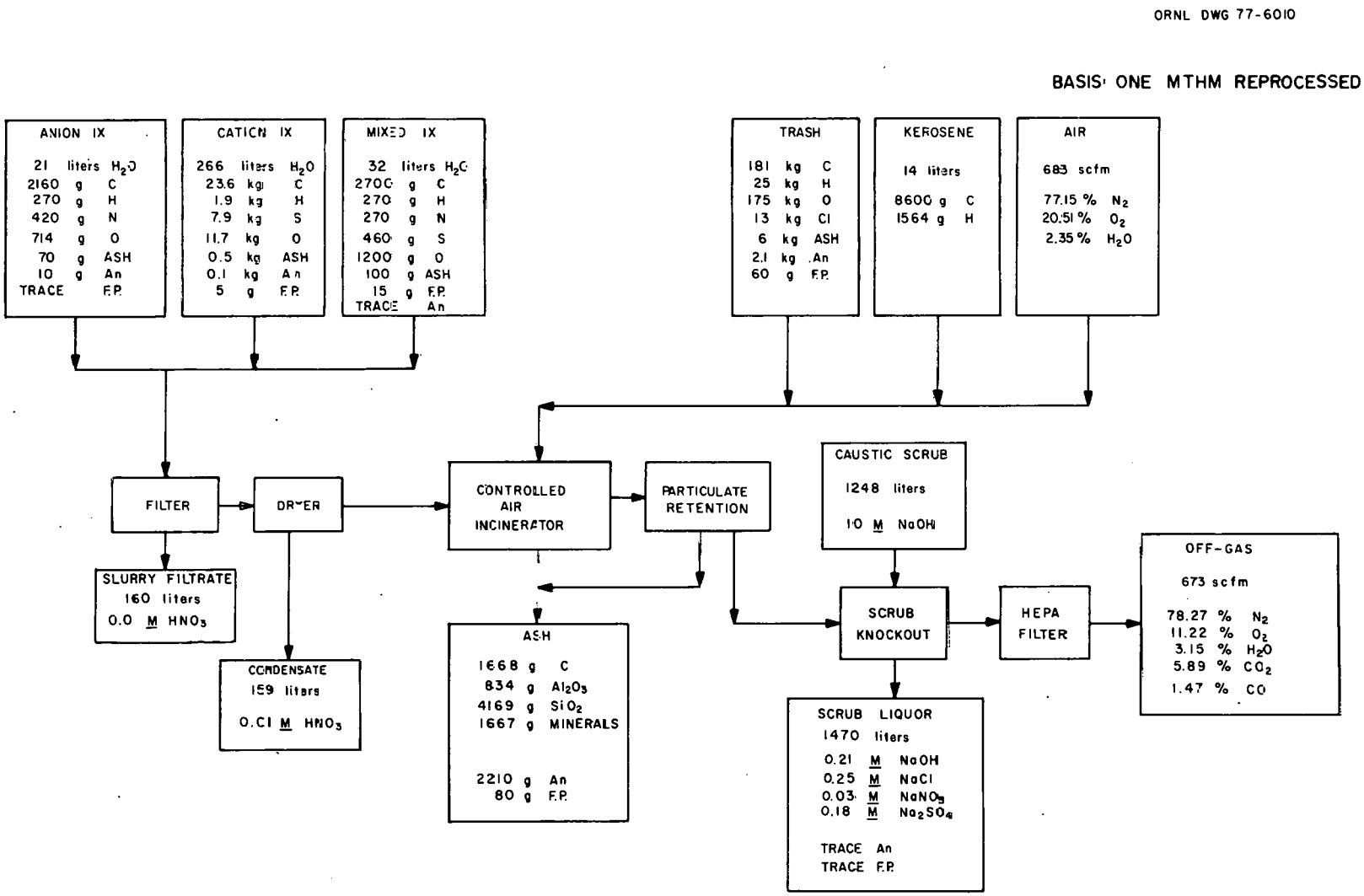

Fig. 16.2. Conventional air incineration.

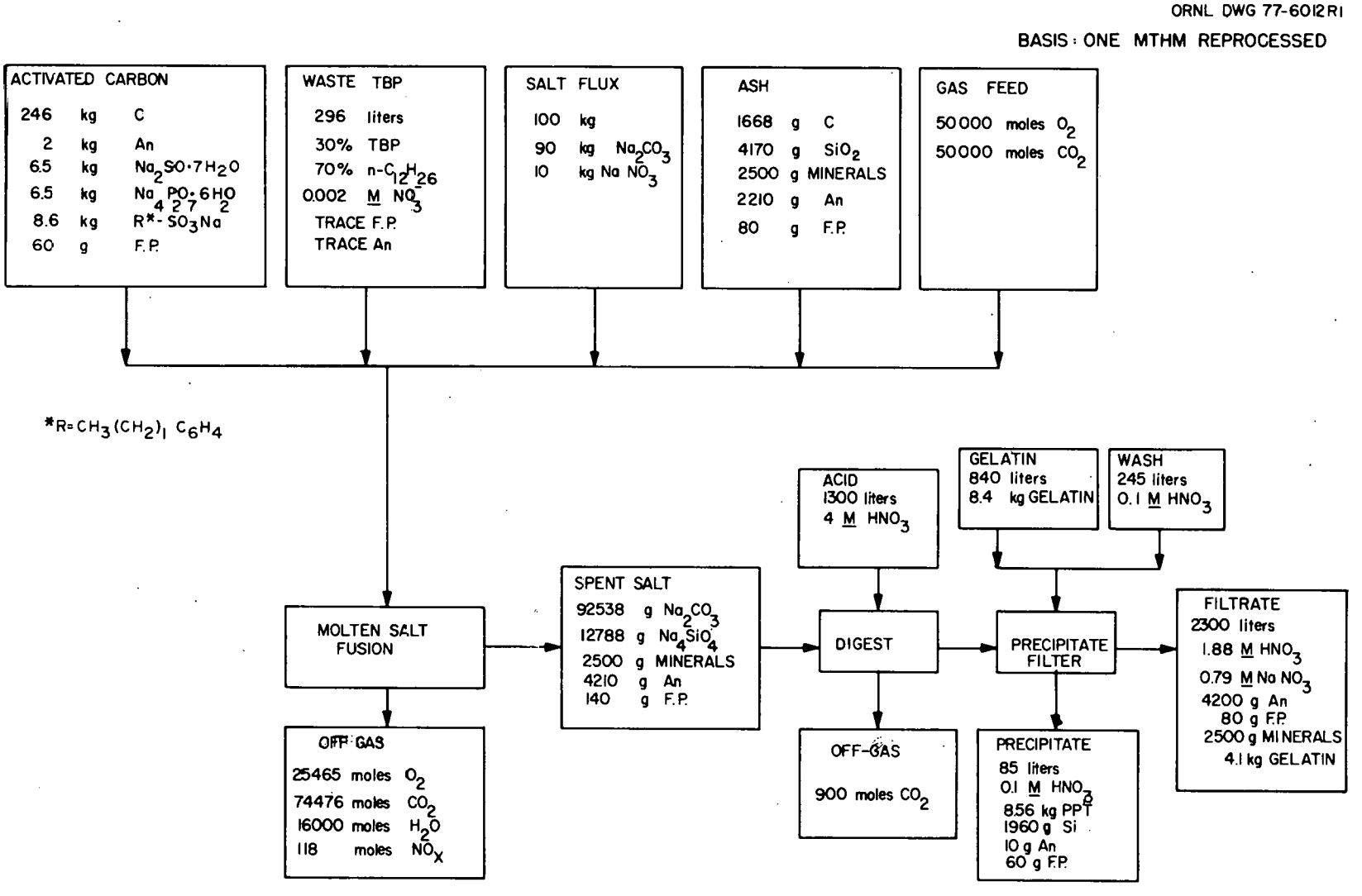

Fig. 16.3. Molten-salt fusion with gelatin strike.

in the wastes from the chloride and sulfate anions. The incineration of TBP in this system might also permit separation of the phosphate anion. In Fig. 16.1, these species are mixed together in the carbonate liquor. On the other hand, the molten-salt system solubilizes the ash materials that would otherwise remain behind during the subsequent HNO_3 leach of the FBI ash.

Table 16.3 summarizes the relative effluent volumes according to general types. The most pronounced advantage for the combination incinerator is the reduction in off-gas rates. (This ratio may be closer to 0.2.) The use of sodium in the combined system could also be further reduced if all the caustic in the off-gas scrub is neutralized, but more than half of the sodium is committed to the salt fusion system. From the standpoint of effluent volume, therefore, it appears that no dramatic reduction is likely except in the relative off-gas rates. However, the combination system may exhibit some additional flexibility since it might be possible to utilize the TBP scrub wastes as a flux in the salt fusion. This approach might further reduce the salt waste volumes, but could also complicate the subsequent actinide recovery since the TBP scrub can be highly contaminated. Consequently, the most clearly perceived advantage for the combined system is its potential for solubilizing refractory actinides.

Table 16.3. Relative effluent volumes

Effluent	Combined system / FBI system
Off-gas rates	0.58
Aqueous volumes	1.30
Solid weights	0.94
Moles of sodium consumed	0.81

16.2 Other Activities

An overview of the program was presented at the Second Annual ERDA Workshop on Actinide Recovery in Richland, Washington. The meeting was generally productive, and several new ideas for waste management were suggested.

Coordination efforts in the various off-site participants continued. The preliminary evaluation of the partitioning-transmutation concept will be completed next quarter, and efforts are now under way to develop a draft report summarizing a set of updated flowsheets which feature the coprocessing of uranium and plutonium, as well as co-sited reprocessing and refabrication facilities.

16.3 References for Section 16

1. D. L. Ziegler et al., Pilot Plant Development of a Fluidized Bed Incineration Process, RFP-2271, Rockwell International, Rocky Flats Plant (October 1974).

2. Transuranic Solid Waste Management Research Programs, October-December 1973, LA-5614-PR, Los Alamos Scientific Laboratory, Los Alamos, N.M. (May 1972).

3. D. E. McKenzie et al., Disposal of Transuranic Solid Waste Using Atomics International Molten Salt Combustion Process, AI-ERDA-13151, Rockwell International, Canoga Park, Calif. (May 1975).

4. H. J. Groh, Removal of Silica from Solutions of Nuclear Fuels, DP-293, E. I. du Pont de Nemours & Co., Savannah River Laboratory (June 1958).

THIS PAGE

WAS INTENTIONALLY

LEFT BLANK

ORNL/TM-6056

INTERNAL DISTRIBUTION

1-2. Central Research Library
3. Document Reference Section
4-6. Laboratory Records
7. Laboratory Records, R.C.
8. ORNL Patent Section
9. C. W. Alexander
10. R. E. Blanco
11-30. J. O. Blomeke
31. W. D. Bond
32. W. D. Burch
33. D. O. Campbell
34. A. G. Croff
35. D. E. Ferguson
36. B. C. Finney
37. L. M. Ferris
38. C. W. Forsberg
39. R. W. Glass
40. H. W. Godbee
41. G. H. Jenks
42. F. A. Kappelmann
43. S. Katz
44. O. L. Keller
45. R. E. Leuze
46. K. H. Lin
47. A. P. Malinauskas
48. W. C. McClain
49. L. E. McNeese
50. J. G. Moore
51. E. Newman
52. E. L. Nicholson
53. K. J. Notz
54. H. Postma
55. F. M. Scheitlin
56. C. D. Scott
57. R. R. Shoun
58. D. W. Tedder
59. L. M. Toth
60. D. B. Trauger
61. B. L. Vondra
62. B. Weaver
63. M. L. Williams
64. R. G. Wymer
65. G. R. Choppin (consultant)
66. E. L. Gaden, Jr. (consultant)
67. C. H. Ice (consultant)
68. L. E. Swabb, Jr. (consultant)
69. K. D. Timmerhaus (consultant)

EXTERNAL DISTRIBUTION

70-96. Technical Information Center, Oak Ridge, TN 37830

ERDA-ORO, Oak Ridge, TN 37830
97. Research and Technical Support Division
98. J. J. Schreiber

ERDA, Washington, DC 20545
99. J. L. Burnett
100. W. K. Eister
101. J. A. Leary

U. S. Nuclear Regulatory Commission, Washington, DC 20555
102. W. P. Bishop
103. R. Cooperstein

Allied Chemical Corp., P. O. Box 2204, Idaho Falls, ID 83401
104. L. D. McIsaac
105. C. M. Slansky

Atlantic Richfield Hanford Company, P. O. Box 250, Richland, WA 99352
106. H. Babad
107. W. W. Schulz

Battelle Northwest, P. O. Box 999, Richland, WA 99352
108. A. M. Platt
109. K. J. Schneider
110. E. J. Wheelwright

Argonne National Laboratory, 9700 South Cass Ave., Argonne, IL 62439
111. E. P. Horwitz
112. G. W. Mason
113. M. Steindler

Hanford Engineering Development Laboratory, P. O. Box 1970, Richland, WA 99352
114. R. Lerch

Sandia Laboratories, P. O. Box 5800, Albuquerque, NM 87115
115. R. L. Schwoebel
116. D. R. Tallant

George C. Marshall Space Flight Center, Marshall Space Flight Center, AL 35812
117. R. E. Burns

Mound Laboratory, P. O. Box 32, Miamisburg, OH 45342
118. E. L. Lewis
119. D. F. Luthy

Rockwell International, Rocky Flats Plant, P. O. Box 464, Golden, CO 80401
120. J. D. Navratil
121. G. H. Thompson

E. I. du Pont de Nemours and Company, Savannah River Laboratory, Aiken, SC 29801
122. T. C. Gorrell

Brookhaven National Laboratory, Upton, NY 11973
123. T. E. Gangwer

Los Alamos Scientific Laboratory, P. O. Box 1663, Los Alamos, NM 37544
124. W. J. Maraman

General Electric, Mail Code S-34, P. O. Box 5020, Sunnyvale, CA 94086
125. S. L. Beaman

Atomic Energy Research Establishment, Harwell, Didcot, Oxon., OX11 ORA, England
126. N. J. Keen
127. G. N. Kelly

Centre d'études nucléaires de Fontenay-aux-Roses, B.P. No. 6, Fontenay-aux-Roses, France
128. Y. Sousselier

OECD-Nuclear Energy Agency, 38, Boulevard Suchet, F-75016 Paris, France
129. M. Takahashi

International Atomic Energy Agency, P. O. Box 590, A-1011 Vienna, Austria
130. J. R. Grover

Institut für Heisse Chemie Kernforschungszentrum, Postfach 3640, 75 Karlsruhe, Germany
131. H. O. Haug

Lab. Teoria e Calcolo Reottori, C.N.E.N. - C.S.N. Casaccia, CP 2400 I-00100 Rome, Italy
132. L. Tondinelli

Commission of the European Communities, CCR Euratom, I-21200 Ispra, Italy
133. F. Girardi

Nuclear Research Institute, 25066 Rez, Czechoslovakia
134. L. Neumann

Chalmers University of Technology, Dept. of Nuclear Chemistry S-402 20 Göteborg, Sweden
135. J. O. Liljenzin

☆ U.S. GOVERNMENT PRINTING OFFICE: 1977-748-189/259